The Role of S6K1 in Development and Maintenance of Nutrient Homeostasis

Inauguraldissertation

zur Erlangung der Würde eines Doktors der Philosophie

vorgelegt der

Philosophisch-Naturwissenschaftlichen Fakultät

der Universität Basel

von

Sung Hee Um

aus Seoul, South Korea

Leiter der Arbeit: PD. Dr. George Thomas

Friedrich Miescher Institute for Biomedical Research

Basel, 2004

Genehmigt von der Philosophisch-Naturwissenschaftlichen Fakultät
auf Antrag von Prof. Michael N. Hall, Prof. Johan Auwerx und PD. Dr. George Thomas.

Basel, den.28.09.2004

Prof. Marcel Tanner

i. ABBREVIATIONS

ii. SUMMARY

I. INTRODUCTION

1. When nutrient homeostasis is normal

1.1. Energy homeostasis in adipose tissue, muscle and liver……..1

1.2. How is dietary fat digested and absorbed?……1

1.3. How is fat stored and mobilized?……..4

1.4. How is fat synthesized and oxidized?……..8

1.5. Adipose tissue……16

1.6. What are the characteristics of white adipose tissue and brown adipose tissue?……16

1.7. How are adipocytes differentiated?……18

2. When nutrient homeostasis is out of order

2.1.Obesity…… 23

2.2. Insulin resistance……25

2.3. What causes insulin resistance? ……29

3. How does nutrient signaling coordinate with insulin signaling?……..34

4. Pancreatic β-cell growth

4.1. What controls nutrient transport required for body growth during development in mammals?……...43

4.2. How is pancreatic β-cell mass is regulated? ……47

4.3. What kind of factors modulate β-cell growth?…….. .48

II. MATERIALS AND METHODS……56

III. RESULTS

Part 1: ……..65

S6K1 (-/-)/S6K2 (-/-) mice exhibit perinatal lethality and rapamycin-sensitive 5'-terminal oligopyrimidine mRNA translation and reveal a mitogen-activated protein kinase-dependent S6 kinase pathway.

Pende M, Um SH, Mieulet V, Sticker M, Goss VL, Mestan J, Mueller M, Fumagalli S, Kozma SC, Thomas G.

Mol Cell Biol. 2004, 24(8):3112-24

Part 2: ……66

Absence of S6K1 protects against age- and diet-induced obesity while enhancing insulin sensitivity.

Um SH, Frigerio F, Watanabe M, Picard F, Joaquin M, Sticker M, Fumagalli S, Allegrini PR, Kozma SC, Auwerx J, Thomas G.

Nature. 2004, 431, 200–205

Part:3:……..68

Regulation of pancreatic β-cell growth by S6K1 during development

Unpublished results and discussion.

IV. DISCUSSION ……..82

V. REFERENCES……92

VI. CURRICULUM VITAE……..106

VII. ACKNOWLEDGEMENTS …….. 109

i. ABBREVIATIONS

4E-BP1	eIF4E binding protein 1
IR	Insulin receptor
IRS	Insulin receptor substrate
GAP	GTPase-activating protein
mRNA	messenger RNA
mTOR	Mammalian target of rapamycin
N-terminal	amino-terminal
p70S6K	S6 kinase 1
PAGE	polyacrylamide gel electrophoresis
PBS	phosphate-buffered saline
PDK1	PtdIns(3,4,5)P_3-dependent protein kinase-1
PI(3)K	phosphatidylinositol-3 kinase
PIP_3	PtdIns(3,4,5)P_3
PKA	protein kinase A
PKB	protein kinase B
PKC	protein kinase C
P-Ser	phosphoserine
P-Thr	phosphothreonine
RNAi	RNA mediated interference
Rb	retinoblastoma tumor suppressor protein
S6	40S ribosomal subunit protein 6
S6K1	S6 kinase 1
S6K2	S6 kinase 2
TOR	Target of rapamycin
5'TOP	Five prime terminal oligopyrimidine tract
TSC	Tuberous sclerosis complex
UTR	Untranslated region

Less frequently used abbreviations are defined upon their first use in the text.

ii. SUMMARY

Insulin signaling at the target tissue results in a large array of biological functions. These events are essential for normal growth and development and for normal nutrient homeostasis. Studying the signaling pathways involved in insulin and nutrient action could lead to better understanding of pathophysiology of insulin resistance associated with obesity and type 2 *diabetes* and identifying key molecules and processes could lead to the development of therapeutic strategies for the treatment of these common disorders.

Previously mice deficient for S6 Kinase 1 (S6K1), an effector of the mammalian target of rapamycin (mTOR) that acts to integrate nutrient and insulin signals, were shown to be hypoinsulinaemic, glucose intolerant and have reduced β-cell mass. However, S6K1-deficient mice maintain normal glucose levels during fasting, suggesting hypersensitivity to insulin, raising the question of their metabolic fate as a function of age and diet. The present study shows that S6K1-deficient mice are protected against obesity owing to enhanced β-oxidation and sensitive to insulin owing to the apparent loss of a negative feedback loop from S6K1 to insulin receptor substrate 1 (IRS1), which blunts S307 and S636/S639 phosphorylation; sites involved in insulin resistance, Thus under conditions of nutrient satiation S6K1 negatively regulates insulin signaling.

The actual cause of diminished β-cell size in adult S6K1-deficient mice has not been fully understood. The present study shows that loss of S6K1 leads to reduced β-cell size during development, intrauterine growth retardation, and impaired placental development. S6K1 deficient embryos supplied with a wild type normal placenta by tetraploid aggregation, developed normally and only β-cell size was still smaller than wild type, suggesting the defect in β-cell growth is independent of placental dysfunction. Furthermore, β-cell specific transgenic expression of S6K1 restores β-cell growth and development in S6K1 deficient embryos.

The present study indicates the impact of S6KI signaling in age- and diet-induced obesity and insulin resistance, and also gives insight into the interaction

between insulin induced IRS-PI3K pathway and nutrient induced mTOR-S6K pathway in pancreatic β-cell growth and nutrient homeostasis.

I. INTRODUCTION

When nutrient homeostasis is normal

1.1. Energy homeostasis in adipose tissue, muscle and liver.

Adipose tissue, which is the main energy storage site, is responsive to both central and peripheral metabolic signals by regulating lipid storage and mobilization. Dietary fat is absorbed through the gastrointestinal tract in the form of circulating chylomicrons and very-low-density lipoprotein (VLDL), part of which is metabolized to provide energy and the rest of which enters the liver and adipose tissues for short- and long-term storage, respectively. As a gauge of energy reserve levels, adipose tissue secretes several adipokines, such as leptin, which regulate energy homeostasis by signaling to the brain and peripheral tissues. Adipose tissues, through the lipolysis and re-esterification process, are also the main sites for fatty-acid cycling, thereby providing an energy supply to oxidative tissues such as skeletal muscle and the heart.

The liver also has an important role as a homeostat for transient energy fluctuation; it protects other tissues from postprandial triglyceridaemia by temporarily storing fatty-acids from the circulation as triacylglycerol (TAG), and secreting them as VLDL when the period of maximum lipid load has passed. The liver is also an important site for energy conversion, exchanging energy sources from one form to another, such as glycogen to glucose, fatty acid to TAG and saturated fatty acid to unsaturated fatty acid (Saltiel and Kahn, 2001).

1.2. How is dietary fat digested and absorbed?

One of the main energy sources, dietary fats are present mainly as mixed TAGs, which comprise one molecule of glycerol and three molecules of fatty acid. Many

fats of animal origin are composed of saturated fatty acids — predominantly palmitic (C16:0) and stearic (C18:0) acids at the sn-1 and sn-3 positions — whereas vegetable oils contain mainly unsaturated fatty acids (70% linoleic acid (C18:2) at the sn-2 position). Dietary TAG undergoes a series of complex biochemical processes before entering intestinal cells and being transported into the circulation (Fig. 1).

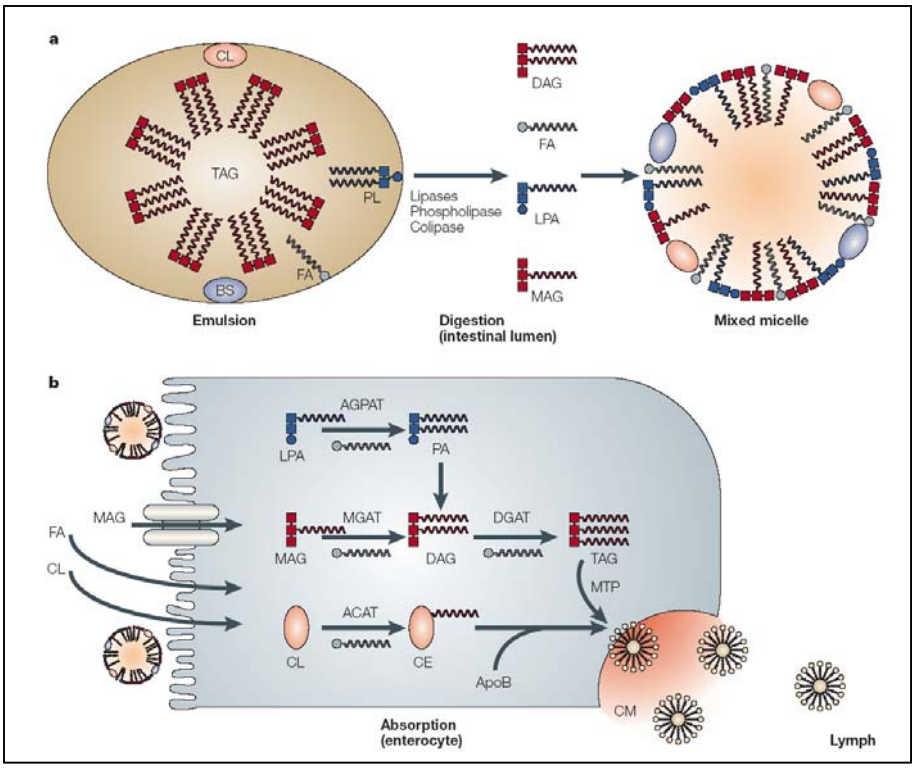

Adapted from (Shi and Burn, 2004)

Fig. 1. The process of dietary lipid digestion and absorption.

a | Dietary lipid digestion begins in the stomach, where lipids are subjected to partial digestion by gastric lipase and form large fat globules with hydrophobic triacylglycerol (TAG) cores surrounded by polar molecules, including phospholipids (PLs), cholesterol (CL), fatty acids (FAs) and ionized proteins. The digestive processes are completed in the intestinal lumen, where large emulsions of fat globules are mixed with bile salts (BS) and pancreatic juice containing lipid digestive enzymes to form an aqueous suspension of small fatty droplets to maximize exposure to the pancreatic lipases for lipid hydrolysis. Monoacylglycerol (MAG), diacylglycerol (DAG) and free FAs that are released by lipid hydrolysis join BS, CL, lysophosphatidic acid (LPA) and fat-soluble vitamins to form mixed micelles that provide a continuous source of digested dietary products for absorption at the brush-border membranes of the enterocytes. b | FAs and MAG enter the enterocytes by passive diffusion and are facilitated by transporters, such as intestinal FA-binding protein (IFABP), CD36 and FA-transport protein-4 (FATP4). They are then re-

esterified sequentially inside the endoplasmic reticulum by MAG acyltransferase (MGAT) and diacylglycerol acyltransferase (DGAT) to form TAG. Phospholipids from the diet as well as bile — mainly LPA — are acylated by 1-acyl-glycerol-3-phosphate acyltransferase (AGPAT) to form phosphatidic acid (PA), which is also converted into TAG. Dietary CL is acylated by acyl-CoA: cholesterol acyltransferase (ACAT) to cholesterol esters (CE). Facilitated by microsomal triglyceride transfer protein (MTP), TAG joins CE and apolipoprotein B (ApoB) to form chylomicrons (CM) that enter circulation through the lymph.

1.2.1. What mediates fat transport inside cells?

Fatty-acid transport and binding proteins.

After digestion, lipolytic products — mainly fatty acids and MAG — are dispersed as vesicles and bile salt-mixed micelles, and are absorbed across the apical brush-border membrane of enterocytes of the small intestine. Both passive (diffusion) and active transport (facilitated by binding protein and/or transporters) diffusion process across adipocyte membranes is rapid and efficient at high or low concentrations of fatty acids (Kamp et al., 2003). In these sense, the transporter-mediated process may only serve to facilitate an appropriate subcellular distribution of lipids.

At least three distinct membrane proteins might participate in long-chain fatty-acid transport across the intestinal epithelial cells: **intestinal fatty-acid-binding protein (IFABP)**, **CD36** and **fatty-acid-transport protein-4 (FATP4)**. Inactivation of IFABP does not attenuate lipid absorption in knockout mice (Vassileva et al., 2000), which indicates the presence of several compensating types of FABP in the small intestine. **CD36**, which is also known as fatty-acid translocase (FAT), is highly expressed in the intestine in a pattern that is consistent with a role in lipid absorption (Chen et al., 2001). Although CD36-deficent mice showed defective fatty-acid uptake by various tissues — including the heart, oxidative skeletal muscle and adipose tissues — no notable impairment of lipid absorption was observed in knockout mice (Goudriaan et al., 2002).

FATP4 is the principal FATP in the small intestine and is thought to have a role in facilitating fatty-acid uptake by intestinal epithelial cells (Schaffer and Lodish, 1994). Targeted deletion of Fatp4 in mice results in embryonic lethality, which prevents the detailed study of its physiological role in dietary fat absorption. Although enterocytes that are isolated from heterozygous mice show a 40% reduction of fatty-acid uptake, this is insufficient to cause detectable effects on fat absorption in heterozygous knockout mice that are fed either a normal or a high-fat diet (Gimeno et al., 2003).

1.3. How is fat stored and mobilized?

In mammals, the main metabolic functions of adipose tissue are the accumulation of surplus energy through triacylglycerol (TAG) synthesis and deposition (lipogenesis), and lipid mobilization by releasing free fatty acids (FFAs) under conditions of negative energy balance (lipolysis). Adipose tissue is the main storage site for TAG. Dysregulation of adipocyte lipogenesis and lipolysis is part of the pathogenesis that is associated with obesity, as well as the development of insulin resistance and *type 2 diabetes* (Kahn and Flier, 2000). For example, excessive accumulation of fat in adipose tissue causes obesity, whereas a deficiency of adipose tissue is associated with a severe form of insulin resistance and development of a fatty liver (Kahn and Flier, 2000). Acute regulation of lipolysis in adipocytes is important in supplying energy to the peripheral tissues in response to fasting and exercise (Fig. 2). The lipolysis re-esterification process also participates in the 'futile cycle' that is believed to preserve fatty acids that are not used to supply energy (Hanson and Reshef, 2003). General processes of fat storage and mobilization are shown in Fig. 2.

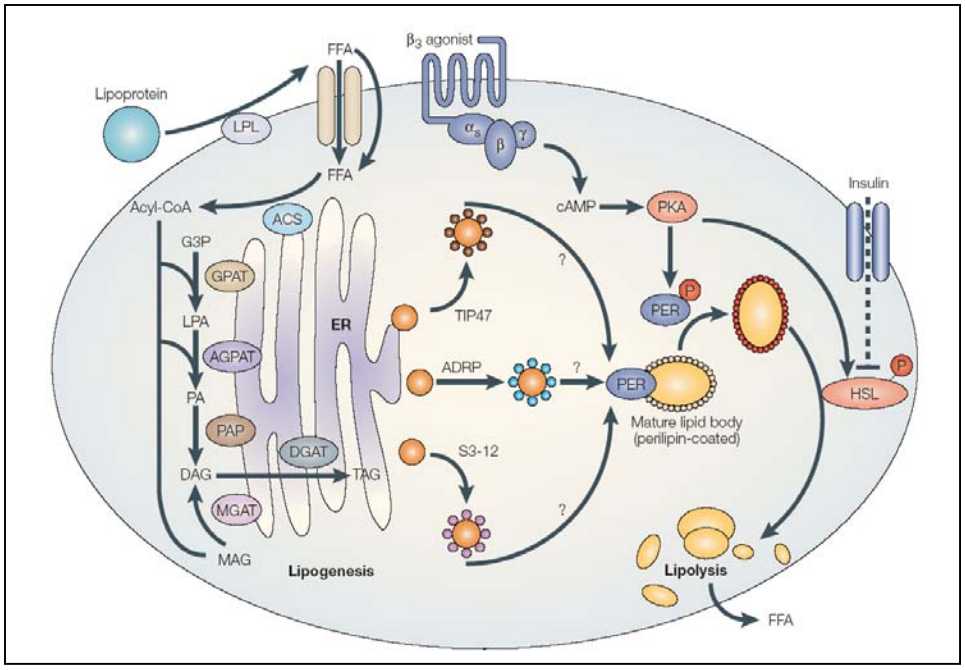

Adapted from (Shi and Burn, 2004)

Fig. 2. Lipid storage and mobilization in adipocytes.
FFAs that are released from lipoprotein — chylomicrons and very-low-density lipoprotein (VLDL) — catalysed by lipoprotein lipase (LPL) enters the adipocytes through both passive diffusion and active transport. Intracellular FFA is first converted to acyl-CoA by acyl-CoA synthase (ACS), and is then used as a substrate by two parallel TAG-synthetic pathways in the endoplasmic reticulum (ER). Glycerol-3-phosphate (G3P) that is generated by glucose metabolism is acylated sequentially by glycerol-3-phosphate acyltransferase (GPAT) and sn-1-acylglycerol-3-phosphate acyltransferase (AGPAT), and converted to diacylglycerol (DAG) by phosphatidic-acid phosphohydrolase (PAP); by contrast, the alternative pathway involves the acylation of monoacylglycerol (MAG) by MAG acyltransferase (MGAT). The two pathways merge with the acylation of DAG to TAG by diacylglycerol acyltransferase (DGAT). Nascent lipid droplets that are generated from the ER are coated by at least one of the PAT family proteins (which includes perilipin (PER), adipose differentiation-related protein (ADRP) and tail-interacting protein of 47 kDa (TIP47)) and S3-12, whereas mature lipid drops are mainly coated with perilipin. The relative rate of lipogenesis and lipolysis is determined by nutritional states and is regulated by endocrine factors, such as catecholamines and insulin, which impose their effect by the phosphorylation of perilipin and hormone-sensitive lipase (HSL). The phosphorylation of perilipin allows HSL to access lipid droplets, which results in the hydrolysis of TAG to FFAs that are then released from the adipocytes. PA, phosphatidic acid; PKA, protein kinase A; LPA, lysophosphatidic acid.

How is fat mobilized?

Adipocyte lipolysis is acutely regulated by hormones, neurotransmitters and other effector molecules, where hormone-sensitive lipase (HSL) is one of the major targets of this regulation. Catecholamines are important stimulators of lipolysis, whereas insulin is believed to be the most important anti-lipolytic hormone (Fig. 3). Binding of agonists to the β-adrenergic receptors, coupled to adenylate cyclase via the stimulatory G-protein, leads to an increased production of cAMP and activation of PKA (protein kinase A). The two main targets for PKA phosphorylation are HSL and the perilipins, which are proteins covering the lipid droplets of adipocytes (Londos et al., 1999). As a result, PKA phosphorylation of HSL and the perilipins causes a dramatic increase in lipolysis. The ability of insulin to antagonize hormone-induced lipolysis is accounted for by its ability to lower cAMP levels and therefore PKA activity. The decrease in cAMP is mainly the result of an insulin-mediated activation of phosphodiesterase 3B (Shakur et al., 2001). The mechanism of hormonal control of adipocyte lipolysis is shown in Fig. 3.

Mechanisms behind PKA-mediated activation of lipolysis

PKA phosphorylates HSL (Holm, 2003). *In vivo*, PKA phosphorylation is known to result in translocation of HSL from the cytosole to the lipid droplets (Londos et al., 1999). Similarly, The perilipin proteins are, besides HSL, major targets for PKA phosphorylation upon β-adrenergic stimulation of adipocytes. They are located on the surface of the lipid droplet, where they seem to serve a dual role as suppressor of basal lipolysis and as necessary components for full lipolytic stimulation to occur (Londos et al., 1999). It has been shown that ERK (extracellular-signal-regulated kinase) 1/2, MAP (mitogen-activated protein) kinases are activated through β3-adrenergic receptor coupling to Gi, raising the possibility that dual Gs/Gi-protein coupling to this receptor allows PKA and ERK1/2 to work in concert to stimulate lipolysis (Soeder et al., 1999).

Transgenic expression of human HSL in mice leads to an increase in hydrolytic activities against TAG, a reduction in fat mass and a decrease in body weight on calorie restriction (Lucas et al., 2003). By contrast, mice that are deficient in HSL manifest adipocyte hypertrophy, reduced fatty-acid release, and decreased hepatic TAG storage (Osuga et al., 2000).

Ectopic overexpression of perilipin A, but not phosphorylation-defective mutants, results in the inhibition of TAG hydrolysis and enhanced lipolytic responses to protein kinase A (PKA) activation (Tansey et al., 2003). Ablation of perilipin leads to animals that are lean, hypermetabolic and resistant to diet-induced obesity. Perilipin-knockout mice show elevated basal lipolysis and resistance to stimulation by β-adrenoceptor agonists (Martinez-Botas et al., 2000). The regulatory mechanism of fat mobilization, lipolysis is shown in Fig. 3.

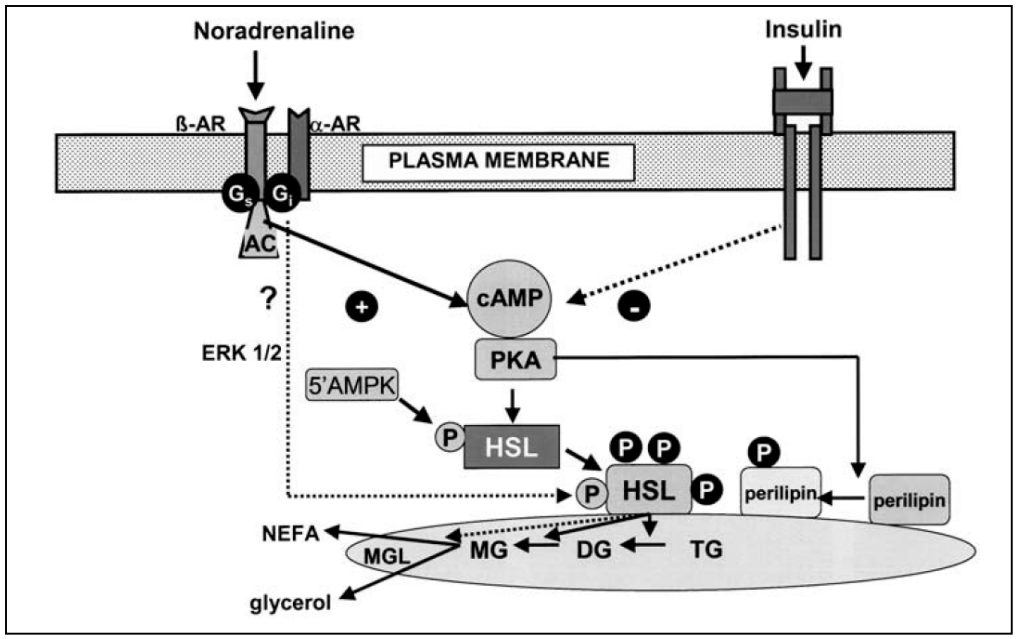

Adapted from (Holm, 2003)

Fig. 3. Hormonal control of adipocyte lipolysis

Binding of agonists to β-adrenergic receptors (β-AR), coupled to the adenylate cyclase (AC) via the stimulatory G-protein (Gs), increases the levels of cAMP. This in turn leads to activation of PKA, which phosphorylates HSL at three serine residues and also perilipin A on multiple sites. PKA phosphorylation of HSL causes translocation from the cytosol to lipid droplets, whereas phosphorylation of perilipin by PKA alleviates the barrier function of this protein and prompts its active participation in the lipolytic process. β3-Adrenergic agonists have been suggested to stimulate lipolysis via a concerted activation of PKA and ERK1/2 MAP kinase, accomplished

through dual coupling of the β3-adrenergic receptor to Gs and Gi. In hormonally quiescent adipocytes, HSL appears to be phosphorylated at a fourth serine residue, presumably by the 5´-AMP-activated protein kinase (5´AMPK). The anti-lipolytic action of insulin can to a large extent be accounted for by its ability to lower cAMP levels. This in turn is mainly the result of an insulin-mediated activation of phosphodiesterase 3B. TG, triglycerides; DG, diglycerides; MG, monoglycerides; MGL, monoglyceride lipase.

1.4. How is fat synthesized and oxidized?

The synthesis and metabolism of fatty acids and TAG is a coordinated process, which is mediated by metabolic enzymes that are regulated by nutritional and hormonal stimuli in response to starvation, exercise and surplus energy (Fig. 4). For example, fasting reduces fat synthesis by decreasing mRNA levels of both fatty-acid synthase (FAS) and glycerol-3-phosphate acyltransferase (GPAT) (Sul and Wang, 1998). In the fed state, the body aims to convert the amino acids, hexoses and triglycerides produced by the digestive tract into forms which can be stored. In the fasted state, the body aims to mobilize stored reserves to provide the necessary metabolic fuels.

Fatty-acid synthase (FAS) mediates synthesis of saturated fatty acids.

Mammalian FAS catalyses the de novo synthesis of saturated fatty acids, such as myristate, palmitate and stearate, using acetyl- and malonyl-CoA. It functions as a homodimer of a multifunctional protein that contains seven catalytic domains and a site for the prosthetic group 4'-phosphopantetheine (Smith et al., 2003). FAS is believed to be important in addition to carnitine palmitoyl transferase (CPT) and acetyl-CoA carboxylase (ACC) in maintaining energy homeostasis by converting excess food intake into lipids for storage and providing energy by upregulating the rate of β-oxidation. In addition to a role for FAS in fat metabolism, the enzyme also has a pivotal role in embryonic development. Targeted deletion of the Fas gene results in mice that die in utero (Chirala et al., 2003), while 50% of heterozygous Fas-knockout mice also fail to survive embryonic development (Chirala et al., 2003). The development of mice with a targeted deletion or inducible knockout of the Fas gene in liver and

adipose tissues will provide a better tool to examine the role of the FAS enzyme in fat synthesis and obesity.

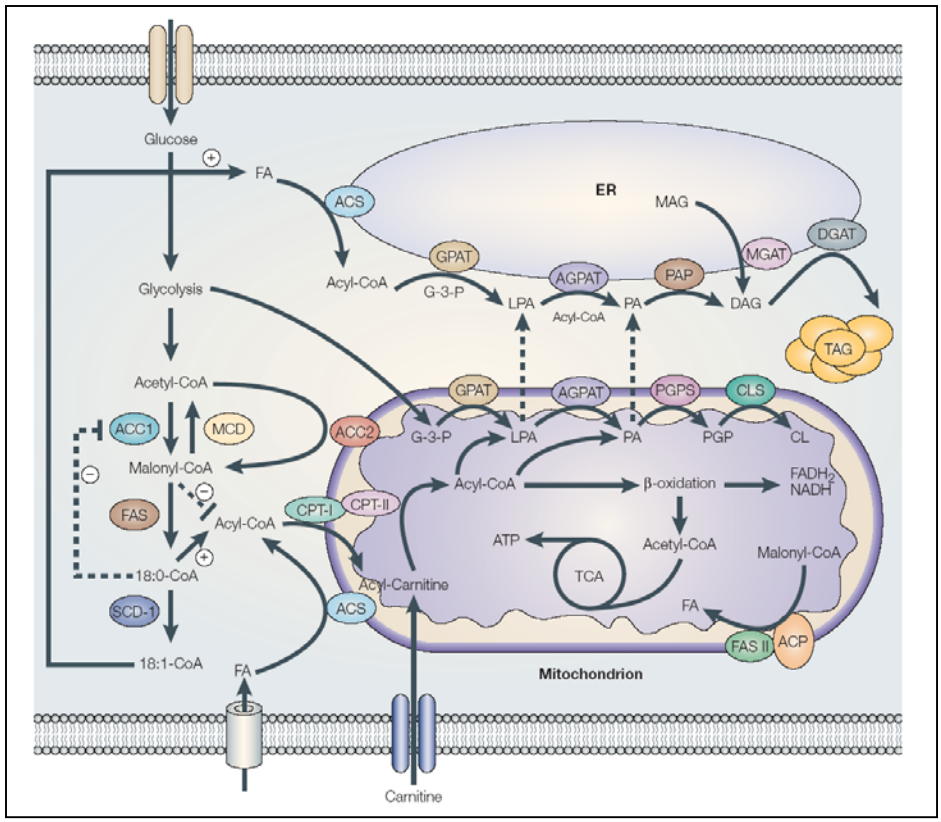

Adapted from (Shi and Burn, 2004)

Fig. 4. | Interconnection of metabolic pathways involved in lipid synthesis in the endoplasmic reticulum and lipid oxidation in mitochondria of liver and skeletal muscle. Among the lipid metabolic enzymes, acetyl-CoA carboxylase (ACC), fatty-acid synthase (FAS) and carnitine palmitoyl transferase (CPT) are the three main enzymes that regulate the synthesis of malonyl-CoA, which is the principal inhibitor of fatty-acid entry into mitochondria for β-oxidation. Stearoyl-CoA desaturase-1 (SCD1) regulates lipid oxidation by converting stearic acid (18:0) to oleic acid (18:1). The saturated fatty acyl-CoAs are known to allosterically inhibit ACC1, whereas monounsaturated fatty acyl-CoAs are the preferred substrates for the lipid synthesis of triacylglycerol (TAG) in the endoplasmic reticulum (ER). Malonyl-CoA and stearic acid reciprocally regulate the entry of acyl-CoA into mitochondria by modulating the activity of CPTA. Lysophosphatidic acid (LPA) and phosphatidic acid (PA) are synthesized in the ER; they are also produced in mitochondria and transported to the ER where the terminal enzymes for TAG synthesis are located. Mitochondrial FAS (FAS II) and acyl-carrier protein (ACP) are involved in fatty-acid synthesis. ACS, acyl-CoA synthase; AGPAT, acylglycerol-3-phosphate acyltransferase; CLS, cardiolipin (CL) synthase; DGAT, diacylglycerol (DAG) acyltransferase; GPAT, glycerol-3-phosphate (G-3-P) acyltransferase; MCD, malonyl-CoA decarboxylase; MGAT, monoacylglycerol (MAG) acyltransferase; PAP, phosphatidic-acid phosphohydrolase; PGPS, phosphatidylglycerophosphate (PGP) synthase; TAG, triacylglycerol; TCA, tricarboxylic-acid cycle.

Carnitine palmitoyl transferase (CPT) mediates fat oxidation.

CPT catalyses the conversion of palmitoyl-CoA to palmitoylcarnitine, which is a rate-limiting step in the transfer of long-chain fatty acyl-CoAs from the cytosol to the mitochondria for β-oxidation. Its activity is inhibited by malonyl-CoA, which acts as an allosteric inhibitor (Fig. 4). In mammals, three CPT enzymes have been identified so far: liver CPT1, muscle CPT1 and CPT2. These enzymes are encoded by three different genes (van der Leij et al., 2000). Muscle CPT1 has a crucial role in controlling the rate of β-oxidation in heart and skeletal muscle; it also has a much higher Michaelis–Menten constant (Km) for carnitine than the liver isoform and is more sensitive to malonyl-CoA inhibition (van der Leij et al., 2000). Several investigations have provided evidence that the malonyl-CoA/CPT1 axis is crucial in controlling the influx of fatty acids into mitochondria for β-oxidation in the heart and skeletal muscle. In addition, abnormal CPT1 activity might also contribute to the cause of obesity in human and rodent models. For example, impairment in CPT1-mediated lipid oxidation in skeletal muscle is observed in obese patients (Kim et al., 2000). Recent studies show that CPT1 inhibition causes insulin resistance, whereas activation of CPT1 through the inhibition of ACC improves insulin sensitivity and lowers blood glucose levels (Abu-Elheiga et al., 2001).

Acetyl-CoA carboxylases (ACC1 and ACC2) regulate fat synthesis and lipid oxidation.

ACC enzymes catalyse the carboxylation of acetyl-CoA to malonyl-CoA, which is a crucial regulator of mitochondrial fatty-acid β-oxidation through its inhibition of CPT1 (Fig. 4). In mammals, ACC exists in two isoforms, ACC1 and ACC2, which are encoded by two different genes. ACC1 is the principal isoform in lipogenic tissues, whereas ACC2 is predominantly expressed in oxidative tissues, such as the heart and skeletal muscle. Both isoforms are expressed in the liver, where fatty-acid synthesis and oxidation coexist (Abu-Elheiga et al., 1997). ACC1 is a cytosolic enzyme, whereas ACC2 is associated with the mitochondrial membrane through its extended amino terminus (Abu-Elheiga et al.,

2000). This difference in compartmentalization might contribute to the diverse roles of the two isoforms in fat metabolism; ACC1 is believed to regulate fat synthesis in lipogenic tissues, whereas ACC2 controls the rate of lipid oxidation (Abu-Elheiga et al., 2000) in oxidative tissues.

ACC activity is mainly regulated by citrate and AMP kinase (AMPK) (Hardie and Pan, 2002). Citrate is believed to be an allosteric activator of ACC, as suggested by a strong positive correlation between levels of malonyl-CoA and citrate concentrations. Phosphorylation of ACC by AMPK inhibits its activity, which is accompanied by a reduction in malonyl-CoA levels. This is seen in skeletal muscle following treadmill exercise (Winder and Hardie, 1996), The incubation of isolated rat soleus muscles with the AMPK activator AICAR decreases ACC2 activity and simultaneously increases the rate of fatty-acid oxidation (Kaushik et al., 2001). Acc2-null mice are hyperphagic and show an elevated rate of fatty-acid oxidation concomitant with decreased malonyl-CoA levels in the skeletal muscle and heart. These knockout mice are resistant to diet-induced obesity and related diabetes, with improved insulin sensitivity and decreased fatty-acid levels (Abu-Elheiga et al., 2003). The mRNA levels of uncoupling proteins (UCPs) are markedly higher in the adipose, heart (UCP2) and muscle (UCP3) tissues of mutant mice, which together with increased β-oxidation might account for an upregulation of energy expenditure (Abu-Elheiga et al., 2003).

What controls energy expenditure?

Most energy is used for the basic maintenance of cells but smaller, variable amounts are expended in physical activity or adaptive thermogenesis (the process of heat production in response to diet or environmental temperature). Adaptive thermogenesis may be an important defense system against obesity. Energy excess or exposure to cold temperatures activates the sympathetic nervous system to enhance energy dissipation. Mice lacking all three isoforms of the β-adrenergic receptor have impaired thermoregulation and increased susceptibility to diet-induced obesity, demonstrating the importance of a central control to adaptive thermogenesis (Bachman et al., 2002).

In brown fat and skeletal muscle, adrenergic signals stimulate the formation of mitochondria and the uncoupling of ATP synthesis from oxidative metabolism. A key effector in this process is the ***PPAR-γ coactivator-1 (PGC-1)*****,** which is induced by adrenergic signals and enhances the transcription of genes involved in mitochondrial biogenesis and uncoupling (Wu et al., 1999a). In skeletal muscle, PGC-1 is preferentially expressed in mitochondria-rich, oxidative type 1 (slow twitch) muscle fibers, and transgenic expression of PGC-1 in muscle induces the conversion of type 2 fibers to type 1 (Lin et al., 2002). Effect of PGC1 expression on thermogenesis is shown in Fig. 5.

Uncoupling protein-1 (UCP-1) is also upregulated by β-adrenergic signals and, in some tissues, by PGC-1 (Lowell and Spiegelman, 2000). As their names imply, UCPs promote leakage of protons and exhaust the electrochemical gradient across the inner mitochondrial membrane. Consistent with this, UCP-1-null mice have impaired cold-induced thermogenesis (Enerback et al., 1997). Overexpression of UCPs induces energy expenditure in mice (Clapham et al., 2000) (Li et al., 2000), while mice deficient in UCP-1 are not susceptible to obesity, suggesting that alternative or additional factors may be important in diet-induced energy dissipation (Enerback et al., 1997).

PPAR-δ as an important mediator of fat burning

Genetic studies and recently developed synthetic PPAR-δ agonists have helped uncover the role of PPAR-δ as a powerful regulator of fatty acid catabolism and energy homeostasis (Dressel et al., 2003; Tanaka et al., 2003). The PPAR- agonist GW501516 was shown to lower plasma triglyceride levels in obese monkeys while raising high-density lipoprotein levels, prompting the initiation of clinical trials to assess its efficacy in hyper-lipidemic patients (Oliver et al., 2001).

Studies in adipose tissue and muscle have begun to uncover the metabolic functions of PPAR-δ. Transgenic expression of an activated form of PPAR-δ in adipose tissue produces lean mice that are resistant to obesity, hyperlipidemia and tissue steatosis induced genetically or by a high-fat diet (Wang et al., 2003). The reason for this is that the activated receptor induces genes required for fatty acid catabolism and adaptive thermogenesis. Taken together, these data identify PPAR-δ as a key regulator of fat-burning. The thermogenic function of PPAR-δ is markedly similar to that of the nuclear cofactor PGC-1(Wu et al., 1999a), Indeed, PPAR-δ strongly associates with PGC-1 both in cultured cells and in tissues (Wang et al., 2003), so it is possible that many metabolic effects of PGC-1 may be mediated through PPAR-δ. Treatment with GW501516 ligand significantly retards weight gain, but does not affect food consumption in animals fed a high-fat diet. Treatment with a PPAR-δ agonist also improves insulin resistance induced by a high-fat diet, probably as a consequence of increased fat-burning by muscle and overall improvement in systemic lipid metabolism (Dressel et al., 2003; Tanaka et al., 2003) (Fig. 6).

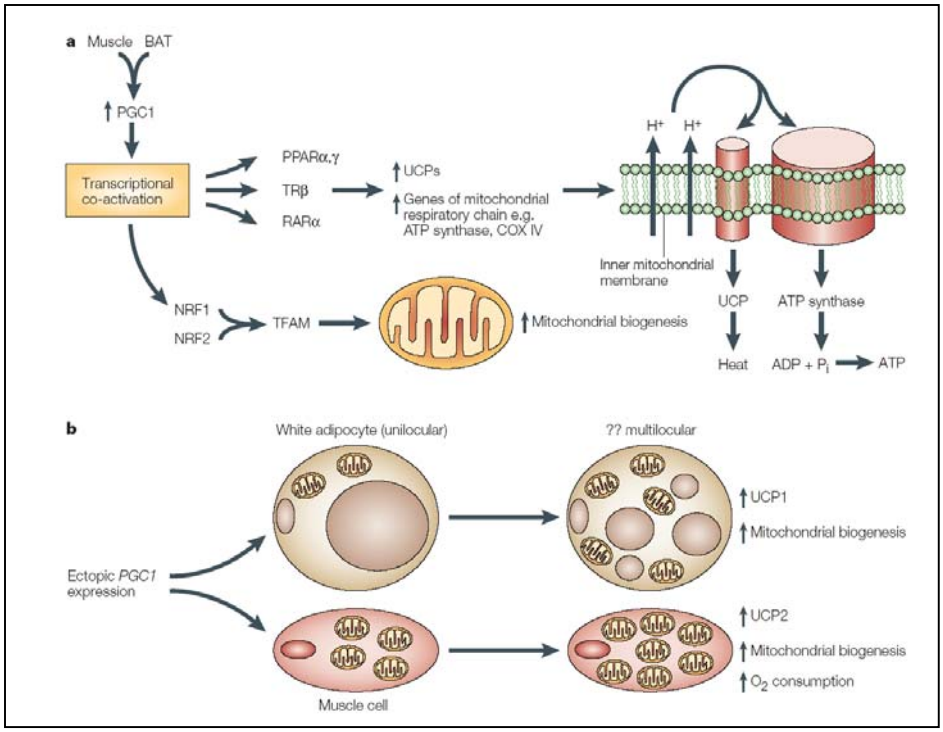

Adapted from (Crowley et al., 2002)

Fig. 5. Effects of PGC1 expression on thermogenesis.

High levels of PGC1 messenger RNA expression occur in brown adipose tissue (BAT), heart, brain and kidney. Cold exposure results in a marked induction of PGC1 expression in BAT and skeletal muscle. PGC1 is a powerful transcriptional co-activator of nuclear hormone receptors, including PPARα and PPARγ, TRβ, RARα and ERα. PGC1 coordinates the transcription of genes that are involved in thermogenesis with the induction of UCPs, genes of the mitichondrial respiratory chain such as ATP synthase and the cytochrome c oxidase subunits (COX) II and IV, and mitochondrial biogenesis. The capacity of PGC1 to promote mitochondrial biogenesis is related to its actions on the transcription of NRF1 and NRF2, both of which are upregulated. PGC1 co-activate directly the transcriptional capacity of NRF1. NRF1 and NRF2 are key trans-acting elements in mitochondrial biogenesis that regulate the transcription of several nuclear-encoded genes, including mitochondrial transcription factor A (TFAM), which is itself a vital coordinator of the transcription and replication of the mitochondrial genome. b | Ectopic PGC1 expression modifies the expression of UCPs, with UCP1 mRNA expression increasing in adipocytes, whereas, UCP2 is upregulated in skeletal muscle cells. There is also a marked induction of the genes that encode proteins of the mitochondrial respiratory chain, and total mitochondrial content is increased in these cells. In muscle cells, basal oxygen consumption is also notably increased. ERα, oestrogen receptor-α; NRF1, nuclear respiratory factor 1; PGC1, peroxisome proliferator-activated receptor-γ co-activator 1; PPAR, peroxisome proliferator-activated receptor; RARα, retinoic-acid receptor-α; TR, thyroid-hormone receptor; UCP, uncoupling protein.

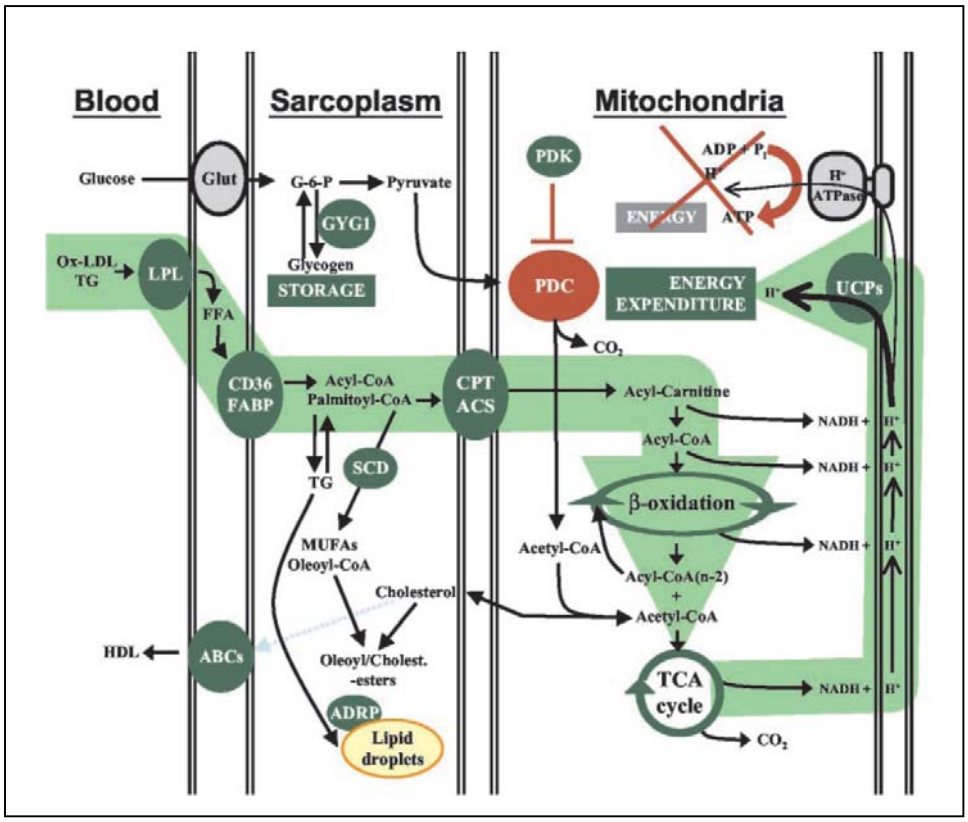

Adapted from ((Dressel et al., 2003)

Fig. 6. Schematic Overview of Metabolic PPARß/δ Action

Enzymes and functions found to be activated by PPARß/δ agonist are marked in green. Red indicates inhibition of pathways. The green arrows underline FA uptake and oxidation, followed by uncoupling oxidation from ATP synthesis.

1.5. Adipose tissue

In humans, the fat-depot consist of white adipose tissue which, at a cellular level, is composed of the lipid-filled adipocytes surrounded by a matrix of collagen fibers, blood vessels, fibroblasts and immune cells (Cinti, 2000; Hirsch et al., 1989; Tiraby and Langin, 2003). The adipocyte is a specialized cell, whose primary function is to store energy in the form of triglycerides when an excess of nutrients are available and, when nutrients are being scarce or absent, release energy again in form of free fatty acids (FFA). The size of the adipose tissue depots are mainly determined by the balance between energy intake and energy expenditure (Hirsch et al., 1989), where the adipose tissue seems to provide a virtually limitless storage site for triglycerides based on its life-long ability to increase fat cell size (hypertrophy) as well as to increase the number of fat cells (hyperplasia)(Couillard et al., 2000; Hirsch and Batchelor, 1976; Hirsch et al., 1989) Obese people tend to have larger adipocytes and more of them than normal weight subjects (Couillard et al., 2000).

1.6. What are the characteristics of white adipose tissue and brown adipose tissue?

The mammalian adipose organ is composed of subcutaneous and visceral fat depots, themselves composed of two tissue types that have critical and interrelated roles in energy balance (Cinti, 2000; Tiraby and Langin, 2003). The main characteristics of these adipose tissue types are briefly listed in Table. 1. White adipose tissue (WAT) is populated mainly by white adipocytes and yet can contain a variable amount of brown adipocytes (Guerra et al., 1998). Conversely, brown adipose tissue (BAT) is composed almost exclusively of brown adipocytes. Cells in certain fat depots appear to be able to "change" between the white and brown adipocyte phenotype in an age- or environment-dependent manner (Cinti, 2000; Tiraby and Langin, 2003). Now under debate in the field is the possibility of

transdifferentiation between WAT and BAT states. Both adipose tissue types are able to store NEFAs as triacylglycerol (TG), but whereas WAT TG hydrolysis satisfies the energy needs of the whole organism, fatty acids released from BAT are used within the tissue to promote non-shivering thermogenesis (Foster and Frydman, 1979; Tiraby and Langin, 2003).

Table 1. Some basic characteristics of WAT and BAT

Characteristics	White fat cell	Brown fat cell
Morphology	Unilocular appearance	Multilocular appearance (numerous small lipid droplets)
	(Single large lipid droplet)	Numerous mitochondria with many cristae
	Large cells (up to 200μm)	
Function	Storage of energy as triglycerides and mobilization as fatty acids	Fat oxidation and thermogenesis
	Secretion of adipocytokines (+++)[a]	Secretion of adipocytokines (+)
Expression of genes involved in metabolism	Uncoupling protein 1 (0)	Uncoupling protein 1 (+++)
	Uncoupling protein 2 (++)	Uncoupling protein 2 (+)
	Uncoupling protein 3 (+/-)	Uncoupling protein 3(+)
	Subunit c of F0-ATPase (+)	Subunit c of F0-ATPase (+/-)
	Respiratory chain genes (+)	Respiratory chain genes (+++)
	Fatty acid oxidation enzymes (+)	Fatty acid oxidation enzymes (+++)
	Glycerol kinase (+/-)	Glycerol kinase (+++)

[a]no (0), very low or uncertain (+/-), moderate (++) and high (+++) expression.

WAT is the predominant type of adipose tissue in adult mammals; its amount usually increases with age, and in obese individuals it can account for more than half of total body weight. In healthy adult humans, it accounts for 15%-20% of body weight in men and 20%-25% in women. The principal cell type of WAT contains a single (unilocular) and large (20-200 μm) lipid droplet, resulting in the near disappearance of the cytoplasm and compression of the nucleus underneath the plasma membrane (Cushman, 1970). These cells are grouped into small lobules surrounded by connective tissue. WAT is considered to be less well vascularized than BAT (Cushman, 1970).

1.7. How are adipocytes differentiated?

At the cellular level, a positive energy balance induces changes in the microenvironment, which stimulate mature adipocytes to accommodate excess energy through enhanced triacylglycerol storage. When adipocytes reach a critical size threshold, it is postulated that signals are transmitted from adipocytes to preadipocytes to stimulate the formation of new adipocytes to store the excess energy (Fruhbeck et al., 2001). Early in life, adipose tissue expansion occurs primarily through new fat cell formation or hyperplasia (Lemonnier, 1972). However, humans and rodents have the capacity to form new fat cells from preadipocytes throughout life (Lemonnier, 1972). Compared with lean animals, obese animals have a greater number of, and larger, adipocytes (Hirsch and Batchelor, 1976). Some studies have suggested that preadipocytes from severely obese individuals display inherent proliferation defects that lead to an excessive number of adipocytes (Ravussin and Smith, 2002).

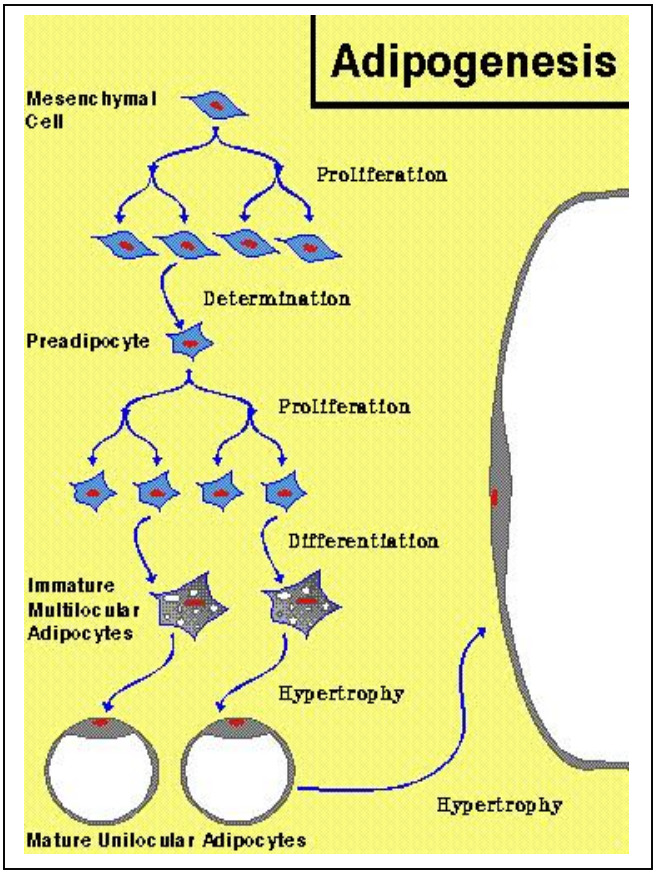

Fig. 7. Adipogenesis is a multistep process.
Mesenchymal cells proliferate (clonal expansion). At some point, some of these cells differentiate into preadipocytes. Preadipocytes proliferate at the site of adipogenesis (clonal expansion). Preadipocytes undergo a second differentiation step and begin to fill with lipids. At first, lipids accumulate within the cell in small droplets (multilocular cells) and eventually the droplets fuse into one large droplet (unilocular cells). The adipocyte can continue to enlarge by accumulating additional lipids. The average mesenchymal cells is 10-20µm in diameter, whereas adipocytes easily reach 100µm (and in some cases 200µm) in diameter. Thus volume of the cell increases as much as a thousand fold largely because of lipid accumulation.

The signal for differentiation of new adipocytes is related to nutritional state. Important stimuli for differentiation include insulin and fatty acids. Fatty acids act through members of the peroxisome proliferator-activated receptor (PPAR) family, PPAR (also known as fatty acid-activated receptor, FAAR (Amri et al., 1995). The natural ligand for PPAR is probably a fatty acid derivative (Forman et al., 1995). In addition, differentiation is regulated by a pathway involving the sterol

regulatory element binding protein-1c (SREBP-1c, also known as adipocyte determination and differentiation factor-1, ADD-1), a pathway that in adipocytes is regulated by insulin (Kim et al., 1998). Given that individual adipocytes can also expand over a very large range as they store more TG, the net effect is that the capacity to store fat can increase seemingly without limit.

Expansion of fat stores, especially if differentiation of new adipocytes is involved, requires new blood vessels. Angiogenesis in adipose tissue appears also to be regulated in part by factors produced within the tissue. Leptin produced by adipocytes has angiogenic properties (Sierra-Honigmann et al., 1998). In addition, expression of genes involved in angiogenesis is upregulated during weight gain in animals (Morimura et al., 2001) and inhibition of angiogenesis reduces fat deposition in various obesity models in mice (Rupnick et al., 2002).

The number of adipocytes present in an organism is determined to a large degree by the adipocyte differentiation process, which generates mature adipocytes from fibroblast-like preadipocytes. One of the first steps in the process of adipogenesis is the re-entry of growth-arrested preadipocytes into the cell cycle and the completion of several rounds of clonal expansion. Hansen et al. demonstrated that mouse lung embryonic fibroblasts (MEFs) with targeted disruption of the gene encoding Rb completely failed to undergo adipocyte differentiation (Hansen et al., 1999). Generally, Rb phosphorylation status correlates well with cell-cycle progression: hypophosphorylated Rb in growth-arrested preadipocytes and hyperphosphorylated Rb in proliferating cells. Hypophosphorylated Rb is complexed with transcription factor E2F, and upon addition of adipogenic hormones, Rb rapidly undergoes hyperphosphorylation by cyclin-dependent kinases (CDKs). This results in the dissociation of Rb and E2F, allowing E2F to promote cell-cycle progression into S phase (Fig. 8). Just before entering the terminal differentiation state, Rb returns to a hypophosphorylated state, sequestering E2F and causing cells to permanently exit from the cell cycle (Hiebert et al., 1992). Many cell-cycle-associated proteins (CDKs and their inhibitors, p18, p21 and p27) play crucial roles during cell-cycle progression that

precedes entry into the terminally differentiated state (Morrison and Farmer, 1999).

Two transcription factor families have emerged as the key determinants of terminal adipocyte differentiation: the CCAAT/enhancer-binding proteins C/EBPα, -β, -δ, and peroxisome proliferator-activated receptor γ (PPARγ , encoded by PPARG) (Yeh et al., 1995b). As cells undergo the differentiation process in response to adipogenic signals, the initial event is the rapid induction of C/EBP-β and -δ expression (Yeh et al., 1995b). A potential role for C/EBP-β and -δ is to increase p21 levels, leading to an inhibition of CDK-mediated Rb phosphorylation. A role for C/EBP -β and -δ and PPARγ2, a key regulator of adipogenesis, has also been reported (Elberg et al., 2000). Overexpression of C/EBP -β and -δ in preadipocytes enhanced adipogenesis (Yeh et al., 1995b), whereas embryonic fibroblast cells (MEFs) derived from mice lacking either C/EBP -β or -δ had reduced levels of adipogenesis compared with the wild type (Tanaka et al., 1997). The induction of C/EBP-β and -δ is immediately followed by an increase in PPARγ and C/EBPα expression. PPARγ is itself a ligand-dependent nuclear receptor transcription factor. In mice there are two isoforms, PPARγ1 and PPARγ2. Interestingly, levels of PPARγ2 expression, but not PPAR1, correlate with the degree of lipid accumulation. Cells with a 95% reduction in PPARγ2 expression completely failed to undergo adipogenesis, whereas cells with a 50% reduction in PPARγ2 expression produced a corresponding 50% loss in adipogenic capacity. These results strongly suggest that PPARγ2, but not PPARγ1, plays a key role in adipogenesis (Ren et al., 2002). During the later stage of differentiation, C/EBPα expression rises immediately after PPARγ2 expression. In summary, PPARγ and C/EBPα are key transcription factors in adipogenesis, acting synergistically to generate fully differentiated, insulin-responsive adipocytes (Rosen et al., 2002)(Fig. 8).

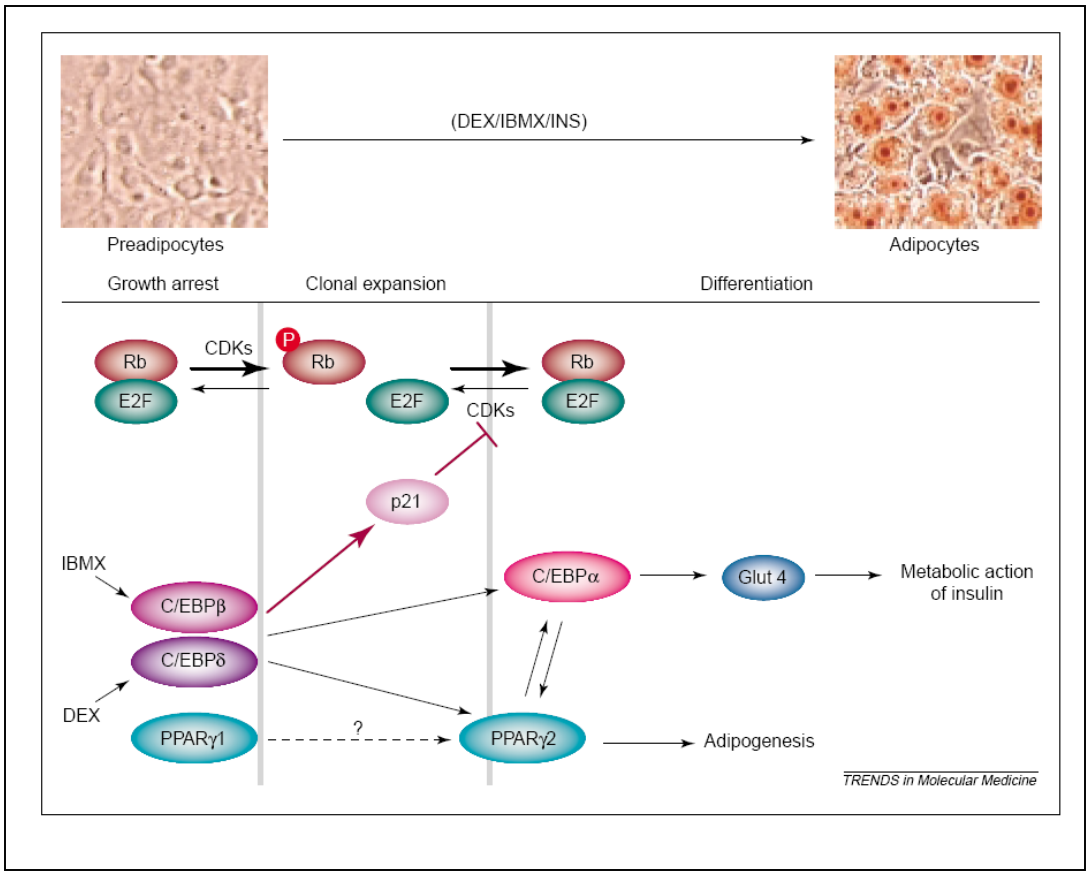

Adapted from (Camp et al., 2002)

Fig. 8. In vitro model of adipogenesis.
Conversion of preadipocytes into lipid-containing adipocytes can be achieved by adding appropriate adipogenic hormones, such as dexamethasone (DEX), isobutylmethylxanthine (IBMX) and insulin (INS). Lipid accumulation is visualized by staining adipocytes with Oil-Red-O stain. The adipogenic process is divided into three distinct stages: growth arrest, clonal expansion and differentiation. A set of distinct genes are induced and activated in each stage during the adipogenic process. Solid arrows represent direct modulation, whereas the dotted arrow represents potential modulatory activity. The bar represents inhibitory action. Abbreviations: CDK, cyclin-dependent kinase; C/EBP, CCAAT/enhancer-binding protein; Glut4, glucose transporter 4; pRb, phosphorylated retinoblastoma protein; Rb, retinoblastoma protein.

2. When nutrient homeostasis is out of order

2.1. Obesity

Obesity can be defined as a condition of abnormal or excessive body fat accumulation, to the extent that health may be impaired (Vega, 2004). A useful (and inexpensive) way of classifying or estimating the prevalence of obesity in a population is done by calculating the Body Mass Index (BMI = the weight in kilograms divided by the square of the height in metres (kg/m^2). However, BMI is a crude estimate of individual adiposity since it does not account for the differences in the amount of body-fat and muscle tissue (Segal et al., 1987) Furthermore, it is well-known that abdominal fat accumulation is an even greater risk factor for disease as is excess body-fat per se (Despres et al., 2001).

Table. 2.: Classification of body weight in adults according to BMI (Frankenfield et al., 2001)

Classification BMI (kg/m^2)	Risk of co-morbidities
Underweight < 18.5	Low
Normal weight 18.5 - 24.9	Average
Overweight	
Pre-obese 25 - 29.9	Increased
Obese class I 30 - 34.9	Moderate
Obese class II 35 - 39.9	Severe
Obese class III 40	Very severe

To obtain more precise and detailed data on the obese phenotype, body composition can be estimated using dual-energy X-ray absorptiometri (DEXA) scans or bioelectrical impedance.

Epidemiology of obesity

During the last twenty years the prevalence of obesity has increased by 50 - 100 %, making it the most common metabolic disorder in the developed parts of the world (Must et al., 1999) . A similar increase in the prevalence of obesity has been observed in United States where 60% of the adult population are considered to be overweight or obese (Must et al., 1999). Obesity is known to be associated with numerous diseases, and consequently with increased morbidity and mortality. Of special interest are the disease states such as insulin resistance, type 2 diabetes, hypertension and cardiovascular disease, which are associated with obesity and often referred to as metabolic syndromes (Despres et al., 2001; Vega, 2004)

Obesity related diseases are
(Must et al., 1999; Vega, 2004)

Certain cancer types (breast, Coronary heart disease Non-insulin dependent
colon and endometrial cancer) Hypertension, *diabetes mellitus*
Polycystic ovary syndrome, Osteoarthritis, Dyslipidaemia
Impaired fertility, Hyperuricaemia, Insulin resistance
Lower back pain, Gout, Sleep apnoea
Increased anaesthetic risk, Gallbladder disease

2.2. Insulin resistance

The term ‘insulin resistance of obesity’, as used currently, refers mainly to resistance to insulin-stimulated glucose disposal (Kahn and Flier, 2000). Under normal homeostasis, binding of insulin to its receptors in skeletal muscle and adipose cells initiates a phosphorylation cascade culminating with the translocation of the glucose transporter, GLUT-4, from intracytoplasmic vesicles to the plasma membrane, thereby facilitating glucose entry into the cell (Wang et al., 1999) (Fig. 9). After phosphorylation to form glucose-6-phosphate, glucose is either stored as glycogen or enters the glycolytic pathway to form pyruvate. Pyruvate is irreversibly decarboxylated to acetyl Co A and enters the mitochondria for oxidation in the citric acid cycle forming CO_2 and H_2O. Any unoxidized surplus is returned to the cytosol via the acetyl-group shuttle and carboxylated to malonyl CoA, the first intermediate in the pathway of fatty acid (FA) synthesis. In addition to being a lipogenic substrate, malonyl CoA inhibits the mitochondrial enzyme, CPT1. This reduction of FA oxidation by malonyl CoA is referred to as the McGarry effect.

In addition to stimulating the uptake of glucose, insulin induces expression of the enzymes of lipogenesis through upregulation of the lipogenic transcription factor, SREBP-1c (Fig. 10)(Shimomura et al., 1999), thereby providing the enzymatic machinery for de novo synthesis of fat. Ironically, insulin-responsive SREBP-1c and its lipogenic target enzymes are expressed at higher levels in tissues of so-called ‘insulin-resistant’ obese rats with defective leptin receptors than in tissues of the ‘insulin-sensitive’ control animals(Kakuma et al., 2000). This implies that the tissues of insulin-resistant animals are not resistant to insulin-stimulated lipogenesis and fits with the idea that glucometabolic insulin resistance is secondary to the overaccumulation of lipids (Boden and Shulman, 2002).

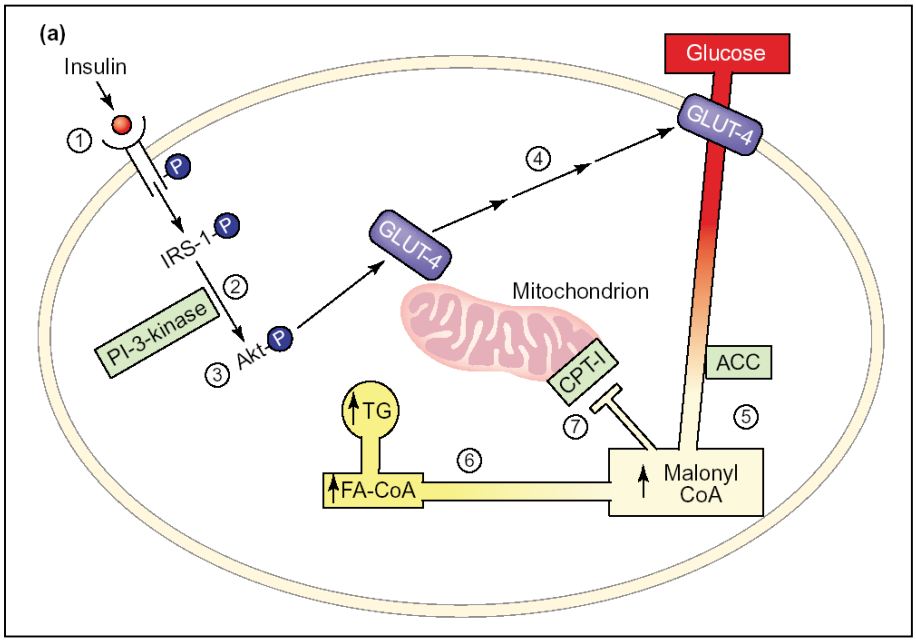

Adapted from (Unger, 2003)

Fig. 9. Glucometabolic insulin resistance development through increased insulin-stimulated lipogenesis.
Insulin action begins when it binds to its receptor (1). This initiates a tyrosine phosphorylation cascade in which insulin receptor substrate-1 (associated with phosphoinositide 3-kinase (PI-3-kinase)) activity (2) and phosphorylation of Akt1 (3) are crucial for the translocation of the glucose transporter, GLUT-4, to the plasma membrane (4), which allows glucose to enter the cell. Surplus glucose not consumed in oxidative metabolism or stored as glycogen enters the lipogenic pathway (5) as acetyl CoA. Acetyl CoA carboxylase (ACC) catalyzes formation of malonyl CoA, the first step in the synthetic pathway of long-chain FAs (FA-CoA) (6) triacylglycerols (TGs) and their lipotoxic derivatives, such as ceramide (not shown). The increase in malonyl CoA inhibits the mitochondrial enzyme carnitine palmitoyl transferase 1 (CPT-1) (7) (McGarry effect), blocking oxidation of long-chain fatty acids (FAs). The resulting increase in intracellular FA-CoA and/or its derivatives, TG and/or ceramide, interferes with the phosphorylation of Akt (3).

The sequence of events postulated to occur during the development of diet-induced obesity and metabolic syndrome

(1)Hyperinsulinemia, stimulated by overnutrition,

(2) upregulates SREBP-1c, the lipogenic transcription factor.

(3)De novo lipogenesis increases.

(4)Newly synthesized fatty acids (FA) and FA from dietary fat are transported as very low-density lipoproteins and stored as triacylglycerol (TG) in adipocytes, resulting in obesity.

(5)Leptin secretion by adipocytes increases in proportion to the increase in fat accumulation.

(6)The hyperleptinemia downregulates SREBP-1c in liver and activates AMP-kinase. This increases FA oxidation in peripheral tissues, thus limiting ectopic deposition of fat.

(7)Despite this, insulin resistance and glucose intolerance result from the small increase in unoxidized FA accumulating in skeletal muscle, although serious lipotoxicity is prevented.

(8)Later in the course of the disorder, leptin-mediated protection against the lipotoxic metabolic syndrome diminishes, in part because of leptin resistance factors that prevent leptin inhibition of SREBP-1c expression and block the compensatory increase in FA oxidation induced by hyperleptinemia. Unoxidized FA increases and lipid derivatives such as TG and ceramide accumulate in nonadipose tissues, compromising their functions and promoting apoptosis (Fig. 10).

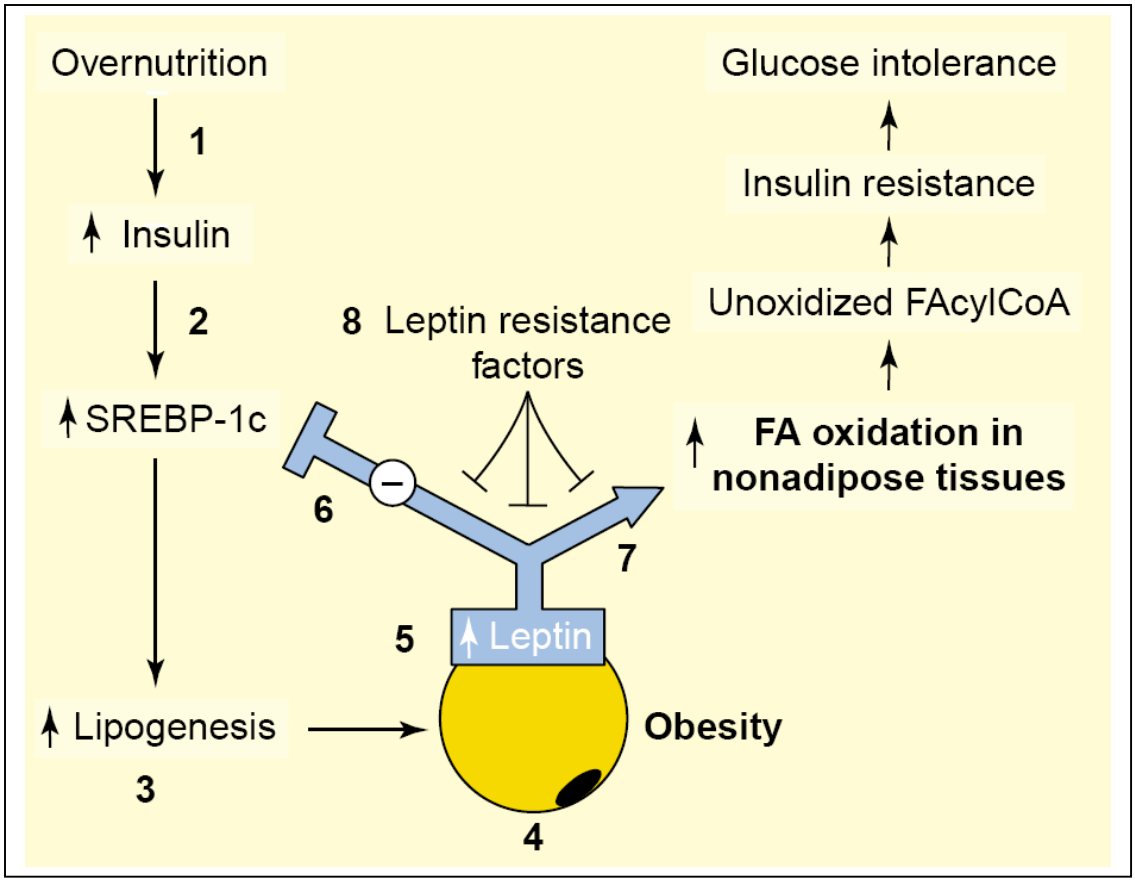

Adapted from (Unger, 2003)

Fig. 10. The sequence of events postulated to occur during the development of diet-induced obesity and metabolic syndrome

2.3. What causes insulin resistance?

Insulin resistance observed in and *type 2 diabetes* is characterized by defects at many levels, with decreases in receptor concentration and kinase activity, in the concentration and phosphorylation of IRS-1 and -2, in PI (3) K activity, in glucose transporter translocation, and in the activity of intracellular enzymes (Kahn and Flier, 2000). Genetic and acquired factors can also profoundly influence insulin sensitivity. Genetic defects in the insulin receptor represent the most severe forms of insulin resistance, and are exemplified by leprechaunism, the Rabson Mendenhall Syndrome, and the type A syndrome of insulin resistance (Taylor and Arioglu, 1998). The high level of insulin resistance may be due to the severity of the genetic defect, the ability of the mutant receptors to form hybrids with IGF-I or other receptors, and other background genetic or acquired factors that modify the insulin-resistant state.

Targeted deletions of the components of insulin signalling *in vivo* have provided some insight into the complexity of insulin resistance. The IRS1 knockout mice have peripheral insulin resistance (Tamemoto et al., 1994), while deletion of IRS2 results in impaired pancreatic β-cell proliferation and *diabetes* (Withers et al., 1998). In addition, defects in the insulin-signalling pathway, such as knockout of PKBβ, can result in insulin resistance and *diabetes* (Cho et al., 2001a).

Combinatorial knockouts have been produced that mimic polygenic type 2 *diabetes* with heterozygous deletion of the insulin receptor and IRS-1 (Bruning et al., 1997a), or of the insulin receptor, IRS-1 and IRS-2 (Kido et al., 2000). In some of these combinations there has been clear evidence of genetic epistasis. For example, although heterozygous knockout of either the insulin receptor or IRS-1 alone does not produce diabetes, the double-heterozygous knockout produces diabetes in up to 50% of mice (Bruning et al., 1997a). This finding gives insight into insulin resistance where insulin-induced downregulation, or genetic polymorphisms in the receptor or IRS-1 alone, might produce modest changes in signalling capacity, but when combined can lead to severe insulin resistance.

The role of specific tissues in the pathogenesis of insulin resistance has been explored using tissue-specific knockouts of the insulin receptor (Michael et al., 2000) (Bruning et al., 1997b). Mice with a knockout of the fat-specific or muscle specific insulin receptor have normal glucose tolerance, whereas the liver-specific insulin-receptor knockout shows both impaired glucose tolerance and decreased insulin clearance with marked hyperinsulinaemia (Bruning et al., 1997b; Michael et al., 2000). Taken together, these findings suggest that impaired insulin-induced signaling results in insulin resistance in insulin target tissues, such as liver and muscle.

Notably, one genetic model with a surprising phenotype regarding glucose homeostasis was the knockout of the p85 regulatory subunit of PI (3) K. Although, PI(3)K is central to the metabolic actions of insulin, p85 heterozygous knockout mice counter-intuitively exhibit improved insulin sensitivity (Fruman et al., 2000). This protection seems to be due to a unique feature of the insulin-signalling pathway in which the stoichiometric balance between p85, the catalytic subunit p110 and IRS proteins is critical for optimal signal transduction.

What is the relationship between fat cells and insulin sensitivity?

Adipose tissue plays a special role in insulin resistance. Circulating FFAs derived from adipocytes are elevated in many insulin-resistant states and have been suggested to contribute to the insulin resistance of diabetes and obesity by inhibiting glucose uptake, glycogen synthesis and glucose oxidation, and by increasing hepatic glucose output (Bergman and Ader, 2000). Elevated FFAs are also associated with a reduction in insulin-stimulated IRS-1 phosphorylation and IRS-1-associated PI(3)K activity (Shulman, 2000). The link between increased circulating FFAs and insulin resistance might involve accumulation of triglycerides and fatty acid-derived metabolites (diacylglycerol, fatty acyl-CoA and ceramides) in muscle and liver. Nuclear magnetic resonance imaging has revealed a close correlation between intramyocellular triglyceride content and

whole-body insulin resistance in patients with obesity and type 2 *diabetes* (Hwang et al., 2001).

Randle proposed that free fatty acids competing with glucose for substrate oxidation, along with increased fat oxidation, may result in insulin resistance seen in obesity and type 2 *diabetes* (Randle, 1998). According to this hypothesis, increased free fatty acids levels lead to elevated mitochondrial acetyl-CoA/CoA and NADH/NAD ratios which, in turn, inhibit pyruvate dehydrogenase activity and lead to an increase in citrate levels that inhibits phosphofructokinase activity. This process induces an increase in glucose 6-phosphate concentration, which inhibits hexokinase and reduces glucose transport/phosphorylation activity. (Randle, 1998).

Does IRS-1 serine phosphorylation relate to cellular insulin resistance?

Prolonged stimulation of cells with insulin also induces Ser phosphorylation of IRS-1, suggesting there may exist a negative-feedback mechanism that uncouples the IRS-1 proteins from their upstream and downstream partners and blocks insulin signal transduction under physiological conditions. For example, TNFα increases serine phosphorylation of IRS-1, resulting in inhibition of insulin-stimulated tyrosine phosphorylation and impaired insulin signaling (Rui et al., 2001). Recently, phosphopeptide mapping, mutational analysis and phosphospecific antibodies allowed the identification of the serine residues phosphorylated in response to insulin and TNFα. Interestingly, insulin and TNFα signaling lead to phosphorylation of the same residues in IRS-1, namely Ser307, Ser612 and Ser632 (Ozes et al., 2001) (Gual et al., 2003b)(Fig.11). (see below.)

Ser307 is located at the end of the phosphotyrosine-binding domain involved in the interaction of IRS-1 with IR, where its phosphorylation blocks this interaction (Fig. 11) (Aguirre et al., 2002). However, its mutation prevents the inhibitory effect of TNFα on insulin-induced IRS-1 tyrosine phosphorylation. Ser307 phosphorylation induces a conformational change of the

phosphotyrosine-binding domain, reducing its affinity for the IR (Aguirre et al., 2002). The mTOR (mammalian target of rapamycin) signalling pathway was shown to be involved in insulin-induced phosphorylation of Ser307 in adipocytes, and muscles (Gual et al., 2003b), (Carlson et al., 2004). Hyperosmotic stress, which also induces insulin resistance, increases the phosphorylation of IRS-1 on Ser307 by an mTOR-dependent pathway (Gual et al., 2003a), indicating the importance of this site in insulin resistance. JNK is also known to be involved in Ser307 phosphorylation of IRS-1 in fat-induced insulin resistance. JNK is activated by fatty acids and JNK activity is abnormally elevated in obesity (Hirosumi et al., 2002). Interestingly, JNK1-knockout mice have a decreased adiposity, resistance to a high-fat diet, an improved insulin sensitivity and an enhanced insulin receptor signalling capacity. Moreover, genetically obese (*ob/ob*) mice with a targeted mutation in Jnk1 put on less weight than their relative control (*ob/ob*) mice and they are partly protected against hyperinsulinaemia and hyperglycaemia (Hirosumi et al., 2002).

Phosphorylation of Ser307 could have a more general role in the regulation of insulin signalling. Its phosphorylation, by inhibiting the interaction between the IR and IRS-1, could favour the dephosphorylation of all IRS-1 tyrosine phosphorylation sites, leading to termination of the insulin signal. Moreover, the regulation of serine versus tyrosine phosphorylation of IRS-1 may regulate IRS-1 degradation, since IRS-1 with a point mutation of Ser307 is more resistant to degradation following long-term exposure to insulin (Greene et al., 2003).

Ser612 and Ser632 are located close to tyrosine residues which are major phosphorylation sites involved in the binding of PI 3-kinase and are required for insulin-stimulated glucose uptake (Fig.11). The role of the phosphorylation of these two serine residues could modulate the interaction between IRS-1 and PI 3-kinase and/or its activation (Mothe and Van Obberghen, 1996). Phosphorylation of these sites is mediated by MAPK and/or mTOR signaling pathways in response to both insulin (Gual et al., 2003b) and TNFα (Ozes et al., 2001). Interestingly, the basal level of IRS-1 phosphorylation on

Ser632 was abnormally high in primary cultures of skeletal muscle cells obtained from type 2 diabetic patients (Bouzakri et al., 2003), suggesting this site may be involved in predisposition of insulin resistance. Phosphorylation of Ser612/Ser632, in addition to the closely located tyrosine residues, could thereby regulate PI 3-kinase activity (Fig. 11).

.

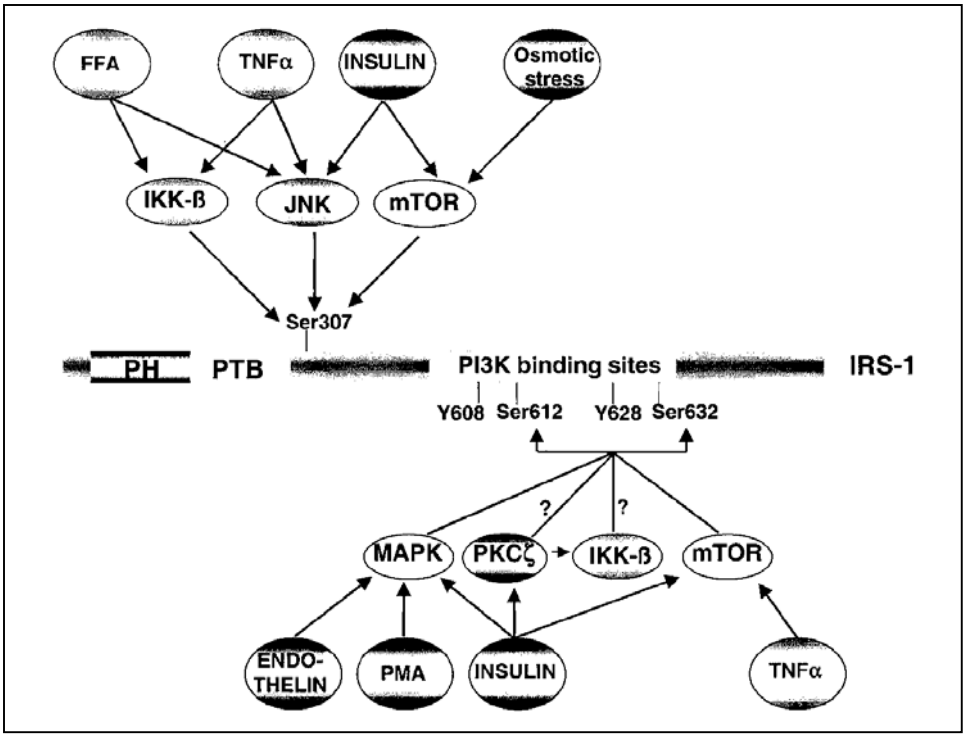

Adapted from (Le Marchand-Brustel et al., 2003)

Fig. 11. Serine phosphorylation of IRS-1 and some of the kinases involved

IRS-1 contains multiple Ser residues which can be phosphorylated. This diagram depicts the action of some kinases which have been identified in the phosphorylation of Ser307, Ser612 and Ser632. The phosphorylation of Ser307 uncouples IRS-1 from the IR and decreases its tyrosine phosphorylation. Phosphorylation of Ser612 and Ser632, which are located close to the tyrosine residues involved in the binding of PI 3-kinase (PI3K) down-regulates insulin action. See text for explanation; FFA refers to NEFA; PTB, phosphotyrosine-binding domain.

3. How does nutrient signaling coordinate with insulin signaling?

Binding of insulin to insulin receptor induces trans-autophosphorylation of receptor on tyrosine residues (Kasuga et al., 1982). The phosphorylated Tyrosine residues serve as docking sites for insulin receptor substrate (IRS) proteins, which themselves become phosphorylated on Tyr residues by the receptor (Whitehead et al., 2000). This leads to recruitment of the heterodimeric PI (3) K to the membrane, which leads to the generation of PIP_3 at the membrane. PIP_3 production is counteracted by the tumor suppressor PTEN or by PI (3) K inhibitors such as wortmanin. PKB translocates to the membrane by virtue of its pleckstrin homology (PH) domain, which also mediates binding to PIP_3. (Burgering and Coffer, 1995; Franke et al., 1997). The interaction of PKB with PIP_3 is thought to cause a change in conformation, which facilitates phosphorylation of the activation loop site (T308) by PDK1 (Alessi et al., 1997) and of the conserved regulatory site in the carboxy terminus (S473) by DNA-dependent protein kinase (Feng et al., 2004). Phosphorylation of the T308 and S473 sites is required for full PKB activation (Bos, 1995). Following activation at the membrane, PKB targets substrates in the cytosol and translocates to the nucleus where it phosphorylates as yet unclear substrates (Brazil et al., 2004). Together this kinase cascades mediate the metabolic and growth functions of insulin, such as the translocation of GLUT4 glucose transporter containing vesicles from intracellular pools to the plasma membrane, stimulation of glycogen and protein synthesis, uptake of amino acids, and the inhibition of specific gene transcription programs (Fig. 12) (Ueki et al., 1998; Yang et al., 2004).

Tuberous sclerosis complex 1/2 heterodimer protein (TSC1/2) and Rheb (Ras homolog enriched in brain) are upstream components of the mTOR (mammalian target of rapamycin) signaling pathway (Gao and Pan, 2001; Gao et al., 2002; Manning and Cantley, 2003). Tuberous sclerosis complex 2 (TSC2) is phosphorylated and inhibited by the pro-growth protein PKB, which is activated

by growth factors such as insulin (Inoki et al., 2002). TSC2 is a GTPase-activating protein (GAP) for the small G protein Rheb (Inoki et al., 2003; Li et al., 2004). Inactivation of Rheb by TSC2 is significant because GTP-bound, activated Rheb leads to an increase in the activation of mTOR, a central regulator of cell growth (Garami et al., 2003; Inoki et al., 2003; Li et al., 2004; Manning and Cantley, 2003) . In response to amino acids and cellular energy levels, mTOR controls translation through activation of S6K1 (p70 ribosomal protein S6 kinase) and inhibition of eukaryotic initiation factor 4E (eIF4E)-binding protein 1 (4E-BP1) (Nojima et al., 2003; Proud, 2004a; Proud, 2004b). It is known that cellular nutrient levels (intracellular amino acids) can regulate the function of mTOR (Beugnet et al., 2003), but it remains to be seen what roles TSC1/2 and Rheb have in the intracellular amino acid and energy-sensing network. (Fig. 12).

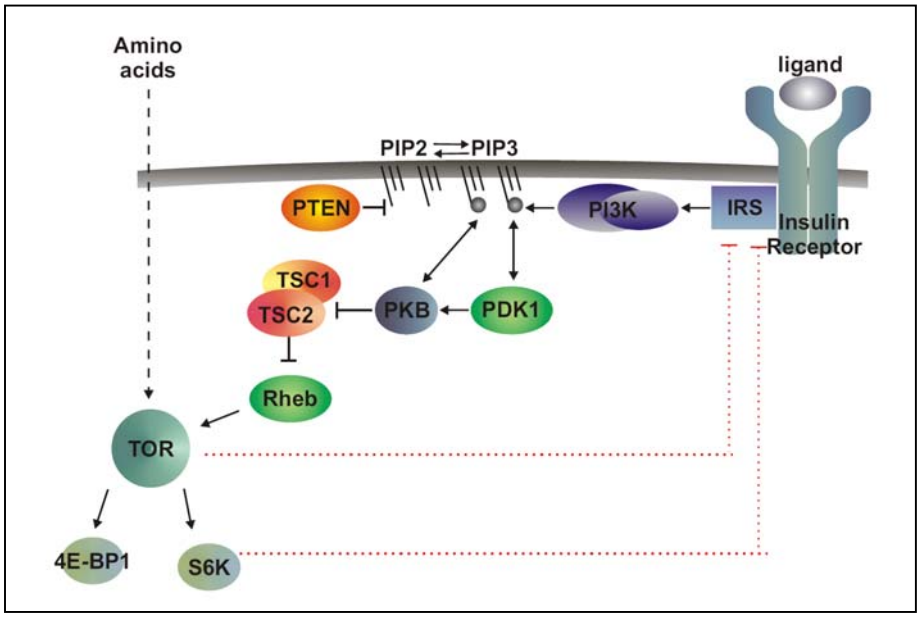

Modified from the book "Cell Growth "(Hall. M., 2004)

Fig. 12. Nutrient signaling coordinates with insulin signaling.

S6K1

S6 kinase (S6K) was first described as a mitogen-stimulated 70kDa kinase which phosphorylates 40S ribosomal protein S6 in Swiss 3T3 cells

(Novak-Hofer and Thomas, 1984). This phosphorylation of S6 was also observed in the liver following partial hepatectomy and during refeeding after starvation, both of which which induce the activation of protein synthesis required for cell growth (Gressner and Wool, 1974; Kozma et al., 1989). S6 phosphorylation by S6K and other unknown kinases occurs in an ordered fashion: Ser 236 > Ser 235 > Ser 240 > Ser 244 (Krieg et al., 1988). Translational upregulation of 5' Terminal Oligopyrimidine tract (5'TOP) mRNA following mitogen stimulation closely follow the multiple phosphorylation events of S6 and activation of S6K, indicating the role of S6K in translational control as a mediator of cell growth (Jefferies and Thomas, 1996). The 5'TOP transcripts represent mRNA encode ribosomal proteins, translational initiation and elongationl factors (Meyuhas et al., 1996).

Deletion of S6K1 gene in mice did not impair either S6 phosphorylation or 5'TOP mRNA translation, leading to the discovery of S6 kinase 2 (Shima et al., 1998), which shows 82% homology in the catalytic domain and in the linker and autoinhibitory domains. S6K1 and S6K2 belong to the AGC family of serine/threonine protein kinases including PKA, PKB, and PKCs where they share high degree of homology in the catalytic domain (Brazil and Hemmings, 2001; Shima et al., 1998).

S6K1 has five distinct domains. The first domain is represented by a short segment at the amino terminus, which confer rapamycin sensitivity. The catalytic domain of S6K1 contains a key site of phosphorylation in the activation loop, T229. The catalytic domain is coupled to the carboxyterminal autoinhibitory domain through a linker domain. The linker domain contains two essential phosphorylation sites, S371, and S/TP site and T389 (Dennis et al., 1998; Pearson et al., 1995). In contrast to most member of the AGC family which end with the linker domain, S6K1 and S6K2 have two additional carboxy-terminal domains which contains four S/T-P phosphorylation sites: S411, S418, T421, and S424 which are critical for T229 phosphorylation (Dennis et al., 1998), and a PDZ-binding domain. The order of S6K1 sequential activation mechanism is described in the legend of Fig. 13. TOS (TOR signaling motif) motif in the amino

terminus of S6K1 binds to Raptor (regulatory associated protein of TOR) which mediates interaction with mTOR (Schalm and Blenis, 2002). The S/TP sites in autoinhibitory domain must be first phosphorylated to facilitate TOR-mediated phosphorylation of T389 (Dennis et al., 1998). Once phosphorylated, T389 in the hydrophobic domain becomes a docking site for PDK1 via its PIF-binding pocket. PDK1 then mediate the first step of S6K1 activation, the phosphorylation of the T -loop site T229 (Alessi et al., 1998; Pullen et al., 1998)(Fig.13).

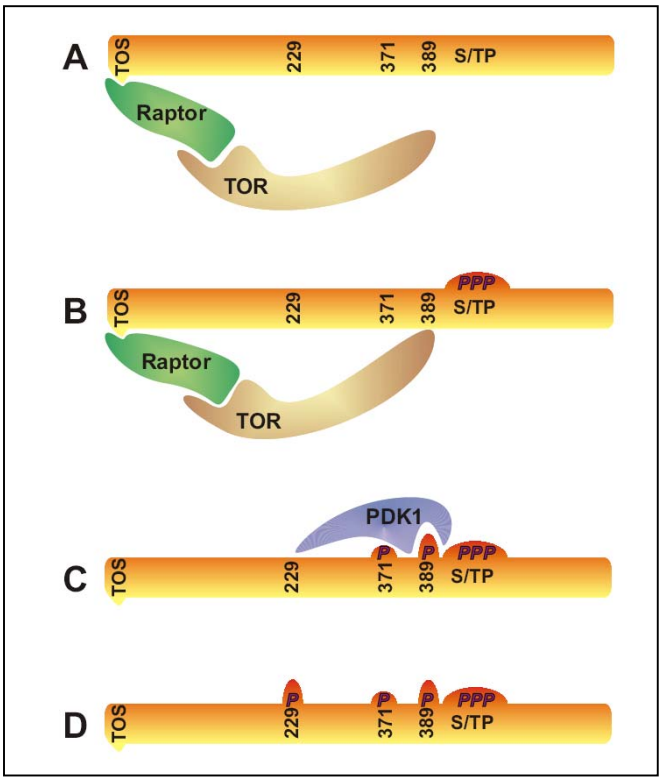

Adapted from book " Cell Growth" (Hall. M., 2004)

Fig. 13. Molecular mechanism of S6K1 sequential activation.
(A) Raptor is able to make a bridge between TOR and S6K1. The S/TP sites within the autoinhibitory domain have first to be phosphorylated to facilitate TOR-mediated phosphorylation of T389. (B), PhosphorylatedbT389 constitutes a docking site for PDK1. (C), which will ultimately phosphorylate the T-loop, T229, within the catalytic domain. (D) S6K1 activity always paralled 371 phosphorylation.

The physiological function of S6K1 has been investigated using S6K1 knockout mice. S6K1 deficient mice revealed that approximately 20% smaller at birth. Unexpectedly, the effects on body size does not appear to be attributable to

a reduction in S6 phosphorylation, as this response proved to be intact in S6K1-deficient animals (Shima et al., 1998). S6 phosphorylation in such animals was still sensitive to rapamycin (Shima et al., 1998). Rapamycin inhibits the mammalian target of rapamycin (mTOR) (Dennis and Thomas, 2002), the upstream S6K1 kinase (Dennis and Thomas, 2002), suggesting there exists a second S6K which may compensate for loss of S6K1. Moreover, proliferation of S6K1 deficient MEFs as well as 5' TOP mRNA translation were intact (Shima et al., 1998), indicating the small body size phenotype may not stem from reduced translational capacity regulating cell cycle. On the other hand, measurements of the humoral environment, such as growth hormone and insulin-like growth factors levels which regulate body growth has not been studied in S6K1 knockout mice. Thus, it is not clear whether reduced body mass in S6K1 knockout mice is due to cell autonomous effects coming from deletion of S6K1 gene. Given that body size differences were more pronounced during embryogenesis, growth retardation in S6K1 deficient mice could be due to defects in fetal development. As efficient nutrient uptake is essential to body growth and development and extraembryonic tissues such as placenta regulate nutrient transport to the embryo (Rossant and Cross, 2001), it remained to be determined whether any impairment of nutrient uptake or function of the placenta was responsible for the growth retardation in S6K1 deficient mice (see results).

Given the differences of S6K2 gene expression level in various tissues of S6K1 deficient mice (Rossant and Cross, 2001), it would be interesting to see if the extents of S6K2 upregulation influence the physiological function of individual tissues operates. Despite the presence of S6K2, S6K1 deficient mice are mildly glucose intolerant and have reduced levels of circulating insulin. Reduced insulin levels result from a selective reduction in β-cell cytosolic endocrine mass indicating reduction in β-cell size (Pende et al., 2000). This would suggest that the function of S6K2 at least in pancreatic β- cell growth and insulin secretion, is different from S6K1. Consistent with this, S6K2 deficient mice did not exhibit the reduced circulating insulin and diminished β-cell size seen in S6K1 deficient mice (S Um, S. Kozma, and G. Thomas, unpublished results).

Raptor

Raptor (regulatory associated protein of TOR) is a conserved 150-kDa protein that also binds the downstream effectors of mTOR, S6K1, and 4E-BP1 (Hara et al., 2002; Kim et al., 2002). Knockdown experiments of Raptor by RNAi in mammalian cells also suggest its positive role in mTOR activity (Hara et al. 2002; Kim et al. 2002). Although Raptor is normally a positive regulator of mTOR, one report indicates that, upon nutrient deprivation, Raptor-mTOR association is stabilized in a manner that inhibits mTOR kinase activity (Kim et al., 2002). Raptor binds S6K1 and 4E-BP1, both downstream effectors of mTOR, leading to efficient phosphorylation of S6K1 (Beugnet et al. 2003; Choi et al. 2003; Nojima et al. 2003; Schalm et al. 2003). The interaction of Raptor with S6K1 and 4E-BP1 is mediated by a 5 amino acid motif termed TOS (TOR signaling) that is present in the N-terminus of S6K1. (Schalm and Blenis, 2002). Taken together, these findings support a model whereby a change in the configuration of the mTOR-Raptor complex, which is mediated by nutrient conditions such as amino acid availability, affects the ability of mTOR to interact with and phosphorylate its substrates such as S6K1 and 4E-BP1 (Hall. M., 2004). In the absence of amino acids, the mTOR-mLST8-Raptor complex precludes mTOR from binding to its substrates and/or prevents the access of mTOR (or mTOR-associated kinases) to the substrates (Chen and Kaiser, 2003; Kim and Sabatini, 2004). Conversely, in the presence of amino acids, a conformational change promotes efficient interaction between Raptor and mTOR substrates and/or increased accessibility of the substrates to mTOR and its associated kinases (Kim and Sabatini, 2004).

mTOR

The mammalian target of rapamycin (mTOR) was identified and cloned (Brown et al. 1994; Chiu et al. 1994; Sabatini et al. 1994) shortly after the discovery of the two yeast genes, TOR1 and TOR2, in the budding yeast *Saccharomyces cerevisiae* during a screening for resistance to the immunosuppressant drug rapamycin (Kunz and Hall, 1993). mTOR is a large protein with homology to members of the lipid kinase family. mTOR regulation of

S6K1 is inhibited by the drug rapamycin, which, in a gain of funtion complex with the small protein FKBP12, specifically binds and inhibits mTOR activity (Brown et al., 1995) . The function of mTOR has also been studied in yeast. Loss of TOR causes effects identical to nutrient starvation: reduction of protein synthesis, accumulation of glycogen, enlargement of vacuoles and specific gene expression reflecting starvation (Hardwick et al., 1999; Kunz and Hall, 1993; Kunz et al., 1993; Noda and Ohsumi, 1998) indicating the critical role of mTOR to mediate nutrient-induced cell growth and protein synthesis.

PKB

Mammalian cells express three unique PKB proteins. A downstream effector of PI3K, PKB is Ser/Thr kinase phosphorylated by 3-phosphoinositide-dependent kinase-1 (PDK1) and by DNA-dependent protein kinase (Feng et al., 2004). Overexpression of a dominant-negative form of PKB impairs insulin-mediated phosphorylation of 4E-BP1 (Gingras et al., 1998). This finding suggests that PKB is an upstream regulator of mTOR. PKB plays a role in directing GLUT4 vesicles to the plasma membrane and thus promotes glucose transport in muscle (Hill et al., 1999). The physiological significance of this process is a net 10- to 40-fold increase in glucose flux into the cells. Constitutively active PKB in quiescent 3T3-L1 adipocytes promotes high levels of lipogenesis (Kohn et al., 1996). Overexpression of active PKBα in cells of transgenic mice leads to a significant expansion of β-cell mass, owing to an increase in both cell size and number indicating the importance of PKBα in pancreatic cell growth (Tuttle et al., 2001).

TSC1/TSC2

Understanding how growth factors and PKB regulate mTOR activity was achieved by the discovery that the TSC1 and TSC2 proteins are upstream regulators of mTOR. TSC1 (also known as hamartin) and TSC2 (also known as tuberin) are encoded by the tuberous sclerosis complex 1 (TSC1) and tuberous sclerosis complex 2 (TSC2) genes, respectively, which are associated with the dominant genetic disorder, tuberous sclerosis complex (TSC), characterized by

hamartomas with large cells in many organs (Cheadle et al., 2000). The similarity between the phenotypes caused by TSC1/TSC2 and dPTEN deficiencies in *Drosophila* prompted genetic epistasis experiments, which showed that TSC1 and TSC2 function between PKB and S6K in the insulin-signaling pathway (Potter et al., 2001). These observations and the fact that S6K1 is highly phosphorylated in mammalian cells lacking functional TSC1 or TSC2 provide potential links between PKB and TSC1/TSC2 and between mTOR and TSC1/TSC2 (Jaeschke et al., 2002). These links were established by the finding that TSC2 is directly phosphorylated by PKB *in vitro* and *in vivo* (Inoki et al., 2002). Further analyses of TSC2-deficient cells, as well as TSC1 and TSC2 overexpression experiments, demonstrate that the TSC1/TSC2 heterodimer is an upstream negative regulator of mTOR (Inoki et al., 2002; Jaeschke et al., 2002). Overexpression of both TSC1 and TSC2 in HEK-293 cells impairs insulin-stimulated phosphorylation of S6K1 and 4E-BP1. In summary, these observations provide strong evidence that PKB activates mTOR, at least in part, through the phosphorylation and inactivation of TSC2. An intriguing phenomenon of a negative regulatory loop was observed in TSC2- or TSC1-deficient cells, in which PKB activity mediated by insulin and other growth factors is significantly diminished (Jaeschke et al., 2002). This negative regulatory loop may serve to coordinate mTOR and PKB functions.

Rheb

Rheb was first identified in a differential screen of mRNAs induced in neurons by agents that provoke seizures. It is ubiquitously expressed, but is particularly abundant in muscle and brain (Yamagata et al., 1994). Recent genetic studies in *Drosophila* place Rheb in the insulin-signaling pathway, downstream of TSC1/2 and upstream of mTOR/S6K1 (Saucedo et al., 2003; Stocker et al., 2003; Zhang et al., 2003). Most significantly, it was recently demonstrated that Rheb is a physiological substrate of TSC2 GAP activity (Garami et al., 2003; Zhang et al., 2003). TSC2 is the functional component of the TSC1/2 complex that inhibits Rheb and mTOR signaling, whereas the

physiological function of TSC1 is to stabilize TSC2 (Inoki et al., 2003; Li et al., 2004; Manning and Cantley, 2003). Biochemical data has shown that Rheb stimulates phosphorylation of S6K1 and 4E-BP1 dramatically (Garami et al., 2003). According to recent data, Rheb could activate mTOR via two proposed mechanisms. First, Rheb may be a direct component of the mTOR signaling complex, regulating either mTOR itself or its binding protein. Second, mTOR signaling has been shown to play a part in sensing intracellular amino acid levels (Rohde et al., 2001). Current data supports the model whereby TSC1/2 antagonizes the mTOR/S6K1/4E-BP1 signaling pathway via stimulation of GTP hydrolysis of Rheb (Inoki et al., 2003). In addition, TSC1/2 and Rheb have pivotal roles in mediating growth factor, nutrient and energy-sensing signals to mTOR-dependent targets.

4. Pancreatic β-cell growth

Previously, mice deficient for S6 Kinase 1 (S6K1) were shown to be hypoinsulinemic, and exhibited reduced β cell size suggesting β-cell growth can be regulated by S6K1 (Pende et al., 2000). Traditionally, genetic factors and nutritional alterations during fetal and postnatal periods have been implicated in β-cell dysfunction and impaired β-cell growth in adult, (Blondeau et al., 2002). We questioned whether diminished β-cell size in adult *S6K1*$^{-/-}$ mice arose from an altered nutritional environment during development *in vivo* or stem from impaired β-cell development due to absence of the S6K1 gene.

As fetal and neonatal life are known to be crucial periods for pancreatic β-cell growth and development, exhibiting the most active β-cell replication and neogenesis, the baseline for β-cell mass occurs is in early life (Rahier et al., 1981), (Bonner-Weir, 2000), (Nielsen et al., 1999), (Finegood et al., 1995), (Kaung, 1994), we next questioned whether diminished β-cell size in adult *S6K1*$^{-/-}$ mice originates from impaired body growth during embryonic development. In addition, given that defects in placental development or dietary protein restriction during gestation lead to fetal growth retardation (Rossant and Cross, 2001), (Parimi et al., 2004), we also questioned whether growth retardation and developmental delay arise from low levels of nutrient availability due to impaired placenta development. A brief overview of placenta development and functions which regulate fetal growth and pancreatic β-cell growth are given below.

4.1. What controls nutrient transport required for body growth during development in mammals?

-Placental development.

The placenta is unique organ exclusive to mammals. It develops from a fertilized egg and is, therefore, an organ of the embryo (Rossant and Cross,

2001). During gestation, development and growth of the fetus depends on the placenta for exchange of gases, nutrients and waste products between mother and fetus (Rossant and Cross, 2001). The placenta also produces pregnancy-associated hormones and growth factors for the fetus. Any genetic or environmental alterations which affects placental development or function may result in placental insufficiency and consequent impairment of fetal development and intra-uterine growth retardation (Tam and Rossant, 2003).

Placental development is initiated from E3.5 and proceeds until E12.5. Functional establishment of the placenta improves the developmental conditions and growth of the fetus. Fetal mass accumulates at an increasing rate from E12.5 to E16.5 and the placenta undergoes remodeling and growth together with the fetus (Rossant and Cross, 2001).

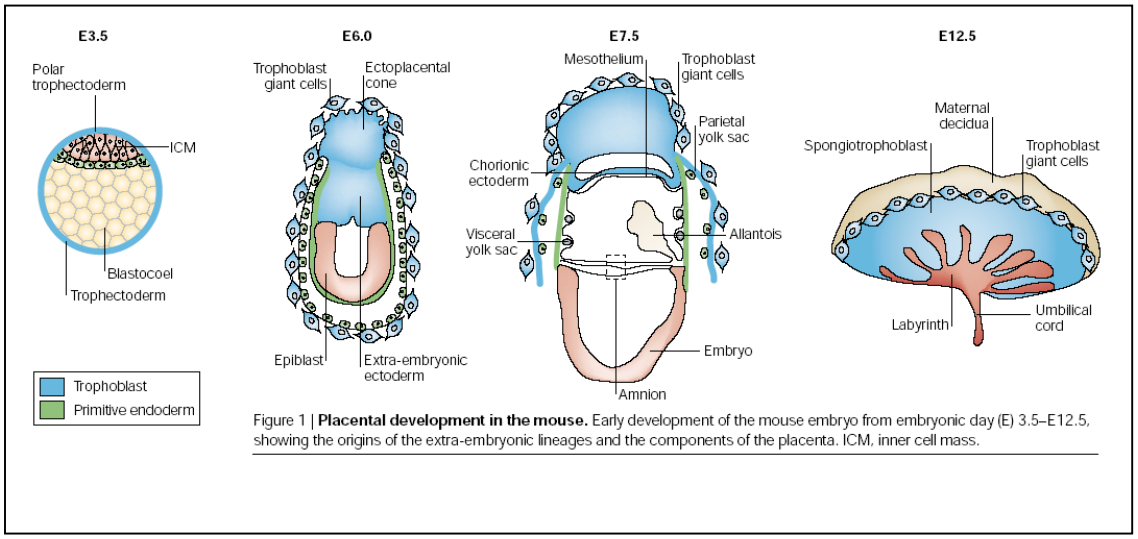

Figure 1 | **Placental development in the mouse.** Early development of the mouse embryo from embryonic day (E) 3.5–E12.5, showing the origins of the extra-embryonic lineages and the components of the placenta. ICM, inner cell mass.

Adapted from (Rossant and Cross, 2001)

Fig. 14. Placental development in the mouse.
Early development of the mouse embryo from embryonic day (E) 3.5–E12.5, showing the origins of the extra-embryonic lineages and the components of the placenta. ICM, inner cell mass.

In early embryo development, there are two populations of cells in early blastocysts, the inner cell mass (ICM) and the trophoblasts, a monolayer of epithelium. The inner cell mass will contribute mainly to the embryo proper, while

the trophoblast develops into a great part of the placenta (Rossant and Cross, 2001). In late blastocysts, a third population of cells appears called the primitive endoderm, and the trophoblast differentiates into the polar trophoectoderm and mural trophoectoderm (Fig. 14) (Rossant and Cross, 2001). In development, the mural trophoectoderm forms the primary trophoblast giant cells from implantation and the polar trophoectoderm or the ectoplacental cone, a primitive placenta (Fig. 14). Later in gastrulation, some mesoderm cells give rise to the allantois and part of the chorion. Meanwhile in the ectoplacental cone, the secondary trophoblast giant cells develop and the chorionononic ectoderm is also formed (Rossant and Cross, 2001) . Thus, the chorion has two different origins, namely the mesoderm of the epiblast and the ectoderm of the ectoplacental cone. By E8.5, the allantois makes contact with the chorion, an event termed chorioallantoic fusion. After several hours of allantoic attachment, folds appear in the chorion where a fetal vascular network will be constructed (Rossant and Cross, 2001) (Tam and Rossant, 2003). The trophoblast, together with its associated fetal blood vessels, subsequently undergoes extensive villous branching and remodeling to generate a densely packed structure, the labyrinth (Tam and Rossant, 2003) (Rossant and Cross, 2001). At the same time, chorionic trophoblast cells begin to differentiate into the various layers of the trophoblast in the labyrinth.

Which components make up the Placenta?

The mature placenta consists of three main layers: maternal decidua basalis (db), junction zone (jz) and labyrinth zone (lb). Below is a schematic representation of a sagittal section of an E15.5 placenta with the maternal side at the top and fetal side at the bottom (Fig. 15) (Georgiades et al., 2001). The placenta is linked to the maternal uterine wall by deciduas basalis. The labyrinth is a vascular network in which the fetal vessel capillaries are immersed in the maternal blood space (mbs) for nutrient, gas, and waste product exchange. Some of the spongiotrophoblast (st) between the decidua basalis and the labyrinth synthesize glycogen (gc). The trophoblast giant cells (tg) line up

between the spongiotrophoblast and the decidua basalis (Georgiades et al., 2001).

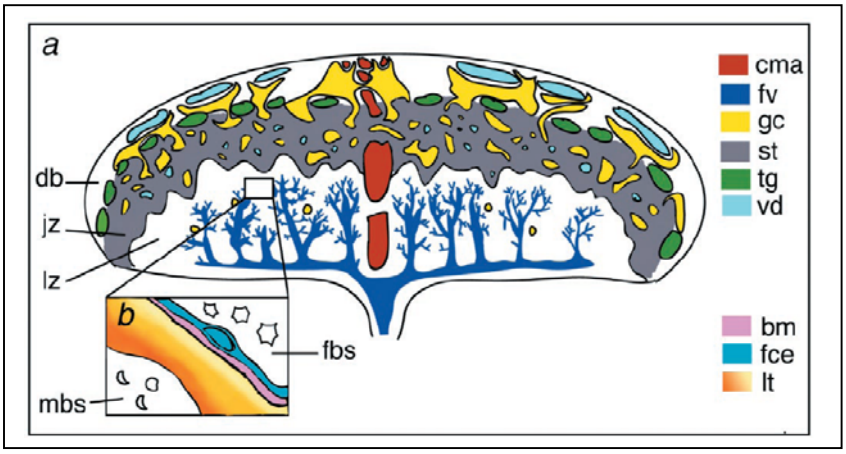

Adapted from (Georgiades et al., 2001)

Fig. 15. The major regions and cell types of the mouse placenta at E15.5. (a) Schematic representation of a sagittal section of the mouse placenta. The placenta is oriented with its maternal side at the top and the fetal (flat) side at the bottom. The plane of sectioning is through the center of the placenta and perpendicular to its flat surface. All sections shown in this study were sectioned in this way. The major placental zones (db, decidua basalis; jz, junctional zone; lz, labyrinth zone) are shown; their constituent cell types are depicted by different colors.

In summary, placental abnormalities often underlie embryonic lethality or growth retardation accompanied by impaired β-cell cell growth. This is caused by the targeted mutation of genes and can arise from defects in embryonic trophoblast and fetal compartments of the placenta.

Pancreatic β-cell growth and development are exclusively sensitive to the level of nutrients provided by the placenta. Why then is pancreatic β-cell size diminished in S6K1 deficient mice? To know the reason, A brief overview of regulation of pancreatic β-cell mass is given below.

4.2. How is pancreatic β-cell mass regulated?

β-Cell mass is dynamically regulated.

β-cell mass is the major factor in determining the amounts of insulin that can be secreted to maintain nutrient homeostasis (Bonner-Weir, 1994). Major contributing factors that regulate β-cell mass is β-cell replication, size of β-cells, incidence of β-cell neogenesis, and rate of β-cell apoptosis (Dor et al., 2004) (Bonner-Weir, 2000).

Phase of pancreatic β-cell growth.

Just after birth, there is a burst of islet cell replication, and then later, during weaning, there is a transient neogenesis that supplements the increased β-cell replication. Postweaning, as the young animal grows up, the rates of β-cell replication, neogenesis, and apoptosis all markedly trail off. In adult life, there remains a very slow turnover of β-cells with the estimated life span of β-cell being 60 days (Bonner-Weir, 2000). About 0.5% of the adult β-cell population is undergoing replication, which is balanced by 0.5% of β-cells entering into apoptosis (Bonner-Weir, 2000). Thus, the most active period of β-cell replication and neogenesis that occurs in early life will dictate the baseline for β-cell mass for the rest of the mammalian organism's life, which could have consequences for the susceptibility to acquiring *type 2 diabetes*. In humans, a low birth weight has been associated with an increased susceptibility for the onset of *type 2 diabetes* later on in life (Hales and Barker, 2001). It is possible that, by being born small, there is a correlatively undersized β-cell population (Hales and Barker,

2001). The neonatal β-cell replication and β-cell neogenesis rates appear to be constant, so that the final β-cell population in the adult that develops from a small neonate will remain relatively low irrespective of how large the adult grows. Therefore, a small β-cell mass in adulthood has less capacity to expand in response to increased insulin demand and/or metabolic homeostasis, which, in turn, contributes to an increased risk of acquiring *type 2 diabetes*. Thus, maintaining β-cell mass is a crucial factor for maintaining nutrient homeostasis and preventing type *2 diabetes.*

4.3. What kind of factors modulates β-cell growth?

Nutrients and growth factors

Certain nutrients and various growth factors stimulate mitogenesis of existing β-cells, and influence the proliferation and differentiation of pancreatic precursor cells into insulin-expressing cells. As a general trend, nutrients that stimulate insulin secretion and synthesis also increase β-cell mass (Bonner-Weir et al., 1989). Glucose is the most physiologically relevant and has been shown to increase rodent β-cell proliferation *in vitro* and *in vivo* in a manner that is dependent on glucose metabolism (Bonner-Weir et al., 1989; Schuppin et al., 1993). The effect of nutrients on β-cell growth has focused primarily on existing adult β-cells, but it is unknown whether nutrients have a direct effect on inducing β-cell neogenesis.

In addition to glucose, feeding normal rats with high fat diet for six weeks results in a modest increase in body weight and insulin resistance, but islet density and β-cell size significantly increases by 30-40%, suggesting the flexibility of β-cell growth to adapt to changes in nutritional status (Fig. 16) (Buettner et al., 2000). β-cell mass is enhanced 50% in glucose infused rats through inducing hyperplasia and hypertrophy (Bonner-Weir et al., 1989). In addition, nutrients, especially amino acids signaling in β-cells are known to promote insulin production, suggesting the importance of nutrients in β-cell

function and mass (McDaniel et al., 2002). Consistent with this model, loss of S6K1, a downstream effector of the mTOR-signaling pathway which integrate nutrient and mitogen signaling results in reduced pancreatic β-cell size leading to hypoinsulinemia (Pende et al., 2000). High fat diet-induced β-cell hypertrophy is shown in Fig. 16.

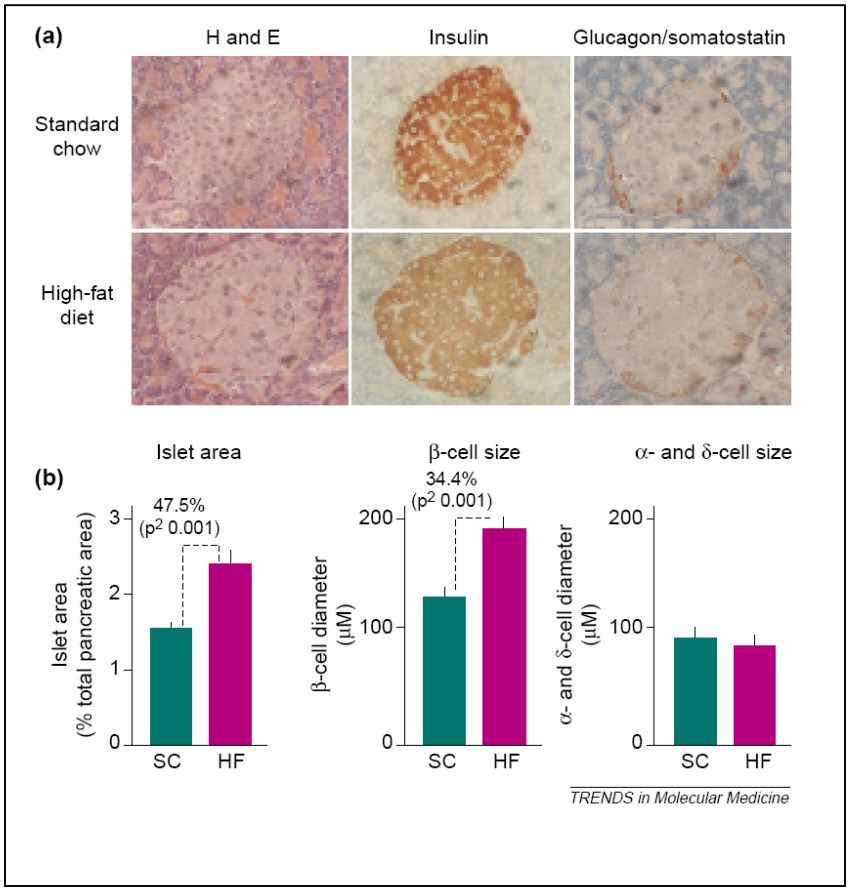

Adapted from (Lingohr et al., 2002a)

Fig. 16. Increased pancreatic β-cell area in normal rats fed a high-fat diet (HF; 42% calories from fat) for six weeks compared with rats fed standard chow (SC; 4% calories from fat).

(a) Serial sections of pancreata were fixed and stained with hematoxylin and eosin (H and E), or immunohistochemically for insulin to detect pancreatic β-cells, or for glucagon and somatostatin to give an indication of non β-cells in the islet. (b) There was a significant increase ($p \leq 0.05$) in β-cell mass in rats fed a high-fat diet compared with controls fed standard chow. This is, presumably, a response to an increase in insulin demand caused by peripheral insulin resistance in these animals (Buettner et al., 2000) .

Can genetic factors modulate β-cell growth?

IRS

IRS-1 knockout mice have peripheral insulin resistance and glucose intolerance, but this is compensated for by a marked increase in β-cell mass ensuring the animals do not develop *diabetes* (Fig. 17) (Tamemoto et al., 1994). By contrast, IRS-2 knockout mice, which also have insulin resistance, do not have the ability to compensate by increasing β-cell mass and these animals are diabetic (Withers et al., 1998). Indeed, β-cell mass in IRS-2 null mice is markedly reduced, and even more so when crossed with mice deficient in one allele for the IGF-1R (Fig. 17) (Withers et al., 1999). These IRS-2 knockout mice studies are complementary to observations that higher IRS-2, but not IRS-1, expression levels increase mitogenesis in rodent β-cell lines (Lingohr et al., 2002b). Thus, IRS-2 appears key in maintaining optimal β-cell mass to compensate for peripheral insulin resistance.

PKB

Overexpression of constitutively active PKBα in pancreatic β-cells of mice produces a significant increase in both β-cell size (Fig. 18) and total islet mass leading to improved glucose tolerance and resistance to streptozotocin-induced *diabetes* without increase of β-cell mitogenesis (Bernal-Mizrachi et al., 2001), (Tuttle et al., 2001). However, PKBα deficient mice display growth retardation but normal glucose homeostasis (Cho et al., 2001b). PKBβ deficient mice display insulin resistance accompanied by hyperinsulinemia and dramatic increase in the size and number of pancreatic islets although no report on individual β-cell size and number (Cho et al., 2001a).

S6K1

S6K1 deficient mice are hypoinsulinemic and mildly glucose intolerant due to reduction in β-cell mass and selective decrease in β-cell size (Fig. 19) (Pende et

al., 2000). Since S6K1 deficient mice are growth retarded (Shima et al., 1998), a similar phenotype to that of nutrient deprivation, further experiments would have to be performed to address if reduction of β-cell mass is likely to be a cell autonomous effect due to loss of S6K1 signaling or secondary consequences from developmental delay (see results).

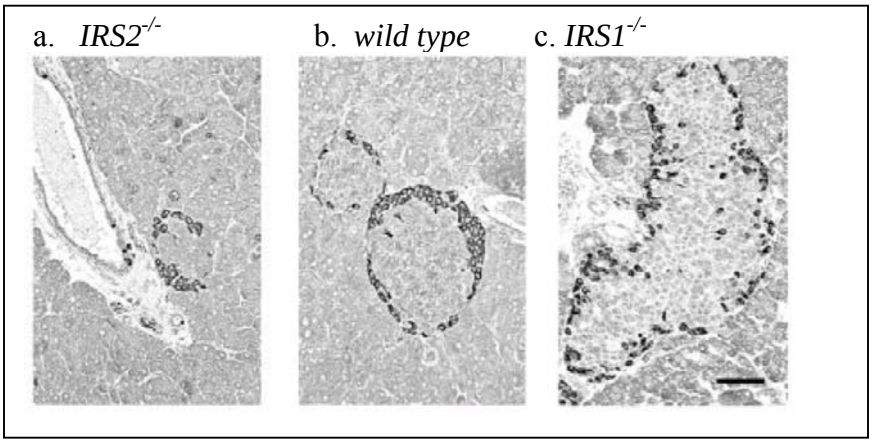

Adapted from (Withers et al., 1998)

Fig. 17. Islet morphology and β-cell mass in *IRS2*$^{-/-}$, *IRS1*$^{-/-}$ and wild-type mice.

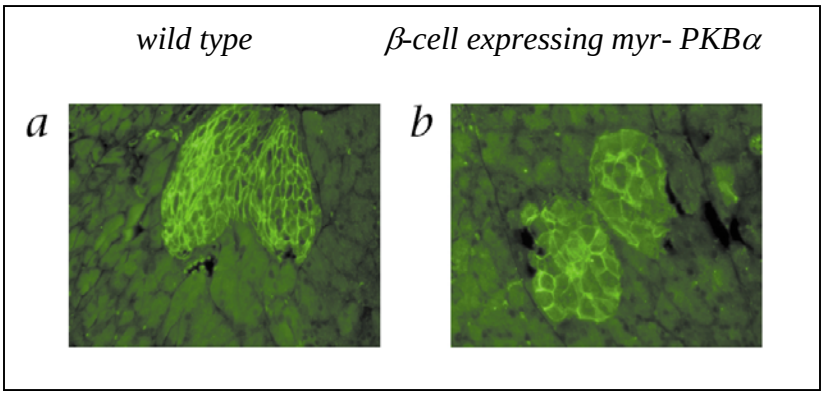

Adapted from (Tuttle et al., 2001)

Fig. 18. Fluorescent staining of GLUT2, glucose transporter. Constitutive active PKBα expression augments β-cell size.

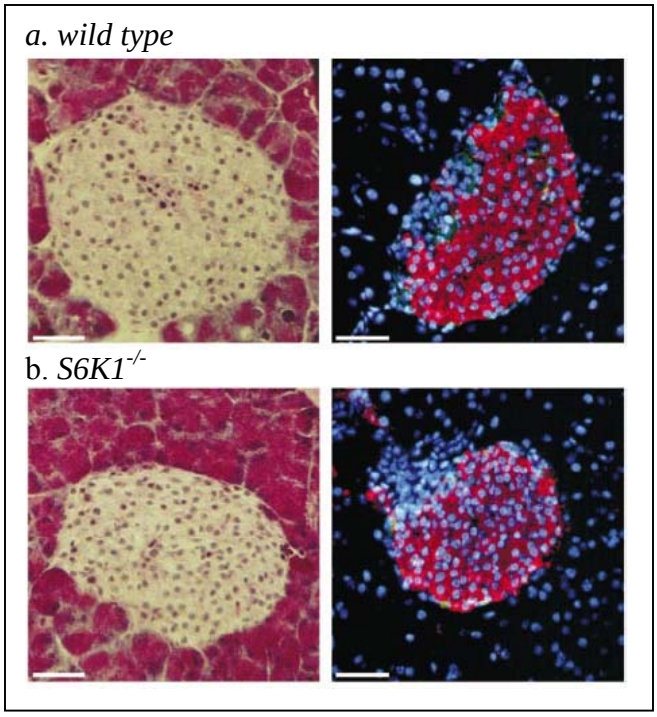

Adapted from (Pende et al., 2000)

Fig. 19. Haematoxyline and eosine stain (left) and immunostain for insulin- and glucagon-containing cells (right) in pancreas sections from wild type and S6K1$^{-/-}$ mice.

How can we distinguish between effects of nutrients provided by the placenta versus genetic defects on reduced β-cell size in S6K1 deficient mice?

-***Distinguishing between primary (due to a genetic defect) versus secondary defects (due to a placental defect).***

Given pancreatic β-cell development is exclusively sensitive to the level of nutrients provided by the placenta (Godfrey, 2002) and general fetal development, the dimished β-cell size phenotype (Pende et al., 2000) in S6K1 deficient mice may be a culmination of the loss of S6K1 gene function in the primary target cells, pancreatic β-cells (the primary effect), or additional effects that are elicited in other tissues such as the placenta (the secondary effect) which regulates nutrient transport required for pancreatic β-cell growth.

Since the main vascularization structure of the placenta originates from the trophoblast of embryo (Georgiades et al., 2001), S6K1 deficient embryos develop with S6K1 deficient placenta. Under these circumstances, it is difficult to dissect S6K1 deficient β-cell phenotype solely because β-cell development and growth are controlled by S6K1 deficient placenta. However, if we were able to provide a wild type placenta to the S6K1 deficient embryo using tetraploid aggregation techniques (Tam and Rossant, 2003), we would be able to distinguish between primary (due to a genetic defect) versus secondary defects (due to a placental defect).

Using ES cell tetraploid embryo chimeras, we could produce mouse fetuses by aggregating homozygous *S6K1*$^{-/-}$ embryonic stem (ES) cells with wild-type tetraploid embryos (Fig. 20). (Rossant and Cross, 2001; Rossant and Spence, 1998; Tam and Rossant, 2003). In the resulting chimeras, the embryos are ES cell derived. The wild type tetraploid cells contribute exclusively to the trophoblast cells of the placenta and endoderm of the yolk sac, but owing to increased ploidity, they are rigorously excluded from the embryo proper. Diploid ES cells cannot make trophoblast tissues *in vivo* but make up the entire embryo proper (Fig. 20). (Tam and Rossant, 2003). If chimeras produced by the

aggregation of *S6K1*$^{-/-}$ ES cells with tetraploid wild type embryos are not growth retarded and have normal β-cell growth and development, it will indicate that these features of *S6K1*$^{-/-}$ phenotype are caused secondarily by extra-embryonic dysfunction, most likely of the placenta (Fig. 20). However, if S6K1$^{-/-}$ ES cell derive fetus which are still small and have impaired pancreatic β-cell growth and development, it will imply that this phenotype occurs as a result of the loss of S6K1 in embryonic tissues, an effect that is unrelated to placental deficiency. Chimera analysis should thus be a useful tool to dissect cell autonomous versus non-cell autonomous roles of S6K1 in fetal growth and pancreatic β-cell development. The principle of tetraploid aggregation is shown in (Fig. 20).

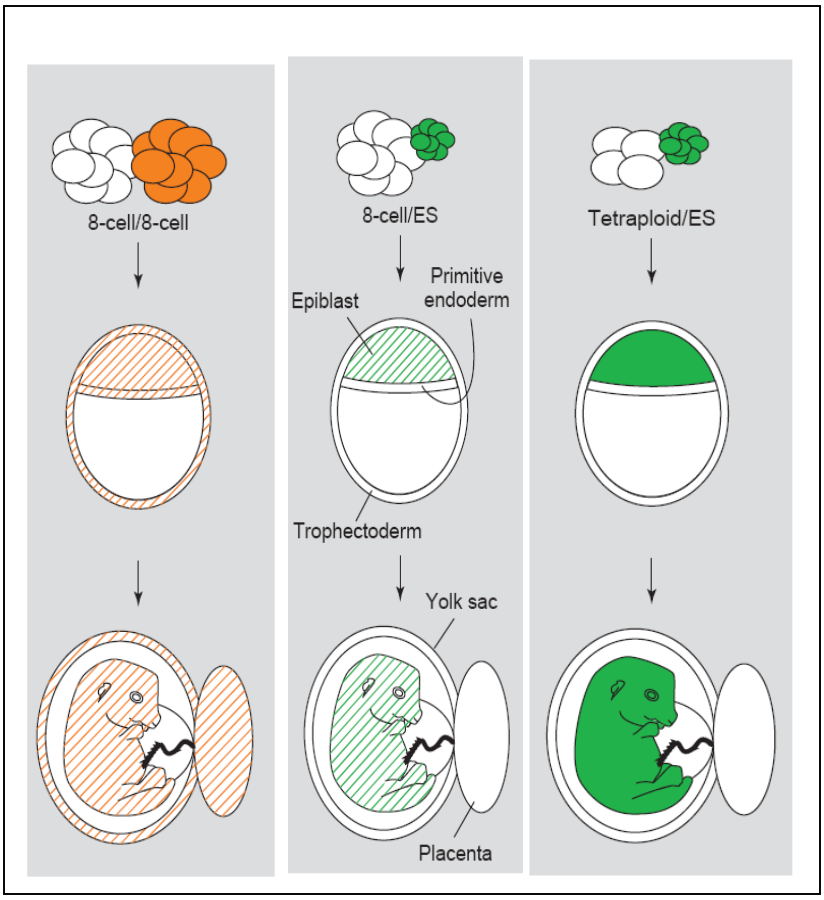

Adapted from (Rossant and Spence, 1998)

Fig. 20. Tissue contribution in chimeras.
The primitive endoderm gives rise to the entire endoderm layer of the yolk sac and the trophectoderm to the trophoblast layers of the placenta, while the epiblast gives rise to the entire

embryo as well as some extraembryonic cells. Orange-white combinations are embryo-embryo combinations; green-white combinations are ES cell-embryo combinations. Solid colours, non-mosaic contribution; stripes, mosaic contribution. Tetraploid embryos are generated by electrofusion of the blastomeres of a two-cell embryo.

II MATERIALS AND METHODS

Part 2: Absence of S6K1 protects against age- and diet-induced obesity while enhancing insulin sensitivity.

Mice

S6K1$^{-/-}$ mice were generated by homologous recombination and genotyped as previously described (Shima et al., 1998). *S6K1*$^{-/-}$ and WT mice were on a hybrid background derived from the C57Bl/6 and 129Ola mouse strains. Animals were maintained on a 12-h light/dark cycle and six month old male mice were used for experiments.

Diet studies and metabolic measurements

At 10 weeks age male mice were placed on either a NCD (Diet #3807, KLIBA-NAFAG, Switzerland) or HFD *ad libitum* (Diet D12492; Researchdiets, New Brunswick, NJ USA) and were followed for a period of 24 weeks. Body weight was recorded weekly and food intake was measured every second day for 15 consecutive days. Insulin tolerance tests were performed by intraperitoneal injection of insulin (0.75 U/kg body weight) after a 3 h fast. Blood was collected before injection and 15, 30, 60 and 90 min after injection. Oxygen consumption and RER were measured every 15 min for 8 h by an indirect calorimetric method, employing an Oxymax (Columbus Instruments, Columbus, OH)(Picard et al., 2002).

Metabolite assays

Blood was collected from retroorbital sinus after an overnight fast or 1 hr after the beginning of the meal followed by an overnight fast. The amount of non-esterified fatty acids, ketone bodies and triglycerides were measured by enzymatic assays (Boehringer-Mannheim, Germany)(Picard et al., 2002). Plasma leptin and total triiodothyronine and thyroxine serum levels were measured using either the Rat

leptin kit (Linco Research, St Louis, MO.) or the radioimmunoassay kit (Immunotech SA, Marseille, France), respectively (Picard et al., 2002).

Histology and morphometric analysis of tissues

Adipose tissue was removed from each animal, fixed in 10% formaldehyde/PBS for 24h, dehydrated and embedded in paraffin. 6µm sections were cut and stained with haematoxylin and eosin. Images were captured and morphometric analysis was performed with ImageJ software (NIH). Epididymal WAT from 500 or more cells from three different animals per genotype was analyzed. Adipose and plantaris muscle tissue were prepared as described for scanning and transmission electron microscopy (Picard et al., 2002).

Magnetic resonance imaging analysis

MRI experiments were carried out on a Biospec 47/30 spectrometer (Bruker Medical, Fällanden CH) at 4.7 T equipped with a self-shielded 12 cm bore gradient system, capable of switching 200 mT/m in 170 µs (Doty et al., 1999). During experiments animals were anaesthetized with 1.5% Isoflurane (Abbott, Cham Switzerland) in a 1:2 mixture of O_2/N_2O administered with a facemask. Adipose tissue was measured with an optimized turbo-RARE2 imaging sequence for body fat visualization 48. Acquisition parameters were: Repetition delay TR = 250 ms, echo delay TE = 8.6 ms, RARE factor = 32 (effective echo time 73.1 ms), number of averages NA = 8, slice orientation transverse, image matrix = 128x128 pixel, field-of-view FOV = 3.5x3.5 cm, slice thickness = 1.2 mm (contiguous). 50 to 64 transverse slices have been recorded. The volumes of fat pads were assessed with an in-house developed software algorithm based on IDL software package (Research Systems Inc., Boulder/CO U.S.A.). The images were filtered using a Gaussian-type filter and then classified in 16 classes followed by quantization, classes 7 to 16 being allocated to adipose tissue. Fat depot volumes were calculated based on the segmented area in each slice and the distance between slices. Body fat indices were calculated by dividing adipose tissue weight (i.e. adipose tissue volume multiplied with the specific weight of fatty tissue of 0.8 g/ml) by body weight.

Lipolysis in isolated adipocytes

Primary adipocytes were prepared from epididymal fat pads by collagenase digestion as described previously (Marette et al., 1991). Cells were incubated for 30 min at 37°C with or without norepinephrine (Sigma-Aldrich SARL, St-Quentin Fallavier, France) at the indicated concentrations.

Real-Time quantitative RT-PCR

Total RNA was extracted from frozen tissue samples or cells using the RNeasy kit (Qiagen, Courtaboeuf, France). cDNA was synthesized from total RNA with the SuperScript First-Strand Synthesis System (Invitrogen) and random hexamer primers. The real-time PCR measurement of individual cDNAs was performed using SYBR green dye to measure duplex DNA formation with the Roche Lightcycler system and normalized to the expression of either β actin or 18S ribosomal rRNA. The primers and probes used in the real time RT-PCR were the following: UCP1 sense, 5'-GGCCCTTGTAAACAACAAAATAC-3', and antisense, 5'-GGCAACAAGAGCTGACAGTAAAT-3'; UCP3 sense, 5'-ACTCCAGCGTCGCC ATCAGGATTCT-3', and antisense, 5'-TAAACAGGTGAGACTCCA GCAACTT-3'; mCPT1 sense, 5'-TTGCCCTACAGCTCTGGCATTTCC-3', and antisense, 5'-GCA CCCAGATGATTGGGATACTGT-3'; mPPAR δ sense, 5'-CTCTTCATCGCGGCCA TCATTCT-3', and antisense, 5'-TCTGCCATCTTCTGC AGCAGCTT-3'; PGC-1 sense 5'-AAGTGTGGAACTCTCTGGAACTG-3', and antisense 5'-GGGTTATCT TGGTTGGCTTTATG-3'.

Measurement of insulin receptor phosphorylation *in vivo*.

After a 6 hour fast, mice were anesthetized and 0.75Ukg^{-1} insulin (Eli Lilly) or an equal volume of vehicle was administered by i.v. injection. Liver, adipose (Epididymal fat pads) and muscle (Gastrocnemius) were collected in liquid nitrogen 5 minutes after injection. Insulin receptor tyrosine phosphorylation was measured in liver. Protein extracts (1mg) from tissue samples were prepared for immunoprecipitation and analyzed as described (Hirosumi et al., 2002). Antibodies

were purchased from Santa Cruz (anti-insulin receptor β, and anti-S6K1), Upstate Biotechnology (anti-phosphotyrosine) and Cell Signaling (anti-PKB, anti-IRS-1, anti-phospho PKB-Ser473, anti-phospho IRS1-Ser 636/639, anti-phospho S6K-Thr 389, anti-phospho S6 240/244). Antibodies to S6 were provided by J. Mestan (Novartis Pharma AG, Basel, Switzerland).

RNA interference

Double stranded RNA duplexes corresponding to mouse and human S6K1 (5'-AAGGGGGCTATGGAAAGGTTT-3') were purified, annealed, and transfected into HeLa cells using oligofectamine (Invitrogen). The effect of RNAi on S6K1 expression and on insulin dependent PKB phosphorylation was measured after 72 hours. Following overnight serum deprivation, cells were either lysed directly or stimulated with 200 nM insulin for 30 minutes. Cell lysates were incubated for 4h with anti IRS1 or anti insulin receptor β antibody pre-absorbed on protein A sepharose beads at 4°C and washed. Equal amounts of cleared lysates were analyzed by Western blot analyses with the indicated antibodies. All RNAi experiments were performed on at least three independent times with comparable results.

Statistical Analysis

Data are presented as mean ± s.e.m. The main and interactive effects were analyzed by ANOVA factorial or repeated measurements (growth curve and insulin tolerance tests) or one-way ANOVA followed by Bonferroni t-test (MRI analysis). Differences between individual group means were analyzed by the Fisher's PLSD test or Student's t test. Analyses were performed using Statview Software (Brainpower, Calabasas, CA). Differences were considered to be statistically significant at $P<0.05$.

Part 3: Regulation of pancreatic β-cell growth by S6K1 during development

Mice

Wild type (*S6K1*$^{+/+}$) and *S6K1*$^{-/-}$ mice were generated by homologous recombination and genotyped as previously described (Pende et al., 2000). Animals were maintained on a 12-h light/dark cycle. Embryos and placentas used in this study were derived from homozygous crosses or intercrosses between *S6K1*$^{+/-}$ mice. The genotypes of dissected embryos and placentas were determined by Southern blot analysis or PCR using DNA isolated from the yolk sac or placenta. The PCR primers corresponded to the S6K1 (S6K1 forward, 5'-GTAGGGCACTTAAATGACCAC-3'; S6K1 reverse, 5'-TGTCCCTATT AATGCTCAAGG-3') and the neo gene (neo reverse, 5'-GCCTTCTTGACGA GTTC TTCTGAG-3').

Histological analysis

Embryos and placentas were freshly collected and fixed in 10% formalin overnight at 4°C. Fixed samples were embedded in paraffin and 5μm-sections were cut and mounted on slides such that series of six slides with comparable sections were created. For general morphological analysis, one slide from each series was stained with haematoxylin and eosin. For immunofluorescence, sections of embryonic pancreas were stained with rabbit anti-glucagon (Zymed, 1:50), guinea pig anti-insulin (Linco, 1:400), and rabbit anti-Glut2 (provided by B. Thorens, 1:200). Detection was performed using Alexa Fluor 488 and 594 (Molecular Probes). Morphometrical analysis and cell counting was done on pancreases from three individuals for each genotype using ImagePro Plus software (Media Cybernetics). α- and β-cell counting was performed on pancreas sections representing 1/6 of the organ. To calculate the mean size of the individual α and β cells, the cell area was divided by the number of cell nuclei in the covered area positive for either insulin or glucagon as previously described (Shima et al., 1998). Immunohistochemistry and *in situ* hybridization on placenta sections was performed using sections from the middle of each placenta from three embryos for each genotype. For anti-PECAM-1

staining, the sections were incubated with 0.1% Trypsin for 12 min at 37°C after rehydration, followed by 20 min incubation with 2N HCl. They were then incubated overnight at 4°C with rat monoclonal anti-PECAM-1 (Pharmingen, 1:50). Biotinylated horse anti-rat (Vector Lab) was used as a secondary antibody, followed by incubation with the ABC-reagent (Vector Lab), detection with DAB (Vector Lab), and nuclear counterstaining with haematoxylin.

In situ hybridization analysis

Dr. Janet Rossant provided the plasmid pKS 4311. The 4311 (*Tpbp*) gene is used as a molecular marker specific for spongiotrophoblast cells. Sections were rehydrated and tissue was permeabilized using 20µg/ml proteinase K in 10mM Tris pH8/20mM EDTA for 15 min at room temperature, refixed in 4% paraformaldehyde/0.2% glutaraldehyde, and dehydrated in a graded series of methanol. Antisense and sense riboprobes were generated by *in vitro* transcription using the DIG RNA Labeling Kit (Roche Diagnostics) (Wilkinson and Nieto, 1993). The DIG-labeled probe was denatured at 70°C for 7 min and used in hybridization buffer. 50µl hybridization solution were applied per section, and incubated in a hybridization oven at 60°C. The next day, slides were washed twice for 30 min in 25% formamide/2x SSC at 60°C, 30 min in 2x SSC at 60°C, 30 min in 0.2% SSC at 60°C, and 3x 10 min in PBS/0.1% Triton X-100 at room temperature. Blocking sections were incubated with 10% sheep serum in PBS/0.1% Triton X-100 for 30 min. Incubation with AP-conjugated anti-DIG antibody (Roche) occurred at 1:2000 in blocking buffer overnight at 4°C. Sections were washed and followed by a 10 min wash in NTMT buffer (100mM TrisHCl pH9.5, 50mM $MgCl_2$, 100mM NaCl, 0.1% Triton X-100). NBT (nitroblue tetrazolium chloride) and BCIP (5-bromo-4-chloro-3-indoyl-phosphate, 4-toluidine salt) (both from Roche) were used as a substrate.

Measurement of insulin content in embryonic pancreas

Isolated embryonic pancreases were placed into phosphate-buffered saline (PBS) and then sonicated three times for 10s. The insulin concentration was measured

using ELISA (Crystal Chem Inc., Illinois, USA) or radioimmunoassay (Linco, St. Louis, USA).

Embryo growth analysis

For the staging of embryos, we considered noon of the day of the vaginal plug appearance as E0.5. For developmental analysis of growth, embryos and placentas were dissected, patted dry with absorbent paper, and wet weights were determined using a microbalance.

Preimplanation development *in vitro*

Following superovulation and mating, E1.5 embryos or E3.5 embryos were collected and individually cultured as described. Each embryo was subsequently transferred to a drop of M16 medium overlaid with mineral oil and incubated at 37°C. The morphology of the embryos was recorded (Nagy, 2002) .

Skeletal staining

Embryos were eviscerated, skinned, fixed in ethanol and then stained with Alcian Blue 8GS (cartilaginous elements) and Alizarin Red S (mineralized elements) for 3-5 days, as adapted from McLeod (McLeod, 1980). The tissues were cleared with 1% KOH and the skeletons stored in glycerol.

Scanning electron microscopic analysis

Embryos were fixed in 1.25% glutaraldehyde, 1% paraformaldehyde in 0.08M cacodylate buffer containing 0.02% $CaCl_2$ for 1h at room temperature, and overnight at 4°C. They were postfixed in 1% OsO_4 in water, washed, and dehydrated by alcohol. Scanning electron microscopic analysis was performed as described (Picard et al., 2002).

Establishment of embryonic stem (ES) cells

Embryos were flushed at the morula stage and incubated overnight in M16 medium. The next day, the blastocysts were transferred to 6cm dishes with

500,000 inactivated mouse fibroblasts and 500,000 inactivated 5637 cells (ATCC HTB9) known to facilitate ES cell development. A few days later, the ICM were picked with a glass pipette, treated with trypsin for 10 min at room temperature, and further propagated on inactivated fibroblasts. The medium was always KO-DMEM supplemented with 15% FBS, pen/strep, glutamin, β-mercaptoethanol, gentamycin, and LIF (Nagy, 2002).

Aggregation of tetraploid wild type embryos with diploid *S6K1*$^{-/-}$ ES cells

Wild type embryos derived from *S6K1*$^{+/+}$ mice were recovered at the 2-cell stage (E1.5). The two blastomeres were fused by elecrofusion (Nagy, 2002), and the resulting tetraploid embryos (Nagy et al., 1993) cultured for 48 hours at 37°C, 5% CO_2, and 100% humidity in M16 medium (Nagy, 2002). Following culture, the zona pellucida was removed from the 4-cell stage tetraploid embryos by Tyrod's Acid treatment (Nagy, 2002). Micro-drops of M16 media were placed in plastic tissue culture dishes, and covered with light mineral oil (Merck). Depression wells were created within the micro-drops using a blunt darning needle. Two tetraploid embryos were placed in each well. Three independent *S6K1*$^{-/-}$ ES cell clones were prepared by 5 min trypsin (Life Technologies) treatment to create a single cell suspension. Residual fibroblast feeder cells were removed by 15 min pre-plating at 37°C, and careful removal of the ES cell-containing suspension from the fibroblasts adhering to the culture dish. The ES cell suspension was allowed to re-aggregate into small clumps by incubation for approximately 1 hour at room temperature. One small clump of approximately 1-15 ES cells was placed in each well containing two tetraploid embryos. The aggregates were incubated overnight at 37°C, 5% CO_2, and 100% humidity. The following day, blastocyst stage embryos could be harvested from the wells, and were implanted into the uterus of E2.5 pseudopregnant recipient CD1 outbred female mice.

Generation of transgenic mice expressing S6K1 in pancreatic β-cells

The transgene consisted of a 720-bp fragment of the rat insulin II promoter (rip) driving transcription of myc-S6K1. Injection of DNA containing rip-S6K1 into fertilized eggs was performed by the FMI transgenic and chimeric mouse facility. Founders were identified using PCR analysis, and germ line transmission was confirmed by Southern blotting. Genotyping was executed by PCR using primers derived from rip and an internal S6K1 sequence. To obtain mice with a homozygous knockout for S6K1 that were rip-S6K1 transgene positive ($S6K1^{-/-}rip^{S6K1}$), $S6K1^{+/-}rip^{S6K1}$ and $S6K1^{+/-}$ were crossed. $S6K1^{+/-}$ were maintained on a pure C57BL/6 background.

Assessment of transgene expression

Genotypes of embryos, placentas, and mice were determined by Southern blot analysis or PCR. Isolated islets were obtained by collagenase P digestion as previously described. For western blot analysis, blots of islet lysates were probed with antibodies against S6K1 (Santa Cruz Biotechnology, Santa Cruz, California, USA) and myc (Upstate Biotechnology). The nested PCR primers corresponding to rip were foward 5'-CAGGCCACCCAGGAGCCCC-3', reverse 1: 5'-GCATGATGTTCTCCGGCTTCAGG-3', reverse 2: 5'-GTAAATGCC CCAAAGCCATGGAG-3'

Statistical analysis

Data are presented as mean ± s.e.m. The main and interactive effects were analyzed using factorial, repeated measures, or one-way ANOVA. Differences between individual group means were analyzed using the Fisher's PLSD test or Student's *t* test. Analyses were performed using Statview Software (Brainpower, Calabasas, California, USA). Differences were considered to be statistically significant at $P<0.05$.

III. RESULTS

Part 1: ……

S6K1 (-/-)/S6K2 (-/-) mice exhibit perinatal lethality and rapamycin-sensitive 5'-terminal oligopyrimidine mRNA translation and reveal a mitogen-activated protein kinase-dependent S6 kinase pathway.

Pende M, Um SH, Mieulet V, Sticker M, Goss VL, Mestan J, Mueller M, Fumagalli S, Kozma SC, Thomas G.
Mol Cell Biol. 2004, 24(8):3112-24

MOLECULAR AND CELLULAR BIOLOGY, Apr. 2004, p. 3112–3124 Vol. 24, No. 8
0270-7306/04/$08.00+0 DOI: 10.1128/MCB.24.8.3112–3124.2004
Copyright © 2004, American Society for Microbiology. All Rights Reserved.

S6K1$^{-/-}$/*S6K2*$^{-/-}$ Mice Exhibit Perinatal Lethality and Rapamycin-Sensitive 5′-Terminal Oligopyrimidine mRNA Translation and Reveal a Mitogen-Activated Protein Kinase-Dependent S6 Kinase Pathway

Mario Pende,[1,2]* Sung Hee Um,[1] Virginie Mieulet,[2] Melanie Sticker,[1] Valerie L. Goss,[3] Jurgen Mestan,[4] Matthias Mueller,[4] Stefano Fumagalli,[1] Sara C. Kozma,[1] and George Thomas[1]*

Friedrich Miescher Institute for Biomedical Research, 4058 Basel,[1] and Novartis Pharma AG, 4057 Basel,[4] Switzerland; INSERM 584, Hormone Targets, 75015 Paris, France[2]; and Cell Signaling Technology, Beverly, Massachusetts 01915[3]

Received 18 July 2003/Returned for modification 18 September 2003/Accepted 14 January 2004

Activation of 40S ribosomal protein S6 kinases (S6Ks) is mediated by anabolic signals triggered by hormones, growth factors, and nutrients. Stimulation by any of these agents is inhibited by the bacterial macrolide rapamycin, which binds to and inactivates the mammalian target of rapamycin, an S6K kinase. In mammals, two genes encoding homologous S6Ks, S6K1 and S6K2, have been identified. Here we show that mice deficient for S6K1 or S6K2 are born at the expected Mendelian ratio. Compared to wild-type mice, *S6K1*$^{-/-}$ mice are significantly smaller, whereas *S6K2*$^{-/-}$ mice tend to be slightly larger. However, mice lacking both genes showed a sharp reduction in viability due to perinatal lethality. Analysis of S6 phosphorylation in the cytoplasm and nucleoli of cells derived from the distinct S6K genotypes suggests that both kinases are required for full S6 phosphorylation but that S6K2 may be more prevalent in contributing to this response. Despite the impairment of S6 phosphorylation in cells from *S6K1*$^{-/-}$/*S6K2*$^{-/-}$ mice, cell cycle progression and the translation of 5′-terminal oligopyrimidine mRNAs were still modulated by mitogens in a rapamycin-dependent manner. Thus, the absence of S6K1 and S6K2 profoundly impairs animal viability but does not seem to affect the proliferative responses of these cell types. Unexpectedly, in *S6K1*$^{-/-}$/*S6K2*$^{-/-}$ cells, S6 phosphorylation persisted at serines 235 and 236, the first two sites phosphorylated in response to mitogens. In these cells, as well as in rapamycin-treated wild-type, *S6K1*$^{-/-}$, and *S6K2*$^{-/-}$ cells, this step was catalyzed by a mitogen-activated protein kinase (MAPK)-dependent kinase, most likely p90rsk. These data reveal a redundancy between the S6K and the MAPK pathways in mediating early S6 phosphorylation in response to mitogens.

Recent studies showed that the 40S ribosomal protein S6 kinase (S6K) p70^{S6K}/p85^{S6K}, termed S6K1 (51), is a major effector of cell growth. This conclusion stems from gene deletion studies with *Drosophila* (39) and with mice (51) as well as recent studies with cell cultures (11). The loss of the *Drosophila* S6K (dS6K) gene is semilethal, with the few surviving adults having a severely reduced body size. The larvae of such flies exhibit a long developmental delay, consistent with a twofold increase in cell cycle doubling times. The few surviving adults are quite lethargic, living no longer than 2 weeks, and females are sterile. Surprisingly, the reduction in mass is strictly due to a decrease in cell size rather than to a decrease in cell number (39).

In mice, removal of this kinase is not lethal, but the mice are approximately 20% smaller at birth (51). Such mice exhibit normal fasting glucose levels but are mildly glucose intolerant due to markedly reduced levels of circulating insulin (42). Reduced insulin levels are caused by a reduction in pancreatic endocrine mass and an impairment of insulin secretion, which can be traced to a selective reduction in β-cell size. Unexpectedly, the effects on body mass and hypoinsulinemia do not appear to be attributable to a reduction in S6 phosphorylation, as this response proved to be largely intact in S6K1-deficient animals (51). However, S6 phosphorylation in such animals was still sensitive to the bacterial macrolide rapamycin (51), which inhibits the mammalian target of rapamycin (mTOR) (1, 7, 16, 48), the upstream S6K1 kinase (4, 8, 18), suggesting the existence of a second S6K. Subsequent searches of expressed sequence tag databases and biochemical studies led to the identification of S6K2, which exhibited overall homology of over 80% with S6K1 in the highly conserved kinase and linker domains (17, 47, 51). In all tissues examined from S6K1-deficient mice, S6K2 transcripts were upregulated (51). From this observation, it was reasoned that S6K1 and S6K2 functions were redundant and that a deletion of the S6K1 gene led to a compensatory increase in the expression of S6K2.

In parallel studies, it was demonstrated that rapamycin suppressed the serum-induced translational upregulation of a family of mRNAs which contain a polypyrimidine tract at their 5′ end (5′-terminal oligopyrimidine [5′TOP] mRNAs) (20, 55). These mRNAs largely code for components of the transla-

* Corresponding author. Mailing address for Mario Pende: INSERM 584, Hormone Targets, 156 Rue de Vaugirard, 75015 Paris, France. Phone: 0033 1 40 61 53 15. Fax: 0033 1 43 06 04 43. E-mail: pende@necker.fr. Mailing address for George Thomas: Friedrich Miescher Institute for Biomedical Research, Maulbeerstr. 66, 4058 Basel, Switzerland. Phone: 0041 61 697 3012. Fax: 0041 61 697 3976. E-mail: gthomas@fmi.ch.

tional apparatus, most notably, ribosomal proteins (37). Earlier studies had shown that the translation of such transcripts is under selective translational control (22) and requires an intact 5′TOP tract (19, 49). In addition, a dominant interfering allele of S6K1 inhibited the mitogen-induced translational upregulation of 5′TOP mRNAs to the same extent as rapamycin, whereas an activated allele of S6K1, which exhibits a substantial degree of rapamycin resistance, largely protected these transcripts from the inhibitory effects of rapamycin (19, 49).

Seemingly consistent with these arguments, in embryonic stem (ES) cells from which S6K1 had been homologously deleted by selection with high doses of G418, serum no longer had an effect on the upregulation of 5′TOP mRNAs, nor was there a redistribution of 5′TOP mRNAs from polysomes to nonpolysomes in the presence of rapamycin (24). However, S6 phosphorylation was initially reported to be abolished in these cells (24), despite the fact that it was largely intact in cells and tissues derived from $S6K1^{-/-}$ mice (51). This difference seemed to be resolved in subsequent studies, where S6 phosphorylation was detected in these same $S6K1^{-/-}$ ES cells and S6K2 was present and active (31, 60). Despite these observations, it was again recently reported that S6 phosphorylation was absent from these same cells (53). Furthermore, it was also claimed in the latter study that S6K activation, S6 phosphorylation, and rapamycin had little impact on 5′TOP mRNA translation in PC12 cells (53), although others working with these same cells had reported earlier that rapamycin treatment abolished the selective recruitment of these transcripts from small to large polysomes (44).

Obviously, cells lacking both S6K1 and S6K2 would facilitate such studies. Therefore, we set out to delete the *S6K2* gene from mice and to determine whether we could generate $S6K1^{-/-}/S6K2^{-/-}$ mice. Here we report on the deletion of the *S6K2* gene and the effects of deleting both *S6K1* and *S6K2* on animal growth and viability as well as on S6 phosphorylation, cell proliferation, and 5′TOP mRNA translation.

MATERIALS AND METHODS

Generation of an S6K2-targeted allele. A P1 129/Ola mouse ES cell library (Genome Systems Inc., St. Louis, Mo.) was screened by PCR with the following S6K2-specific primers: 5′-CCTTTGAGGGGTTCCGG and 5′-TTCTCACAGC TGCCCTCTCTTCCTCTATTCTCCTAACG. A positive clone containing a genomic DNA fragment larger than 70 kb encompassed all of the S6K2 coding exons. The 1.3-kb EcoRI-PstI fragment of the S6K2 gene was ligated to the ClaI-NotI sites of a targeting vector containing a neomycin resistance gene and a thymidine kinase gene for negative selection and positive selection, respectively (2). The 5.5-kb SmaI fragment of the S6K2 gene was ligated to the HpaI site of the targeting vector (Fig. 1A). The S6K2 targeting vector was linearized at the ClaI site and electroporated into E14 129/Ola ES cells as described previously (51). Homologous recombination events were identified by Southern blot analysis of ES cell DNA after digestion with BamHI and hybridization with the probe corresponding to the 1-kb BamHI-SpeI fragment of the S6K2 gene (Fig. 1A). Three clones were found to be positive for the homologous recombination event. Hybridization with a probe for the neomycin resistance gene revealed a single integration site.

Animals and cell cultures. S6K2-targeted ES cells from clone 36 were aggregated with morula-stage embryos as described previously (51). Chimeric mice were crossed with C57BL/6 mice, and germ line transmission was assessed by Southern blot analysis. $S6K2^{-/-}$ mice were crossed with $S6K1^{-/-}$ mice (51) to generate mice carrying the combined deletions. Wild-type and mutant mice initially were kept in a hybrid C56BL/6-129/Ola background and subsequently were backcrossed in a pure C57BL/6 background for 10 generations. Animals were maintained on a 12-h light-dark cycle and were allowed free access to food. Mouse embryonic fibroblasts (MEFs) were prepared from embryos at embryonic day 13.5 and analyzed for cell proliferation and mRNA translation as previously described (51).

Primary hepatocytes from 12- to 14-week-old male mice were isolated by liver perfusion by the method of Seglen (50) as modified by Klaunig et al. (25). After cannulation in the subhepatic vena cava, the liver was perfused at a flow rate of 10 ml/min with calcium-free HEPES buffer (0.33 mM, pH 7.6) for 3 min and then with HEPES buffer containing 7 μg of collagenase (Liberase; Roche)/ml and 5 mM calcium chloride for 5 min. The solutions were allowed to run through a cut made in the portal vein. After enzymatic digestion, cells were collected in L-15 medium (Invitrogen Corporation) supplemented with 1 mg of bovine serum albumin (BSA)/ml, filtered, and centrifuged for 2 min at $100 \times g$. Viable hepatocytes were purified by centrifugation on a 45% Percoll gradient for 10 min at $100 \times g$. The pellet was collected and washed twice in L-15 medium containing 1 mg of BSA/ml. Hepatocytes were plated at 12×10^4 cells/cm^2 in Primaria dishes (Falcon) or on coverslips coated with collagen I (Sigma) in M-199 medium (Invitrogen) supplemented with 10% fetal calf serum (FCS), 1 mg of BSA/ml, and 100 nM dexamethasone in a 37°C incubator with a 5% CO_2 atmosphere. After 3 h of adhesion, cells were incubated in serum-free M-199 medium containing 1 mg of BSA/ml. On the next day, hepatocytes were treated as indicated above. All of the media contained penicillin (100 U/ml), streptomycin (100 μg/ml), and amphotericin B (Fungizone) (250 ng/ml).

Antibody production. S6K2 cDNA sequences coding for amino acids 1 to 43 or 440 to 484 were cloned into vector pMAL (New England Biolabs) to bacterially express N-terminal or C-terminal S6K2 peptides fused to maltose binding protein. Fusion proteins were purified according to the manufacturer's protocol. Monoclonal antibodies (MAbs) were generated by immunization of BALB/c mice with the following protocol. Two mice were immunized by intrasplenic injection (52) of 13.5 μg of purified antigen, 10 μg of adjuvant peptide (*N*-acetylmuramyl-L-alanyl-D-isoglutamine; Sigma A5919), and 10 mg of liposomes, with encapsulated muramyl tripeptide phosphatidylethanolamine as an additional adjuvant (mixed in phosphate-buffered saline [PBS]; total volume, 70 μl). Booster injections with mixtures of 15 μg of antigen, 10 μg of adjuvant peptide, 550 U of interleukin 2, and 560 U of gamma interferon with 10 mg of liposomes in PBS were administered at days 17 (subcutaneously [s.c.]), 33 (s.c. and intrperitoneally [i.p.]), 49 (s.c.), and 67 (s.c. and i.p.).

Serum samples were taken on days 40 and 73 and tested for the presence of specific antibodies by using an enzyme-linked immunosorbent assay with full-length S6K2 protein fused to glutathione *S*-transferase (GST) (N terminus free and C terminus free, respectively). A final booster injection (same composition) was administered i.p. at day 86, followed by fusion of the spleen cells (30) at day 89. The fusion partner cell line was mouse myeloma line SP2/0-AG-14. After hypoxanthine-aminopterin-thymidine selection, hybridomas were grown in HB101 hybridoma medium containing 10% CLEX serum supplement, and hybridoma supernatants were screened for the presence of antibodies to the GST-S6K2 fusion protein. Positive hybridoma cells were subcloned, and clones producing specific MAbs were selected (enzyme-linked immunosorbent assay, Western blotting, and immunocytochemical analysis). MAbs to the S6K2 N terminus (140.9.11 and 140.8.1) and to the S6K2 C terminus (141.8.5 and 141.5.23) were identified, and milligram amounts were produced by using a Miniperm culture system (Heraeus). Clones were screened for binding to the full-length S6K2 protein fused to GST.

2D PAGE, immunoprecipitation, immunoblotting, kinase assays, and nuclear fractionation. Total 80S ribosomal proteins were isolated from either MEFs or mouse liver, and the level of in vivo S6 phosphorylation was examined by two-dimensional (2D) polyacrylamide gel electrophoresis (PAGE) as previously described (36, 41). For the preparation of total protein extracts, MEFs and hepatocytes were washed twice with cold PBS, scraped from the culture dish into egg lysis buffer, and homogenized with 10 strokes in a Teflon-glass homogenizer. To remove cell debris, homogenates were spun at $8{,}000 \times g$ for 10 min. For the preparation of nuclear and cytosolic extracts, cells were scraped into hypotonic buffer (10 mM morpholinepropanesulfonic acid [MOPS] [pH 7.4], 10 mM KCl, 2 mM $MgCl_2$, 0.1 mM EDTA, 5 mM dithiothreitol [DTT]), homogenized with 10 strokes in a glass-glass homogenizer, and spun at $8{,}000 \times g$ for 3 min. The supernatants represented the cytosolic extracts. To purify nuclear proteins, pellets were resuspended in buffer I (0.32 mM sucrose, 3 mM $CaCl_2$, 2 mM Mg acetate, 0.1 mM EDTA, 0.1% Triton X-100, 1 mM DTT, 10 mM Tris [pH 8]), layered onto a sucrose cushion (2 M sucrose, 5 mM Mg acetate, 0.1 mM EDTA, 1 mM DTT, 10 mM Tris [pH 8]), and spun at $30{,}000 \times g$ for 45 min. Protein concentrations were measured by using a Bio-Rad D/C protein assay.

For immunoblot analysis, protein extracts were resolved by sodium dodecyl sulfate-PAGE before transfer to Immobilon membranes and incubation with the following primary antibodies: mouse anti-N-terminal or anti-C-terminal S6K2, rabbit anti-ribosomal protein L7a (62), rabbit anti-phosphorylated ribosomal

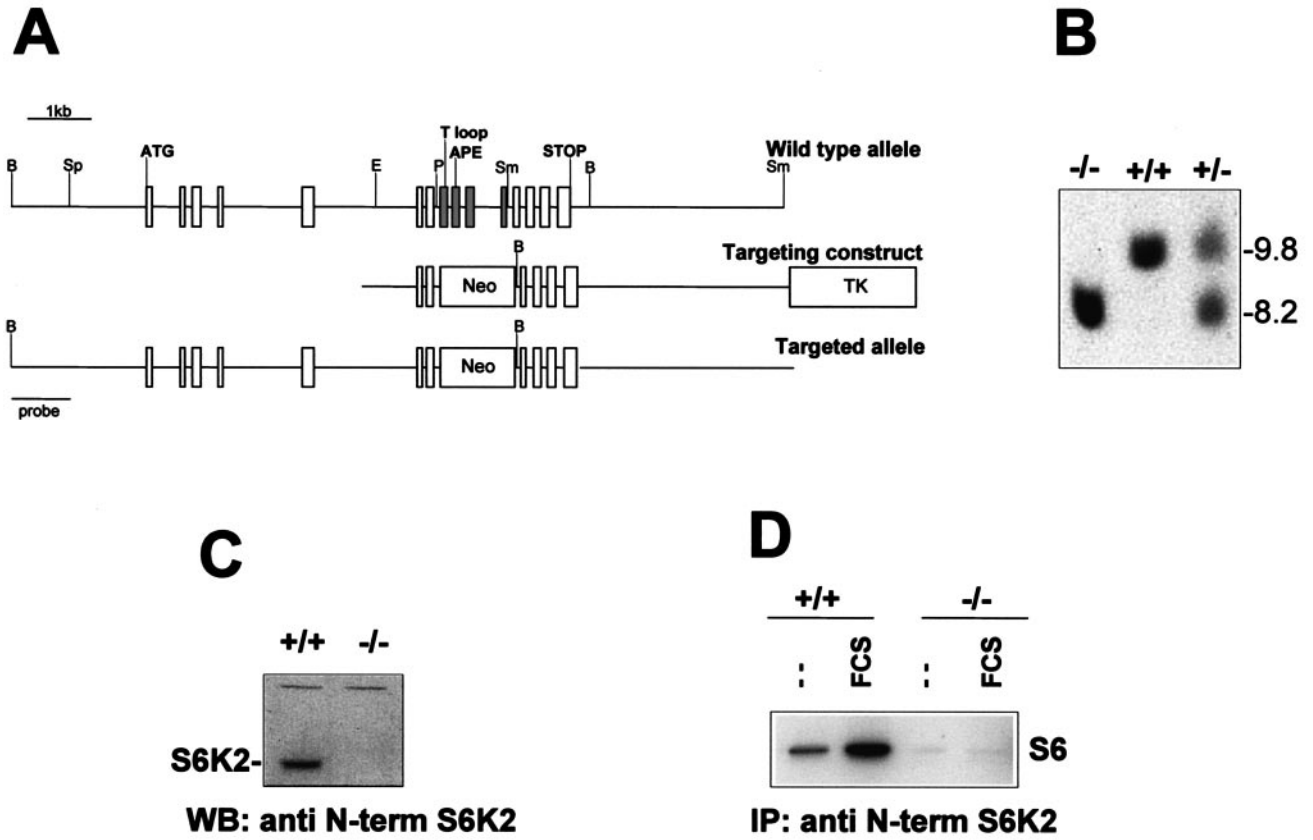

FIG. 1. Generation of an *S6K2*-null allele. (A) Murine *S6K2* gene map and targeting vector. Rectangles represent the coding exons of the *S6K2* gene as well as the neomycin resistance (Neo) and thymidine kinase (TK) genes. The exons containing the T loop and APE sequences and the initiation and stop codons are indicated. The four exons deleted following the homologous recombination event are shown in grey. Restriction sites: B, BamHI; Sp, SpeI; E, EcoRI; P, PstI; Sm, SmaI. (B) Genotypes of littermates from $S6K2^{+/-}$ crosses. Tail DNA was digested with BamHI, analyzed by Southern blotting, and hybridized with the probe depicted in panel A. The corresponding BamHI fragments of genomic DNA are 9.8 kb in the wild-type allele and 8.2 kb in the targeted allele. (C and D) Loss of S6K2 protein and kinase activity in S6K2 homozygous mutant cells. (C) Western blot (WB) analysis of fibroblast cell extracts from wild-type or $S6K2^{-/-}$ embryos with a MAb against the N-terminal (N-term) region of S6K2. The apparent molecular mass of S6K2 is 68 kDa. (D) MEFs from wild-type or $S6K2^{-/-}$ embryos were starved overnight and either stimulated with 10% FCS for 30 min or left untreated. Equal amounts of protein extracts were immunoprecipitated (IP) with the anti-S6K2 antibody, and S6K activity was measured with an immune complex assay (see Materials and Methods).

protein S6 (Ser235 and Ser236 [Ser235/236] and Ser240 and Ser244 [Ser240/244]), and anti-phosphorylated ERK1/ERK2 (Cell Signaling Technology). The specificity of the anti-phoshorylated S6 antibodies was demonstrated by competition with differentially phosphorylated S6 peptides (V. L. Goss and R. Polakiewicz, unpublished data). For immunoprecipitation, 300 μg of protein extract was incubated with 4 μg of MAb precoupled to protein G-Sepharose beads. S6K activity was measured by using an immune complex assay with 40S ribosomal subunits as a substrate as previously described (45).

Immunofluorescence analysis. Primary hepatocytes were plated at 12×10^4 cells/cm^2 on coverslips coated with collagen I and incubated overnight in M-199 medium containing 1 mg of BSA/ml. Hepatocytes were stimulated with 1 μM insulin, 25 ng of epidermal growth factor (EGF)/ml, and 10% FCS for 1 h in the presence or absence of 20 nM rapamycin. Cells were washed twice with Tris-buffered saline (TBS) (50 mM Tris [pH 7.4], 150 mM NaCl), fixed with 4% paraformaldehyde for 10 min at room temperature, and washed once again with TBS. Cells were permeabilized with methanol for 5 min at −20°C and washed three times for 5 min each time with TBS. Incubation in fresh 0.1% sodium borohydride in TBS for 5 min quenched the activity of the cells. Cells were rinsed once in TBS, blocked for 1 h at room temperature with PBS containing 10% goat serum, 1% BSA, and 0.02% sodium azide, and washed for 5 min with TBS. Prior to use, anti-phosphorylated ribosomal protein S6 (Ser235/236) primary antibodies or anti-60S ribosomal protein L7a primary antibodies were centrifuged at $13{,}000 \times g$ for 5 min at 4°C, diluted 1:200 in TBS containing 0.1% BSA, and applied to the cells during overnight incubation at 4°C. After three washes for 5 min each time with TBS, the cells were incubated with a secondary fluorescent antibody (anti-rabbit Alexa 488; Molecular Probes) diluted 1:200 in TBS containing 0.1% BSA for 45 min at room temperature. After the cells were washed three times for 5 min each time with TBS in the dark, coverslips were mounted with a ProLong antifade kit (Molecular Probes) and observed under a confocal microscope.

Histological analysis. Newborn mice were left for several minutes on ice before being anaesthetized and sacrificed. Tissues were fixed by injecting at several points under the skin 10% formalin in 0.1 M phosphate buffer (pH 7.4) (Baker) and incubating overnight at 4°C. Bodies were cut into three parts: the head, the thorax, and the abdomen. Samples were embedded in paraffin, and five consecutive transverse sections 5 μm thick were obtained at different levels (100 μm apart) of each mouse pup with a Leica RM2135 microtome. Sections were mounted, and one out of five consecutive slides was stained with hematoxylin and eosin for histological examination.

RESULTS

Deletion of the *S6K2* gene in mice. The coding sequence of the murine *S6K2* gene spans a 7-kb region of genomic DNA containing 15 exons (Fig. 1A). The overall structure of the *S6K2* gene was similar to that of the homologous *S6K1* gene, as

TABLE 1. Genotype analysis of littermates from crosses of $S6K1^{+/-}$ and $S6K2^{+/-}$ mice at postnatal day 21

Genotype	% of mice	
	Expected	Obtained
$S6K1^{+/+}/S6K2^{+/+}$	6.25	10.0
$S6K1^{+/+}/S6K2^{+/-}$	12.5	18.1
$S6K1^{+/-}/S6K2^{+/+}$	12.5	12.4
$S6K1^{+/-}/S6K2^{+/-}$	25	24.7
$S6K1^{-/-}/S6K2^{+/+}$	6.25	6.4
$S6K1^{+/+}/S6K2^{-/-}$	6.25	5.9
$S6K1^{+/-}/S6K2^{-/-}$	12.5	12.6
$S6K1^{-/-}/S6K2^{+/-}$	12.5	8.1
$S6K1^{-/-}/S6K2^{-/-}$	6.25	1.9

most of the intron-exon boundaries were conserved between the two genes (data not shown). To generate a targeted deletion of the *S6K2* gene by homologous recombination in ES cells (6), we used a vector in which a neomycin resistance cassette replaced four exons of the catalytic domain, including the activation loop and the conserved APE motif (Fig. 1A). Heterozygous mice carrying the targeted allele were identified by Southern blot analysis and mated to obtain homozygous mutant offspring (Fig. 1B). The resulting $S6K2^{-/-}$ homozygous mice were viable and showed no obvious phenotypic abnormalities. That the *S6K2* gene had been correctly targeted was demonstrated by the absence of S6K2 protein on Western blots of extracts from $S6K2^{-/-}$ MEFs compared to MEFs from wild-type mice with monoclonal antibodies directed against either the N terminus or the C terminus of the protein (Fig. 1C and data not shown). Moreover, with either of the two antibodies, S6K2 activity was undetectable by immunoprecipitation in extracts derived from either quiescent or serum-stimulated MEFs of $S6K2^{-/-}$ mice compared to those of wild-type mice (Fig. 1D and data not shown). These results indicated that the gene had been correctly deleted without causing any obvious phenotype.

Phenotypes of $S6K1^{-/-}/S6K2^{-/-}$ mice. As the *S6K1* and *S6K2* genes share a high degree of homology and as *S6K2* mRNA is upregulated in $S6K1^{-/-}$ mice (51), the two genes might compensate functionally for one another in vivo. To fully evaluate the impact of the S6K pathway on mouse development, we set out to generate mice lacking both protein kinases. We intercrossed mice null for the *S6K1* and *S6K2* genes to obtain mice with combined heterozygous mutations in both alleles. The $S6K1^{+/-}/S6K2^{+/-}$ mice were bred, and the genotypes of the progeny were identified by Southern blot analysis. As shown in Table 1, all possible genotypic combinations were represented, although $S6K1^{-/-}/S6K2^{+/-}$ and $S6K1^{-/-}/S6K2^{-/-}$ mice were born at lower frequencies than expected, 65 and 30%, respectively (Table 1). Indeed, only 10 $S6K1^{-/-}/S6K2^{-/-}$ mice were viable from among 526 offspring. However, analysis of embryos at 18.5 days of gestation indicated a normal Mendelian distribution of genotypes (data not shown). These data suggested that the reduced viability of $S6K1^{-/-}/S6K2^{+/-}$ and $S6K1^{-/-}/S6K2^{-/-}$ mice was due to wastage between delivery and the time of weaning. Close observation of the litters revealed that approximately one-third of the $S6K1^{-/-}/S6K2^{-/-}$ mice were born dead. The corpses were found in a fetal position, still lying in the yolk sac and attached to the placenta (Fig. 2A). Among the $S6K1^{-/-}/S6K2^{-/-}$ mice that were born alive and emerged from the yolk sac, the majority developed signs of cyanosis, and approximately half of them died shortly after birth. The mice surviving the first day after delivery usually reached adulthood and were fertile. However, the litters from the viable $S6K1^{-/-}/S6K2^{-/-}$ parents were small and showed a high incidence of perinatal lethality (data not shown). Caesarean delivery appeared to rescue neonatal viability, although the $S6K1^{-/-}/S6K2^{-/-}$ mice were more likely to develop transient signs of hypoxia, as indicated by a bluish discoloration of the skin (Fig. 2B).

To analyze the rates of growth of $S6K1^{-/-}$, $S6K2^{-/-}$, and $S6K1^{-/-}/S6K2^{-/-}$ mice during development, mice homozygous for each genotype were inbred, and the weights of their offspring were compared to those of wild-type mice during embryonic development and early postnatal life (Fig. 2C and D). As previously reported, at birth, $S6K1^{-/-}$ mice were about 15% smaller than wild-type mice (51). This growth defect was more evident in embryos at midgestation, when the difference in body weight was approximately 30% at embryonic day 12.5 (Fig. 2C). During postnatal growth, the $S6K1^{-/-}$ mice failed to attain the same body size as wild-type mice and remained about 20% smaller at 2 months of age (Fig. 2D). Conversely, the $S6K2^{-/-}$ mice tended to be larger at later stages of embryonic development and during the postnatal period; however, their weights did not differ significantly from those of wild-type mice throughout the entire period of observation (Fig. 2C and D). Moreover, the growth defect of the $S6K1^{-/-}$ mice was not reduced further in an $S6K2^{-/-}$ background, as $S6K1^{-/-}$ mice and the surviving $S6K1^{-/-}/S6K2^{-/-}$ mice had similar growth rates (Fig. 2C and D). Growth rates and newborn viability were initially assessed with mice in a hybrid C57BL/6-129Ola genetic background and were confirmed following backcrossing for 10 generations in a C57BL/6 genetic background (data not shown). Thus, the impairment of body growth appears to be caused selectively by deletion of the *S6K1* gene, whereas perinatal lethality is revealed only when the *S6K1* and *S6K2* gene products are both absent.

To assess the possible causes of reduced viability of the $S6K1^{-/-}/S6K2^{-/-}$ mice, histopathological analyses of mice born dead, viable mice with signs of cyanosis, and viable mice with no signs of cyanosis were compared to those of wild-type mice at postnatal day 0. Such analyses failed to reveal any gross anatomical defects in $S6K1^{-/-}/S6K2^{-/-}$ neonates. Moreover, in all viable neonates, the lungs were inflated and properly developed. However, in the nonviable neonates and in the cyanotic neonates, the internal organs were hyperemic and the heart chambers tended to be more dilated. In addition, the nonviable neonates showed several hemorrhagic sites, as revealed by diapedesis of red blood cells throughout the entire myocardium (Fig. 2E).

S6 phosphorylation in S6K-deficient mice. Upon growth factor stimulation, ribosomal protein S6 is multiply phosphorylated at the carboxy terminus on five serine residues in an ordered fashion beginning with Ser236, followed sequentially by Ser235, Ser240, Ser244, and Ser247 (27, 36). This response is readily measured by the decreased electrophoretic mobility of S6 following the separation of its differentially phosphorylated derivatives by 2D PAGE. To determine whether the deletion of the *S6K2* gene affected the mitogen-induced phos-

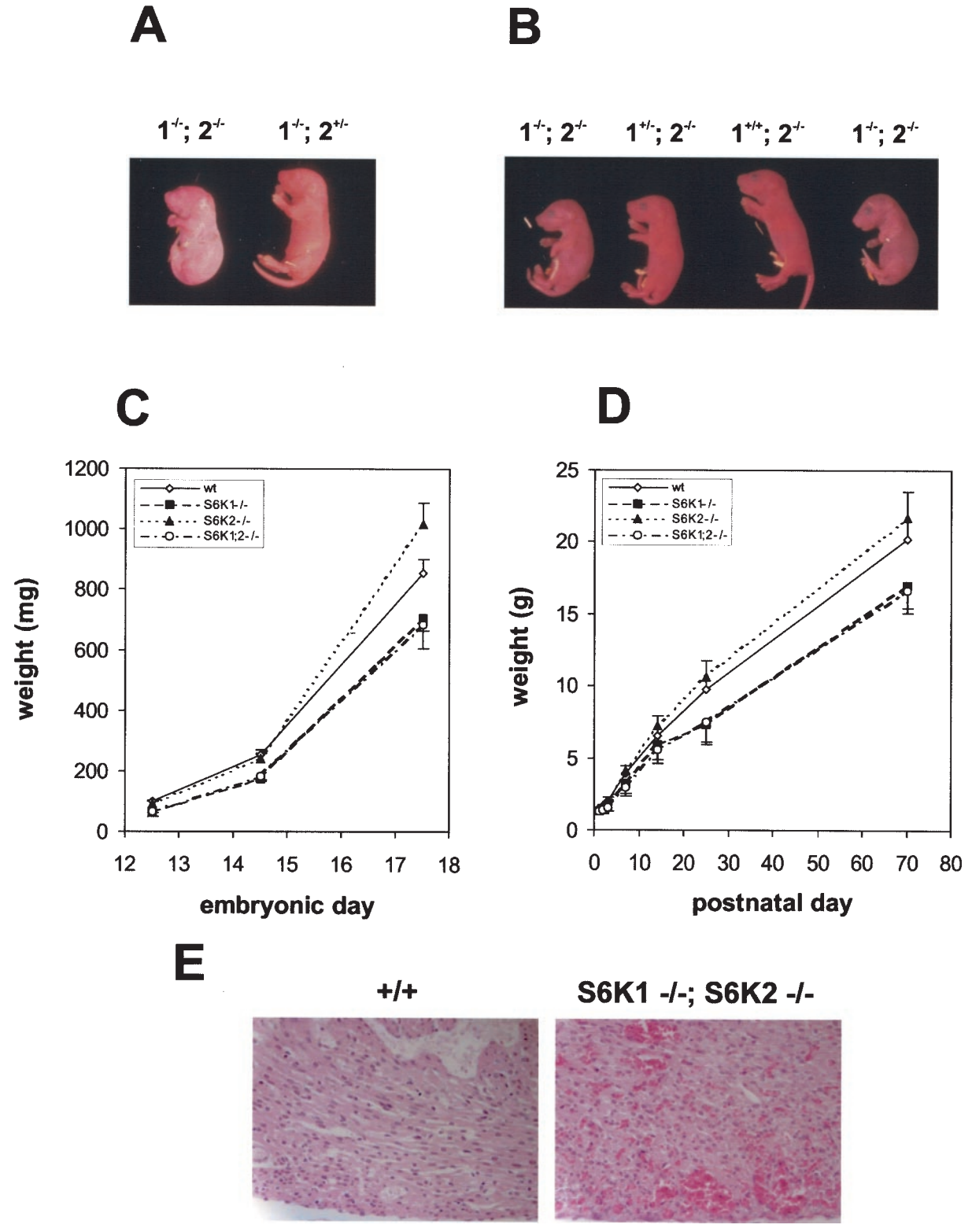

FIG. 2. Phenotypes of *S6K1*$^{-/-}$/*S6K2*$^{-/-}$ mice. (A) Littermates from an *S6K1*$^{-/-}$/*S6K2*$^{+/-}$ cross a few minutes after natural delivery. The genotypes of the mice are indicated. The *S6K1*$^{-/-}$/*S6K2*$^{-/-}$ mouse was born dead and left in the yolk sac. (B) Littermates from an *S6K1*$^{+/-}$/*S6K2*$^{-/-}$ cross at embryonic day 19.5 a few minutes after caesarean delivery. The genotypes of the mice are indicated. *S6K1*$^{-/-}$/*S6K2*$^{-/-}$ mice were more prone to develop transient signs of cyanosis. (C and D) Fetal (C) and postnatal (D) growth curves for mice from homozygous crosses. Values for mice with the same genotype did not differ from those for mice derived from heterozygous crosses. Data represent the average and standard deviation for at least 10 mice per genotype. wt, wild type. (E) Heart histologic findings for wild-type and *S6K1*$^{-/-}$/*S6K2*$^{-/-}$ mice a few minutes after delivery. The *S6K1*$^{-/-}$/*S6K2*$^{-/-}$ mouse was born dead. Note hemorrhages in the myocardium.

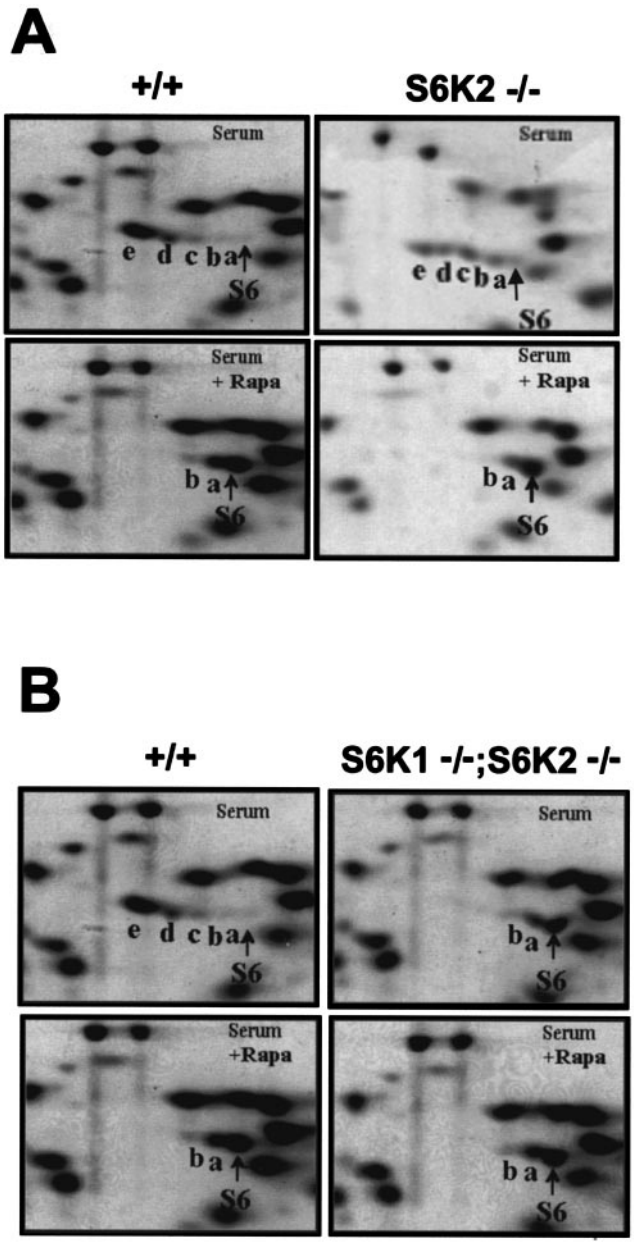

FIG. 3. Regulation of S6 phosphorylation. (A) In $S6K2^{-/-}$ cells, S6 phosphorylation was reduced yet regulated by mitogens and inhibited by rapamycin (Rapa). 2D PAGE was carried out with 80S ribosomal proteins from wild-type and $S6K2^{-/-}$ MEFs. Cells were stimulated with 10% FCS for 1 h, with or without pretreatment with 20 nM rapamycin. (B) S6 phosphorylation in $S6K1^{-/-}/S6K2^{-/-}$ cells was reduced to the same extent as in rapamycin-treated cells. 2D PAGE was carried out with 80S ribosomal proteins from wild-type and $S6K1^{-/-}/S6K2^{-/-}$ MEFs. Cells were treated as described for panel A. See the text for an explanation of a to e on the panels.

phorylation of ribosomal protein S6, total ribosomal proteins from serum-stimulated MEFs were analyzed by 2D PAGE. As shown in Fig. 3A, in serum-stimulated wild-type MEFs, the majority of S6 migrated in highly phosphorylated derivatives d and e, corresponding to proteins phosphorylated on four and five serine residues, respectively (36, 41). Under similar experimental conditions, Shima et al. previously demonstrated that the extent of S6 phosphorylation in $S6K1^{-/-}$ cells was largely comparable to that in wild-type MEFs (51). In $S6K2^{-/-}$ MEFs, S6 was still highly phosphorylated in response to serum, although to a lesser extent than in wild-type and $S6K1^{-/-}$ MEFs; a considerable amount of S6 was present in phosphorylated derivatives a, b, and c, representing phosphorylation on one, two, and three serine residues, respectively (Fig. 3A). Pretreatment with rapamycin drastically decreased S6 phosphorylation in all three genotypes, resulting in the presence of the unphosphorylated, monophosphorylated, or biphosphorylated forms of S6 (Fig. 3A) (51). These data suggest that in $S6K2^{-/-}$ cells, S6 phosphorylation was catalyzed by a second rapamycin-sensitive kinase, most likely S6K1, although somewhat less efficiently. To test this hypothesis, we assessed S6 phosphorylation in MEFs from $S6K1^{-/-}/S6K2^{-/-}$ mice. As shown in Fig. 3B, the combined deletion of the *S6K1* and *S6K2* genes severely suppressed S6 phosphorylation compared to that in wild-type cells. Moreover, rapamycin treatment attenuated S6 phosphorylation in wild-type MEFs, bringing it to the same level as that in serum-stimulated $S6K1^{-/-}/S6K2^{-/-}$ MEFs, where rapamycin had no effect on S6 phosphorylation (Fig. 3B). S6 phosphorylation was also attenuated in the liver of $S6K1^{-/-}/S6K2^{-/-}$ mice following refeeding of starved animals (data not shown). These data suggested that S6K1 and S6K2 are the sole kinases responsible for mediating rapamycin-sensitive phosphorylation.

Intracellular localization of S6K activity. The majority of S6 is found in the cytoplasm as an integral component of the 40S ribosomal subunit. However, S6 is also present in nucleoli, the site of ribosome biogenesis, and in perinucleolar structures called coiled bodies (or Cajall bodies). Given the large relative abundance of S6 in the cytoplasm compared to the nucleus, the quantitation of S6 phosphorylation by 2D PAGE would largely reflect the status of S6 phosphorylation in the cytoplasm. However, as the $p85^{S6K}$ isoform of S6K1 is targeted to the nucleus (46) and S6K2 also contains a nuclear targeting sequence (17, 47, 51), it is possible that one of the two kinases is responsible for mediating selective phosphorylation of S6 in the nucleolus. Consistent with this idea, previous studies demonstrated that S6K1 and S6K2 are differentially targeted within the cell (26, 46, 57). In wild-type hepatocytes, growth factors predominantly stimulated S6 Ser235/236 phosphorylation in the cytosol and nucleoli (Fig. 4A). This staining matched the localization of the ribosomal subunits, as shown by immunostaining with antibodies against 60S ribosomal protein L7a (Fig. 4A) (62). In agreement with the 2D PAGE analysis (Fig. 3A), the deletion of *S6K2* caused a sharper reduction of S6 phosphorylation in the cytosol than did the deletion of *S6K1* (Fig. 4A). Interestingly, this also appeared to be the case in nucleoli (Fig. 4A). The overall intensity of S6 phosphorylation was further reduced by combining the deletion of *S6K1* with the deletion of *S6K2*. In addition to the immunofluorescence analysis, nuclear fractionation of hepatocytes was performed following growth factor stimulation (Fig. 4B). The purity of the fractions was assessed with specific nuclear and cytosolic protein markers, CREB and α-tubulin, respectively (Fig. 4B). Consistent with the results of the immunofluorescence experiments, the deletion of *S6K2* significantly affected S6 phosphorylation in both cell compartments, and the combination of the two gene deletions further reduced the levels of the phosphorylated protein. Moreover, in

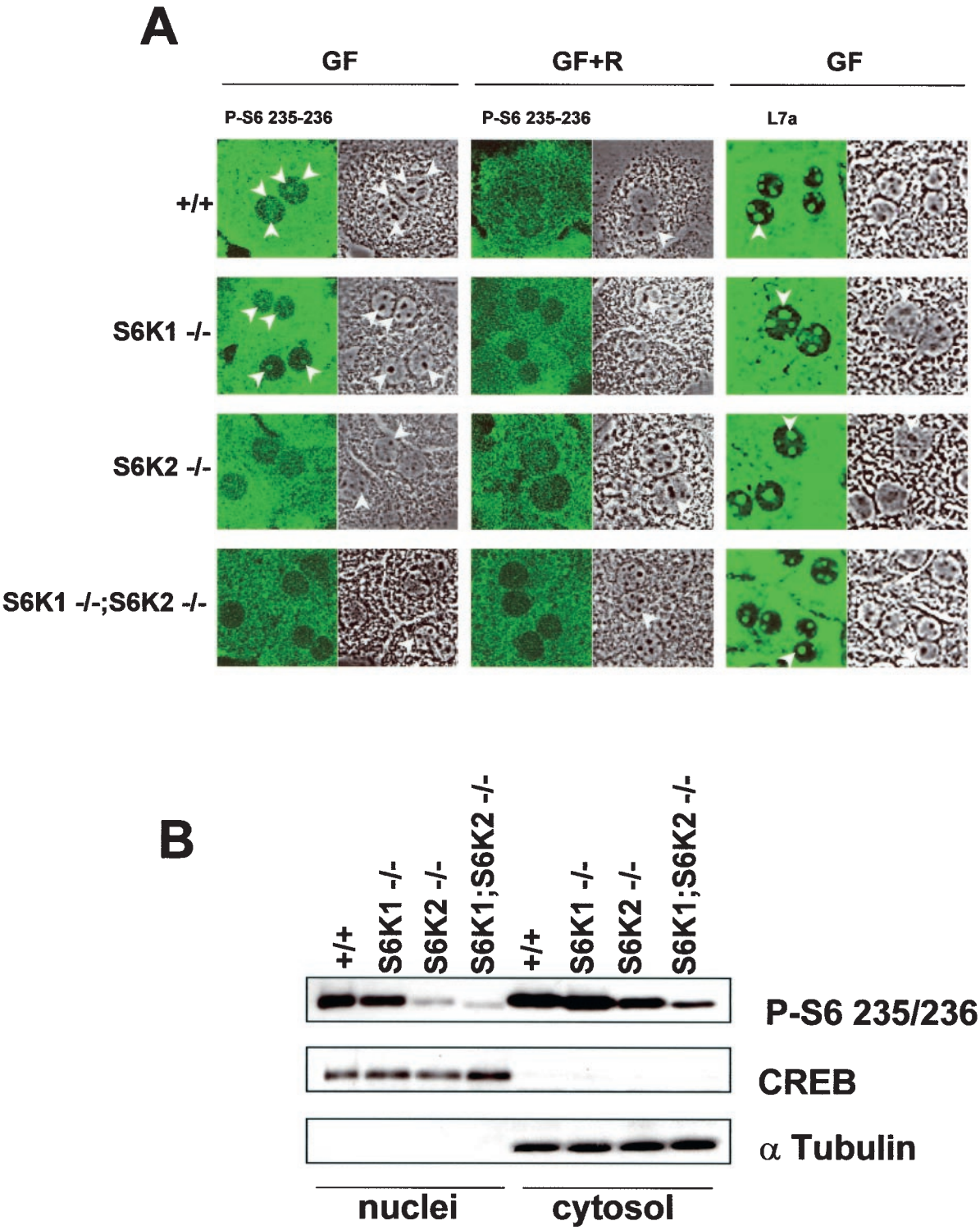

FIG. 4. Intracellular localization of S6K activity. (A) Immunostaining of wild-type, *S6K1*$^{-/-}$, *S6K2*$^{-/-}$, and *S6K1*$^{-/-}$/*S6K2*$^{-/-}$ hepatocytes with anti-phosphorylated S6 (Ser235/236) and anti-L7a antibodies (left panels). The right panels represent phase-contrast images of the same fields. Cells were growth factor deprived for 1 day and stimulated with 4 nM EGF (25 ng/ml) and 1 μM insulin for 1 h (GF), with or without pretreatment with 20 nM rapamycin (R). Arrowheads indicate nucleoli. (B) Immunoblot analysis of nuclear and cytosolic extracts from wild-type, *S6K1*$^{-/-}$, *S6K2*$^{-/-}$, and *S6K1*$^{-/-}$/*S6K2*$^{-/-}$ hepatocytes with anti-phosphorylated S6 (Ser235/236), anti-α-tubulin, and anti-CREB antibodies. The latter two were used as cytosolic and nuclear markers, respectively.

contrast to the results obtained with the other genotypes, the residual S6 phosphorylation staining observed with the anti-phosphorlyated S6 (Ser235/236) antibody in the cytosol and the nuclei of *S6K1*$^{-/-}$/*S6K2*$^{-/-}$ hepatocytes was not inhibited by rapamycin treatment (Fig. 4A) (also see below).

5′TOP mRNA translation and cell cycle progression of *S6K1*$^{-/-}$/*S6K2*$^{-/-}$ cells. It was previously demonstrated that rapamycin inhibits the selective upregulation of 5′TOP mRNAs following mitogen stimulation (20, 55) and that this effect requires intact 5′TOP (19, 49) and may be mediated by S6K1 (19, 49). However, recently it was claimed that neither the S6Ks nor rapamycin appears to be involved in this response (53). As 5′TOP mRNAs code for ribosomal proteins, their increased expression is essential to sustaining translation during the phases of cell growth (56). To examine the roles of S6K1, S6K2, and rapamycin in this response, we used cells derived from *S6K1*$^{-/-}$/*S6K2*$^{-/-}$ mice. Initially, we examined the distribution of 5′TOP elongation factor 1α (EF1α) mRNA on polysomes in MEFs derived from wild-type and *S6K1*$^{-/-}$/*S6K2*$^{-/-}$ mice. As shown in Fig. 5A, serum induced the recruitment of EF1α mRNA into polysomes in both cell types to almost the same extent, and this effect was largely abolished by rapamycin in both *S6K1*$^{-/-}$/*S6K2*$^{-/-}$ and wild-type cells. Furthermore, the combined deletion of *S6K1* and *S6K2* did not alter the cell doubling times or the saturation densities compared to that of wild-type MEFs (data not shown). Rapamycin inhibited the S-phase entry of cells from both genotypes with similar potencies and 50% inhibitory concentrations (Fig. 5B).

The analysis of 5′TOP mRNA translation was extended to ES cells, as Kawasome et al. (24) previously reported that 5′TOP mRNAs are constitutively upregulated in *S6K1*$^{-/-}$ ES cells and resistant to the effects of rapamycin, although these findings were not consistent with those of a later study with the same ES cells (53). To examine this possibility, we analyzed the distribution of EF1α mRNA on polysomes in ES cells derived from embryos of *S6K1*$^{-/-}$/*S6K2*$^{-/-}$, *S6K1*$^{-/-}$, and wild-type mice. Similar to what was observed for MEFs, the deletion of *S6K1* alone or the deletion of both *S6K1* and *S6K2* in ES cells did not alter the upregulation of 5′TOP mRNA or sensitivity to rapamycin (Fig. 5C). Thus, despite a pronounced effect on the development and growth of the animal, in two distinct cell types, neither the reduction of S6 phosphorylation nor the loss of S6K1 and S6K2 function is sufficient to deregulate 5′TOP mRNA translation; these findings suggest that other rapamycin-sensitive events are required.

Evidence for functional redundancy with the mitogen-activated protein kinase (MAPK) pathway. The findings described above raised the possibility of either a compensatory or a redundant S6K pathway. On closer analysis of S6 phosphorylation, a small amount of partially phosphorylated S6 was still detected in MEFs from *S6K1*$^{-/-}$/*S6K2*$^{-/-}$ mice as well as in rapamycin-treated wild-type MEFs, as evidenced by the presence of derivatives a and b (Fig. 3B). The residual S6 phosphorylation in wild-type MEFs could have been due to the relatively short treatment in the presence of rapamycin, as longer times were reported for complete S6 dephosphorylation (20). However, this finding was unexpected for *S6K1*$^{-/-}$/*S6K2*$^{-/-}$ MEFs, as the level of S6 phosphorylation was low in these cells and was unaffected by rapamycin (Fig. 3B). To examine this situation further, we monitored S6 phosphorylation in primary hepatocytes stimulated with EGF and insulin by using phosphospecific antibodies directed against the first and second phosphorylation sites, Ser236 and Ser235, or the third and fourth phosphorylation sites, Ser240 and Ser244. Following insulin stimulation, phosphorylation at both Ser235/236 and Ser240/244 increased in wild-type, *S6K1*$^{-/-}$, and *S6K2*$^{-/-}$ hepatocytes, whereas only Ser235/236 phosphorylation was detectable in *S6K1*$^{-/-}$/*S6K2*$^{-/-}$ hepatocytes (Fig. 6A and B); these results were consistent with the order and extent of S6 phosphorylation (Fig. 3B) (3). In wild-type hepatocytes as well as in *S6K1*$^{-/-}$ and *S6K2*$^{-/-}$ hepatocytes, the increase in S6 phosphorylation was sensitive to rapamycin (Fig. 6A). However, in *S6K1*$^{-/-}$/*S6K2*$^{-/-}$ hepatocytes, the increase in S6 phosphorylation was resistant to rapamycin (Fig. 6B), suggesting that a rapamycin-resistant S6K was operating in the absence of *S6K1* and *S6K2*.

It is known that Akt has a substrate recognition motif similar to that of S6K1 and S6K2 (32) and phosphorylates S6 in vitro (23). However, the phosphatidylinositide-3OH kinase inhibitor wortmannin, which blocks Akt activation, had no effect on insulin-induced S6 phosphorylation in *S6K1*$^{-/-}$/*S6K2*$^{-/-}$ hepatocytes, whereas it was as potent as rapamycin in blocking S6 phosphorylation in wild-type hepatocytes (Fig. 6B). As p90rsk appears to be the rapamycin-resistant kinase responsible for regulating S6 phosphorylation during progesterone-induced meiotic maturation of *Xenopus* oocytes (9, 49), we next tested the effect of the MEK inhibitor U0126 on S6 phosphorylation in *S6K1*$^{-/-}$/*S6K2*$^{-/-}$ hepatocytes. MEK mediates MAPK activation, which in turn phosphorylates and activates p90rsk (13, 54). Such treatment had no measurable effect on S6 phosphorylation in wild-type cells; however, it inhibited Ser235/236 and MAPK phosphorylation in a dose-dependent manner in *S6K1*$^{-/-}$/*S6K2*$^{-/-}$ cells (Fig. 6C).

The MAPK-dependent phosphorylation of S6 could represent either the upregulation of a compensatory pathway or the presence of a pathway that normally operates in wild-type cells but whose activity is masked by S6Ks. It was difficult to distinguish between these possibilities, given the high level of basal S6 phosphorylation displayed by wild-type hepatocytes. To circumvent this problem, hepatocytes were deprived of nutrients as well as serum, a step which resulted in the complete dephosphorylation of S6 (Fig. 6D). Under these conditions, rapamycin abolished the insulin-induced increase in Ser240/244 phosphorylation but only attenuated the phosphorylation of Ser235/236 (Fig. 6D). In contrast, PD184352, an MKK1/ERK1/ERK2 pathway inhibitor that is more specific than U0126 (38), had little effect on S6 phosphorylation when used alone but, when used together with rapamycin, totally abolished the insulin-induced response. In contrast, in *S6K1*$^{-/-}$/*S6K2*$^{-/-}$ hepatocytes, rapamycin had no effect on Ser235/236 phosphorylation, whereas PD184352 abolished this response (Fig. 6C). Thus, in the absence of S6K1 and S6K2 activity, an MAPK pathway which cooperates in the regulation of S6 phosphorylation was unveiled.

DISCUSSION

Studies with gene deletions or RNA interference can be instructive in revealing biological functions. For S6Ks, such studies have been carried out by double-stranded RNA inter-

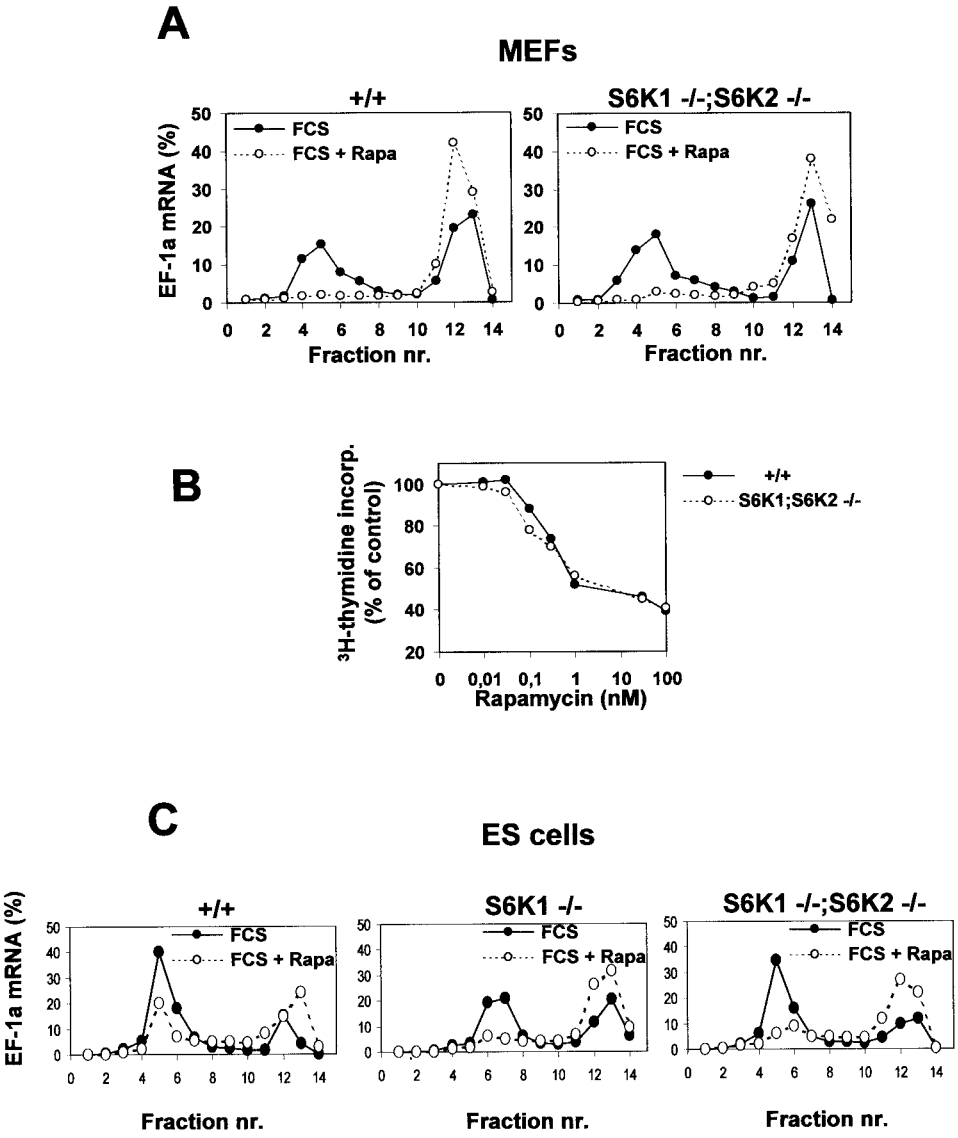

FIG. 5. Regulation of 5′TOP mRNA translation and cell cycle progression is preserved in *S6K1*$^{-/-}$/*S6K2*$^{-/-}$ MEFs. (A and C) 5′TOP mRNA translation is modulated by serum and rapamycin (Rapa), although S6 phosphorylation is resistant to rapamycin treatment. Cytoplasmic extracts were prepared from wild-type (+/+), *S6K1*$^{-/-}$, and *S6K1*$^{-/-}$/*S6K2*$^{-/-}$ MEFs (A) or ES cells (C) that had been stimulated with 10% serum (FCS) in the presence (empty circles) or absence (filled circles) of 20 nM rapamycin after serum deprivation for 48 h. Extracts were centrifuged on a sucrose gradient prior to fractionation as previously described (22). RNA from the different fractions was analyzed by Northern blotting with a probe specific for EF1α (EF-1a) mRNA. The relative amount of mRNA present in each fraction is expressed as a percentage. Fractions 1 to 7 contain polysomes, whereas fractions 8 to 14 are enriched in monosomes, ribosomal subunits, and mRNPs. nr., number. (B) Inhibitory effect of rapamycin on the proliferation of S6K-null cells. Wild-type MEFs (filled circles) and *S6K1*$^{-/-}$/*S6K2*$^{-/-}$ MEFs (empty circles) were seeded in a 24-well plate at a density of 2×10^4 cells per well. Cells then were treated with 0.5% serum for 48 h and stimulated for 20 h with 10% serum in the absence or presence of rapamycin concentrations ranging from 0 to 100 nM. Cells were labeled with [^{3}H]thymidine (1 μCi/ml) throughout the entire stimulation period Radioactivity incorporated (incorp.) into the DNA was measured, and the average values for triplicate samples were determined. Data are expressed as the percent inhibition of [^{3}H]thymidine incorporation by rapamycin-treated cells compared to untreated cells.

ference with *Caenorhabditis elegans* (33) and by gene deletion with *Drosophila melanogaster* (39) and mice (42). In *C. elegans*, disruption of the gene encoding the S6K1/S6K2 orthologue, Cep70, by double-stranded RNA interference led to only minor growth deficits (33). In contrast, deletion of the *Drosophila* gene encoding the S6K1/S6K2 orthologue, the dS6K gene, resulted in semilethality, with most flies dying during the late third larval instar or early pupation (39). In addition, the surviving flies were strikingly reduced in size and lived only a few weeks, and the females were sterile (39). However, S6K1-deficient mice are viable and fertile, although they are 15 to 20% smaller than wild-type mice at birth and are hypoinsulinemic (42, 51). Furthermore, these mice, unlike *Drosophila*, have a second S6K, S6K2, which is upregulated in all tissues examined in S6K1-deficient mice, suggesting a compensatory response for the loss of S6K1. Consistent with this argument,

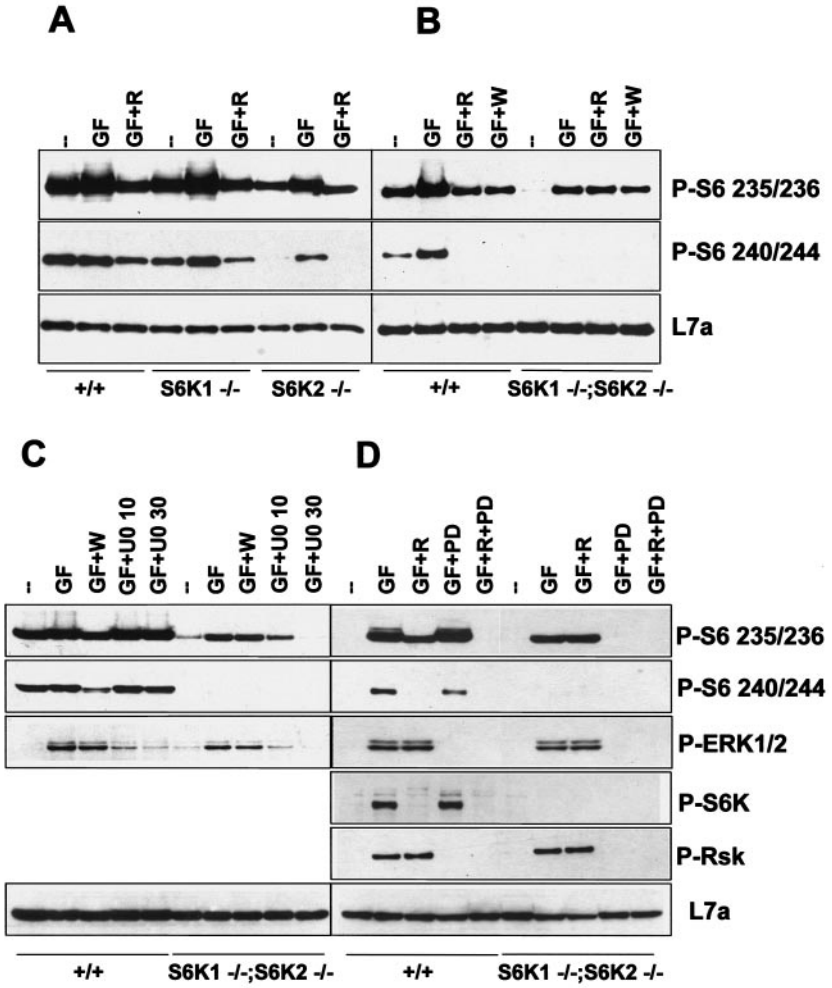

FIG. 6. Evidence for a rapamycin-insensitive S6K. Western blot analysis of protein extracts from wild-type, $S6K1^{-/-}$, $S6K2^{-/-}$, and $S6K1^{-/-}/S6K2^{-/-}$ hepatocytes was carried out with anti-phosphorylated S6 (Ser235/236 and Ser240/244), anti-phosphorylated ERK1/ERK2, anti-phosphorylated S6K (Thr389), anti-phosphorylated Rsk (Thr359 and Ser363), and anti-L7a antibodies, the latter being used as a loading control. Cells were stimulated with 4 nM EGF (25 ng/ml) and 1 μM insulin for 30 min (GF), with or without pretreatment with 20 nM rapamycin (R), 1 μM wortmannin (W), 10 or 30 μM U0126 (U0 10 or U0 30, respectively), and 3 μM PD184352 (PD). Extracts in panels A and C were derived from cells deprived of GFs for 1 day, whereas those in panels B and D were derived from cells deprived of GFs for 2 days. In panel D, cells were also deprived of nutrients (all of the amino acids and glucose) for 3 h.

we show here that deletion of S6K1 and S6K2 in mice, as for dS6K in flies, is also semilethal, with pups dying at the time of delivery or shortly thereafter. A potential difference between the findings for *C. elegans* or *D. melanogaster* and mice is that small interfering RNAs reduce gene expression, whereas it is abolished by gene deletion. It should also be noted that the combined inactivation of two other elements of the phosphatidylinositide-3OH kinase pathway, Akt1 and Akt2, also leads to perinatal lethality of unknown cause (43). The results of macroscopic and histological analyses of newborns lacking S6K1 and S6K2 were compatible with the mutant mice experiencing a period of hypoxic stress. This finding might have been partly due to heart failure or a placentation defect, a possibility which is presently being addressed.

One of the early intracellular responses to growth factor stimulation in both invertebrates and vertebrates is multiple phosphorylation of 40S ribosomal protein S6 (14, 58). Although many kinases have been shown to mediate this response in vitro, only two have been demonstrated to phosphorylate S6 in the same specific order and extent as those observed in vivo: S6K1 (10) and p90rsk from *Xenopus* (61). Although a role for p90rsk in this response has been controversial, studies of progesterone-induced meiotic maturation of *Xenopus* oocytes support such a function (29, 49). That S6K1 is not involved in this response is further supported by the fact that rapamycin, which selectively inhibits S6K1 but not p90rsk activation (28), abolished S6K1 activity, with little effect on progesterone-induced S6 phosphorylation (49). In contrast to the findings in progesterone-treated *Xenopus* oocytes, rapamycin eliminates serum-induced S6 phosphorylation in mammalian cells (20), an inhibitory effect that is reversed by the use of an S6K1 variant that is largely rapamycin resistant (19, 59). In seeming agreement with the findings in mammalian cells, $S6K1^{-/-}$ ES cells were reported to be devoid of phosphory-

lated S6 (24, 53). However, in tissues derived from *S6K1*$^{-/-}$ mice, S6 phosphorylation was shown to be intact but still rapamycin sensitive (51), leading to the discovery of S6K2 (17, 47, 51). Although studies with ES cells have been difficult to rationalize, some investigators recently demonstrated that growth factor stimulation of these same cells leads to S6K2 activation and increased S6 phosphorylation in a rapamycin-sensitive manner (31, 60). These conflicting results may be attributable to different stimulation conditions or detection methods.

The studies presented here reveal two novel aspects of S6 phosphorylation in mammalian cells in vivo, i.e., the major role of S6K2 in this response and the involvement of an MAPK pathway, whose function is detectable when S6K1 and S6K2 are inactive. S6K2 appears to be the dominant S6K in embryo fibroblasts as well as in adult hepatocytes and skeletal and heart muscle, as *S6K2*$^{-/-}$ mice showed a more dramatic reduction in the amount of phosphorylated S6 in these tissues than did *S6K1*$^{-/-}$ mice (Fig. 3 and 6 and data not shown). In addition, the nucleolar phosphorylation of S6 was greatly affected in *S6K2*$^{-/-}$ hepatocytes (Fig. 4), implying that the nucleus-targeted isoform of S6K1, p85^{S6K} (46), may not efficiently mediate phosphorylation in nucleoli. Ectopically expressed S6K2 predominantly resides in the nucleus due to a nuclear localization signal in the C-terminal region of the protein (26, 57). Upon mitogen stimulation, protein kinase C-dependent phosphorylation of S6K2 in the C-terminal region masks the nuclear localization signal, causing the retention of the kinase in the cytosol (57). Our data are compatible with this model and suggest the presence of active S6K2 in the cytosol and nucleoli, where it can phosphorylate S6. However, S6K1 clearly contributes to the overall amount of S6 phosphorylation, as deletion of both kinases was required to reduce S6 phosphorylation to the same extent as rapamycin (Fig. 3). Indeed, with our experimental model, we cannot conclusively determine to what extent each kinase contributes to this response under physiological conditions, as it was previously reported that in *S6K1*$^{-/-}$ mice, S6K2 mRNA transcripts are upregulated in all tissues examined (51). Such upregulation of S6K2 could explain its dominance as an S6K and the reliance of complete S6 phosphorylation on S6K1. That *S6K1* and *S6K2* are the only genes coding for rapamycin-sensitive S6Ks is consistent with two other S6K genes identified by the human genome project representing pseudogenes (34). However, the combined inactivation of *S6K1* and *S6K2* revealed the presence of another S6K, most likely p90rsk, which is rapamycin resistant and phosphorylates at least the first two Ser residues of S6 (Fig. 3 and 6). p90rsk appears to be the physiological S6K during *Xenopus* (49) and mouse (15) meiotic maturation. The murine p90rsk family includes several members which are directly phosphorylated and activated by ERK1 and ERK2 (12). p90rsk family members have two kinase domains; the N-terminal one shows approximately 60% sequence identity with S6K1 and S6K2 and has a similar consensus substrate recognition motif (32). The functional redundancy among the S6K pathways indicates the importance of the phosphorylation of S6 or another common substrate at one or more steps of embryonic development.

The functional compensation between S6K1 and S6K2 was initially proposed based on the upregulation of S6K2 in *S6K1*$^{-/-}$ mice and could represent a mechanism to ensure the survival of the animal (51). This suggestion is supported by the data presented here, showing semilethality in both S6K1$^{-/-}$/S6K2$^{-/-}$ and S6K1$^{-/-}$/S6K2$^{+/-}$ mice. Interestingly, Wang et al. (60) showed that S6 phosphorylation was reduced in the *S6K1*$^{-/-}$ ES cells described above (24) but found no difference in the level of S6K2 protein. These ES cells were obtained by selection in vitro with high doses of G418 (24), rather than from crossing heterozygous founders. Therefore, they may not have upregulated S6K2 compensatorily, as they have not undergone the stress associated with embryonic development. Following a similar reasoning, the MAPK-dependent S6K activity described here could alleviate the phenotype of the double-mutant mice. Surprisingly, the body size phenotype of the single-mutant mice did not appear to correlate with the extent of S6 phosphorylation. For *S6K1*$^{-/-}$ mice, body size was clearly reduced, with little effect on S6 phosphorylation, whereas *S6K2*$^{-/-}$ mice exhibited normal body size but had reduced levels of S6 phosphorylation. Similarly, the defect in β-cell growth and insulin levels was associated mainly with the deletion of S6K1, which has a minor effect on S6 phosphorylation in β cells (data not shown). These data raise the interesting possibility that S6K1 and S6K2 also exert specific functions through distinct substrates. Consistent with such a model, the two kinases have been reported to be differentially localized and regulated (5, 31, 35). Despite these observations, it should be noted that recent studies with phosphospecific site mutations in *Drosophila* S6 suggested that *Drosophila* S6 is epistatic to dS6K, the single S6K gene in *Drosophila*, arguing that it may be required to elicit the dS6K growth response (T. Radimerski and G. Thomas, unpublished data).

Initial studies showed that rapamycin selectively inhibited the translation of 5′TOP mRNAs (20, 55), with the extent of inhibition varying between cell types (21). This finding led to the conclusion that some cell types use both rapamycin-sensitive and rapamycin-resistant pathways to control this response, whereas other cell types are largely reliant on the rapamycin-sensitive pathway (20). Such an explanation is consistent with the ability of rapamycin to inhibit cell proliferation in certain cell types, such as endothelial, smooth muscle, and naive T cells, while having a less dramatic impact on other cell types. Here we show, as previously demonstrated (51), that the inhibitory effect of rapamycin on 5′TOP mRNA translation is complete in MEFs derived from wild-type cells (Fig. 5). Earlier it was also demonstrated that the effect of rapamycin requires an intact polypyrimidine tract, that dominant interfering alleles of S6K1 were as effective in blocking the upregulation of 5′TOP mRNAs as rapamycin, and that the inhibitory effects of rapamycin could be largely prevented by the use of a rapamycin-resistant allele of S6K1 (19, 49). Unexpectedly, we found here that rapamycin still inhibited the translation of 5′TOP mRNAs despite the absence of S6K1 and S6K2 (Fig. 5). The effect of the dominant-negative S6K1 allele can be rationalized by its ability to titrate mTOR, potentially through Raptor (40), and block mTOR from phosphorylating other key downstream targets (19, 59). However, in view of the findings presented here, it is more difficult to understand the ability of the rapamycin-resistant allele of S6K1 to protect 5′TOP mRNA translation from the inhibitory effects of rapamycin (19, 49). One possibility is that S6K1 is not involved in this

response but that ectopic expression of the rapamycin-resistant allele can lead to the phosphorylation of a target protein that is involved in 5′TOP mRNA translation and whose phosphorylation is not mediated by endogenous S6K1. It is also possible that in the absence of S6K1 and S6K2, a rapamycin-sensitive, compensatory pathway is activated during development. Stolovich et al. (53) recently reported that S6 phosphorylation, S6K1, and rapamycin had little impact on 5′TOP mRNA translation. However, they used ES cells in which the S6K pathway was not completely inhibited, as S6K2 was still expressed (31, 60). To resolve this issue and the discrepancies concerning the inhibitory effect of rapamycin on 5′TOP mRNA translation in nerve growth factor-treated PC12 cells (42, 51), an understanding of the molecular mechanisms which control 5′TOP mRNA translation is required.

In summary, these studies provide a first comparative analysis of the distinct phenotypes of S6K1- and S6K2-deficient mice and should serve as a basis to search for other specific cellular targets of these enzymes. They also reveal an alternative mechanism leading to S6 phosphorylation in the absence of S6K1 and S6K2, i.e, an MAPK pathway; this function should be taken into account when the impact of this pathway on growth and development is evaluated.

ACKNOWLEDGMENTS

We thank P. Kopp and J.-F. Spetz for expert technical assistance in generating *S6K2*$^{-/-}$ mice. We are grateful to R. Polakiewicz, A. Sobering, A. Sotiropoulos, and T. Nobukuni for critical reading of the manuscript and for helpful discussions. We also thank A. Ziemiecki for providing L7a antibodies and Paul Schofield and M. Stumm for help with histological studies.

M.P. is a recipient of a stipend from the Foundation pour la Recherche Medicale. This work was supported in part by a grant to M.P. from the INSERM Avenir Program (R01131KS) and a grant to S.C.K. and G.T. from the EEC (EU BIO4-CT97-2071) and the Novartis Research Foundation.

REFERENCES

1. **Abraham, R. T.** 2002. Identification of TOR signaling complexes: more TORC for the cell growth engine. Cell **111:**9–12.
2. **Arber, S., J. J. Hunter, J. Ross, Jr., M. Hongo, G. Sansig, J. Borg, J. C. Perriard, K. R. Chien, and P. Caroni.** 1997. MLP-deficient mice exhibit a disruption of cardiac cytoarchitectural organization, dilated cardiomyopathy, and heart failure. Cell **88:**393–403.
3. **Bandi, H. R., S. Ferrari, J. Krieg, H. E. Meyer, and G. Thomas.** 1993. Identification of 40 S ribosomal protein S6 phosphorylation sites in Swiss mouse 3T3 fibroblasts stimulated with serum. J. Biol. Chem. **268:**4530–4533.
4. **Burnett, P. E., R. K. Barrow, N. A. Cohen, S. H. Snyder, and D. M. Sabatini.** 1998. RAFT1 phosphorylation of the translational regulators p70 S6 kinase and 4E-BP1. Proc. Natl. Acad. Sci. USA **95:**1432–1437.
5. **Burnett, P. E., S. Blackshaw, M. M. Lai, I. A. Qureshi, A. F. Burnett, D. M. Sabatini, and S. H. Snyder.** 1998. Neurabin is a synaptic protein linking p70 S6 kinase and the neuronal cytoskeleton. Proc. Natl. Acad. Sci. USA **95:** 8351–8356.
6. **Capecchi, M. R.** 1989. Altering the genome by homologous recombination. Science **244:**1288–1292.
7. **Dennis, P. B., S. Fumagalli, and G. Thomas.** 1999. Target of rapamycin (TOR): balancing the opposing forces of protein synthesis and degradation. Curr. Opin. Genet. Dev. **9:**49–54.
8. **Dennis, P. B., A. Jaeschke, M. Saitoh, B. Fowler, S. C. Kozma, and G. Thomas.** 2001. Mammalian TOR: a homeostatic ATP sensor. Science **294:** 1102–1105.
9. **Erikson, E., and J. L. Maller.** 1989. In vivo phosphorylation and activation of ribosomal protein S6 kinases during Xenopus oocyte maturation. J. Biol. Chem. **264:**13711–13717.
10. **Ferrari, S., H. R. Bandi, B. M. Bussian, and G. Thomas.** 1991. Mitogen-activated 70K S6 kinase. J. Biol. Chem. **266:**22770–22775.
11. **Fingar, D. C., S. Salama, C. Tsou, E. Harlow, and J. Blenis.** 2002. Mammalian cell size is controlled by mTOR and its downstream targets S6K1 and 4EBP1/eIF4E. Genes Dev. **16:**1472–1487.
12. **Frodin, M., and S. Gammeltoft.** 1999. Role and regulation of 90 kDa ribosomal S6 kinase (RSK) in signal transduction. Mol. Cell. Endocrinol. **151:** 65–77.
13. **Frodin, M., C. J. Jensen, K. Merienne, and S. Gammeltoft.** 2000. A phosphoserine-regulated docking site in the protein kinase RSK2 that recruits and activates PDK1. EMBO J. **19:**2924–2934.
14. **Fumagalli, S., and G. Thomas.** 2000. S6 phosphorylation and signal transduction, p. 695–717. *In* M. B. Mathews (ed.), Translational control of gene expression. Cold Spring Harbor Laboratory Press, Cold Spring Harbor, N.Y.
15. **Gavin, A. C., and S. Schorderet-Slatkine.** 1997. Ribosomal S6 kinase p90rsk and mRNA cap-binding protein eIF4E phosphorylations correlate with MAP kinase activation during meiotic reinitiation of mouse oocytes. Mol. Reprod. Dev. **46:**383–391.
16. **Gingras, A. C., B. Raught, and N. Sonenberg.** 2001. Regulation of translation initiation by FRAP/mTOR. Genes Dev. **15:**807–826.
17. **Gout, I., T. Minami, K. Hara, Y. Tsujishita, V. Filonenko, M. D. Waterfield, and K. Yonezawa.** 1998. Molecular cloning and characterization of a novel p70 S6 kinase, p70 S6 kinase b, containing a proline-rich region. J. Biol. Chem. **273:**30061–30064.
18. **Isotani, S., K. Hara, C. Tokunaga, H. Inoue, J. Avruch, and K. Yonezawa.** 1999. Immunopurified mammalian target of rapamycin phosphorylates and activates p70 S6 kinase alpha in vitro. J. Biol. Chem. **274:**34493–34498.
19. **Jefferies, H. B. J., S. Fumagalli, P. B. Dennis, C. Reinhard, R. B. Pearson, and G. Thomas.** 1997. Rapamycin suppresses 5′TOP mRNA translation through inhibition of p70^{s6k}. EMBO J. **12:**3693–3704.
20. **Jefferies, H. B. J., C. Reinhard, S. C. Kozma, and G. Thomas.** 1994. Rapamycin selectively represses translation of the "polypyrimidine tract" mRNA family. Proc. Natl. Acad. Sci. USA **91:**4441–4445.
21. **Jefferies, H. B. J., and G. Thomas.** 1996. Ribosomal protein S6 phosphorylation and signal transduction, p. 389–409. *In* N. Sonenberg (ed.), Translational control. Cold Spring Harbor Laboratory Press, Cold Spring Harbor, N.Y.
22. **Jefferies, H. B. J., G. Thomas, and G. Thomas.** 1994. Elongation factor-1a mRNA is selectively translated following mitogenic stimulation. J. Biol. Chem. **269:**4367–4372.
23. **Jones, P. F., T. Jakubowicz, F. J. Pitossi, F. Maurer, and B. A. Hemmings.** 1991. Molecular cloning and identification of a serine/threonine protein kinase of the second-messenger subfamily. Proc. Natl. Acad. Sci. USA **88:** 4171–4175.
24. **Kawasome, H., P. Papst, S. Webb, G. M. Keller, G. L. Johnson, E. W. Gelfand, and N. Terada.** 1998. Targeted disruption of p70^{s6k} defines its role in protein synthesis and rapamycin sensitivity. Proc. Natl. Acad. Sci. USA **95:**5033–5038.
25. **Klaunig, J. E., P. J. Goldblatt, D. E. Hinton, M. M. Lipsky, J. Chacko, and B. F. Trump.** 1981. Mouse liver cell culture. I. Hepatocyte isolation. In Vitro **17:**913–925.
26. **Koh, H., K. Jee, B. Lee, J. Kim, D. Kim, Y. H. Yun, J. W. Kim, H. S. Choi, and J. Chung.** 1999. Cloning and characterization of a nuclear S6 kinase, S6 kinase-related kinase (SRK): a novel nuclear target of Akt. Oncogene **18:** 5115–5119.
27. **Krieg, J., J. Hofsteenge, and G. Thomas.** 1988. Identification of the 40 S ribosomal protein S6 phosphorylation sites induced by cycloheximide. J. Biol. Chem. **263:**11473–11477.
28. **Kuo, C. J., J. Chung, D. F. Fiorentino, W. M. Flanagan, J. Blenis, and G. R. Crabtree.** 1992. Rapamycin selectively inhibits interleukin-2 activation of p70 S6 kinase. Nature **358:**70–73.
29. **Lane, H. A., S. J. Morley, M. Doree, S. C. Kozma, and G. Thomas.** 1992. Identification and early activation of a Xenopus laevis p70^{s6k} following progesterone-induced meiotic maturation. EMBO J. **11:**1743–1749.
30. **Lane, R. D., R. S. Crissman, and S. Ginn.** 1986. High efficiency fusion procedure for producing monoclonal antibodies against weak immunogens. Methods Enzymol. **121:**183–192.
31. **Lee-Fruman, K. K., C. J. Kuo, J. Lippincott, N. Terada, and J. Blenis.** 1999. Characterization of S6K2, a novel kinase homologous to S6K1. Oncogene **18:**5108–5114.
32. **Leighton, I. A., K. N. Dalby, F. B. Caudwell, P. T. Cohen, and P. Cohen.** 1995. Comparison of the specificities of p70 S6 kinase and MAPKAP kinase-1 identifies a relatively specific substrate for p70 S6 kinase: the N-terminal kinase domain of MAPKAP kinase-1 is essential for peptide phosphorylation. FEBS Lett. **375:**289–293.
33. **Long, X., C. Spycher, Z. S. Han, A. M. Rose, F. Muller, and J. Avruch.** 2002. TOR deficiency in C. elegans causes developmental arrest and intestinal atrophy by inhibition of mRNA translation. Curr. Biol. **12:**1448–1461.
34. **Manning, G., D. B. Whyte, R. Martinez, T. Hunter, and S. Sudarsanam.** 2002. The protein kinase complement of the human genome. Science **298:** 1912–1934.
35. **Martin, K. A., S. S. Schalm, C. Richardson, A. Romanelli, K. L. Keon, and J. Blenis.** 2001. Regulation of ribosomal S6 kinase 2 by effectors of the phosphoinositide 3-kinase pathway. J. Biol. Chem. **276:**7884–7891.
36. **Martin-Pèrez, J., and G. Thomas.** 1983. Ordered phosphorylation of 40S ribosomal protein S6 after serum stimulation of quiescent 3T3 cells. Proc. Natl. Acad. Sci. USA **80:**926–930.

37. **Meyuhas, O., D. Avni, and S. Shama.** 1996. Translational control of ribosomal protein mRNAs in eukaryotes, p. 363–388. *In* N. Sonenberg (ed.), Translational control. Cold Spring Harbor Laboratory Press, Cold Spring Harbor, N.Y.
38. **Mody, N., J. Leitch, C. Armstrong, J. Dixon, and P. Cohen.** 2001. Effects of MAP kinase cascade inhibitors on the MKK5/ERK5 pathway. FEBS Lett. **502:**21–24.
39. **Montagne, J., M. J. Stewart, H. Stocker, E. Hafen, S. C. Kozma, and G. Thomas.** 1999. Drosophila S6 kinase: a regulator of cell size. Science **285:** 2126–2129.
40. **Nojima, H., C. Tokunaga, S. Eguchi, N. Oshiro, S. Hidayat, K. I. Yoshino, K. Hara, N. Tanaka, J. Avruch, and K. Yonezawa.**2003. The mammalian target of rapamycin (mTOR)partner, raptor, binds the mTOR substratesp70 S6 kinase and 4E-BP1 through their TOR signaling (TOS) motif. J. Biol. Chem.**78:**5461–15464.
41. **Olivier, A. R., L. M. Ballou, and G. Thomas.** 1988. Differential regulation of S6 phosphorylation by insulin and epidermal growth factor in Swiss mouse 3T3 cells: insulin activation of type 1 phophatase. Proc. Natl. Acad. Sci. USA **85:**4720–4724.
42. **Pende, M., S. C. Kozma, M. Jaquet, V. Oorschot, R. Burcelin, Y. Le Marchand-Brustel, J. Klumperman, B. Thorens, and G. Thomas.** 2000. Hypoinsulinaemia, glucose intolerance and diminished beta-cell size in S6K1-deficient mice. Nature **48:**994–997.
43. **Peng, X. D., P. Z. Xu, M. L. Chen, A. Hahn-Windgassen, J. Skeen, J. Jacobs, D. Sundararajan, W. S. Chen, S. E. Crawford, K. G. Coleman, and N. Hay.** 2003. Dwarfism, impaired skin development, skeletal muscle atrophy, delayed bone development, and impeded adipogenesis in mice lacking Akt1 and Akt2. Genes Dev. **17:**1352–1365.
44. **Petroulakis, E., and E. Wang.** 2002. Nerve growth factor specifically stimulates translation of eukaryotic elongation factor 1A-1 (eEF1A-1) mRNA by recruitment to polyribosomes in PC12 cells. J. Biol. Chem. **277:**18718–18727.
45. **Pullen, N., P. B. Dennis, M. Andjelkovic, A. Dufner, S. C. Kozma, B. A. Hemmings, and G. Thomas.** 1998. Phosphorylation and activation of $p70^{s6k}$ by PDK1. Science **279:**707–710.
46. **Reinhard, C., A. Fernandez, N. J. C. Lamb, and G. Thomas.** 1994. Nuclear localization of $p85^{s6k}$: functional requirement for entry into S phase. EMBO J. **13:**1557–1565.
47. **Saitoh, M., P. ten Dijke, K. Miyazono, and H. Ichijo.** 1998. Cloning and characterization of $p70^{s6kb}$ defines a novel family of p70 S6 kinases. Biochem. Biophys. Res. Commun. **253:**470–476.
48. **Schmelzle, T., and M. N. Hall.** 2000. TOR, a central controller of cell growth. Cell **1**3:193–200.
49. **Schwab, M. S., S. H. Kim, N. Terada, C. Edfjall, S. C. Kozma, G. Thomas, and J. L. Maller.** 1999. p70(S6K) controls selective mRNA translation during oocyte maturation and early embryogenesis in *Xenopus laevis*. Mol. Cell. Biol. **19:**2485–2494.
50. **Seglen, P. O.** 1976. Preparation of isolated rat liver cells. Methods Cell Biol. **13:**29–83.
51. **Shima, H., M. Pende, Y. Chen, S. Fumagalli, G. Thomas, and S. C. Kozma.** 1998. Disruption of the $p70^{s6k}/p85^{s6k}$ gene reveals a small mouse phenotype and a new functional S6 kinase. EMBO J. **17:**6649–6659.
52. **Spitz, M.** 1986. "Single-shot" intrasplenic immunization for the production of monoclonal antibodies. Methods Enzymol. **121:**33–41.
53. **Stolovich, M., H. Tang, E. Hornstein, G. Levy, R. Cohen, S. S. Bae, M. J. Birnbaum, and O. Meyuhas.** 2002. Transduction of growth or mitogenic signals into translational activation of TOP mRNAs is fully reliant on the phosphatidylinositol 3-kinase-mediated pathway but requires neither S6K1 nor rpS6 phosphorylation. Mol. Cell. Biol. **22:**8101–8113.
54. **Sturgill, T. W., L. B. Ray, and J. L. Maller.** 1988. Insulin-stimulated MAP-2 kinase phosphorylates and activates ribosomal protein S6 kinaseII. Nature **334:**715–718.
55. **Terada, N., H. R. Patel, K. Takase, K. Kohno, A. C. Narin, and E. W. Gelfand.** 1994. Rapamycin selectively inhibits translation of mRNAs encoding elongation factors and ribosomal proteins. Proc. Natl. Acad. Sci. USA **91:**11477–11481.
56. **Thomas, G.** 2000. An "encore" for ribosome biogenesis in cell proliferation. Nat. Cell Biol. **2:**E71-E72.
57. **Valovka, T., F. Verdier, R. Cramer, A. Zhyvoloup, T. Fenton, H. Rebholz, M. L. Wang, M. Gzhegotsky, A. Lutsyk, G. Matsuka, V. Filonenko, L. Wang, C. G. Proud, P. J. Parker, and I. T. Gout.** 2003. Protein kinase C phosphorylates ribosomal protein S6 kinase βII and regulates its subcellular localization. Mol. Cell. Biol. **23:**852–863.
58. **Volarevic, S., and G. Thomas.** 2001. Role of S6 phosphorylation and S6 kinase in cell growth. Prog. Nucleic Acids Res. Mol. Biol. **65:**101–127.
59. **von Manteuffel, S. R., P. B. Dennis, N. Pullen, A. C. Gingras, N. Sonenberg, and G. Thomas.** 1997. The insulin-induced signalling pathway leading to S6 and initiation factor 4E binding protein 1 phosphorylation bifurcates at a rapamycin-sensitive point immediately upstream of p70s6k. Mol. Cell. Biol. **17:**5426–5436.
60. **Wang, X., W. Li, M. Williams, N. Terada, D. R. Alessi, and C. G. Proud.** 2001. Regulation of elongation factor 2 kinase by p90(RSK1) and p70 S6 kinase. EMBO J. **20:**4370–4379.
61. **Wettenhall, R. E., E. Erikson, and J. L. Maller.** 1992. Ordered multisite phosphorylation of Xenopus ribosomal protein S6 by S6 kinase II. J. Biol. Chem. **267:**9021–9027.
62. **Ziemiecki, A., R. G. Müller, F. Xiao-Chang, N. E. Hynes, and S. Kozma.** 1990. Oncogenic activation of the human trk proto-oncogene by recombination with the ribosomal large subunit protein L7a. EMBO J. **9:**191–196.

III. RESULTS

Part 2: ……

Absence of S6K1 protects against age- and diet-induced obesity while enhancing insulin sensitivity.

Um SH, Frigerio F, Watanabe M, Picard F, Joaquin M, Sticker M, Fumagalli S, Allegrini PR, Kozma SC, Auwerx J, Thomas G.
Nature. 2004, 431, 200–205

Absence of S6K1 protects against age- and diet-induced obesity while enhancing insulin sensitivity

Sung Hee Um[1], Francesca Frigerio[1], Mitsuhiro Watanabe[2], Frédéric Picard[2]*, Manel Joaquin[1], Melanie Sticker[1], Stefano Fumagalli[1], Peter R. Allegrini[3], Sara C. Kozma[1]*, Johan Auwerx[2] & George Thomas[1]

[1]*Friedrich Miescher Institute for Biomedical Research, Maulbeerstrasse 66, 4058 Basel, Switzerland*
[2]*Institut de Génétique et de Biologie Moléculaire et Cellulaire, CNRS/INSERM/ULP, and Institut Clinique de la Souris, Génopole Strasbourg, 67404 Illkirch, France*
[3]*Novartis Pharma AG, Klybeckstrasse 141, 4057 Basel, Switzerland*

* Present address: Laval Hospital Research Center, 2725 chemin Ste-Foy, Ste-Foy, Quebec G1V 4G5, Canada (F.P.); Genome Research Institute, University of Cincinnati, 2180 E. Galbraith Road, Cincinnati, Ohio 45237, USA (S.C.K.)

Elucidating the signalling mechanisms by which obesity leads to impaired insulin action is critical in the development of therapeutic strategies for the treatment of diabetes[1]. Recently, mice deficient for S6 Kinase 1 (S6K1), an effector of the mammalian target of rapamycin (mTOR) that acts to integrate nutrient and insulin signals[2], were shown to be hypoinsulinaemic, glucose intolerant and have reduced β-cell mass[3]. However, *S6K1*-deficient mice maintain normal glucose levels during fasting, suggesting hypersensitivity to insulin[3], raising the question of their metabolic fate as a function of age and diet. Here, we report that *S6K1*-deficient mice are protected against obesity owing to enhanced β-oxidation. However on a high fat diet, levels of glucose and free fatty acids still rise in *S6K1*-deficient mice, resulting in insulin receptor desensitization. Nevertheless, *S6K1*-deficient mice remain sensitive to insulin owing to the apparent loss of a negative feedback loop from S6K1 to insulin receptor substrate 1 (IRS1), which blunts S307 and S636/S639 phosphorylation; sites involved in insulin resistance[4,5]. Moreover, wild-type mice on a high fat diet as well as *K/K A^y* and *ob/ob* (also known as *Lep/Lep*) mice—two genetic models of obesity—have markedly elevated S6K1 activity and, unlike *S6K1*-deficient mice, increased phosphorylation of IRS1 S307 and S636/S639. Thus under conditions of nutrient satiation S6K1 negatively regulates insulin signalling.

As animals reach adulthood their growth rate decreases and fatty acids are largely converted into triglycerides and stored as an energy reserve in adipose tissue. To investigate the effect of age on growth, a matched set of *S6K1*-deficient (*S6K1*$^{-/-}$) and wild-type male mice were placed on a normal chow diet (NCD) (4% total calories derived from fat, 3,035 kcal kg^{-1}) and monitored over a period of 17 weeks from 10 weeks of age. The rate at which *S6K1*$^{-/-}$ mice increased body weight on the NCD was significantly reduced compared with wild-type mice: at 27 weeks of age the difference in body weight was 25% (Fig. 1a). Dissection of *S6K1*$^{-/-}$ mice revealed a marked reduction in epididymal white adipose tissue (WAT) (Supplementary Fig. 1a). When normalized for body weight, epididymal, inguinal and retroperitoneal fat pads (Fig. 1b), as well as the brown fat pad (Supplementary Fig. 1b) were significantly reduced. Furthermore, the decrease was specific for fat, as the weight of other major organs such as liver was not affected after correction for total body weight (Fig. 1b).

Analysis of adipocytes in epididymal fat pads by either scanning electron microscopy or by haematoxylin and eosin staining showed a sharp reduction in size, with some adipocytes exhibiting a multilocular-like phenotype (Fig. 1c and see below). Morphometric analysis revealed that *S6K1*$^{-/-}$ adipocytes were consistently smaller compared with adipocytes from wild-type mice (Fig. 1c), with an average 71% decrease in size (Supplementary Fig. 1c). The decrease in fat accumulation in *S6K1*$^{-/-}$ mice was not due to less food intake, which was increased 17% when food consumption was adjusted for body weight (Fig. 1d). Moreover, on the basis of normal fasting and feeding glucose levels and no increase in ketone body formation[3] (Table 1), *S6K1*$^{-/-}$ mice did not seem to be starving, nor was there an alteration in adaptive thermogenesis (data not shown). This raised the possibility that triglycerides were being broken down rather than stored in WAT. Consistent with this, basal rates of lipolysis were fivefold higher in *S6K1*$^{-/-}$ versus wild-type adipocytes, although norepinephrine-induced fatty acid and glycerol release increased in both genotypes in a dose-dependent manner to the same final extent (Fig. 1e; see also Supplementary Fig. 1d). Moreover the metabolic rate was greatly enhanced in *S6K1*$^{-/-}$ mice, as indicated by the 27% increase in oxygen consumption versus wild-type mice (Fig. 1f). The respiratory exchange ratio (RER) of 0.713 ± 0.004 for wild-type mice and 0.709 ± 0.003 for *S6K1*$^{-/-}$ mice ($P < 0.01$) showed that both animals were largely using fatty acids as an energy source. Thus the failure to accumulate fat with age in *S6K1*$^{-/-}$ mice seems to stem from a sharp increase in lipolytic and metabolic rates.

These increased responses, combined with the finding that levels of circulating triglycerides and free fatty acids (FFAs) were similar in both genotypes (Table 1), suggested that in *S6K1*$^{-/-}$ mice triglycerides were being rapidly oxidized in WAT and/or muscle. WAT is not an energy-consuming tissue; however, electron micrographs revealed multi-locular adipocytes, with mitochondria of increased size and number—phenotypes that are absent in wild-type adipocytes (Fig. 2a). Consistent with this, analysis of the messenger RNA levels of genes involved in energy combustion and oxidative phosphorylation were found to be strongly increased in *S6K1*$^{-/-}$ adipocytes compared with wild-type adipocytes, including uncoupling protein 1 (UCP1), UCP3, carnitine palmitoyltransferase 1 (CPT1) and PPAR-γ co-activator 1-α (PGC1-α) (Fig. 2a; see also Supplementary Fig. 2a). Mitochondrial content was also affected in *S6K1*$^{-/-}$ skeletal muscle (Fig. 2b), consistent with increased expression of peroxisome proliferator-activated receptor β/δ (PPAR-β/δ), PGC1-α, UCP3 and CPT1 (Fig. 2b; see also Supplementary Fig. 2b). As *S6K1*$^{-/-}$ mice have reduced WAT and increased oxidative phosphorylation, this raised the possibility that *S6K1*$^{-/-}$ mice are protected against diet-induced obesity, which is linked to the oxidative phosphorylation pathway[6–10]. Indeed, when *S6K1*$^{-/-}$ mice were challenged with a high fat diet (HFD) (60% total calories derived from fat, 4,057 kcal kg^{-1}) weight accumulation was significantly reduced compared with wild-type mice during the 4-month feeding period (Figs 2c, d). Although food intake in *S6K1*$^{-/-}$ mice is similar to that of wild-type mice, when normalized to body weight they consume 44% more food (Supplementary Fig. 2c). Metabolic rate measured by indirect calorimetry increased for both genotypes on the HFD, with the effect more pronounced for *S6K1*$^{-/-}$ mice (compare Figs 2e and 1f).

Table 1 **One-hour post-prandial values after overnight fasting of wild-type and *S6K1*$^{-/-}$ mice**

	Wild type		*S6K1*$^{-/-}$	
Diet	Normal	High fat	Normal	High fat
Insulin (μg l^{-1})	0.57 ± 0.09	2.22 ± 0.87	0.38 ± 0.08†	0.27 ± 0.06†
Triglycerides (mmol l^{-1})	0.61 ± 0.09	1.08 ± 0.15	0.55 ± 0.06	0.95 ± 0.14
FFAs (mmol l^{-1})	0.26 ± 0.05	0.27 ± 0.02	0.19 ± 0.04	0.56 ± 0.10†
Leptin (ng ml^{-1})	6.11 ± 0.82	12.6 ± 0.00	3.22 ± 0.50	6.34 ± 2.35†
β-Hydroxybutyrate (mg dl^{-1})*	1.30 ± 0.05	ND	1.40 ± 0.16	ND

Values are for 6-month-old male mice of the indicated genotype fed a normal or high fat diet. Data represent mean ± s.e.m. ND, not determined.
*The level of β-hydroxybutyrate was measured in 6-h-fasted mice.
†$P < 0.05$ compared with wild type ($n = 6$–18).

©2004 Nature Publishing Group

Moreover RER remained unchanged in *S6K1* $^{-/-}$ mice on a HFD (0.708 ± 0.002), whereas in wild-type mice it increased from 0.713 ± 0.004 to 0.729 ± 0.002 ($n = 6$, $P < 0.01$), indicating an increase in carbohydrate relative to fatty acid oxidation. To determine the weight gain corresponding to fat, mice were subjected to magnetic resonance imaging (MRI) analysis at 2-month intervals while on the HFD. A transverse section through the abdomen showed a marked reduction in fat depots, depicted by the less intense signal (Supplementary Fig. 2d). MRI assessment of total fat, corrected for body weight, revealed that the body fat index for *S6K1* $^{-/-}$ mice increased by 20% over this period, whereas it doubled for wild-type mice (Fig. 2f). Thus, consistent with the increase in oxidative phosphorylation, *S6K1* $^{-/-}$ mice are protected against diet-induced obesity.

Although *S6K1* $^{-/-}$ mice have a high metabolic rate when on a HFD, they exhibit a threefold increase in circulating FFAs (Table 1), consistent with an increase in fat on their skin and hair (data not shown). As increased circulating FFAs are implicated in insulin resistance[11–13] and *S6K1* $^{-/-}$ mice are hypoinsulinaemic[3], it seemed likely that they would become insulin resistant on the HFD. On a NCD both *S6K1* $^{-/-}$ and wild-type mice exhibited similar fasting levels of glucose (Fig. 3a), although *S6K1* $^{-/-}$ mice were more insulin sensitive, as indicated by faster glucose clearance in the insulin tolerance test (Fig. 3a). In contrast, both genotypes displayed increased hyperglycaemia on a HFD, although the effect was more pronounced in wild-type mice (Fig. 3b). However, despite the increases in glucose and in FFAs, *S6K1* $^{-/-}$ mice remain as insulin sensitive on a HFD as on a NCD (Fig. 3b versus a). In the case of wild-type mice, insulin resistance on a HFD (Fig. 3b) can be explained by persistently elevated insulin levels (Table 1), inducing insulin receptor desensitization, as measured by reduced receptor auto-phosphorylation in response to insulin (Fig. 3c). In *S6K1* $^{-/-}$ mice insulin levels fail to rise on a HFD (Table 1), consistent with higher insulin receptor auto-phosphorylation (Fig. 3c). However, insulin receptors still desensitize in *S6K1* $^{-/-}$ mice on a HFD (Fig. 3c), probably due to the large increase in FFA levels (Table 1). That insulin receptors desensitize in *S6K1* $^{-/-}$ mice but remain insulin sensitive suggests that absence of S6K1 facilitates insulin signalling downstream of the insulin receptor. To test this we monitored protein kinase B (PKB) phosphorylation, as insulin sensitivity is tightly linked to the phosphatidylinositol-3-OH kinase (PI(3)K)–PKB signalling pathway[14]. As with insulin receptor auto-phosphorylation in wild-type mice on a HFD, insulin-induced PKB phosphorylation was suppressed in fat, liver and muscle compared with wild-type mice maintained on a NCD (Fig. 3d). However, there was no significant effect on PKB phosphorylation in *S6K1* $^{-/-}$ mice,

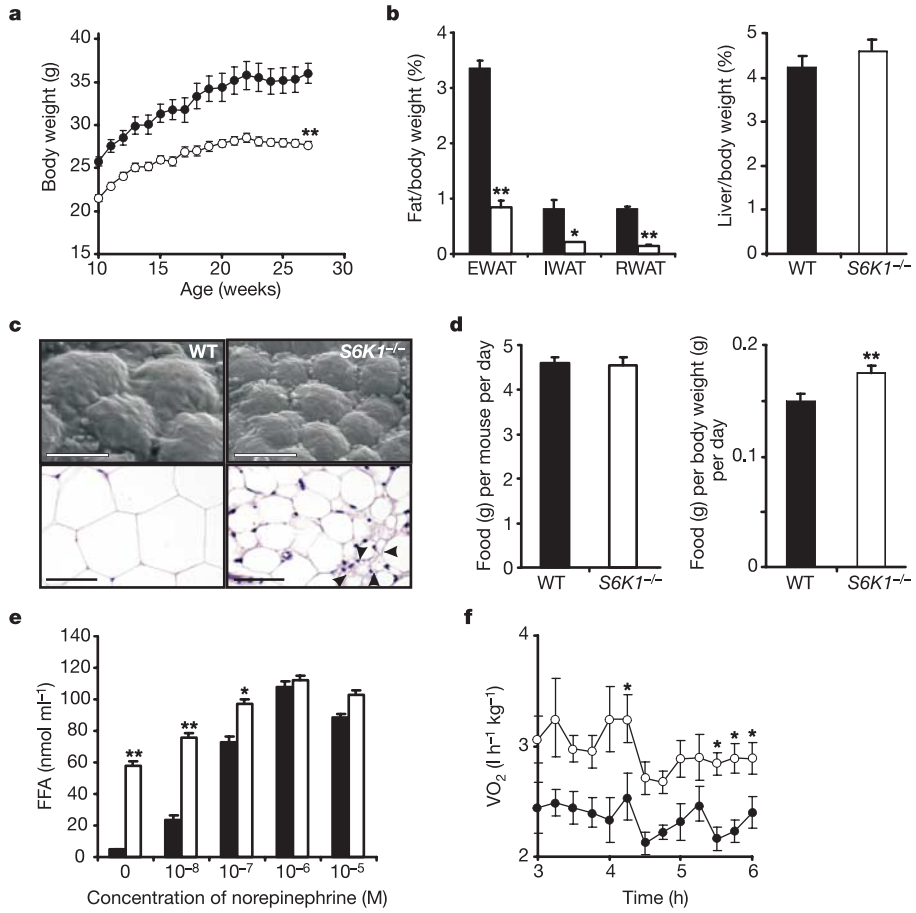

Figure 1 Reduced adiposity in *S6K1* $^{-/-}$ mice. **a**, Growth curves of wild-type and *S6K1* $^{-/-}$ mice on a NCD. Wild type, $n = 11$; *S6K1* $^{-/-}$, $n = 13$. **b**, Weights of epididymal, inguinal and retroperitoneal adipose tissue (EWAT, IWAT and RWAT, respectively) and liver normalized by body weight ($n = 6$ each genotype). WT, wild type. **c**, Scanning electron microscopic (top) and histological analysis of epididymal WAT (bottom). Arrowheads indicate multi-locular adipocytes. Magnification for scanning microscopy and for histology are × 500 and × 200, respectively. Mice were 6-month-old males in **b** and **c**. **d**, Food intake per mouse measured over 15 days ($n = 12$; $P = 0.8$) or normalized by body weight ($n = 12$). **e**, Enhanced lipolysis in *S6K1* $^{-/-}$ adipocytes. **f**, Oxygen consumption (VO_2) in wild-type and *S6K1* $^{-/-}$ mice fed a NCD ($n = 6$ each genotype). All values are given as mean ± s.e.m. Asterisk, $P < 0.01$; double asterisk, $P < 0.001$. Filled symbols/columns indicate wild type; open symbols/columns, *S6K1* $^{-/-}$ mice.

©2004 Nature Publishing Group

regardless of diet or tissue (Fig. 3d). This suggested that S6K1 elicited a selective inhibitory effect on PKB activation at a point downstream of the insulin receptor, consistent with little effect on mitogen activated protein kinase and S6K1 activation in wild-type animals on a HFD (see below and data not shown).

Recently, we demonstrated in *Drosophila* that dS6K negatively regulates dPKB activity in a cell-autonomous manner[15]. To test whether this was the mechanism responsible for the observed responses, S6K1 levels were reduced with small interfering RNAs. The results show that lowering S6K1 levels potentiates insulin-induced PKB phosphorylation, with no effect on insulin receptor auto-phosphorylation (Fig. 3e), suggesting that the target of inhibition resided downstream of the insulin receptor. Indeed, reduction of S6K1 levels is paralleled by a decrease in phosphorylation of S307 and S636/S639 of insulin receptor substrate 1 (IRS1) (Fig. 3e), sites shown to inhibit PI(3)K binding to IRS1 (ref. 4) and

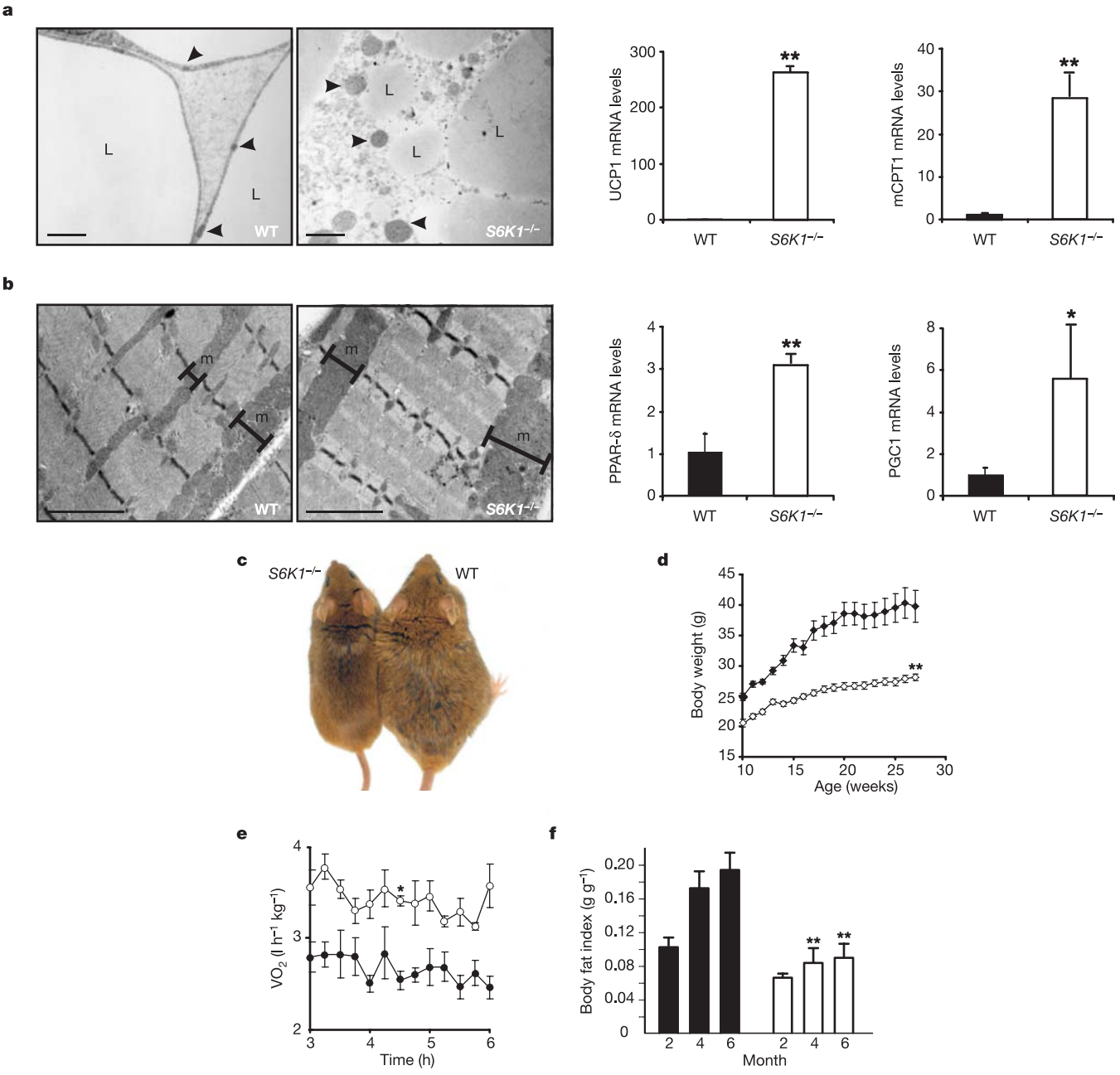

Figure 2 Increased mitochondria and resistance to diet-induced obesity. **a**, The left panels show transmission electron microscopic analysis of epididymal fat. Arrowheads indicate mitochondria and lipid droplets (L) (× 5,000 magnification). The right panels show UCP1 and mCPT1 mRNA (relative values) measured by quantitative RT–PCR (see Methods). **b**, The left panels show transmission electron microscopic analysis of plantaris muscle (× 10,000 magnification). m, mitochondria. The right panels show PPAR-δ and PGC1 mRNA levels (relative values) measured by quantitative RT–PCR. In **a**, **b**, $n = 4$–7; asterisk, $P < 0.01$; double asterisk, $P < 0.001$. **c**, Representative wild-type and *S6K1* $^{-/-}$ mice after 6 months feeding on a HFD. **d**, Growth curves of wild-type and *S6K1* $^{-/-}$ mice maintained on a HFD. WT, $n = 11$; *S6K1* $^{-/-}$, $n = 15$; $P < 0.001$. **e**, Oxygen consumption (VO_2) in wild-type and *S6K1* $^{-/-}$ mice maintained on a HFD for 6 months ($n = 6$ each genotype). **f**, Body fat index determined by MRI analysis of wild-type ($n = 10$) and *S6K1* $^{-/-}$ mice ($n = 12$) maintained on a HFD for 4 months. Filled symbols/columns indicate wild type; open symbols/columns, *S6K1* $^{-/-}$ mice. Values are mean ± s.e.m. Asterisk, $P < 0.01$; double asterisk, $P < 0.001$ in **d**–**f**.

©2004 Nature Publishing Group

to be involved in insulin resistance in skeletal muscle cells from patients with type 2 diabetes[5]. Thus, removal of S6K1 can facilitate insulin signalling in a cell-autonomous manner.

Hyperglycaemia, hyperaminoacidaemia and hyperlipidaemia are associated with obesity and insulin resistance[16]; however, the role of increased nutrients in insulin action is not well understood[17–19]. As S6K1 is activated by nutrients[20–22] and acts negatively on PI(3)K signalling, this raised the possibility that on a HFD S6K1 is involved in inducing insulin resistance. This hypothesis is supported by the reversal of amino acid inhibition of insulin-induced PI(3)K signalling by rapamycin, which inhibits mTOR[23], an immediate upstream S6K1 kinase[2]. Consistent with this hypothesis, phosphorylation of S6K1 T389, S6 S240/S244, IRS1 S307 and IRS1 S636/S639 is highly elevated in wild-type mice maintained on a HFD compared with wild-type mice maintained on a NCD (Fig. 4a, b). Furthermore, the increase in IRS1 S307 and S636/S639 phosphorylation is absent in *S6K1* $^{-/-}$ mice on a HFD (Fig. 4b). Under these conditions there were no apparent alterations in IRS1 levels (Fig. 4b). These findings suggest that nutrient-induced S6K1 activation acts to suppress insulin signalling through modulating IRS1 S307 and S636/S639 phosphorylation. To test this further, two genetic models of obesity were examined: *K/K A*^{y} and *ob/ob* mice[24,25]. The results show that the *K/K A*^{y} and *ob/ob* mice maintained on a NCD have elevated S6K1 T389, S6 S240/S244, IRS1 S307 and IRS1 S636/S639 phosphorylation as compared with wild-type mice on a NCD (Fig. 4c). Moreover, in contrast with PKB S473 phosphorylation in adipose and muscle (Fig. 3d), insulin stimulates S6K1 T389 phosphorylation to even higher levels in wild-type animals on a HFD compared with a NCD (Fig. 4d), potentially further suppressing PI(3)K signalling. Thus, either nutritionally or genetically driven obesity leads to the upregulation of S6K1, which may in turn act to suppress PI(3)K signalling, contributing to insulin resistance.

The results presented here indicate that *S6K1* $^{-/-}$ mice are protected against obesity and insulin resistance due to the upregulation of the oxidative phosphorylation pathway and increased insulin sensitivity. Enhanced oxidative metabolism is consistent with the increase in mitochondria number, as well as the induction of genes that control the oxidative phosphorylation pathway. That *S6K1* $^{-/-}$ mice remain insulin sensitive despite high circulating FFAs may be explained by the strong protection against metabolic syndrome by overexpression or activation of PPAR-δ[6–8]. Despite the increase in the oxidative phosphorylation pathway and reduced insulin levels, circulating glucose and FFA levels still rise in *S6K1* $^{-/-}$ mice; however, these animals remain sensitive to insulin, and PI(3)K

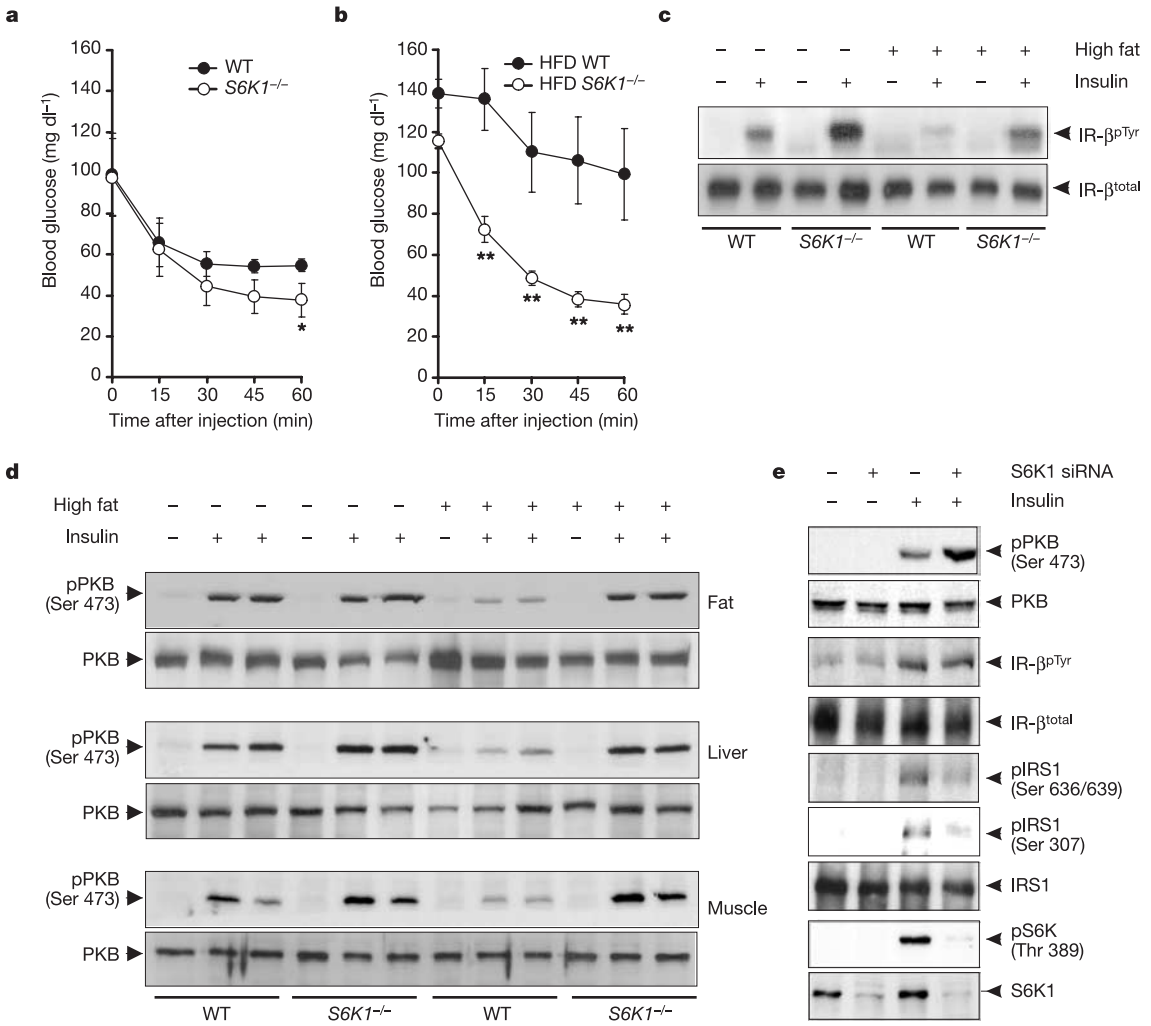

Figure 3 Enhanced insulin sensitivity and insulin signalling in the absence of S6K1. **a**, **b**, Insulin tolerance test in 3-h-fasted mice on a NCD (**a**) or HFD (**b**) at 6 months of age. Asterisk, $P < 0.05$; double asterisk, $P < 0.01$. Values are mean ± s.e.m. **c**, Insulin receptor tyrosine phosphorylation in liver of wild-type and *S6K1* $^{-/-}$ mice before (−) or after (+) insulin stimulation on a NCD or HFD. **d**, Level of phosphorylation of PKB Ser 473 in fat, liver and muscle ($n = 3$–8 for each genotype in **c**, **d**). **e**, Lowering S6K1 expression by siRNA potentiates insulin-induced PKB phosphorylation in HeLa cells.

©2004 Nature Publishing Group

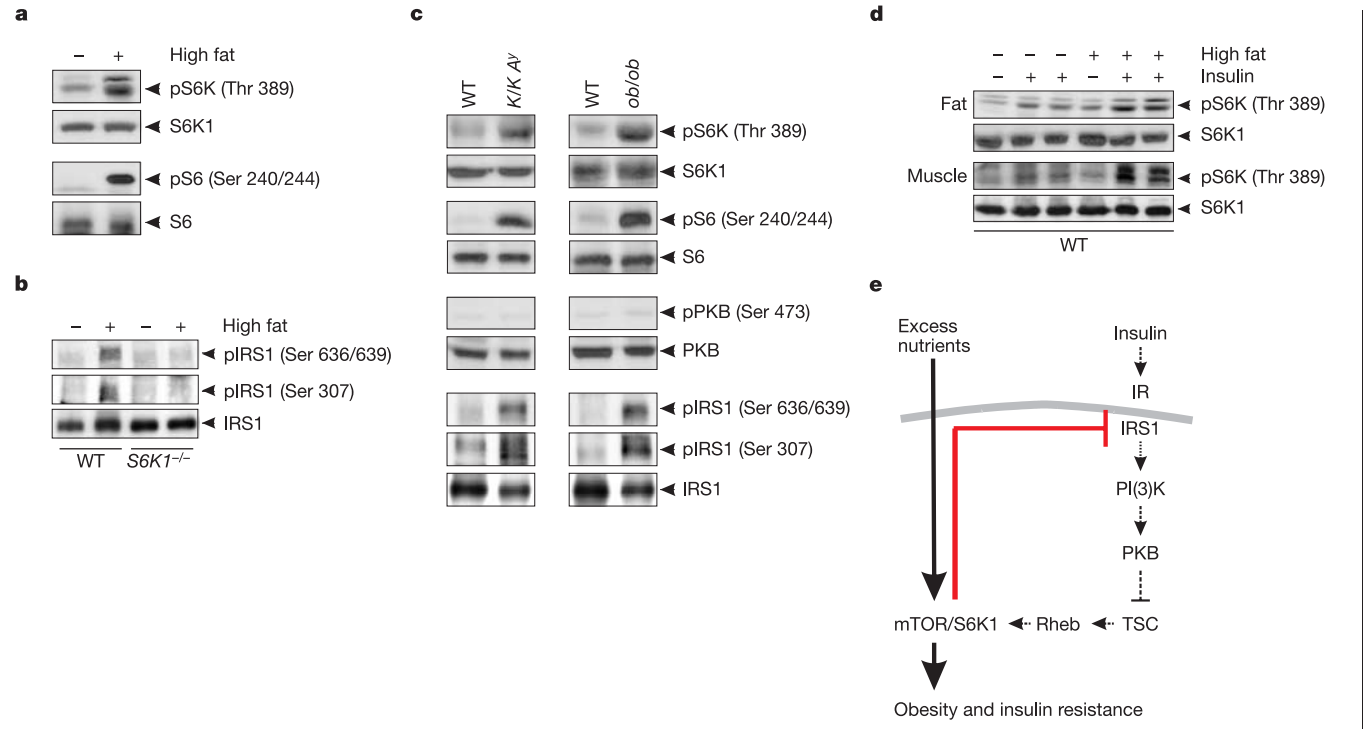

Figure 4 S6K1 activation in obesity. **a**, S6K1 Thr 389 and S6 Ser 240/244 phosphorylation in fat of wild-type mice maintained on a NCD (−) or HFD (+) for 4 months. **b**, IRS1 Ser 307 and Ser 636/639 phosphorylation in fat of wild-type or *S6K1* $^{-/-}$ mice maintained on a NCD (−) or HFD (+). **c**, S6K1 Thr 389, S6 Ser 240/244, IRS1 Ser 307 and IRS1 Ser 636/639 phosphorylation in fat of wild-type, *K/K A* ^{y} or *ob/ob* mice maintained on a NCD. **d**, S6K1 Thr 389 phosphorylation in fat or muscle of wild-type mice maintained on a NCD or HFD for 4 months before (−) or after (+) injection of insulin (0.75 U kg^{-1} of body weight). All mice of each genotype (n = 3–8) in **a**–**d** were fasted for 6 h and were 6 months old. **e**, Model of inhibition of IRS1 signalling through activation of S6K1.

signalling is unaffected. This observation may be explained by the loss of S6K1, whose activation by either nutrients or insulin leads to increased IRS1 serine phosphorylation (Fig. 4e). In the case of insulin, this is mediated by a negative feedback loop triggered by PKB phosphorylation of the TSC1/2 tumour suppressor complex, leading to Rheb activation and stimulation of S6K1 (ref. 26). Thus, in a homeostatic setting, as nutrients and amino acids are consumed, mTOR/S6K1 activity would decrease, restoring PI(3)K signalling, whereas the incessant supply of nutrients associated with the obese state would lead to constitutive activation of mTOR/S6K1 and desensitization of insulin signalling (Fig. 4e). Taken together the results suggest that S6K1 may have a central function along with other signalling components in development of obesity and insulin resistance, and may be an important drug target in the treatment of patients suffering from these pathological disorders. □

Methods

Mice

S6K1 $^{-/-}$ mice were generated as previously described[3]. Male C57BL/6J, *K/K A* ^{y} and *ob/ob* (C57BL/6J background) mice were obtained from E. Janvier, CLEA Japan Inc., and The Jackson Laboratory, respectively.

Metabolic studies

At 10 weeks of age male mice were placed on either a NCD (diet number 3807, KLIBA-NAFAG) or HFD *ad libitum* (diet D12492, Researchdiets) and monitored for 24 weeks. Body weight was recorded weekly and food intake was measured every second day for 15 consecutive days. Insulin tolerance tests, oxygen consumption, RER measurements and quantification of blood metabolites were performed as previously described[27].

Histology and morphometric analysis of tissues

Adipose tissue was analysed by haematoxylin and eosin staining as previously described[27]. Morphometric analysis of epididymal WAT from 500 or more cells from three different animals per genotype was performed with ImageJ software (NIH). Adipose and plantaris muscle tissue were prepared as described for scanning and transmission electron microscopy[27].

Magnetic resonance imaging analysis

MRI experiments were carried out on a Biospec 47/30 spectrometer (Bruker Medical) at 4.7 T equipped with a self-shielded 12-cm bore gradient system[28]. Animals were anaesthetized with 1.5% isoflurane (Abbott). Adipose tissue was measured with an optimized turbo-RARE2 imaging sequence. Acquisition parameters were: repetition delay (TR) = 250 ms; echo delay (TE) = 8.6 ms; RARE factor = 32 (effective echo time 73.1 ms); number of averages = 8; slice orientation transverse, image matrix = 128 × 128 pixels; field-of-view = 3.5 × 3.5 cm; slice thickness = 1.2 mm (contiguous). Fat pad volumes were assessed with an in-house software algorithm based on IDL software package (Research Systems Inc.). Body fat indices were calculated by dividing adipose tissue weight by body weight.

Lipolysis in isolated adipocytes

Primary adipocytes were prepared from epididymal fat pads as described previously[29]. Cells were incubated for 30 min at 37 °C with or without norepinephrine (Sigma-Aldrich SARL) at the indicated concentrations.

Real-time quantitative RT–PCR

Total RNA was extracted from frozen tissue samples or cells using the RNeasy kit (Qiagen). Complementary DNA was synthesized from total RNA with the SuperScript First-Strand Synthesis System (Invitrogen) and random hexamer primers. The real-time polymerase chain reaction (PCR) measurement of individual cDNAs was performed using SYBR green dye to measure duplex DNA formation with the Roche Lightcycler system and normalized to the expression of either β-actin or 18S ribosomal RNA. The primers and probes used in the real time RT–PCR were the following: UCP1 sense 5′-GGCCCTTGT AAACAACAAAATAC-3′, antisense 5′-GGCAACAAGAGCTGACAGTAAAT-3′; UCP3 sense 5′-ACTCCAGCGTCGCCATCAGGATTCT-3′, antisense 5′-TAAACAGGTGAG ACTCCAGCAACTT-3′; mCPT1 sense 5′-TTGCCCTACAGCTCTGGCATTTCC-3′, antisense 5′-GCACCCAGATGATTGGGATACTGT-3′; mPPAR-δ sense 5′-CTCTTCATC GCGGCCATCATTCT-3′, antisense 5′-TCTGCCATCTTCTGCAGCAGCTT-3′; PGC-1 sense 5′-AAGTGTGGAACTCTCTGGAACTG-3′, antisense 5′-GGGTTATCTTGGTTGG CTTTATG-3′.

©2004 Nature Publishing Group

Measurement of insulin receptor and IRS1 phosphorylation *in vivo*

After a 6-h fast mice were injected intravenously with 0.75 U kg^{-1} insulin (Eli Lilly) or equal volume of vehicle. All indicted tissues were collected in liquid nitrogen 5 min after injection. Protein extracts from tissue samples were analysed as described[30]. Antibodies were from Santa Cruz (anti-insulin receptor β and anti-S6K1 antibodies), Upstate Biotechnology (anti-phosphotyrosine and anti-IRS1 antibodies) and Cell Signaling (anti-PKB, anti-phospho-PKB Ser 473, anti-phospho-IRS1 Ser 636/639, anti-phospho-S6K Thr 389 and anti-phospho-S6 240/244 antibodies). Antibodies to S6 and phospho-IRS1 Ser 307 were from J. Mestan and Y. Le Marchand-Brustel, respectively.

RNA interference

RNA interference (RNAi) duplexes corresponding to human S6K1 (5′-AAGGGGGCTATGGAAAGGTTT-3′) were purified, annealed and transfected into HeLa cells using oligofectamine (Invitrogen). After 60 h cells were deprived of serum overnight and either lysed directly or stimulated with 200 nM insulin for 30 min. The effect of RNAi on S6K1 expression and PKB phosphorylation was measured by western blot analysis. Cell lysates were incubated for 4 h with anti-IRS1 or anti-insulin receptor β antibody pre-absorbed on protein A Sepharose at 4 °C, and analysed by western blot analyses after gel electrophoresis.

Statistical analysis

Data are presented as mean ± s.e.m. The main and interactive effects were analysed by analysis of variance (ANOVA) factorial, repeated measurements or by one-way ANOVA followed by Bonferroni *t*-test (MRI analysis). Differences between individual group means were analysed by Fisher's PLSD test. Analyses were performed using Statview Software (Brainpower).

Received 19 April; accepted 21 July 2004; doi:10.1038/nature02866.
Published online 11 August 2004.

1. Saltiel, A. R. & Kahn, C. R. Insulin signalling and the regulation of glucose and lipid metabolism. *Nature* **414,** 799–806 (2001).
2. Fingar, D. C., Salama, S., Tsou, C., Harlow, E. & Blenis, J. Mammalian cell size is controlled by mTOR and its downstream targets S6K1 and 4EBP1/eIF4E. *Genes Dev.* **16,** 1472–1487 (2002).
3. Pende, M. *et al.* Hypoinsulinaemia, glucose intolerance and diminished β-cell size in S6K1-deficient mice. *Nature* **408,** 994–997 (2000).
4. Zick, Y. Insulin resistance: a phosphorylation-based uncoupling of insulin signaling. *Trends Cell Biol.* **11,** 437–441 (2001).
5. Bouzakri, K. *et al.* Reduced activation of phosphatidylinositol-3 kinase and increased serine 636 phosphorylation of insulin receptor substrate-1 in primary culture of skeletal muscle cells from patients with type 2 diabetes. *Diabetes* **52,** 1319–1325 (2003).
6. Tanaka, T. *et al.* Activation of peroxisome proliferator-activated receptor delta induces fatty acid β-oxidation in skeletal muscle and attenuates metabolic syndrome. *Proc. Natl Acad. Sci. USA* **100,** 15924–15929 (2003).
7. Luquet, S. *et al.* Peroxisome proliferator-activated receptor delta controls muscle development and oxidative capability. *FASEB J.* **17,** 2299–2301 (2003).
8. Dressel, U. *et al.* The peroxisome proliferator-activated receptor beta/delta agonist, GW501516, regulates the expression of genes involved in lipid catabolism and energy uncoupling in skeletal muscle cells. *Mol. Endocrinol.* **17,** 2477–2493 (2003).
9. Patti, M. E. *et al.* Coordinated reduction of genes of oxidative metabolism in humans with insulin resistance and diabetes: Potential role of PGC1 and NRF1. *Proc. Natl Acad. Sci. USA* **100,** 8466–8471 (2003).
10. Mootha, V. K. *et al.* PGC-1α-responsive genes involved in oxidative phosphorylation are coordinately downregulated in human diabetes. *Nature Genet.* **34,** 267–273 (2003).
11. Boden, G. Role of fatty acids in the pathogenesis of insulin resistance and NIDDM. *Diabetes* **46,** 3–10 (1997).
12. Kahn, B. B. Type 2 diabetes: when insulin secretion fails to compensate for insulin resistance. *Cell* **92,** 593–596 (1998).
13. Le Marchand-Brustel, Y. *et al.* Fatty acid-induced insulin resistance: role of insulin receptor substrate 1 serine phosphorylation in the retroregulation of insulin signalling. *Biochem. Soc. Trans.* **31,** 1152–1156 (2003).
14. Jiang, G. & Zhang, B. B. Pi 3-kinase and its up- and down-stream modulators as potential targets for the treatment of type II diabetes. *Front. Biosci.* **7,** d903–d907 (2002).
15. Radimerski, T., Montagne, J., Hemmings-Mieszczak, M. & Thomas, G. Lethality of *Drosophila* lacking TSC tumor suppressor function rescued by reducing dS6K signaling. *Genes Dev.* **16,** 2627–2632 (2002).
16. Kahn, B. B. & Flier, J. S. Obesity and insulin resistance. *J. Clin. Invest.* **106,** 473–481 (2000).
17. Proietto, J., Filippis, A., Nakhla, C. & Clark, S. Nutrient-induced insulin resistance. *Mol. Cell. Endocrinol.* **151,** 143–149 (1999).
18. Greiwe, J. S., Kwon, G., McDaniel, M. L. & Semenkovich, C. F. Leucine and insulin activate p70 S6 kinase through different pathways in human skeletal muscle. *Am. J. Physiol. Endocrinol. Metab.* **281,** E466–E471 (2001).
19. Patti, M. E. Nutrient modulation of cellular insulin action. *Ann. NY Acad. Sci.* **892,** 187–203 (1999).
20. Hara, K. *et al.* Amino acid sufficiency and mTOR regulate p70 S6 kinase and eIF-4E BP1 through a common effector mechanism. *J. Biol. Chem.* **273,** 14484–14494 (1998).
21. Patti, M. E., Brambilla, E., Luzi, L., Landaker, E. J. & Kahn, C. R. Bidirectional modulation of insulin action by amino acids. *J. Clin. Invest.* **101,** 1519–1529 (1998).
22. Dennis, P. B. *et al.* Mammalian TOR: a homeostatic ATP sensor. *Science* **294,** 1102–1105 (2001).
23. Tremblay, F. & Marette, A. Amino acid and insulin signaling via the mTOR/p70 S6 kinase pathway. A negative feedback mechanism leading to insulin resistance in skeletal muscle cells. *J. Biol. Chem.* **276,** 38052–38060 (2001).
24. Iwatsuka, H., Shino, A. & Suzuoki, Z. General survey of diabetic features of yellow KK mice. *Endocrinol. Jpn* **17,** 23–35 (1970).
25. Zhang, Y. *et al.* Positional cloning of the mouse obese gene and its human homologue. *Nature* **372,** 425–432 (1994).
26. Manning, B. D. & Cantley, L. C. Rheb fills a GAP between TSC and TOR. *Trends Biochem. Sci.* **28,** 573–576 (2003).
27. Picard, F. *et al.* SRC-1 and TIF2 control energy balance between white and brown adipose tissues. *Cell* **111,** 931–941 (2002).
28. Doty, F. D., Entzminger, G. Jr, Hauck, C. D. & Staab, J. P. Practical aspects of birdcage coils. *J. Magn. Reson.* **138,** 144–154 (1999).
29. Marette, A., Tulp, O. L. & Bukowiecki, L. J. Mechanism linking insulin resistance to defective thermogenesis in brown adipose tissue of obese diabetic SHR/N-cp rats. *Int. J. Obes.* **15,** 823–831 (1991).
30. Hirosumi, J. *et al.* A central role for JNK in obesity and insulin resistance. *Nature* **420,** 333–336 (2002).

Supplementary Information accompanies the paper on **www.nature.com/nature**.

Acknowledgements We thank T. Opgenorth and C. Rondinone for sharing their results before publication; G. S. Hotamisligil, S. Y. Kim and D. J. Withers for their critical reading of the manuscript; and S. Cinti, P. B. Dennis, A. Dulloo, L. Fajas, A. Greenberg, B. M. Spiegelman, G. Solinas, J. Tanti and M. Wymann for discussions. We are also grateful to M.-F. Champy, W. Theilkaes, N. Messaddeq, I. Obergfoell and J. F. Spetz for the blood analysis, studies with MRI, technical assistance with electron microscopy, for photography and for assistance in the animal experiments, respectively. Work in the laboratory of J.A. is supported by grants from CNRS, INSERM, ULP, Hôpital Universitaire de Strasbourg, NIH, EMBO and the European community, and the laboratory of S.C.K. and G.T. is supported by the Novartis Institutes for Biomedical Research and a grant from the Swiss Cancer League.

Competing interests statement The authors declare that they have no competing financial interests.

Correspondence and requests for materials should be addressed to G.T. (gthomas@fmi.ch).

Cytoplasmic PML function in TGF-β signalling

Hui-Kuan Lin, Stephan Bergmann & Pier Paolo Pandolfi

Cancer Biology and Genetics Program, Department of Pathology, Memorial Sloan-Kettering Cancer Center, Sloan-Kettering Institute, 1275 York Avenue, New York, New York, 10021, USA

Transforming growth factor β (TGF-β) is a pluripotent cytokine that controls key tumour suppressive functions[1–3], but cancer cells are often unresponsive to it[1,4]. The promyelocytic leukaemia (PML) tumour suppressor of acute promyelocytic leukaemia (APL) accumulates in the PML nuclear body, but cytoplasmic PML isoforms of unknown function have also been described[5,6]. Here we show that cytoplasmic *Pml* is an essential modulator of TGF-β signalling. *Pml*-null primary cells are resistant to TGF-β-dependent growth arrest, induction of cellular senescence and apoptosis. These cells also have impaired phosphorylation and nuclear translocation of the TGF-β signalling proteins Smad2 and Smad3, as well as impaired induction of TGF-β target genes. Expression of cytoplasmic *Pml* is induced by TGF-β. Furthermore, cytoplasmic PML physically interacts with Smad2/3 and SARA (Smad anchor for receptor activation) and is required for association of Smad2/3 with SARA and for the accumulation of SARA and TGF-β receptor in the early endosome. The PML–RARα oncoprotein of APL can antagonize cytoplasmic PML function and APL cells have defects in TGF-β signalling similar to those observed in *Pml*-null cells. Our findings identify cytoplasmic PML as a critical TGF-β regulator, and further implicate deregulated TGF-β signalling in cancer pathogenesis.

APL is almost invariably associated with chromosomal translocations involving the *PML* tumour suppressor and *RARα* genes, resulting in the generation of a PML–RARα leukaemogenic fusion protein that can function as a dominant-negative PML and RARα mutant[7–9]. PML–RARα physically interacts with nuclear PML isoforms causing their delocalization from the PML nuclear body (PML-NB) into aberrant microspeckled nuclear structures[7,8]. Until

©2004 Nature Publishing Group

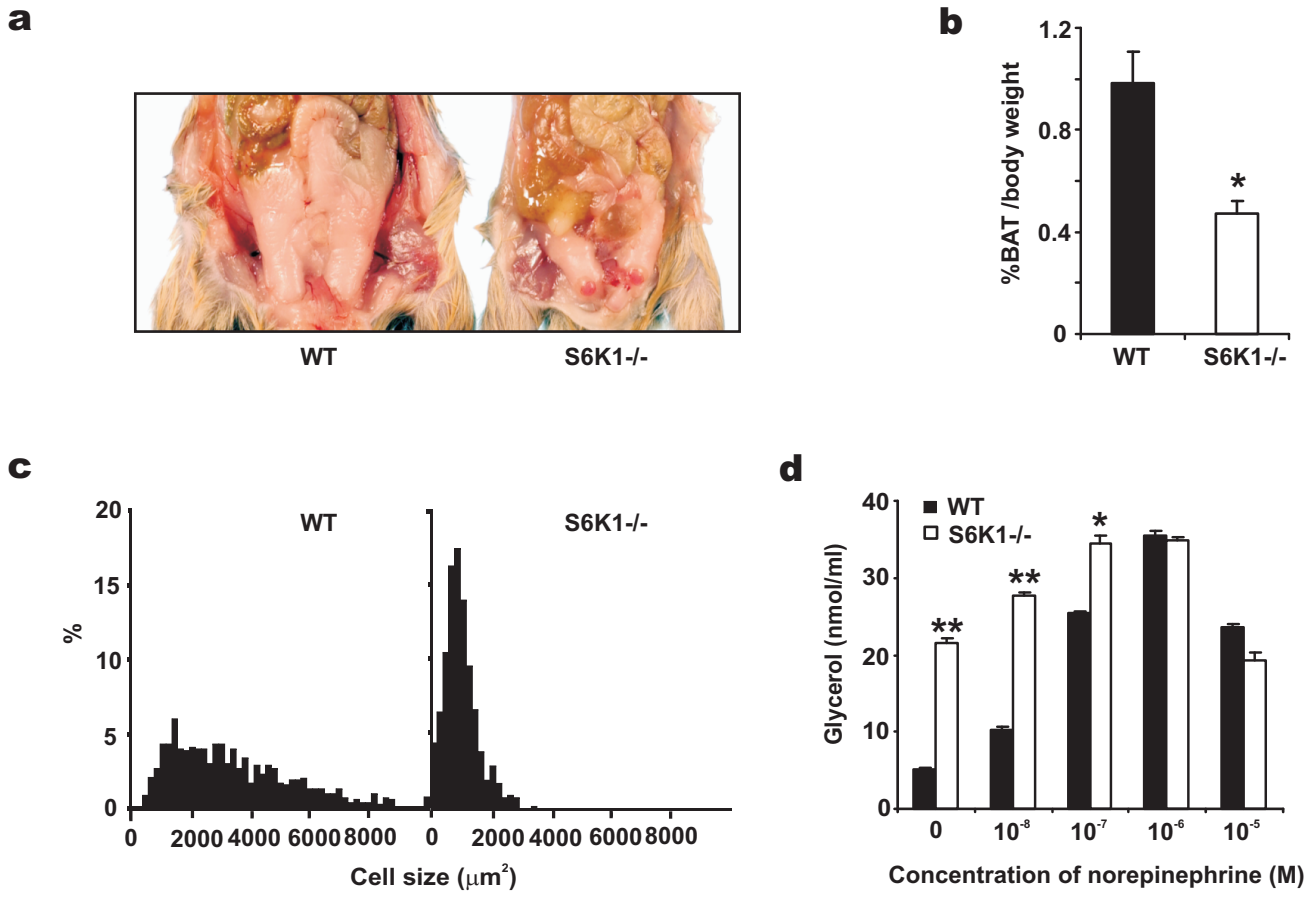

Supplementary Figure 1: Reduced adiposity in *S6K1*$^{-/-}$ mice. **a**, A ventral view of *WT* and *S6K1*$^{-/-}$ mouse. **b,** Weight of brown adipose tissue normalized by body weight (n=6 each genotype). **c**, Epididymal fat sections were stained by haematoxilin and eosin and used to measure cell size and cell number of *WT* and *S6K1*$^{-/-}$ mice (n=3). **d**, Enhanced lipolysis in *S6K1*$^{-/-}$ adipocytes. *, $P < 0.01$, **, $P < 0.001$.

Supplementary Figure 1

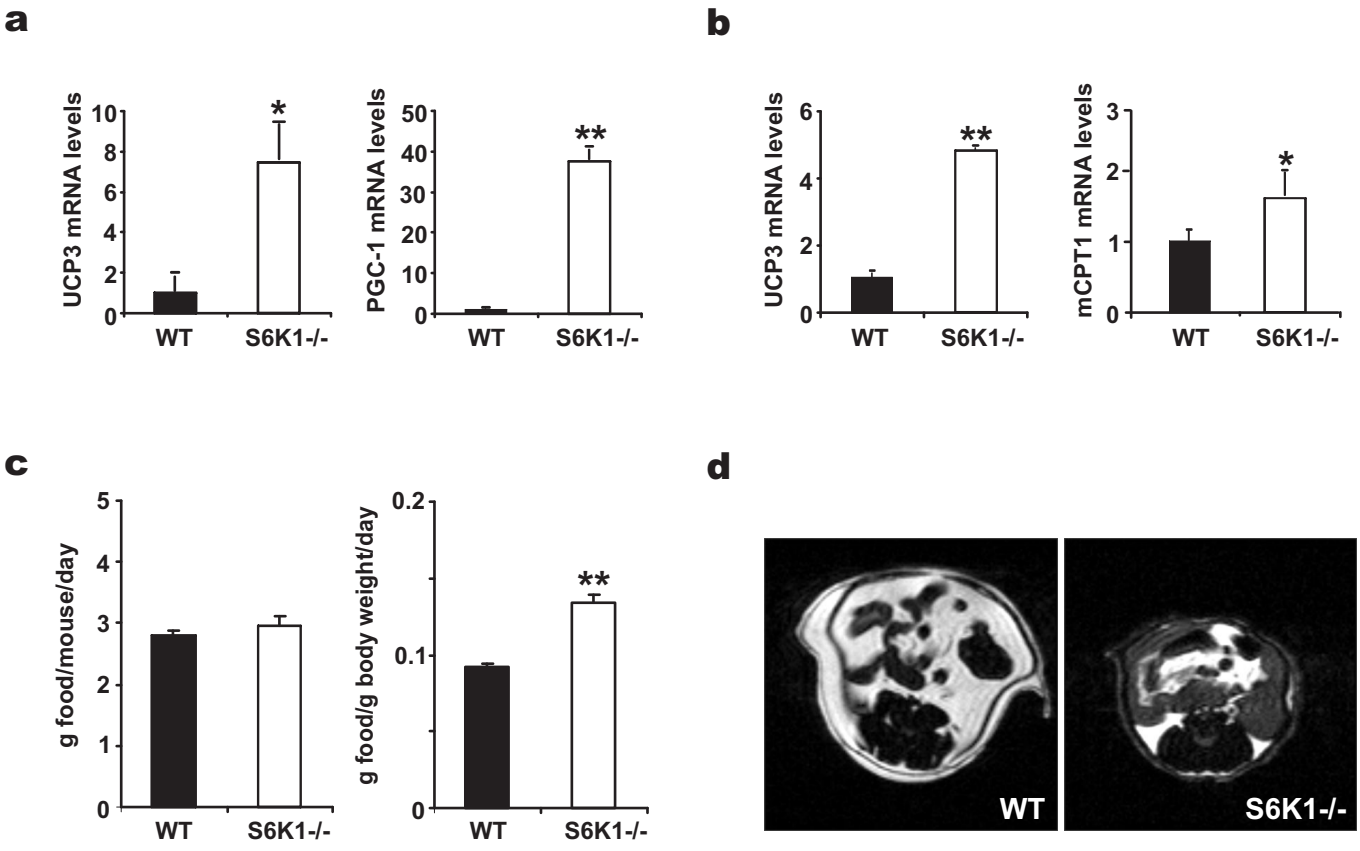

Supplementary Figure 2: Increased mitochondria and resistance to diet-induced obesity. a, UCP3 and PGC1 mRNA levels were measured by quantitative RT-PCR (see Methods,). **b,** UCP3 and mCPT1 mRNA levels were measured by quantitative RT-PCR. n=4-7 in a-b. **c**, Food intake per mouse measured, *WT*: 2.81 ± 0.07 (n=12); *S6K1*$^{-/-}$: 2.96 ± 0.15 g/day (n=15), P=0.2, or normalized by body weight over 15 days on a high fat diet: *WT*: 0.09 ± 0.01 (n=12); *S6K1*$^{-/-}$: 0.13 ± 0.01 g/ g of body weight/day (n=15). **d,** Representative MRI sections from the abdominal region of a *WT* and *S6K1*$^{-/-}$ mouse, where white regions indicate fat. *, $P < 0.01$, **, $P < 0.001$.

Supplementary Figure 2

Part2:

Unpublished results

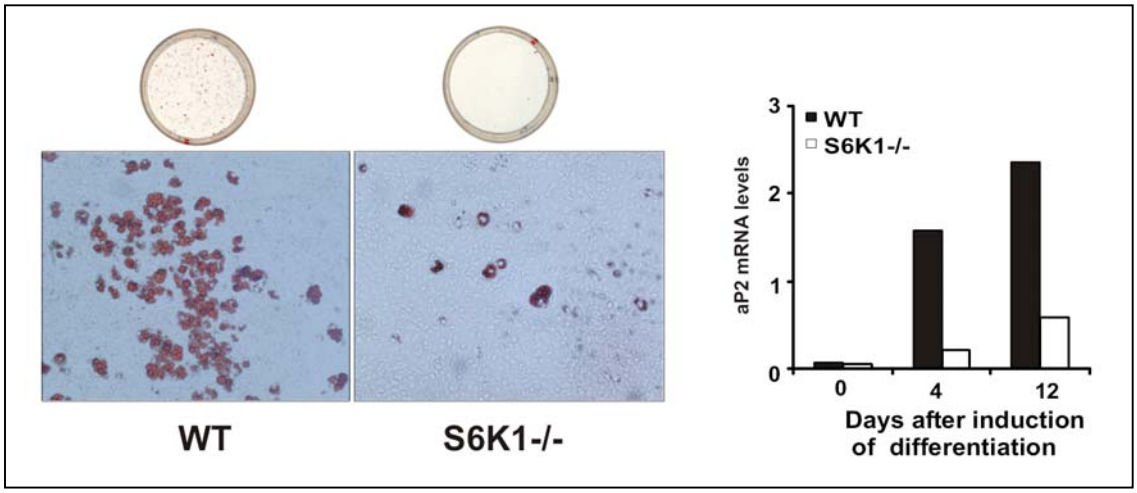

Impaired adipogenesis in *S6K1*$^{-/-}$ mouse embryonic fibroblasts *in vitro*.

Oil red O staining in wild type and *S6K1*$^{-/-}$ MEFs induced to differentiate into adipocytes by treatment with a differentiation cocktail (see Methods). aP2 mRNA levels measured by quantitative RT-PCR (Right).

Supplementary Method: Induction of adipocyte differentiation

Mouse embryonic fibroblasts (MEFs) were prepared as previously described (Shima et al., 1998). To induce adipogenesis in MEFs, the medium was supplemented with 2 μM insulin, 1 μM dexamethasone, and 0.25 mM isobuthyl methyl xanthine for 2 days. The cells were then incubated with insulin and 10^{-7} M rosiglitazone for another 12 days, changing the medium every second day. Fat accumulation was scored by determination of mRNA and protein levels of adipocyte-specific genes and by staining of lipids with Oil Red O.

III. RESULTS

Part:3:……...

Regulation of pancreatic β-cell growth by S6K1 during development

Um SH, Sticker M, Vintersten K, Gangloff YG, Adams R., Mueller M, Pyo S, Thomas G and Kozma S.

Unpublished results and discussion.

Abstract

The pancreatic β-cell mass is dynamically regulated in order to maintain nutrient homeostasis by changing β-cell number and size (Bernard et al., 1999). S6K1 is a downstream effector of the mTOR-signalling pathway which integrates nutrient and mitogen signalling to regulate cell growth (Fingar et al., 2002). Consistent with this, *S6K1*$^{-/-}$ mice have previously been shown to be hypoinsulinemic and mildly glucose intolerant due to reduced β-cell size (Pende et al., 2000). However, the actual cause of diminished β-cell size in adult *S6K1*$^{-/-}$ mice was not fully understood. Here, we show that the loss of S6K1 leads to reduced β-cell size and number during development, retarded intrauterine growth, and impaired placental development. We used two complementary techniques, tetraploid aggregation (Tam and Rossant, 2003), and transgenic expression (Dandoy-Dron et al., 1995) to dissect the role of S6K1 in body growth and β-cell-specific growth during development. S6K1-deficient embryos supplied with a wild type normal placenta by tetraploid aggregation developed normally without any growth retardation. However, despite the normal growth of S6K1-deficient embryos when the placental defect was compensated for, β-cells were still smaller than in the wild type, suggesting the defect in β-cell growth is independent of placental dysfunction. Furthermore, β-cell-specific transgenic expression of S6K1 restores β-cell growth and development in S6K1-deficient embryos. These findings would suggest a novel function for S6K1 in extraembryonic cell lineages, that are required for embryonic growth, and indicate a cell autonomous role of S6K1 in β-cell size regulation during development.

Introduction

β-cell mass in the pancreas plays an important role in determining the amounts of insulin that are secreted to maintain glucose homeostasis (Bonner-Weir, 1994). Changes in β-cell mass are dynamic, and is regulated to meet metabolic demands in various metabolic conditions such as obesity, pregnancy, glucose infusion, partial pancretectomy, and islet transplantation (Bernard-Kargar and Ktorza, 2001). β-cell mass has a remarkable ability to adapt to different nutritional conditions by changing β-cell number and size (Chan et al., 1999). Increases in β-cell number are result of β-cell neogenesis, which is replication from existing β-cells or from pancreatic precursor stem cells, or by the proliferation of differentiated β-cells (Dor et al., 2004), (Bonner-Weir, 2000).

Decreases in β-cell number are accomplished by β-cell apoptosis (Bernard et al., 1999). Recently, studies have shown that important components of the increases in β-cell mass after pancreatectomy are not only β-cell neogenesis and replication, but also increases in β-cell size (Jonas et al., 1999). Failure of the pancreatic β-cell mass to adapt to changes in metabolic demands can lead to type 2 *diabetes* (Kloppel et al., 1985). Understanding what regulates β-cell number and size, and how β-cell growth is coordinated with physiological demands, is important for developing therapeutic strategies for the treatment of any metabolic disease associated with pancreatic β-cell dysfunction.

Previous studies in mammalian models have shown that the insulin signaling cascade regulates β-cell growth, signaling, and survival (Withers et al., 1999). Despite a number of reports on the regulation of β-cell mass by β-cell number and survival, the regulation of β-cell size in mass and function is not fully understood. Overexpression of active PKBα in mouse β-cells results in increases of β-cell size and total islet mass, leading to resistance to streptozotocin-induced *diabetes*, suggesting that the genetic modulation of insulin signaling regulates β-cell size although the mechanism is not fully understood (Tuttle et al., 2001). The growth of pancreatic β-cells is also regulated by growth factors and nutrients.

Feeding normal rats with a high fat diet for six weeks results in a modest increases in body weight and insulin resistance, but islet density and β-cell size significantly increase by 30-40% suggesting that β-cell growth adapts to changes in nutritional status (Buettner et al., 2000). β-cell mass is enhanced 50% in glucose-infused rats through inducing hyperplasia and hypertrophy (Bonner-Weir et al., 1989). In addition, nutrient signaling (especially that of amino acids) is found in β-cells and is known to promote insulin production, indicating that nutrients are important for β-cell function and mass (McDaniel et al., 2002).

Previously, mice deficient in S6 Kinase 1 (S6K1), an effector of the mammalian Target Of Rapamycin (mTOR) which is activated in response to amino acids and insulin and mediates cell growth, were shown to be hypoinsulinemic and exhibited reduced β-cell size, suggesting β-cell growth can be regulated by S6K1 (Pende et al., 2000). Notably, that genetic factors and nutritional alterations during fetal and postnatal periods have been implicated in β-cell dysfunction and impaired β-cell growth in the adult (Blondeau et al., 2002), we questioned whether diminished β-cell size in adult *S6K1*$^{-/-}$ mice arose from altered nutritional environment during development *in vivo* or stemmed from impaired β-cell development due to the absence of the S6K1 gene.

Results and discussion

Given that fetal and neonatal life are known to be crucial periods for pancreatic β-cell growth and development, and most active for β-cell replication and neogenesis (Rahier et al., 1981), (Bonner-Weir, 2000), (Nielsen et al., 1999), (Finegood et al., 1995), (Kaung, 1994), we first questioned whether diminished β-cell size in adult *S6K1*$^{-/-}$ mice originates from impaired pancreatic β-cell growth during embryonic development. We first analyzed haematoxylin- and eosin-stained embryonic pancreas sections at E16.5. S6K1-deficient pancreatic sections appeared to have more dense nuclei per endocrine pancreas area, reflecting a reduction in cell size during pancreas development (Fig. 1a). To

further examine pancreatic development, embryonic pancreas sections were stained for insulin and glucagon. Consecutive sections were scored for the number of insulin- or glucagon-positive cells per pancreatic area (Fig. 1b). The morphometric analysis of the pancreas at E16.5 showed a decrease in β-cell number in the *S6K1*$^{-/-}$ embryo compared to the wild type (wt: 594±87, n=3; *S6K1*$^{-/-}$: 446±58, n=3, 18 sections each genotype, $P<0.05$) indicating delayed pancreatic β-cell development, but no significant difference in α cell number in *S6K1*$^{-/-}$ embryos, although there tended to be fewer α cells (Fig. 1d). Reduced β-cell number was not due to increased cell death, as judged by TUNEL staining (data not shown). Morphometric analysis revealed that β-cells in *S6K1*$^{-/-}$ embryos were smaller than β-cells from wild type embryos (Fig. 1e), with an average of 27% decrease in size (wt: 95.60±2.69 μm^2, n=3; *S6K1*$^{-/-}$: 69.54±1.5 μm^2, n=3, $P<0.01$). Notably, there were no significant differences in size and number of glucagon-positive cells between genotypes, suggesting that the impairment observed was limited to β-cells in adult *S6K1*$^{-/-}$ mice (Fig. 1d and Fig. 1e). Diminished β-cell size in *S6K1*$^{-/-}$ embryos was more obvious in sections of the embryonic pancreas which were labeled with an antibody directed against the GLUT2 glucose transporter, residing in the plasma membrane of cells (Fig. 1c). In addition, the reduction in β-cell size was consistent with lower insulin levels in *S6K1*$^{-/-}$ compared to wild type mice (Fig. 1f). Because pancreatic weights of embryos could not be reliably ascertained due to the small size of embryos, and the total numbers of pancreatic sections were correlated with whole embryo weight, insulin content normalized with embryo body weight. Such measurements revealed that *S6K1*$^{-/-}$ pancreas had about 50% reduced insulin content at E16.5 (Fig. 1f) indicating the reduction in β-cell size was consistent with lower insulin levels in *S6K1*$^{-/-}$ mice. Reduced β-cell size and number were persistent at E19.5 (data not shown). In summary, reduced insulin levels in the *S6K1*$^{-/-}$ embryonic pancreas was due to a reduction in the number and size of insulin-positive β-cells in the *S6K1*$^{-/-}$ embryonic pancreas, suggesting that the β-

cell phenotype in adult *S6K1*$^{-/-}$ mice may be arising from impaired pancreatic β-cell growth and development during embryogenesis.

Since the reduced β-cell number and size, and diminished insulin contents in the *S6K1*$^{-/-}$ embryonic pancreas might be due to a general developmental delay, we next questioned whether general fetal growth and developmental retardation would be the cause of impaired pancreatic β-cell growth in the *S6K1*$^{-/-}$ embryo. To examine this, the body weight of embryos was measured from E12.5 to E18.5. The results showed that *S6K1*$^{-/-}$ mice displayed growth retardation during embryogenesis (Fig. 2a), which became apparent at E12.5. In general, the overall embryo weight was about 80% of that of wild type, while the growth curve of *S6K1*$^{-/-}$ and wild type embryos exhibited parallel slopes between stages E12.5 and E18.5 (Fig. 2a). Interestingly, In utero growth retardation did not arise from maternal malnutrition during pregnancy, as *S6K1*$^{-/-}$ mice displayed normal glucose levels in both fasting and fed states in addition to normal food intake (Um et al., in press). Moreover, fetal growth retardation was observed in *S6K1*$^{-/-}$ embryos from heterozygous matings, indicating the maternal nutritional environment was not likely to be the main cause of fetal growth retardation (Shima et al., 1998).

To examine whether fetal growth retardation was accompanied by developmental delay, we analyzed bone development at E16.5. Such an analysis confirmed a delay in the formation of an ossification centers, as illustrated by the alcian blue (stains cartilaginous regions) and alizarin red S (stains ossified regions) staining and the chondrocyte hypertrophy in cervical vertebrae (Fig. 2b). To determine whether developmental delay starts earlier than E12.5, we analyzed the developmental hallmarks of whole embryos using scanning electron microscopy. At day E9.5, *S6K1*$^{-/-}$ embryos exhibited a decrease in somite number, delayed formation of limb buds and an opened otic pit, indicating a developmental delay at this stage (Fig. 2c). Thus, the absence of S6K1 has an effect on both fetal growth and developmental timing. In addition, based on the knowledge that the appearance of growth retardation in *S6K1*$^{-/-}$ embryos starts around E9.5 while insulin plays an role in late stage of development (Duvillie et

al., 1997), (Fowden, 1989), low levels of insulin production accompanied by delayed pancreatic β-cell development may not likely be the primary cause of growth retardation. Moreover, given the fact that mice lacking the insulin receptor are born with 10% growth retardation and die with severe *diabetes* (Kitamura et al., 2003), altered levels of insulin or impaired insulin receptor signaling are unlikely the main cause of growth retardation in *S6K1*$^{-/-}$ embryos.

To address whether the developmental delay starts even at the preimplantation stage, and examine whether the growth retardation and developmental delay in *S6K1*$^{-/-}$ embryos are due to the defective intrinsic ability to develop, we examined preimplantation development using one-cell eggs *in vitro.* Single-cell fertilized eggs from wild type or *S6K1*$^{-/-}$ mice were collected for their ability to develop tested *in vitro* for 5 days. Single-cell fertilized eggs from *S6K1*$^{-/-}$ mice developed normally *in vitro*, with 60% of blastocysts recovered at day 3.5, and the rate of development from the one cell to the blastocyst stage was same as wild type (Fig. 2d), suggesting that developmental delay starts after implantation. Moreover, S6K1$^{-/-}$ blastocysts didn't appear have different growth rates than wild type ones (data not shown). Despite general growth retardation and developmental delay, no difference in the *in vitro* development of fertilized eggs and in the proliferation rate of blastocysts suggests that developmental phenotypes may arise from extraembryonic tissues.

Impaired placental function or placental insufficiency accounts for 70-80% of fetal growth retardation and newborns that are born small for their gestational age (Rossant and Cross, 2001), (Baschat and Hecher, 2004). Placenta is specifically mammalian organ which allows oxygen exchange between mother and fetus and regulates nutrient levels in fetal tissues (Rossant and Cross, 2001). The differentiation of the trophoblasts, the most important placental cell type of the placenta, starts at E4.5, the time of implantation. Mature placenta, established after stage E10, is composed of three principal layers derived from the fetus: the outer trophoblast giant cells; a middle spongiotrophoblast layer; and the innermost labyrinth (Rossant and Cross, 2001). The labyrinth contains cells of both trophoblast and mesodermal origin that together undergo branching

morphogenesis to produce a large surface area of the placenta for nutrient and gas exchange. (Cross et al 2000) (Rossant and Cross, 2001).

Given defects in placental development or dietary protein restriction during gestation lead to fetal growth retardation (Rossant and Cross, 2001), (Parimi et al., 2004), we next questioned whether growth retardation and developmental delay arise from low nutrient availability due to impaired placental development. We first examined the morphology of the placenta at E13.5. At the equivalent gestational stage, *S6K1*$^{-/-}$ placentas from a homozygous or heterozygous matings were smaller than the placentas of wild type mice (Fig. 4d). Analysis of haematoxylin- and eosin-stained cross-sections revealed that the spongiotrophoblast layer in *S6K1*$^{-/-}$ placentas was thinner than in wild type placentas (Fig. 3a, b). The spongiotrophoblast layer was further analyzed by *in situ* hybridization using the spongiotrophoblast-specific gene *Tpbp*. The results confirmed a significantly reduced layer of *Tpbp*-expressing cells (Fig. 3b). However, a typical feature was observed for the giant cells that form the multiple cell layers between maternal decidual tissue and the embryonic labyrinth (data not shown). As an intact spongiotrophoblast layer is required for the normal development of the labyrinthine trophoblast layer, and secretes the vascular endothelial growth factor needed for blood vessel function (Rossant and Cross, 2001), we examined the labyrinthine layer. Closer examination of the labyrinthine layer using haemotoxylin and eosin staining revealed reduced intermingling of embryonic and maternal blood vessels (Fig. 3c). Embryonic blood vessels in the *S6K1*$^{-/-}$ labyrinthine layer appeared to be dilated and filled with more blood cells than vessels in wild type mice. (Fig. 3c, d). Morphometric analysis and immunohistochemical detection of PECAM-1, a fetal endothelial cell marker, revealed that the number of fetal blood vessels in the labyrinthine layer of *S6K1*$^{-/-}$ was reduced and that fetal blood vessels were irregular in diameter (Fig. 3d). Taken together, these observations indicate a decreased vascular capacity in *S6K1*$^{-/-}$ placentas and a role of S6K1 in the normal vascularization of the labyrinthine layer. Decreases in intermingling between maternal and fetal blood vessels may indicate restricted nutrient or oxygen exchange between the mother

and developing embryos. In addition, the *S6K1*$^{-/-}$ placentas had improperly positioned *Tpbp*-expressing cells in the labyrinthine region at E19.5. (Fig. 3e, f). Therefore, it appeared likely that the defect in spongiotrophoblast and the labyrinthine layer could be one of the causes for fetal growth retardation in *S6K1*$^{-/-}$ mice. In addition, our results indicate that S6K1 is required for placental morphogenesis and vascularization.

Considering the impaired placental development in *S6K1*$^{-/-}$ mice and the fact pancreatic β-cell development is exclusively sensitive to the level of nutrients provided by placenta (Godfrey, 2002), we questioned whether a faulty *S6K1*$^{-/-}$ placenta might be the primary cause of the embryonic growth retardation resulting in impaired pancreatic β-cell growth. To explore this possibility, we supplied *S6K1*$^{-/-}$ embryos with normal placenta by the tetraploid aggregation technique (Tanaka et al., 2001). To this end, we produced mouse fetuses by aggregating homozygous *S6K1*$^{-/-}$ embryonic stem (ES) cells with wild type tetraploid embryos. In the resulting chimeras, the embryos are ES-cell derived. The wild type tetraploid cells contribute exclusively to the placental trophoblast cells and the endoderm of the yolk sac, but owing to increased ploidity, they are rigorously excluded from the embryo proper. Conversely, diploid ES cells cannot make trophoblast tissues *in vivo*, but make up the entire embryo proper (Tam and Rossant, 2003). The absence of S6K1 in ES cell- derived embryos after tetraploid aggregation was confirmed by Southern blotting (Fig. 4a). Analysis of tetraploid wild type placenta at E13.5 using haematoxylin and eosin staining demonstrated extensive intermingling of blood vessels between mother and fetus and a well-organized placenta structure, indicating the tetraploid aggregation technique provided histologically normal wild type placenta for *S6K1*$^{-/-}$ embryos (Fig. 4c). When tetraploid wild type morulae and diploid *S6K1*$^{-/-}$ ES cells were aggregated, the S6K1$^{-/-}$ ES-cell derived fetuses associated with wild type reconstituted placentas (indicated as *S6K1*$^{-/-}$*TR*) appeared normal without developmental delay or growth retardation (Fig. 4b, d), indicating that growth retardation in *S6K1*$^{-/-}$ embryos was secondary to impaired placental development. No growth retardation in *S6K1*$^{-/-}$*TR* embryos was visible throughout the

embryonic stages from E13.5 to E19.5 (Fig. 4d and data not shown). Thus, the absence of S6K1 in the trophoblasts leads to impaired placental development associated with fetal growth retardation, suggesting a new role of S6K1 in extra-embryonic cell lineage.

As maturation of pancreatic β-cell growth and function takes place during early development, the pancreatic β-cells are particularly susceptible to the effects of poor nutrition and impaired placental development (Blondeau et al., 2002). We next questioned whether impaired β-cell growth in *S6K1*$^{-/-}$ embryos during development was also a secondary phenotype due to low levels of nutrient availability, potentially due to placental dysfunction driven by the loss of S6K1. To explore this possibility, we analysed pancreatic β-cell size, number, and insulin content in *S6K1*$^{-/-}$ embryos at E16.5 with a tetraploid wild type placentas. Consistent with a full resumption of body growth in the presence of tetraploid wild type placentas, there was also an increase in β-cell numbers in *S6K1*$^{-/-}$*TR* embryos to the same level as wild type (indicated as *S6K1*$^{-/-}$*TR,* Fig. 4h). Surprisingly, β-cell density was higher in *S6K1*$^{-/-}$*TR* embryos (Fig. 4e) although pancreatic β-cells in *S6K1*$^{-/-}$*TR* embryos were still 27% smaller than those of wild type embryos (Fig. 4g and Fig. 4i), suggesting that the reduced number of β-cells, but not diminished β-cell size, could be rescued by providing wild type placentas. Despite a nutrient-rich environment provided by the tetraploid placenta, loss of S6K1 function in β-cells results in smaller cells indicating the requirement of S6K1 for maintaining normal β-cell size during development. Consistent with reduced β-cell size, there was a more striking reduction in insulin levels, when normalized with the body weight of the embryo, probably due to further increases in body weight in tetraploid embryo rescue experiments (Fig. 4j). Despite completely rescue of body size and development in the presence of a tetraploid wild type placentas, *S6K1*$^{-/-}$*TR* embryos still had diminished β-cells (Fig. 4g. i), indicating that defects in placental development or nutritional environment during gestation *in vivo* may not be the primary cause for

reduced β-cell size in *S6K1*$^{-/-}$ embryos, but rather a specific effect of the genetic lesion.

To further investigate the actual genetic cause of smaller β-cells in adult *S6K1*$^{-/-}$ mice, we generated transgenic mice in which a wild type form of S6K1 was expressed in pancreatic β-cells. For this purpose, we used the rat insulin II promoter to drive expression of S6K1 in pancreatic β-cells (Dandoy-Dron et al., 1995). We confirmed transgene expression by PCR and western blot analysis of pancreatic islet β-cell lysates using antibodies against S6K1 and the myc tag present on the N terminus of the expressed transgene. Transgenic S6K1 (indicated as *rip*^{S6K1}) was detected in both *WTrip*^{S6K1} and *S6K1*$^{-/-}$*rip*^{S6K1} islet extracts, but was undetectable in WT and *S6K1*$^{-/-}$ islets (Fig. 5a). By breeding *S6K1*$^{+/-}$*rip*^{S6K1} mice with *S6K1*$^{+/-}$ mice, we were able to generate S6K1-deficient embryos expressing S6K1 only in pancreatic β-cell (indicated as *S6K1*$^{-/-}$*rip*^{S6K1}). *S6K1*$^{-/-}$*rip*^{S6K1} mice are viable and fertile but smaller than wild type mice. Morphometric analysis revealed that β-cell density (Fig. 5b), number (Fig. 5e), and size (Fig. 5f) in *S6K1*$^{-/-}$*rip*^{S6K1} embryos were restored to wild type levels. Consistent with complete rescue of β-cell size and number in *S6K1*$^{-/-}$*rip*^{S6K1}, measurements of insulin levels also revealed no differences in insulin contents between *WTrip*^{S6K1} and *S6K1*$^{-/-}$*rip*^{S6K1} (Fig. 5g). Notably, smaller β-cell size and reduced cell number in the *S6K1*$^{-/-}$ embryos during development were completely restored by transgene expression in β-cells (Fig. 5e, f), but diminished β-cell size was not restored by providing tetraploid wild type placentas (Fig. 4e, i), indicating that extrinsic nutrients provided by the placenta cannot restore β-cell size in the absence of S6K1. Furthermore, morphometric analysis in 3-month-old adult mice revealed that higher β-cell density due to smaller cell size in *S6K1*$^{-/-}$ mice was also restored in adult transgenic *S6K1*$^{-/-}$*rip*^{S6K1} mice with an average 19% decrease in β-cell density (wild type: 86.59±1.78 (n=32 islets); *S6K1*$^{-/-}$: 100.54±1.24 (n=31 islets), *S6K1*$^{-/-}$*rip*^{S6K1}: 81.53±2.39 (n=28 islets), wt vs. *S6K1*$^{-/-}$ *rip*^{S6K1} P=0.09, wt vs. *S6K1*$^{-/-}$ P<0.001, *S6K1*$^{-/-}$ vs. *S6K1*$^{-/-}$*rip*^{S6K1} P<0.001, four female mice of each genotype). This indicates that the restoration of β-cell size

by transgene expression during embryonic development persists throughout adult life. Thus, transgenic expression of S6K1 in S6K1-deficient β-cells restores β-cell size and thereby restores β-cell development. (Fig. 5e, f). Consistent with this, we observed recently that overexpression of wild type mammalian S6K1 in *dS6K*-deficient *Drosophila* could rescue cell size defects as well as developmental delay by restoring cell cycle time (J. Montagne, unpublished data). Thus, these results suggest that the loss of S6K1 function in β-cells during development may lead to delayed β-cell development at a smaller size, but that the loss of S6K1 in the trophoblasts, results in impaired placental development, potentially leading to a general growth retardation and reduced β-cell number as demonstrated in tetraploid aggregation experiments. (Fig. 4e, 5b).

Despite increases in β-cell size and number in $S6K1^{-/-}rip^{S6K1}$ embryos compared to $S6K1^{-/-}$ embryos, the expression of S6K1 in a wild type background fails to increase β-cell size further, and even resulting in a slightly decreased β-cell size compared to wild type (Fig. 5f). Although the levels of S6K1 expression in a S6K1-deficient background were higher than in a wild type mice (Fig. 5a), it did not increase β-cell size further than the wild type and exhibited no differences in insulin levels compared to wild type or wild type transgenic mice (Fig. 5f, g). These results suggest that there may be a critical cell size threshold operated by S6K1. Slightly reduced β-cell size in $WTrip^{S6K1}$ compared with wild type mice (Fig. 5f) could be explained by the fact that overexpression of S6K1 in a wild type background is a dominant negative to itself as well as other downstream targets (Jefferies et al., 1997), (Von Manteuffel et al., 1996). This may be due to titrating out the mTOR/Raptor/LST8-signaling complex by the overexpression of transgenic S6K1 and the requirement for multi-site phosphorylation for S6K1 activation (Von Manteuffel et al., 1996), (Kim et al., 2002). In contrast to β-cell-enlargement phenotypes seen following increased PKB activity in mice (Tuttle et al., 2001), the failure of S6K1 overexpression to increase β-cell size over that of wild type (Fig. 5f) suggests that S6K1 does not function downstream of the PKB pathway, as demonstrated in the *Drosophila* system (Radimerski et al., 2002).

Given the difference in the β-cell size phenotype in wild type background versus transgenic mice expressing active PKB or S6K1 in β-cells, it would be interesting to investigate how the PKB and S6K1 pathways regulate β-cell size differently when there is a demand to increase β-cell mass in order to compensate insulin resistance in peripheral tissues. Nevertheless, transgenic expression of S6K1 could revert the diminished β-cell size phenotype in S6K1$^{-/-}$ mice in a cell autonomous manner (Fig. 5f), indicating that S6K1 is clearly required for maintaining normal β-cell size. Furthermore, the results show the conservation of β-cell size (Fig. 5b, d, f) and prevention of hyperinsulinemia in *S6K1*$^{-/-}$*rip*^{S6K1} embryo under normal nutrient homeostasis suggesting that transgenic expression of S6K1 may be helpful for selectively restoring the function of β-cells under pathological conditions associated with reduced β-cell size and mass. It will be interesting to determine whether a loss of S6K1 in pancreatic β-cells using conditional knockout strategies is sufficient to induce reduced β-cell size or a growth retardation phenotype in embryos and adult mice.

Previous studies were unable to establish a cell autonomous vs. non-autonomous role of S6K1 during development. Here we find that the histological structure of the spongiotrophoblast layer is altered, and that vascularization in the labyrinth is reduced, in the *S6K1*$^{-/-}$ placenta resulting in growth retardation and developmental delay. Analysis using tetraploid aggregation indicates that a defect in *S6K1*$^{-/-}$ placental trophoblast cells leads to growth retardation and developmental delay phenotypes of S6K1$^{-/-}$ embryos because embryos, when supplied with a functionally normal placenta, grew to a normal size without delay in development and only diminished β-cell size (Fig. 4d, e, g, i). Our studies would suggest non-cell-autonomous role for S6K1 in fetal growth during development and a new role for S6K1 in trophoblast development. The molecular mechanism underlying the defect in *S6K1*$^{-/-}$ trophoblasts remains to be investigated. Importantly, restoration of S6K1 function in pancreatic β-cells by transgenic expression is sufficient to rescue the pancreatic β-cell size defect of

S6K1$^{-/-}$ embryonic and adult mice (Fig. 5d and Fig. 5f), indicating a cell autonomous role for S6K1 specifically in β-cell size determination.

It has been shown that protein malnutrition during the fetal stages of pancreatic development leads to a reduction in pancreatic insulin content and β-cell mass in the adult age, underscoring the importance of nutritional stimuli on β-cell growth during fetal development (Swenne et al., 1992). Alterations in this stimulation may result in impaired β-cell growth and β-cell dysfunction in later life (Swenne et al., 1992), (Swenne et al., 1987). Our results suggest that S6K1 signaling may be one key signaling molecule mediating β-cell growth for maintainance of the competence of β-cells to grow in response to nutrients and growth factors during development. Despite impaired β-cell growth, mild glucose intolerance, and hypoinsulinemia, *S6K1*$^{-/-}$ mice were not diabetic and maintained normal feeding and fasting glucose levels (Um et al., in press), (Pende et al., 2000). The absence of *diabetes* in these mice can be explained by the presence of high insulin sensitivity in peripheral tissues through a negative feedback loop from S6K1 to IRS1 serine phosphorylation (Um et al., in press). Similarly, low protein diets during late gestation leads to reduced β-cell size and hypoinsulinemia as in *S6K1*$^{-/-}$ mice but the effect of hypoinsulinemia was attenuated by high insulin sensitivity (Grace et al., 1990) through decreases of IRS1 serine phosphorylation in human and rats (Toyoshima et al., 2004). Thus, the absence of S6K1 results in a phenotype strongly reminiscent of a human on a limited protein diet during gestation (Rigalleau et al., 1998). Taken together, these studies suggest that S6K1 acts as an important mediator in nutrient-induced β-cell growth and placental development, and that loss of S6K1 may lead to the failure to integrate of nutrient and mitogen signaling required for β-cell growth under normal nutrient conditions. This observation may help to develop therapeutic interventions for the treatment of pathological conditions associated with reduced β-cell growth, such as malnutrition-induced *diabetes*.

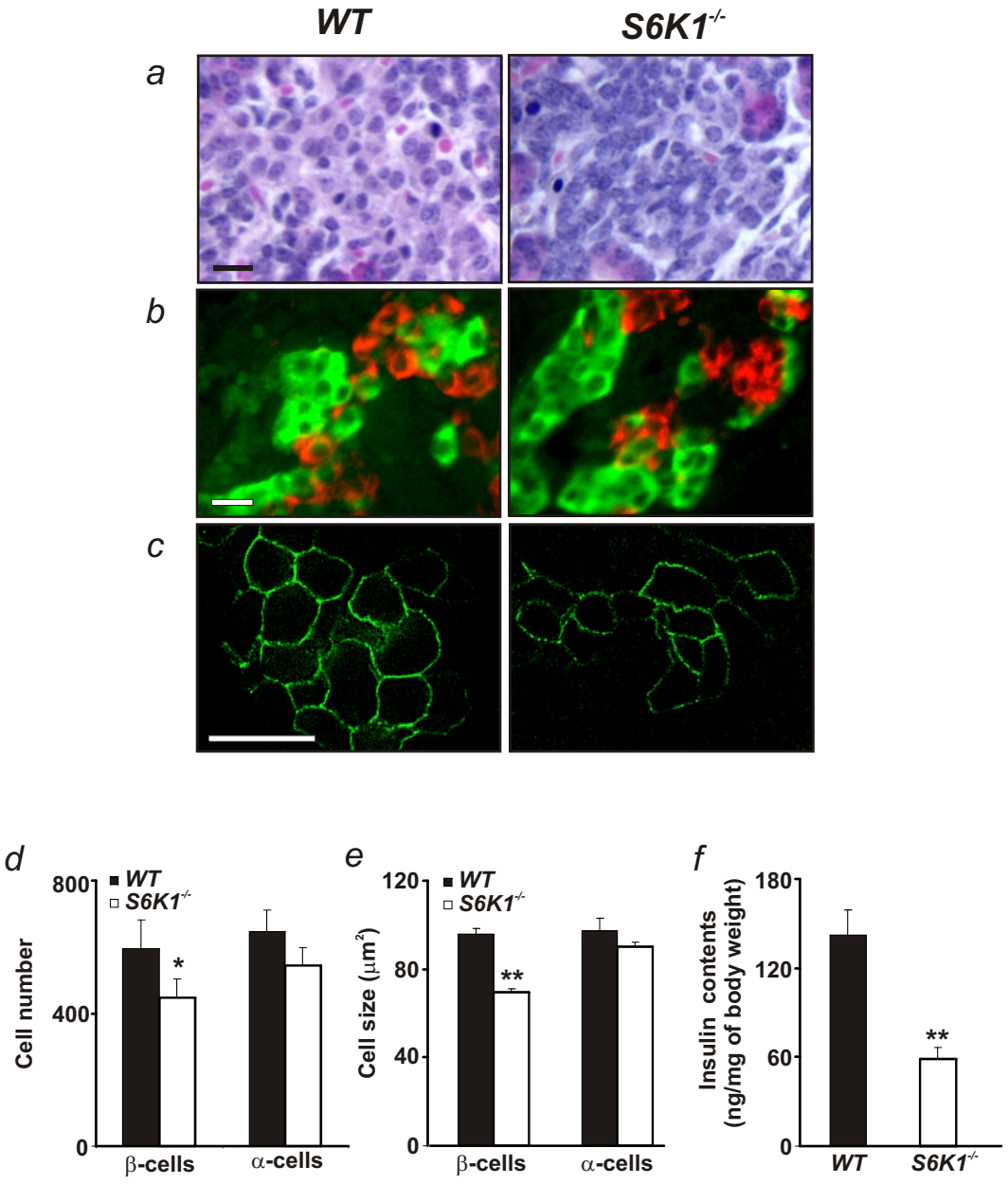
WT
S6K1-/-
a
b
c
d
WT
S6K1-/-
800
400
0
Cell number
*
β-cells
α-cells
e
120
80
40
0
Cell size (μm2)
**
β-cells
α-cells
f
180
120
60
0
Insulin contents (ng/mg of body weight)
**
WT
S6K1-/-

Fig. 1

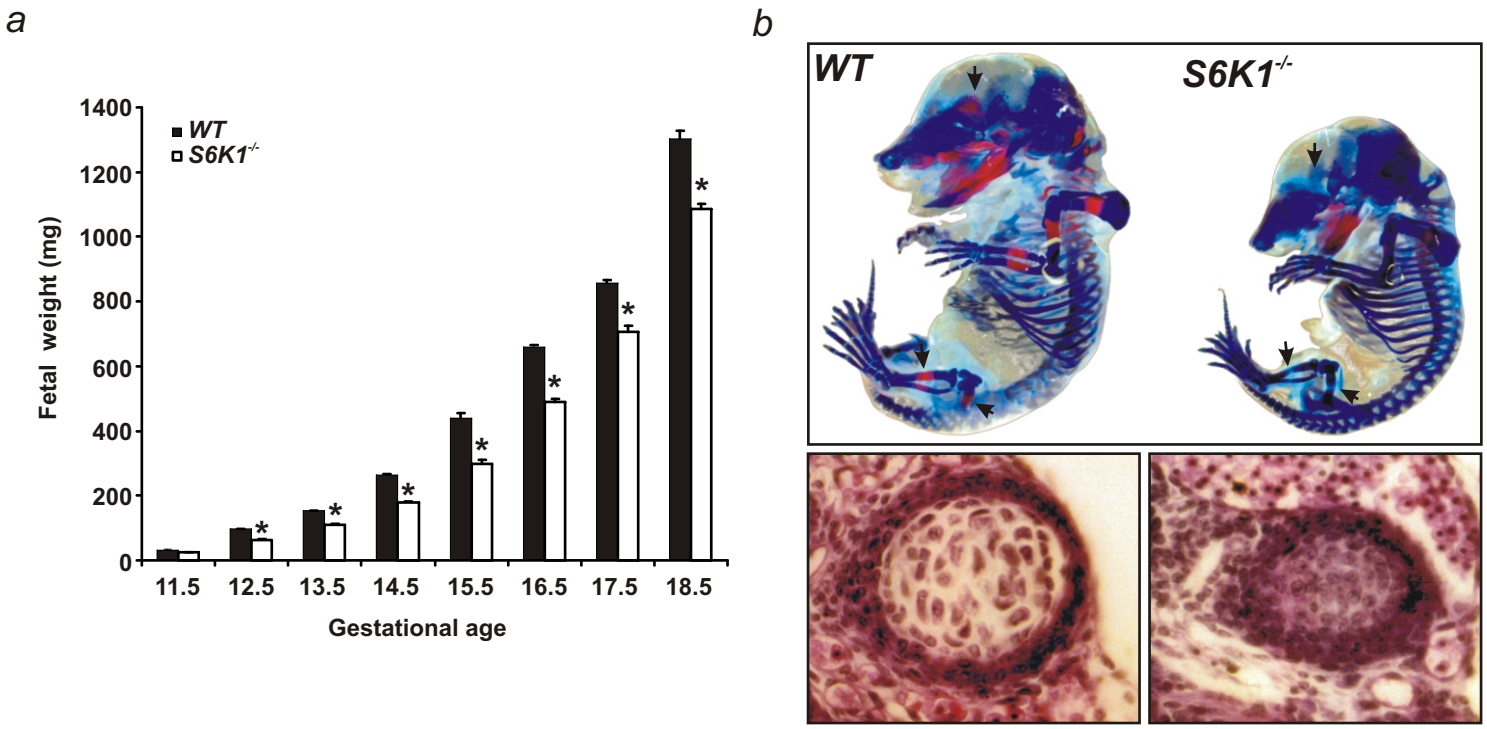
a
b
c
d
WT
S6K1-/-
Fetal weight (mg)
Gestational age
11.5
12.5
13.5
14.5
15.5
16.5
17.5
18.5
Somite number
% of embryo
Early blastocyst
Blastocyst

Fig. 2

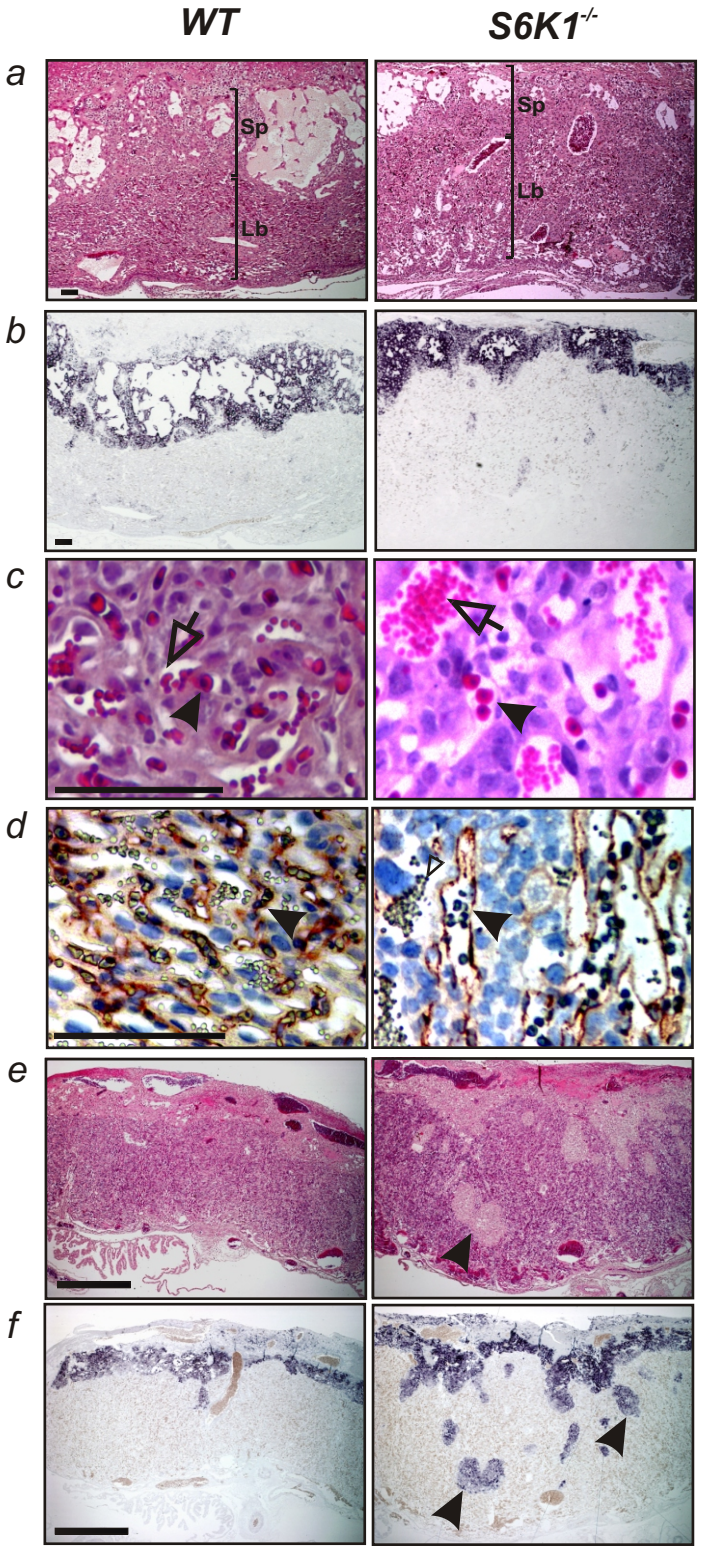

Fig. 3

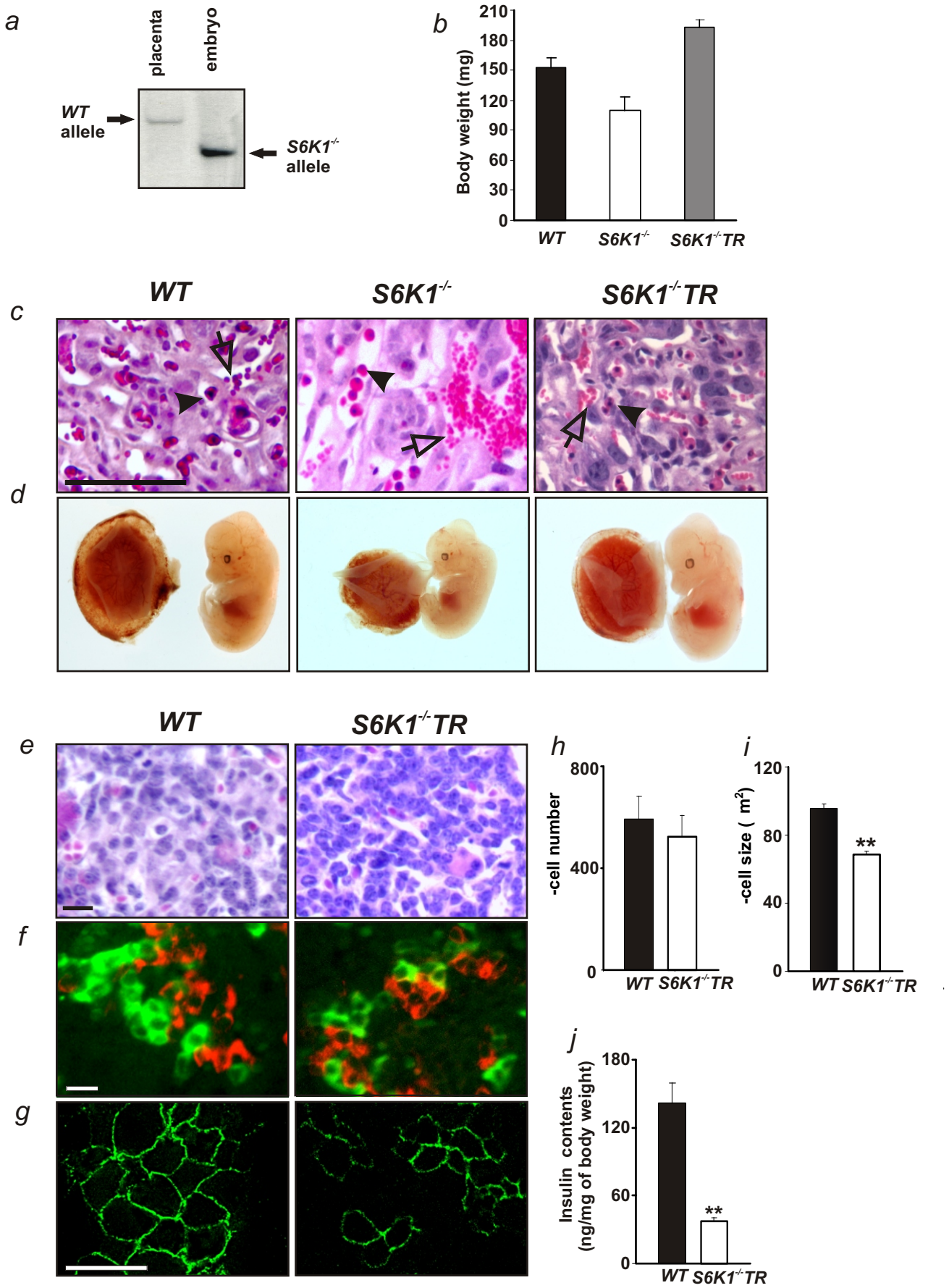
a
placenta
embryo
WT allele
S6K1-/- allele
b
Body weight (mg)
210
180
150
120
90
60
30
0
WT
S6K1-/-
S6K1-/-TR
c
d
WT
S6K1-/-
S6K1-/-TR
e
f
g
WT
S6K1-/-TR
h
-cell number
800
400
0
WT S6K1-/-TR
i
-cell size (m2)
120
80
40
0
**
WT S6K1-/-TR
j
Insulin contents (ng/mg of body weight)
180
120
60
0
**
WT S6K1-/-TR

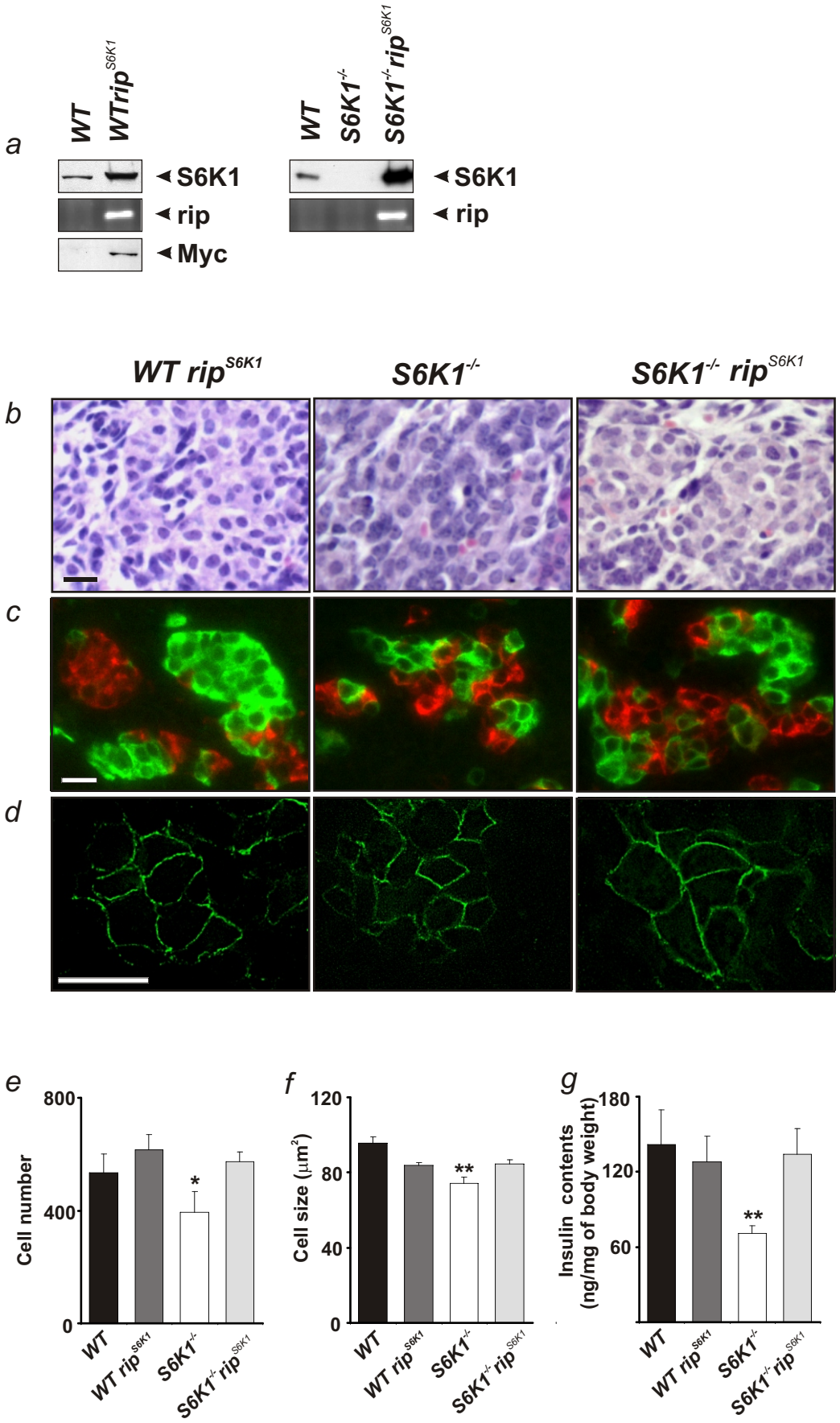
a
WT
WTrip S6K1
S6K1
rip
Myc
WT
S6K1-/-
S6K1-/- rip S6K1
S6K1
rip
b
c
d
WT rip S6K1
S6K1-/-
S6K1-/- rip S6K1
e
Cell number
800
400
0
*
f
Cell size (μm2)
120
80
40
0
**
g
Insulin contents (ng/mg of body weight)
180
120
60
**
WT
WT rip S6K1
S6K1-/-
S6K1-/- rip S6K1

Fig. 5

Figure legends

Figure 1: Diminished β cell size in *S6K1*$^{-/-}$ embryonic pancreas. **a.** Histology of pancreas from wild type (left) and *S6K1*$^{-/-}$ embryo (right) at E16.5. Tissue sections were stained by haematoxilin and eosin. **b**, Immunofluorescence staining of embryonic pancreas for insulin (red) and glucagon (green). **c**, Fluorescent staining for the GLUT2 glucose transporter. **d**, Reduced β cell number in *S6K1*$^{-/-}$ embryonic pancreas. **e**, Diminished β cell size in *S6K1*$^{-/-}$ embryonic pancreas. **f,** Reduced insulin contents normalized by body weight in *S6K1*$^{-/-}$ embryonic pancreas. (see Methods). ***,** $P < 0.05$, ****,** $P < 0.01$

Figure 2: Growth retardation and developmental delay in *S6K1*$^{-/-}$ embryos.
a, Fetal weights of wild type (WT) and *S6K1*$^{-/-}$ embryos at the indicated gestational ages. *, $P < 0.05$. **b**, Delayed bone development in *S6K1*$^{-/-}$ embryo. Lateral view of skeleton at E16.5 analyzed for ossification using alcian blue and alizarine red (Top). Arrows indicate that ossification is present in frontal bone on the cranium and fibula and tibia bone on hind limb of WT, whereas cartilaginous regions are still present in the same regions of *S6K1*$^{-/-}$ embryo. Presence of hypertrophic chondrocytes in WT but not in *S6K1*$^{-/-}$ at E14.5. (Bottom). **c**, Side views of embryos at E9.5 by scanning electron microscopic analysis (left) and somite numbers in embryos at E9.5 (right). Asterisk indicates somite. Note opened otic pit (open arrow) and the absence of limb bud (filled arrow) in *S6K1*$^{-/-}$ embryo. **d**, Normal preimplantation development in *S6K1*$^{-/-}$ *, $P < 0.05$, WT, wild type.

Figure 3: Abnormal placental development in *S6K1*$^{-/-}$ mice.
a and c, Hematoxylin/eosin-stained cross sections of placenta from wild type (left) and *S6K1*$^{-/-}$ embryo (right) at E13.5. Labyrinthine trophoblast (Lb) and spongiotrophoblast layers (Sp) are indicated. **b**, RNA *in situ* hybridization analysis of the spongiotrophoblast-specific marker *Tpbp* in E13.5 placenta. Note that spongiotrophoblast layer is thinner in *S6K1*$^{-/-}$ placenta. **c**, Reduced intermingling of maternal (containing enucleated erythrocytes, open arrow) and embryonic blood

vessels (identified by nucleated erythrocytes, filled arrow) in labyrinthine layer of *S6K1*$^{-/-}$ placenta. Size bar 100 μm. **d**, Anti-PECAM staining (brown color) shows dilated fetal blood vessels with irregular in diameter in *S6K1*$^{-/-}$ placenta. **e**, Hematoxylin/eosin-stained cross-sections of placenta from wild type and *S6K1*$^{-/-}$ embryo at E19.5. Size bar 1mm. **f**. RNA *in situ* hybridization analysis of the spongiotrophoblast-specific marker *Tpbp* in E19.5 placenta. Arrows indicate the improperly positioned *Tpbp* -expressing cells in the labyrinthine region of *S6K1*$^{-/-}$ placenta.

Figure 4: Tetraploid wild type placenta rescues growth retardation but not β cell size in *S6K1*$^{-/-}$ embryos. **a**, Southern blot of genomic DNA from tetraploid placenta and ES cell derived embryo. **b**, Fetal weights of wild type, *S6K1*$^{-/-}$, *S6K1*$^{-/-}$ after tetraploid aggregation (*S6K1*$^{-/-}$ *TR*) at E13.5. **c**, Placenta after tetraploid aggregation (*S6K1*$^{-/-}$*TR*) as visualized in hematoxylin/eosin-stained sections. Note that well-developed intermingling of maternal (open arrow) and embryonic blood vessels (filled arrow) in labyrinthine layer of placenta after tetraploid aggregation. **d**, Appearance of wild type, *S6K1*$^{-/-}$, *S6K1*$^{-/-}$ embryos after tetraploid aggregation (*S6K1*$^{-/-}$*TR)*. **e**, Histology of pancreas from wild type, and *S6K1*$^{-/-}$*TR* embryo (right) after tetraploid aggregation at E16.5. **f**, Immunofluorescence staining of embryonic pancreas for insulin (green) and glucagon (red). **g**, Fluorescent staining for the GLUT2 glucose transporter. **h,** β cell number in WT and *S6K1*$^{-/-}$*TR.* **i**, Diminished β cell size in *S6K1*$^{-/-}$ embryonic pancreas supplied with a normal placenta by tetraploid aggregation. **j**, Reduced insulin contents in *S6K1*$^{-/-}$*TR*. **, $P < 0.01$

Figure 5: Pancreatic β cell specific expression of S6K1 rescues diminished β cell size in *S6K1*$^{-/-}$ mice. **a**, Confirmation of transgene expression by western blot and PCR. Islet lysates of transgenic and nontransgenic mice were immunoblotted with antibodies against myc or S6K1 or PCR of genomic DNA to detect rat insulin promotor (rip). **b**, Histology of pancreas from *WTrip*^{S6K1}(left), *S6K1*$^{-/-}$ (middle), transgenic embryo (*S6K1*$^{-/-}$*rip*^{S6K1}, right) at E16.5. Tissue sections were stained by haematoxilin and eosin. **c**, Immunofluorescence staining of pancreas for insulin

(green) and glucagon (red). **d**, Fluorescent staining for the GLUT2 glucose transporter. **e**, β cell number in transgenic pancreas. **f,** Rescued β cell size in transgenic pancreas. **g**, Rescued insulin contents in transgenic pancreas. *, $P < 0.05$, **, $P < 0.01$

IV. DISSCUSSION

Why are S6K deficient mice resistant to age-and diet-induced obesity?

Negative feed back from S6K1 activation to IRS1 serine phosphorylation

S6K1 deficient mice were shown to be mild glucose intolerance and hypoinsulinemic due to selective reduction in pancreatic β-cell size (Pende et al., 2000). However, such mice have normal fasting and feeding glucose levels despite their hypoinsulinemia (Pende et al., 2000; Um et al., in press). This suggests that they may have hypersensitivity to insulin in the peripheral tissues. Indeed, the present study revealed that S6K1 deficient mice exhibit slightly higher insulin sensitivity on a normal chow diet and that this phenotype was more pronounced when they were on a high fat diet (Um et al., in press). Why is insulin sensitivity increased in the absence of S6K1? Is S6K1 one of the signaling molecules responsible for dampening insulin signaling?

Previously, hyperglycemia, hyperaminocidemia, and hyperlipidemia, have been shown to be associated with obesity and insulin resistance (Kahn and Flier, 2000; Pijl et al., 1994), suggesting insulin resistance may be caused by excess nutrient supply. Consistent with this, hyperglycemia, high protein diet, and high fat diet induce insulin resistance by inhibiting the early steps of the insulin signaling pathway, such as IRS tyrosine phosphorylation and PI3K activation (Hresko et al., 1998; Patti, 1999; Rossetti et al., 1989; Shulman, 2000). Given that the mTOR/S6K1-signaling pathway is activated by nutrients (Hara et al., 1998; Patti et al., 1998) and insulin (Dennis et al., 2001), S6K1 could be involved in inducing insulin resistance by inhibiting an early events in insulin signaling. The involvement of S6K1 in this process is supported by the observation that amino acids inhibit insulin-induced PI3K signaling, an inhibitory response which is reversed by the inhibition of mTOR/S6K1 signaling by rapamycin(Tremblay and Marette, 2001).

One of the inhibitory signals for insulin action is the phosphorylation of IRS1 on serine residues such as S307, S632, and S612 of mouse IRS1, or

alternatively S312 and S636 of human IRS1. Ser307 phosphorylation induces a conformational change of the phosphotyrosine-binding domain that reduces its affinity for the IR (Aguirre et al., 2002), while Ser612 and Ser632 phosphorylation of IRS1 inhibits the binding of PI 3-kinase to IRS1 (Mothe and Van Obberghen, 1996).

How does nutrient-induced S6K1 activation dampen insulin signaling and which signaling molecules are involved in this process? The present study has shown that the insulin receptor is still desensitized in response to insulin injection in S6K1 deficient mice on a high fat diet. Furthermore, there are no changes at the level of insulin receptor tyrosine autophosphorylation, despite increases in insulin-induced PKB phosphorylation in S6K1 siRNA treated cells. This would suggest that S6K1 may elicit a selective inhibitory effect on PKB activation at a point downstream of the insulin receptor. Further analysis of IRS1 serine phosphorylation in S6K1 siRNA treated cells and S6K1 deficient mice on a high fat diet revealed that phosphorylation of S307 and S632 in IRS1 was abrogated both *in vitro* and *in vivo,* suggesting S6K1 may have a selective positive effect on serine phosphorylation of IRS1 leading to inhibition of PKB signaling and to insulin resistance.

Given that phosphorylation of S307 and S632 in IRS1 is known to be elevated in animal models of obesity and in muscle from *type 2 diabetes* patients (Bouzakri et al., 2003) and phosphorylation of those sites are abrogated in S6K1 deficient mice and siRNA treated cells, how then does S6K1 influence serine phosphorylation of IRS1 to inhibit insulin signaling?

Is S6K1 able to phosphorylate directly serine sites of IRS1?

Interestingly, Harmann et al have shown that insulin-activated S6K1 phosphorylates IRS1 between residues 511 and 772 *in vitro* suggesting the S6K1 may directly regulate of IRS serine phosphorylation. However, no serine sites were identified to be phosphorylated by S6K1. Given the fact that S6K1 recognizes the RXRXXS/T motif in ribosomal protein S6 (Flotow and Thomas, 1992), S307 and S632 in IRS may not be good candidates as S6K1 substrates.

(Gual et al., 2003b; Ozes et al., 2001). An intriguing the findings by Harrington et al revealed that Ser302 proximal to the IRS1 PTB domain is phosphorylated by S6K *in vitro* (Harrington et al., 2004) and that this site contains an S6K1 recognition motif. Moreover, they have shown that phosphorylation of this site disrupts the ability of the PTB domain to interact with activated insulin receptors. Their finding supports the model that S6K1 directly mediate IRS1 serine phosphorylation leading to dampening of insulin signaling. Consistent with this study, a recent study showed that the level of phosphorylation of serine 302 in IRS1 is indeed increased along with S307 in animal models of obesity and insulin resistance, including genetically obese *ob/ob* mice, diet-induced obesity, and upon induction of hyperinsulinemia although the relevance of S6K1 in these models has not been tested (Werner et al., 2004). Interestingly, phosphorylation on both S307 and S302 sites is necessary for IR/IRS1 disruption but not sufficient for disruption (Werner et al., 2004), suggesting an additional site or sites are required for disruption of the IR/IRS1 interaction and insulin resistance. It will be interesting to determine whether the loss of S6K1 in cells and/or mice abrogates phosphorylation of S302 in IRS1 along with other sites such as S307 and S632. In addition, further experiments are required to determine if S302 phosphorylation alone is involved in predisposition of insulin resistance *in vivo* and *in vitro.* Measurement of biological functional outcomes such as glucose uptake in cells or mice expressing an IRS1 S302 substitution mutant could be informative to evaluate this. To test the physiological significance of this site *in vivo,* a more precise approach would involve generate knock-in mice expressing an IRS1 S302 mutant instead of wild type IRS1, and test their ability to maintain glucose homeostasis and insulin sensitivity following either high fat diet feeding or a genetic cross with *ob/ob* or *K/K Ay* mice. Crossing these mice with S6K1 deficient mice can also be useful to determine the direct versus indirect roles of S6K1 on IRS1 serine phosphorylation in the context of insulin sensitivity.

-Does S6K1 interact with molecules, which mediate serine phosphorylation of IRS1 to regulate IRS1 indirectly?

The mTOR (mammalian target of rapamycin) signalling pathway has been shown to be involved in insulin-induced phosphorylation of Ser307 in adipocytes, and muscles (Gual et al., 2003b), (Carlson et al., 2004). In addition, hyperosmotic stress, which also induces insulin resistance, increases the phosphorylation of IRS1 on S307 by an mTOR-dependent pathway (Carlson et al., 2004) indicating the relevance of mTOR on phosphorylation of IRS1 on S307 in insulin resistance. Moreover, mTOR can catalyse the phosphorylation of set of Ser/Thr-Pro sites which may make an IRS1 S307 and S632 as mTOR substrates (McMahon et al., 2002). Recent studies have also supported this by showing the physical association between IRS1 and mTOR (Gual et al., 2003b; Ozes et al., 2001). Surprisingly, the association between IRS1 and mTOR was not changed by insulin treatment (Gual et al., 2003b; Ozes et al., 2001) suggesting that there may be other regulators besides insulin which control the association of these two signalling components leading to further change of mTOR activity. Given the fact that amino acids activate mTOR signalling, it would be interesting to determine whether the association between IRS1 and mTOR is regulated by exogenous nutrients such as amino acids or free fatty acids. Those studies would aid in understanding the mechanism of insulin resistance arising not only from hyperinsulinemia but also from incessant nutrient supply. Given that mTOR binds S6K1 and 4E-BP1 via raptor (Hara et al., 2002; Kim et al., 2002; Nojima et al., 2003), one interesting question arises; Does S6K1 regulate the association between IRS1 and mTOR? Further experiments will be required to address whether lowering S6K1 level or loss of S6K1 influences the association between IRS1 and mTOR to modulate mTOR activity.

As raptor enhances the mTOR-catalyzed phosphorylation of S6K1 *in vitro* via TOR signaling (TOS) motif (Schalm et al., 2003) and the TOS motif is found in mTOR substrates and responsible for association with mTOR through interaction with raptor, we examined whether IRS1 also has a TOS motif by sequence analysis. Surprisingly, IRS1 does not have a TOS motif, even though

mTOR is known to mediate phosphorylation of serine 307 in IRS1 in response to insulin and TNF-α (Carlson et al., 2004). This would indicate that the interaction between mTOR and IRS1 may not require a TOS motif. Nevertheless, it would be interesting to investigate whether raptor is required for the ability of mTOR to phosphorylate IRS1, thereby assessing the relevance of this molecule in insulin sensitivity. These studies will be helpful to understand how nutrient sensitive signaling components integrate with insulin signaling through the interaction between mTOR or S6K1 and IRS1.

On the other hand, Harrington et al showed that reduced IRS1 mRNA levels in TSC2 deficient cells where mTOR/S6K signaling is hyperactivated, were restored by rapamycin treatment but reversed by actinomycin D (Harrington et al., 2004), suggesting mTOR/S6K signaling reduces mRNA abundance at the level of transcription. Furthermore, they have shown that suppression of S6K1 mimics the effect of rapamycin treatment and restores IRS1 mRNA. In contrast to this, the level of IRS1 protein in S6K1 deficient mice and S6K1 siRNA treated cells was not obviously different from wild type mice either on a normal chow diet or a high fat diet in our study. Because measurement of IRS mRNA expression levels has not been done in our study, it is difficult to compare these conflicting results. However, it will be valuable to test whether IRS1 gene transcription is enhanced in S6K1 deficient mice given that the level of IRS1 gene expression is important for maintaining insulin sensitivity on the long term.

Upregulation of the OXPHOS pathway in S6K1 deficient mice.

Another mechanism of protection against obesity and insulin resistance in S6K1 deficient mice is the upregulation of the oxidative phosphorylation (OXPHOS) pathway. Our study showed an increased metabolic rate, enhanced oxidative metabolism, consistent with the increase in mitochondria number, as well as the induction of genes that control the OXPHOS pathway. That S6K1 deficient mice remain insulin sensitive, despite high circulating FFAs, may be explained by overexpression or activation of PPARδ. More specifically, an interesting finding of this work was that the deletion of S6K1 results in an

increase of PGC1, UCP1, mCPT, and PPARδ expression *in vivo*. These genes induce expression of mitochondrial respiratory genes and enhance fatty acid β-oxidation (Lowell and Spiegelman, 2000; Puigserver et al., 1998). How then does the loss of S6K1 increase OXPHOS pathway? Interestingly, Serkova et al have shown that SDZ-RAD, a rapamycin analogue, antagonizes the effects of cyclosporine by stimulating oxidative phosphorylation in isolated rat brain slices (Serkova et al., 2000). It would be informative to assess whether the S6 kinases might be involved in the transcriptional activation of PGC1, UCP1, mCPT, and PPARδ by using rapamycin or RNA interference against S6K1 or S6K2 gene expression. Given that S6K2 gene expression is upregulated in all tissues examined of S6K1 deficient mice and that S6K2 is localized in the nucleus (Shima et al., 1998) (Savinska et al., 2004), it remains to be addressed whether upregulation of the OXPHOS pathway is due to direct genetic deletion of S6K1 or to compensatory S6K2 gene upregulation.

Infusion of glucosamine under hyperinsulinemic conditions leads to down-regulation of OXPHOS gene expression and lower oxygen consumption (Obici et al., 2002). Similar changes in OXPHOS gene expression occur with overfeeding (Obici et al., 2002). Conversely, caloric restriction and exercise are associated with lower glucosamine production and high insulin sensitivity (Koubova and Guarente, 2003). Previous and present findings in S6K1 deficient mice are closely parallel by some of the effects of a low protein diet or low calorie diet feeding, despite the fact that these mice are not starved (Pende et al., 2000; Um et al., in press): small body size during gestation, reduced pancreatic β-cell size, hypoinsulinemia, high insulin sensitivity in peripheral tissues, and enhanced OXPHOS gene expression. Thus, these results indicate that S6K1 may be one of signaling molecules mediating the effect of overnutrition to induce insulin resistance by downregulation of OXPHOS pathway, although the mechanism is not fully understood.

How is an enhanced OXPHOS pathway coordinated with insulin sensitivity by loss of S6K1?

The activation of increased energy expenditure and PGC1 expression in S6K1 deficient muscle ultimately requires an increased uptake and metabolism of fuels. Therefore, is increased expression of PGC1 able to induce glucose uptake leading to hypersensitivity to insulin? Indeed, adenovirus-mediated PGC1 expression induces gene expression of the insulin-sensitive glucose transporter (Glut-4) in muscle *in vivo* and increases glucose uptake, although this process occurs even in the absence of insulin (Michael et al., 2001). Thus, it would be interesting to investigate whether S6K signaling is involved in PGC1 induced Glut-4 expression. Signaling responsible for the effects of PGC1 on glucose uptake and metabolism is of particular interest in *type 2 diabetes* because there are numerous studies indicating that the rates of mitochondrial oxidation can affect glucose uptake, where PGC1α gene expression is altered in type 2 diabetic patients with insulin resistance (Mootha et al., 2003). Interestingly, the phenotype of increased mitochondrial number and size and UCP1 gene expression in S6K1 deficient adipose tissue could be attributed to PGC1 expression, based on previous findings showing that PGC1 induces endogenous UCP1 gene expression and mitochondrial biogenesis when PGC1 is introduced into white fat cells (Puigserver et al., 1998).

What is the relationship between an enhanced OXPHOS pathway and reduced adiposity in S6K1 deficient mice?

Why do S6K1 deficient mice have reduced adipose tissue mass?

Is an enhanced OXPHOS pathway responsible for reduced adipocyte cell number and size? We showed that deletion of S6K1 results in increased PGC1, UCP1, mCPT, and PPAR-δ expression. Expression of PGC1 in white fat cells turned on UCP1 gene expression but fails to activate the adipocyte specific aP2 gene (Puigserver et al., 1998), the first gene actually identified as a target of PPAR- γ2(Tontonoz et al., 1994). This indicates that increased PGC1 expression

in adipose tissue may not be involved in reduced adiposity although it may enhance insulin sensitivity (Michael et al., 2001).

Increased PPAR-δ expression could be related to reduced adiposity in such mice. Tanaka et al have shown that the PPAR-δ agonist, GW501516, stimulates fatty acid β-oxidation and energy expenditure in skeletal muscle, leading to reduced lipid content in both skeletal muscle and liver (Tanaka et al., 2003). Moreover, accumulation of excess lipid in skeletal muscle or liver disturbs insulin signaling. In skeletal muscle, this disturbance has been linked to impaired activity of the insulin receptor substrate (IRS)-1-associated phosphatidyl inositol 3-kinase (PI3-kinase) (Dresner et al., 1999; Shulman, 2000; Yu et al., 2002).

Is reduced adiposity arising from a defect in adipogenesis?

Adipose tissue expands as existing adipocytes enlarge and as new adipocytes mature from fibroblast-like preadipocytes (MacDougald and Mandrup, 2002). Tontonoz et al have shown that expression of PPAR-γ2 and RXR α activates the adipocyte specific aP2 enhancer in cultured fibroblasts, and this activation is potentiated by peroxisome proliferators, fatty acids, and 9-cis retinoic acid (Tontonoz et al., 1994). They therefore suggested a mechanism whereby fatty acids, peroxisome proliferators, 9-cis retinoic acid, and other lipids may regulate adipocyte gene expression and differentiation (Tontonoz et al., 1994). Despite the disappearance of the smaller adipocyte size phenotype in S6K1 deficient mice fed on a high fat diet compared to a normal chow diet (Um SH, Thomas G, unpublished results), such mice exhibited dramatically reduced adipose tissue mass, indicating the defect may reside in adipogenesis stimulated by high fat diet. Thus, reduced adipogenesis in S6K1 deficient mouse embryonic fibroblasts *in vitro* (Frigerio F, Um SH, Kozma S, Thomas G, unpublished results) may arise from impaired signalling from adipogenic stimuli such as fatty acids or PPAR- gamma agonist due to the loss of S6K1. Consistent with this, rapamycin inhibits adipogenesis partially in 3T3 L1 cells *in vitro* (El-Chaar et al., 2004; Yeh et al., 1995a) although the molecular mechanisms by which rapamycin inhibits adipogenesis remains unclear. Furthermore, Bell et al have demonstrated that

rapamycin can interrupt adipogenesis independently from its antiproliferative effect. These experiments were performed in primary human adipocytes which undergo differentiation in the absence of clonal expansion (Bell et al., 2000). Therefore, this study would imply that the mTOR/S6K pathway may be involved in adipogenesis at the differentiation stage following clonal expansion. It would be interesting to determine whether PPAR-γ2 (Peroxisome proliferator-activated receptor-γ2) and C/EBPα (CCAAT/enhancer-binding protein), two key transcription factors for adipocyte differentiation (Wu et al., 1999b), are regulated by the S6K pathway. Given that rapamycin inhibits many mTOR targets besides S6K1, including S6K2, the 4EBPs, eIF4B, and eEF2 kinase (Gingras et al., 2001; Hay and Sonenberg, 2004), it will be informative to determine whether lowering S6K1 levels or other mTOR target levels using lentiviral vector expressing short hairpin RNA inhibit adipogenesis *in vivo* and *in vitro* (Katayama et al., 2004). By analyzing what kind of factors are involved in this process, this approach will serve to clarify the role of S6K1 pathway in adipocyte differentiation and to identify potential targets of mTOR/S6K pathway during adipogenesis.

Furthermore, because of the role of S6K1 in many important metabolic processes in adipose tissue and muscle, it is worth asking whether and how the activities of S6K1 might be modulated in a tissue specific manner. Conditional knockout approaches could be useful to understand the tissue specific physiological action of S6K1 in metabolism.

Human obesity and S6K1

Human body fat mass is to a large extent genetically determined, but little is known about the susceptibility genes for common obesity (Barsh et al., 2000; Snyder et al., 2004). So far, single gene mutations have only been identified as the cause of morbid obesity in about 5% of young individuals (Barsh et al., 2000; Vaisse et al., 2000). One of the most successful routes for identification of body fat regulative mechanisms as well as genetic causes of obesity in humans has been systematic investigation of genes shown to affect energy metabolism in gene knockout mice (Butler and Cone, 2001; Snyder et al., 2004). Based on

resistance to age- and diet- induced obesity and insulin resistance in S6K1 knockout mice, it would be particularly informative to analyze single-nucleotide polymorphisms (SNPs) and repeat polymorphisms in the human S6K1 gene region which may drive constitutive activation of this pathway, thereby finding a relationship between S6K1 and susceptibility for insulin resistance and obesity.

The present study indicates the impact of S6KI signaling in age- and diet-induced obesity and insulin resistance, and gives insight into the interaction between insulin induced IRS-PI3K pathway and nutrient induced mTOR-S6K pathway in metabolism and nutrient homeostasis. Furthermore, S6K1's function in insulin sensitivity and regulation of the oxidative phosphorylation pathway, as shown in this study, all suggest that S6K1 could be an attractive target for antiobesity or *diabetes* drugs.

In analyzing the role of S6K1 in obesity and diabetes, one must also consider S6K2. S6K1-deficient mice are smaller, have reduced pancreatic β cell size, and are resistant to age- and diet-induced obesity. In contrast, S6K2-deficient mice are not reduced in body size nor do they exhibit reduced pancreatic β cell size, despite reduced S6 phosphorylation. These findings indicate that each kinase may have distinct targets independent of S6. Interestingly, Richardson et al have shown that SKAR, a RNA binding protein is a specific target for S6K1 but not S6K2 (Richardson et al., 2004), suggesting differential substrate specificity for each kinase. Interestingly, Zhu et al have shown that main mutational locus for Bardet Biedl syndrome, which presents hypogonadism with predisposition to diabetes, hypertension, obesity and mental retardation, maps within or nearby the S6K2 gene (Zhu and Gerhard, 1998) suggesting that potential relevance of S6K2 gene mutation in predisposition of metabolic disorders. Analyzing the phenotype of S6K2 deficient mice and comparing it with that of S6K1 deficient mice in the context of insulin sensitivity and OXPHOS pathway may improve our understanding of the role of each kinase in metabolism and potential mechanism by which substrate specificity is driven.

V. REFERENCES

Abu-Elheiga, L., Almarza-Ortega, D.B., Baldini, A. and Wakil, S.J. (1997) Human acetyl-CoA carboxylase 2. Molecular cloning, characterization, chromosomal mapping, and evidence for two isoforms. *J Biol Chem*, **272**, 10669-10677.

Abu-Elheiga, L., Brinkley, W.R., Zhong, L., Chirala, S.S., Woldegiorgis, G. and Wakil, S.J. (2000) The subcellular localization of acetyl-CoA carboxylase 2. *Proc Natl Acad Sci U S A*, **97**, 1444-1449.

Abu-Elheiga, L., Matzuk, M.M., Abo-Hashema, K.A. and Wakil, S.J. (2001) Continuous fatty acid oxidation and reduced fat storage in mice lacking acetyl-CoA carboxylase 2. *Science*, **291**, 2613-2616.

Abu-Elheiga, L., Oh, W., Kordari, P. and Wakil, S.J. (2003) Acetyl-CoA carboxylase 2 mutant mice are protected against obesity and diabetes induced by high-fat/high-carbohydrate diets. *Proc Natl Acad Sci U S A*, **100**, 10207-10212.

Aguirre, V., Werner, E.D., Giraud, J., Lee, Y.H., Shoelson, S.E. and White, M.F. (2002) Phosphorylation of Ser307 in insulin receptor substrate-1 blocks interactions with the insulin receptor and inhibits insulin action. *J Biol Chem*, **277**, 1531-1537.

Alessi, D.R., Deak, M., Casamayor, A., Caudwell, F.B., Morrice, N., Norman, D.G., Gaffney, P., Reese, C.B., MacDougall, C.N., Harbison, D., Ashworth, A. and Bownes, M. (1997)

3-Phosphoinositide-dependent protein kinase-1 (PDK1): structural and functional homology with the Drosophila DSTPK61 kinase. *Curr Biol*, **7**, 776-789.

Alessi, D.R., Kozlowski, M.T., Weng, Q.P., Morrice, N. and Avruch, J. (1998) 3-Phosphoinositide-dependent protein kinase 1 (PDK1) phosphorylates and activates the p70 S6 kinase in vivo and in vitro. *Curr Biol*, **8**, 69-81.

Amri, E.Z., Bonino, F., Ailhaud, G., Abumrad, N.A. and Grimaldi, P.A. (1995) Cloning of a protein that mediates transcriptional effects of fatty acids in preadipocytes. Homology to peroxisome proliferator-activated receptors. *J Biol Chem*, **270**, 2367-2371.

Bachman, E.S., Dhillon, H., Zhang, C.Y., Cinti, S., Bianco, A.C., Kobilka, B.K. and Lowell, B.B. (2002) betaAR signaling required for diet-induced thermogenesis and obesity resistance. *Science*, **297**, 843-845.

Barsh, G.S., Farooqi, I.S. and O'Rahilly, S. (2000) Genetics of body-weight regulation. *Nature*, **404**, 644-651.

Baschat, A.A. and Hecher, K. (2004) Fetal growth restriction due to placental disease. *Semin Perinatol*, **28**, 67-80.

Bell, A., Grunder, L. and Sorisky, A. (2000) Rapamycin inhibits human adipocyte differentiation in primary culture. *Obes Res*, **8**, 249-254.

Bergman, R.N. and Ader, M. (2000) Free fatty acids and pathogenesis of type 2 diabetes mellitus. *Trends Endocrinol Metab*, **11**, 351-356.

Bernal-Mizrachi, E., Wen, W., Stahlhut, S., Welling, C.M. and Permutt, M.A. (2001) Islet beta cell expression of constitutively active Akt1/PKB alpha induces striking hypertrophy, hyperplasia, and hyperinsulinemia. *J Clin Invest*, **108**, 1631-1638.

Bernard, C., Berthault, M.F., Saulnier, C. and Ktorza, A. (1999) Neogenesis vs. apoptosis As main components of pancreatic beta cell ass changes in glucose-infused normal and mildly diabetic adult rats. *Faseb J*, **13**, 1195-1205.

Bernard-Kargar, C. and Ktorza, A. (2001) Endocrine pancreas plasticity under physiological and pathological conditions. *Diabetes*, **50 Suppl 1**, S30-35.

Beugnet, A., Tee, A.R., Taylor, P.M. and Proud, C.G. (2003) Regulation of targets of mTOR (mammalian target of rapamycin) signalling by intracellular amino acid availability. *Biochem J*, **372**, 555-566.

Blondeau, B., Avril, I., Duchene, B. and Breant, B. (2002) Endocrine pancreas development is altered in foetuses from rats previously showing intra-uterine growth retardation in response to malnutrition. *Diabetologia*, **45**, 394-401.

Boden, G. and Shulman, G.I. (2002) Free fatty acids in obesity and type 2 diabetes: defining their role in the development of insulin resistance and beta-cell dysfunction. *Eur J Clin Invest*, **32 Suppl 3**, 14-23.

Bonner-Weir, S. (1994) Regulation of pancreatic beta-cell mass in vivo. *Recent Prog Horm Res*, **49**, 91-104.

Bonner-Weir, S. (2000) Life and death of the pancreatic beta cells. *Trends Endocrinol Metab*, **11**, 375-378.

Bonner-Weir, S., Deery, D., Leahy, J.L. and Weir, G.C. (1989) Compensatory growth of pancreatic beta-cells in adult rats after short- term glucose infusion. *Diabetes*, **38**, 49-53.

Bos, J.L. (1995) A target for phosphoinositide 3-kinase: *Akt*/PKB. *Trends in biochemical science*, **20**, 441-442.

Bouzakri, K., Roques, M., Gual, P., Espinosa, S., Guebre-Egziabher, F., Riou, J.P., Laville, M., Le Marchand-Brustel, Y., Tanti, J.F. and Vidal, H. (2003) Reduced activation of phosphatidylinositol-3 kinase and increased serine 636 phosphorylation of insulin receptor substrate-1 in primary culture of skeletal muscle cells from patients with type 2 diabetes. *Diabetes*, **52**, 1319-1325.

Brazil, D.P. and Hemmings, B.A. (2001) Ten years of protein kinase B signalling: a hard Akt to follow. *Trends Biochem Sci*, **26**, 657-664.

Brazil, D.P., Yang, Z.Z. and Hemmings, B.A. (2004) Advances in protein kinase B signalling: AKTion on multiple fronts. *Trends Biochem Sci*, **29**, 233-242.

Brown, E.J., Beal, P.A., Keith, C.T., Chen, J., Shin, T.B. and Schreiber, S.L. (1995) Control of p70 S6 kinase by kinase activity of FRAP *in vivo*. *Nature*, **377**, 441-446.

Bruning, J.C., Winnay, J., Bonner-Weir, S., Taylor, S.I., Accili, D. and Kahn, C.R. (1997a) Development of a novel polygenic model of NIDDM in mice heterozygous for IR and IRS-1 null alleles. *Cell*, **88**, 561-572.

Bruning, J.C., Winnay, J., Cheatham, B. and Kahn, C.R. (1997b) Differential signaling by insulin receptor substrate 1 (IRS-1) and IRS-2 in IRS-1-deficient cells. *Mol Cell Biol*, **17**, 1513-1521.

Buettner, R., Newgard, C.B., Rhodes, C.J. and O'Doherty, R.M. (2000) Correction of diet-induced hyperglycemia, hyperinsulinemia, and skeletal muscle insulin resistance by moderate hyperleptinemia. *Am J Physiol Endocrinol Metab*, **278**, E563-569.

Burgering, B.M.T. and Coffer, P.J. (1995) Protein Kinase B (c-*Akt*) in phosphatidylinositol-3-OH kinase signal transduction. *Nature*, **376**, 599-602.

Butler, A.A. and Cone, R.D. (2001) Knockout models resulting in the development of obesity. *Trends Genet*, **17**, S50-54.

Camp, H.S., Ren, D. and Leff, T. (2002) Adipogenesis and fat-cell function in obesity and diabetes. *Trends Mol Med*, **8**, 442-447.

Carlson, C.J., White, M.F. and Rondinone, C.M. (2004) Mammalian target of rapamycin regulates IRS-1 serine 307 phosphorylation. *Biochem Biophys Res Commun*, **316**, 533-539.

Chan, C.B., MacPhail, R.M., Sheu, L., Wheeler, M.B. and Gaisano, H.Y. (1999) Beta-cell hypertrophy in fa/fa rats is associated with basal glucose hypersensitivity and reduced SNARE protein expression. *Diabetes*, **48**, 997-1005.

Cheadle, J.P., Reeve, M.P., Sampson, J.R. and Kwiatkowski, D.J. (2000) Molecular genetic advances in tuberous sclerosis. *Hum Genet*, **107**, 97-114.

Chen, E.J. and Kaiser, C.A. (2003) LST8 negatively regulates amino acid biosynthesis as a component of the TOR pathway. *J Cell Biol*, **161**, 333-347.

Chen, M., Yang, Y., Braunstein, E., Georgeson, K.E. and Harmon, C.M. (2001) Gut expression and regulation of FAT/CD36: possible role in fatty acid transport in rat enterocytes. *Am J Physiol Endocrinol Metab*, **281**, E916-923.

Chirala, S.S., Chang, H., Matzuk, M., Abu-Elheiga, L., Mao, J., Mahon, K., Finegold, M. and Wakil, S.J. (2003) Fatty acid synthesis is essential in embryonic development: fatty acid synthase null mutants and most of the heterozygotes die in utero. *Proc Natl Acad Sci U S A*, **100**, 6358-6363.

Cho, H., Mu, J., Kim, J.K., Thorvaldsen, J.L., Chu, Q., Crenshaw, E.B., 3rd, Kaestner, K.H., Bartolomei, M.S., Shulman, G.I. and Birnbaum, M.J. (2001a) Insulin resistance and a diabetes mellitus-like syndrome in mice lacking the protein kinase Akt2 (PKB beta). *Science*, **292**, 1728-1731.

Cho, H., Thorvaldsen, J.L., Chu, Q., Feng, F. and Birnbaum, M.J. (2001b) Akt1/PKBalpha is required for normal growth but dispensable for maintenance of glucose homeostasis in mice. *J Biol Chem*, **276**, 38349-38352.

Cinti, S. (2000) Anatomy of the adipose organ. *Eat Weight Disord*, **5**, 132-142.

Clapham, J.C., Arch, J.R., Chapman, H., Haynes, A., Lister, C., Moore, G.B., Piercy, V., Carter, S.A., Lehner, I., Smith, S.A., Beeley, L.J., Godden, R.J., Herrity, N., Skehel, M., Changani, K.K., Hockings, P.D., Reid, D.G., Squires, S.M., Hatcher, J., Trail, B., Latcham, J., Rastan, S., Harper, A.J., Cadenas, S., Buckingham, J.A., Brand, M.D. and Abuin, A. (2000) Mice overexpressing human uncoupling protein-3 in skeletal muscle are hyperphagic and lean. *Nature*, **406**, 415-418.

Couillard, C., Mauriege, P., Imbeault, P., Prud'homme, D., Nadeau, A., Tremblay, A., Bouchard, C. and Despres, J.P. (2000) Hyperleptinemia is more closely associated with adipose cell hypertrophy than with adipose tissue hyperplasia. *Int J Obes Relat Metab Disord*, **24**, 782-788.

Crowley, V.E., Yeo, G.S. and O'Rahilly, S. (2002) Obesity therapy: altering the energy intake-and-expenditure balance sheet. *Nat Rev Drug Discov*, **1**, 276-286.

Cushman, S.W. (1970) Structure-function relationships in the adipose cell. I. Ultrastructure of the isolated adipose cell. *J Cell Biol*, **46**, 326-341.

Dandoy-Dron, F., Itier, J.M., Monthioux, E., Bucchini, D. and Jami, J. (1995) Tissue-specific expression of the rat insulin 1 gene in vivo requires both the enhancer and promoter regions. *Differentiation*, **58**, 291-295.

Dennis, P.B., Jaeschke, A., Saitoh, M., Fowler, B., Kozma, S.C. and Thomas, G. (2001) Mammalian TOR: a homeostatic ATP sensor. *Science*, **294**, 1102-1105.

Dennis, P.B., Pullen, N., Pearson, R.B., Kozma, S.C. and Thomas, G. (1998) Phosphorylation sites in the autoinhibitory domain participate in $p70^{s6k}$ activation loop phosphorylation. *J Biol Chem*, **273**, 14845-14852.

Dennis, P.B. and Thomas, G. (2002) Quick guide: target of rapamycin. *Curr Biol*, **12**, R269.

Despres, J.P., Lemieux, I. and Prud'homme, D. (2001) Treatment of obesity: need to focus on high risk abdominally obese patients. *Bmj*, **322**, 716-720.

Dor, Y., Brown, J., Martinez, O.I. and Melton, D.A. (2004) Adult pancreatic beta-cells are formed by self-duplication rather than stem-cell differentiation. *Nature*, **429**, 41-46.

Doty, F.D., Entzminger, G., Jr., Hauck, C.D. and Staab, J.P. (1999) Practical aspects of birdcage coils. *J Magn Reson*, **138**, 144-154.

Dresner, A., Laurent, D., Marcucci, M., Griffin, M.E., Dufour, S., Cline, G.W., Slezak, L.A., Andersen, D.K., Hundal, R.S., Rothman, D.L., Petersen, K.F. and Shulman, G.I. (1999) Effects of free fatty acids on glucose transport and IRS-1-associated phosphatidylinositol 3-kinase activity. *J Clin Invest*, **103**, 253-259.

Dressel, U., Allen, T.L., Pippal, J.B., Rohde, P.R., Lau, P. and Muscat, G.E. (2003) The peroxisome proliferator-activated receptor beta/delta agonist, GW501516, regulates the expression of genes involved in lipid catabolism and energy uncoupling in skeletal muscle cells. *Mol Endocrinol*, **17**, 2477-2493.

Duvillie, B., Cordonnier, N., Deltour, L., Dandoy-Dron, F., Itier, J.M., Monthioux, E., Jami, J., Joshi, R.L. and Bucchini, D. (1997) Phenotypic alterations in insulin-deficient mutant mice. *Proc Natl Acad Sci U S A*, **94**, 5137-5140.

Elberg, G., Gimble, J.M. and Tsai, S.Y. (2000) Modulation of the murine peroxisome proliferator-activated receptor gamma 2 promoter activity by CCAAT/enhancer-binding proteins. *J Biol Chem*, **275**, 27815-27822.

El-Chaar, D., Gagnon, A. and Sorisky, A. (2004) Inhibition of insulin signaling and adipogenesis by rapamycin: effect on phosphorylation of p70 S6 kinase vs eIF4E-BP1. *Int J Obes Relat Metab Disord*, **28**, 191-198.

Enerback, S., Jacobsson, A., Simpson, E.M., Guerra, C., Yamashita, H., Harper, M.E. and Kozak, L.P. (1997) Mice lacking mitochondrial uncoupling protein are cold-sensitive but not obese. *Nature*, **387**, 90-94.

Feng, J., Park, J., Cron, P., Hess, D. and Hemmings, B.A. (2004) Identification of a PKB/Akt hydrophobic motif Ser-473 kinase as DNA-dependent protein kinase. *J Biol Chem*.

Finegood, D.T., Scaglia, L. and Bonner-Weir, S. (1995) Dynamics of beta-cell mass in the growing rat pancreas. Estimation with a simple mathematical model. *Diabetes*, **44**, 249-256.

Fingar, D.C., Salama, S., Tsou, C., Harlow, E. and Blenis, J. (2002) Mammalian cell size is controlled by mTOR and its downstream targets S6K1 and 4EBP1/eIF4E. *Genes Dev*, **16**, 1472-1487.

Flotow, H. and Thomas, G. (1992) Substrate recognition determinants of the mitogen-activated 70K S6 kinase from rat liver. *Journal of Biological Chemistry*, **267**, 3074-3078.

Forman, B.M., Tontonoz, P., Chen, J., Brun, R.P., Spiegelman, B.M. and Evans, R.M. (1995) 15-Deoxy-delta 12, 14-prostaglandin J2 is a ligand for the adipocyte determination factor PPAR gamma. *Cell*, **83**, 803-812.

Foster, D.O. and Frydman, M.L. (1979) Tissue distribution of cold-induced thermogenesis in conscious warm- or cold-acclimated rats reevaluated from changes in tissue blood flow: the dominant role of brown adipose tissue in the replacement of shivering by nonshivering thermogenesis. *Can J Physiol Pharmacol*, **57**, 257-270.

Fowden, A.L. (1989) The role of insulin in prenatal growth. *J Dev Physiol*, **12**, 173-182.

Franke, T.F., Kaplan, D.R., Cantley, L.C. and Toker, A. (1997) Direct regulation of the Akt proto-oncogene product by phosphatidylinositol-3,4-bisphosphate [see comments]. *Science*, **275**, 665-668.

Frankenfield, D.C., Rowe, W.A., Cooney, R.N., Smith, J.S. and Becker, D. (2001) Limits of body mass index to detect obesity and predict body composition. *Nutrition*, **17**, 26-30.

Fruhbeck, G., Gomez-Ambrosi, J., Muruzabal, F.J. and Burrell, M.A. (2001) The adipocyte: a model for integration of endocrine and metabolic signaling in energy metabolism regulation. *Am J Physiol Endocrinol Metab*, **280**, E827-847.

Fruman, D.A., Mauvais-Jarvis, F., Pollard, D.A., Yballe, C.M., Brazil, D., Bronson, R.T., Kahn, C.R. and Cantley, L.C. (2000) Hypoglycaemia, liver necrosis and perinatal death in mice lacking all isoforms of phosphoinositide 3-kinase p85 alpha. *Nat Genet*, **26**, 379-382.

Gao, X. and Pan, D. (2001) TSC1 and TSC2 tumor suppressors antagonize insulin signaling in cell growth. *Genes Dev*, **15**, 1383-1392.

Gao, X., Zhang, Y., Arrazola, P., Hino, O., Kobayashi, T., Yeung, R.S., Ru, B. and Pan, D. (2002) Tsc tumour suppressor proteins antagonize amino-acid-TOR signalling. *Nat Cell Biol*, **4**, 699-704.

Garami, A., Zwartkruis, F.J., Nobukuni, T., Joaquin, M., Roccio, M., Stocker, H., Kozma, S.C., Hafen, E., Bos, J.L. and Thomas, G. (2003) Insulin activation of Rheb, a mediator of mTOR/S6K/4E-BP signaling, is inhibited by TSC1 and 2. *Mol Cell*, **11**, 1457-1466.

Georgiades, P., Watkins, M., Burton, G.J. and Ferguson-Smith, A.C. (2001) Roles for genomic imprinting and the zygotic genome in placental development. *Proc Natl Acad Sci U S A*, **98**, 4522-4527.

Gimeno, R.E., Hirsch, D.J., Punreddy, S., Sun, Y., Ortegon, A.M., Wu, H., Daniels, T., Stricker-Krongrad, A., Lodish, H.F. and Stahl, A. (2003) Targeted deletion of fatty acid transport protein-4 results in early embryonic lethality. *J Biol Chem*, **278**, 49512-49516.

Gingras, A.-., C., Kennedy, S., G., O'Leary, M., A., Sonenberg, N. and Hay., N. (1998) 4E-BP1, a Repressor of mRNA Translation, is Phosphorylated and activated by the Akt (PKB) Signaling Pathway. *Genes and Development*, **12**, 502-513.

Gingras, A.C., Raught, B. and Sonenberg, N. (2001) Regulation of translation initiation by FRAP/mTOR. *Genes Dev*, **15**, 807-826.

Godfrey, K.M. (2002) The role of the placenta in fetal programming-a review. *Placenta*, **23 Suppl A**, S20-27.

Goudriaan, J.R., Dahlmans, V.E., Febbraio, M., Teusink, B., Romijn, J.A., Havekes, L.M. and Voshol, P.J. (2002) Intestinal lipid absorption is not affected in CD36 deficient mice. *Mol Cell Biochem*, **239**, 199-202.

Grace, C.J., Swenne, I., Kohn, P.G., Strain, A.J. and Milner, R.D. (1990) Protein-energy malnutrition induces changes in insulin sensitivity. *Diabete Metab*, **16**, 484-491.

Greene, M.W., Sakaue, H., Wang, L., Alessi, D.R. and Roth, R.A. (2003) Modulation of insulin-stimulated degradation of human insulin receptor substrate-1 by Serine 312 phosphorylation. *J Biol Chem*, **278**, 8199-8211.

Gressner, A.M. and Wool, I.G. (1974) The phosphorylation of liver ribosomal proteins *in vivo* Evidence that only a single small subunit (S6) is phosphorylated. *Journal of Biological Chemistry*, **249**, 6917-6925.

Gual, P., Gonzalez, T., Gremeaux, T., Barres, R., Le Marchand-Brustel, Y. and Tanti, J.F. (2003a) Hyperosmotic stress inhibits insulin receptor substrate-1 function by distinct mechanisms in 3T3-L1 adipocytes. *J Biol Chem*, **278**, 26550-26557.

Gual, P., Gremeaux, T., Gonzalez, T., Le Marchand-Brustel, Y. and Tanti, J.F. (2003b) MAP kinases and mTOR mediate insulin-induced phosphorylation of insulin receptor substrate-1 on serine residues 307, 612 and 632. *Diabetologia*, **46**, 1532-1542.

Guerra, C., Koza, R.A., Yamashita, H., Walsh, K. and Kozak, L.P. (1998) Emergence of brown adipocytes in white fat in mice is under genetic control. Effects on body weight and adiposity. *J Clin Invest*, **102**, 412-420.

Hales, C.N. and Barker, D.J. (2001) The thrifty phenotype hypothesis. *Br Med Bull*, **60**, 5-20.

Hall. M., R.M., Thomas G. (2004) *Cell Growth: Control of Cell Size (Cold Spring Harbor Monograph Series)*. Cold Spring Harbor Laboratory Press, New York.

Hansen, J.B., Petersen, R.K., Larsen, B.M., Bartkova, J., Alsner, J. and Kristiansen, K. (1999) Activation of peroxisome proliferator-activated receptor gamma bypasses the function of the retinoblastoma protein in adipocyte differentiation. *J Biol Chem*, **274**, 2386-2393.

Hanson, R.W. and Reshef, L. (2003) Glyceroneogenesis revisited. *Biochimie*, **85**, 1199-1205.

Hara, K., Maruki, Y., Long, X., Yoshino, K., Oshiro, N., Hidayat, S., Tokunaga, C., Avruch, J. and Yonezawa, K. (2002) Raptor, a binding partner of target of rapamycin (TOR), mediates TOR action. *Cell*, **110**, 177-189.

Hara, K., Yonezawa, K., Weng, Q.P., Kozlowski, M.T., Belham, C. and Avruch, J. (1998) Amino acid sufficiency and mTOR regulate p70 S6 kinase and eIF-4E BP1 through a common effector mechanism. *J Biol Chem*, **273**, 14484-14494.

Hardie, D.G. and Pan, D.A. (2002) Regulation of fatty acid synthesis and oxidation by the AMP-activated protein kinase. *Biochem Soc Trans*, **30**, 1064-1070.

Hardwick, J.S., Kuruvilla, F.G., Tong, J.K., Shamji, A.F. and Schreiber, S.L. (1999) Rapamycin-modulated transcription defines the subset of nutrient-sensitive signaling pathways directly controlled by the Tor proteins. *Proc Natl Acad Sci U S A*, **96**, 14866-14870.

Harrington, L.S., Findlay, G.M., Gray, A., Tolkacheva, T., Wigfield, S., Rebholz, H., Barnett, J., Leslie, N.R., Cheng, S., Shepherd, P.R., Gout, I., Downes, C.P. and Lamb, R.F. (2004) The TSC1-2 tumor suppressor controls insulin-PI3K signaling via regulation of IRS proteins. *J Cell Biol*, **166**, 213-223.

Hay, N. and Sonenberg, N. (2004) Upstream and downstream of mTOR. *Genes Dev*, **18**, 1926-1945.

Hiebert, S.W., Chellappan, S.P., Horowitz, J.M. and Nevins, J.R. (1992) The interaction of RB with E2F coincides with an inhibition of the transcriptional activity of E2F. *Genes Dev*, **6**, 177-185.

Hill, M.M., Clark, S.F., Tucker, D.F., Birnbaum, M.J., James, D.E. and Macaulay, S.L. (1999) A role for protein kinase Bbeta/Akt2 in insulin-stimulated GLUT4 translocation in adipocytes. *Mol Cell Biol*, **19**, 7771-7781.

Hirosumi, J., Tuncman, G., Chang, L., Gorgun, C.Z., Uysal, K.T., Maeda, K., Karin, M. and Hotamisligil, G.S. (2002) A central role for JNK in obesity and insulin resistance. *Nature*, **420**, 333-336.

Hirsch, J. and Batchelor, B. (1976) Adipose tissue cellularity in human obesity. *Clin Endocrinol Metab*, **5**, 299-311.

Hirsch, J., Fried, S.K., Edens, N.K. and Leibel, R.L. (1989) The fat cell. *Med Clin North Am*, **73**, 83-96.

Holm, C. (2003) Molecular mechanisms regulating hormone-sensitive lipase and lipolysis. *Biochem Soc Trans*, **31**, 1120-1124.

Hresko, R.C., Heimberg, H., Chi, M.M. and Mueckler, M. (1998) Glucosamine-induced insulin resistance in 3T3-L1 adipocytes is caused by depletion of intracellular ATP. *J Biol Chem*, **273**, 20658-20668.

Hwang, J.H., Pan, J.W., Heydari, S., Hetherington, H.P. and Stein, D.T. (2001) Regional differences in intramyocellular lipids in humans observed by in vivo 1H-MR spectroscopic imaging. *J Appl Physiol*, **90**, 1267-1274.

Inoki, K., Li, Y., Xu, T. and Guan, K.L. (2003) Rheb GTPase is a direct target of TSC2 GAP activity and regulates mTOR signaling. *Genes Dev*, **17**, 1829-1834.

Inoki, K., Li, Y., Zhu, T., Wu, J. and Guan, K.L. (2002) TSC2 is phosphorylated and inhibited by Akt and suppresses mTOR signalling. *Nat Cell Biol*, **4**, 648-657.

Jaeschke, A., Hartkamp, J., Saitoh, M., Roworth, W., Nobukuni, T., Hodges, A., Sampson, J., Thomas, G. and Lamb, R. (2002) Tuberous sclerosis complex tumor suppressor-mediated S6 kinase inhibition by phosphatidylinositide-3-OH kinase is mTOR independent. *J Cell Biol*, **159**, 217-224.

Jefferies, H.B.J., Fumagalli, S., Dennis, P.B., Reinhard, C., Pearson, R.B. and Thomas, G. (1997) Rapamycin suppresses 5'TOP mRNA translation through inhibition of $p70^{s6k}$. *EMBO Journal*, **12**, 3693-3704.

Jefferies, H.B.J. and Thomas, G. (1996) Ribosomal Protein S6 Phosphorylation and Signal Transduction. In Hershey, J.W.B., Mathews, M.B. and Sonenberg, N. (eds.), *Translational Control*. Cold Spring Harbor Laboratory Press, Cold Spring Harbor, USA, pp. 389-409.

Jonas, J.C., Sharma, A., Hasenkamp, W., Ilkova, H., Patane, G., Laybutt, R., Bonner-Weir, S. and Weir, G.C. (1999) Chronic hyperglycemia triggers loss of pancreatic beta cell differentiation in an animal model of diabetes. *J Biol Chem*, **274**, 14112-14121.

Kahn, B.B. and Flier, J.S. (2000) Obesity and insulin resistance. *J Clin Invest*, **106**, 473-481.

Kakuma, T., Lee, Y., Higa, M., Wang, Z., Pan, W., Shimomura, I. and Unger, R.H. (2000) Leptin, troglitazone, and the expression of sterol regulatory element binding proteins in liver and pancreatic islets. *Proc Natl Acad Sci U S A*, **97**, 8536-8541.

Kamp, F., Guo, W., Souto, R., Pilch, P.F., Corkey, B.E. and Hamilton, J.A. (2003) Rapid flip-flop of oleic acid across the plasma membrane of adipocytes. *J Biol Chem*, **278**, 7988-7995.

Kasuga, M., Zick, Y., Blithe, D.L., Crettaz, M. and Kahn, C.R. (1982) Insulin stimulates tyrosine phosphorylation of the insulin receptor in a cell-free system. *Nature*, **298**, 667-669.

Katayama, K., Wada, K., Miyoshi, H., Ohashi, K., Tachibana, M., Furuki, R., Mizuguchi, H., Hayakawa, T., Nakajima, A., Kadowaki, T., Tsutsumi, Y., Nakagawa, S., Kamisaki, Y. and Mayumi, T. (2004) RNA interfering approach for clarifying the PPARgamma pathway using lentiviral vector expressing short hairpin RNA. *FEBS Lett*, **560**, 178-182.

Kaung, H.L. (1994) Growth dynamics of pancreatic islet cell populations during fetal and neonatal development of the rat. *Dev Dyn*, **200**, 163-175.

Kaushik, V.K., Young, M.E., Dean, D.J., Kurowski, T.G., Saha, A.K. and Ruderman, N.B. (2001) Regulation of fatty acid oxidation and glucose metabolism in rat soleus muscle: effects of AICAR. *Am J Physiol Endocrinol Metab*, **281**, E335-340.

Kido, Y., Burks, D.J., Withers, D., Bruning, J.C., Kahn, C.R., White, M.F. and Accili, D. (2000) Tissue-specific insulin resistance in mice with mutations in the insulin receptor, IRS-1, and IRS-2. *J Clin Invest*, **105**, 199-205.

Kim, D.H. and Sabatini, D.M. (2004) Raptor and mTOR: subunits of a nutrient-sensitive complex. *Curr Top Microbiol Immunol*, **279**, 259-270.

Kim, D.H., Sarbassov, D.D., Ali, S.M., King, J.E., Latek, R.R., Erdjument-Bromage, H., Tempst, P. and Sabatini, D.M. (2002) mTOR interacts with raptor to form a nutrient-sensitive complex that signals to the cell growth machinery. *Cell*, **110**, 163-175.

Kim, J.B., Sarraf, P., Wright, M., Yao, K.M., Mueller, E., Solanes, G., Lowell, B.B. and Spiegelman, B.M. (1998) Nutritional and insulin regulation of fatty acid synthetase and leptin gene expression through ADD1/SREBP1. *J Clin Invest*, **101**, 1-9.

Kim, J.Y., Hickner, R.C., Cortright, R.L., Dohm, G.L. and Houmard, J.A. (2000) Lipid oxidation is reduced in obese human skeletal muscle. *Am J Physiol Endocrinol Metab*, **279**, E1039-1044.

Kitamura, T., Kahn, C.R. and Accili, D. (2003) Insulin receptor knockout mice. *Annu Rev Physiol*, **65**, 313-332.

Kloppel, G., Lohr, M., Habich, K., Oberholzer, M. and Heitz, P.U. (1985) Islet pathology and the pathogenesis of type 1 and type 2 diabetes mellitus revisited. *Surv Synth Pathol Res*, **4**, 110-125.

Kohn, A.D., Takeuchi, F. and Roth, R.A. (1996) Akt, a pleckstrin homology domain containing kinase, is activated primarily by phosphorylation. *J Biol Chem*, **271**, 21920-21926.

Koubova, J. and Guarente, L. (2003) How does calorie restriction work? *Genes Dev*, **17**, 313-321.

Kozma, S.C., Lane, H.A., Ferrari, S., Luther, H., Siegmann, M. and Thomas, G. (1989) A stimulated S6 kinase from rat liver: identity with the mitogen-activated S6 kinase from 3T3 cells. *EMBO Journal*, **8**, 4125-4132.

Krieg, J., Hofsteenge, J. and Thomas, G. (1988) Identification of the 40 S ribosomal protein S6 phosphorylation sites induced by cycloheximide. *Journal of Biological Chemistry*, **263**, 11473-11477.

Kunz, J. and Hall, M.N. (1993) Cyclosporin A, FK506 and rapamycin more than just immunosupression. *Trends in biochemical science*, **18**, 334-338.

Kunz, J., Henriquez, R., Scheider, U., Deuter-Reinhard, M., Movva, N.R. and Hall, M.N. (1993) Target of rapamycin in yeast, TOR2 is an essential phosphatidylinosito kinase homolog required for G_1 progression. *Cell*, **73**, 585-596.

Le Marchand-Brustel, Y., Gual, P., Gremeaux, T., Gonzalez, T., Barres, R. and Tanti, J.F. (2003) Fatty acid-induced insulin resistance: role of insulin receptor substrate 1 serine phosphorylation in the retroregulation of insulin signalling. *Biochem Soc Trans*, **31**, 1152-1156.

Lemonnier, D. (1972) Effect of age, sex, and sites on the cellularity of the adipose tissue in mice and rats rendered obese by a high-fat diet. *J Clin Invest*, **51**, 2907-2915.

Li, B., Nolte, L.A., Ju, J.S., Han, D.H., Coleman, T., Holloszy, J.O. and Semenkovich, C.F. (2000) Skeletal muscle respiratory uncoupling prevents diet-induced obesity and insulin resistance in mice. *Nat Med*, **6**, 1115-1120.

Li, Y., Corradetti, M.N., Inoki, K. and Guan, K.L. (2004) TSC2: filling the GAP in the mTOR signaling pathway. *Trends Biochem Sci*, **29**, 32-38.

Lin, J., Wu, H., Tarr, P.T., Zhang, C.Y., Wu, Z., Boss, O., Michael, L.F., Puigserver, P., Isotani, E., Olson, E.N., Lowell, B.B., Bassel-Duby, R. and Spiegelman, B.M. (2002) Transcriptional co-activator PGC-1 alpha drives the formation of slow-twitch muscle fibres. *Nature*, **418**, 797-801.

Lingohr, M.K., Buettner, R. and Rhodes, C.J. (2002a) Pancreatic beta-cell growth and survival--a role in obesity-linked type 2 diabetes? *Trends Mol Med*, **8**, 375-384.

Lingohr, M.K., Dickson, L.M., McCuaig, J.F., Hugl, S.R., Twardzik, D.R. and Rhodes, C.J. (2002b) Activation of IRS-2-mediated signal transduction by IGF-1, but not TGF-alpha or EGF, augments pancreatic beta-cell proliferation. *Diabetes*, **51**, 966-976.

Londos, C., Brasaemle, D.L., Schultz, C.J., Segrest, J.P. and Kimmel, A.R. (1999) Perilipins, ADRP, and other proteins that associate with intracellular neutral lipid droplets in animal cells. *Semin Cell Dev Biol*, **10**, 51-58.

Lowell, B.B. and Spiegelman, B.M. (2000) Towards a molecular understanding of adaptive thermogenesis. *Nature*, **404**, 652-660.

Lucas, S., Tavernier, G., Tiraby, C., Mairal, A. and Langin, D. (2003) Expression of human hormone-sensitive lipase in white adipose tissue of transgenic mice increases lipase activity but does not enhance in vitro lipolysis. *J Lipid Res*, **44**, 154-163.

MacDougald, O.A. and Mandrup, S. (2002) Adipogenesis: forces that tip the scales. *Trends Endocrinol Metab*, **13**, 5-11.

Manning, B.D. and Cantley, L.C. (2003) Rheb fills a GAP between TSC and TOR. *Trends in Biochemical Sciences*, **28**, 573-576.

Marette, A., Tulp, O.L. and Bukowiecki, L.J. (1991) Mechanism linking insulin resistance to defective thermogenesis in brown adipose tissue of obese diabetic SHR/N-cp rats. *Int J Obes*, **15**, 823-831.

Martinez-Botas, J., Anderson, J.B., Tessier, D., Lapillonne, A., Chang, B.H., Quast, M.J., Gorenstein, D., Chen, K.H. and Chan, L. (2000) Absence of perilipin results in leanness and reverses obesity in Lepr(db/db) mice. *Nat Genet*, **26**, 474-479.

McDaniel, M.L., Marshall, C.A., Pappan, K.L. and Kwon, G. (2002) Metabolic and autocrine regulation of the mammalian target of rapamycin by pancreatic beta-cells. *Diabetes*, **51**, 2877-2885.

McLeod, M.J. (1980) Differential staining of cartilage and bone in whole mouse fetuses by alcian blue and alizarin red S. *Teratology*, **22**, 299-301.

McMahon, L.P., Choi, K.M., Lin, T.A., Abraham, R.T. and Lawrence, J.C., Jr. (2002) The rapamycin-binding domain governs substrate selectivity by the mammalian target of rapamycin. *Mol Cell Biol*, **22**, 7428-7438.

Meyuhas, O., Avni, D. and Shama, S. (1996) Translational control of ribosomal protein mRNAs in eukaryotes. In Hershey, J.W.B., Mathews, M.B. and Sonenberg, N. (eds.), *Translational Control*. Cold Spring Harbor Laboratory Press, Cold Spring Harbor, pp. 363-388.

Michael, L.F., Wu, Z., Cheatham, R.B., Puigserver, P., Adelmant, G., Lehman, J.J., Kelly, D.P. and Spiegelman, B.M. (2001) Restoration of insulin-sensitive glucose transporter (GLUT4) gene expression in muscle cells by the transcriptional coactivator PGC-1. *Proc Natl Acad Sci U S A*, **98**, 3820-3825.

Michael, M.D., Kulkarni, R.N., Postic, C., Previs, S.F., Shulman, G.I., Magnuson, M.A. and Kahn, C.R. (2000) Loss of insulin signaling in hepatocytes leads to severe insulin resistance and progressive hepatic dysfunction. *Mol Cell*, **6**, 87-97.

Mootha, V.K., Lindgren, C.M., Eriksson, K.F., Subramanian, A., Sihag, S., Lehar, J., Puigserver, P., Carlsson, E., Ridderstrale, M., Laurila, E., Houstis, N., Daly, M.J., Patterson, N., Mesirov, J.P., Golub, T.R., Tamayo, P., Spiegelman, B., Lander, E.S., Hirschhorn, J.N., Altshuler, D. and Groop, L.C. (2003) PGC-1alpha-responsive genes involved in oxidative phosphorylation are coordinately downregulated in human diabetes. *Nat Genet*, **34**, 267-273.

Morimura, M., Ishiko, O., Sumi, T., Yoshida, H. and Ogita, S. (2001) Angiogenesis in adipose tissues and skeletal muscles with rebound weight-gain after diet-restriction in rabbits. *Int J Mol Med*, **8**, 499-503.

Morrison, R.F. and Farmer, S.R. (1999) Role of PPARgamma in regulating a cascade expression of cyclin-dependent kinase inhibitors, p18(INK4c) and p21(Waf1/Cip1), during adipogenesis. *J Biol Chem*, **274**, 17088-17097.

Mothe, I. and Van Obberghen, E. (1996) Phosphorylation of insulin receptor substrate-1 on multiple serine residues, 612, 632, 662, and 731, modulates insulin action. *J Biol Chem*, **271**, 11222-11227.

Must, A., Spadano, J., Coakley, E.H., Field, A.E., Colditz, G. and Dietz, W.H. (1999) The disease burden associated with overweight and obesity. *Jama*, **282**, 1523-1529.

Nagy, A., Gertsenstein M., Vinterstein K.,Behringer R. (2002) *Manipulating the Mouse Embryo: A Laboratory Manual*.

Nagy, A., Rossant, J., Nagy, R., Abramow-Newerly, W. and Roder, J.C. (1993) Derivation of completely cell culture-derived mice from early-passage embryonic stem cells. *Proc Natl Acad Sci U S A*, **90**, 8424-8428.

Nielsen, J.H., Svensson, C., Galsgaard, E.D., Moldrup, A. and Billestrup, N. (1999) Beta cell proliferation and growth factors. *J Mol Med*, **77**, 62-66.

Noda, T. and Ohsumi, Y. (1998) Tor, a phosphatidylinositol kinase homologue, controls autophagy in yeast. *J Biol Chem*, **273**, 3963-3966.

Nojima, H., Tokunaga, C., Eguchi, S., Oshiro, N., Hidayat, S., Yoshino, K.I., Hara, K., Tanaka, N., Avruch, J. and Yonezawa, K. (2003) The mTOR partner, Raptor binds the mTOR substrates, p70 S6 kinase and 4E-BP1 through their TOS (TOR signaling) motif. *J Biol Chem*.

Novak-Hofer, I. and Thomas, G. (1984) An activated S6 kinase in extracts from serum- and epidermal growth factor-stimulated Swiss 3T3 cells. *Journal of Biological Chemistry*, **259**, 5995-6000.

Obici, S., Wang, J., Chowdury, R., Feng, Z., Siddhanta, U., Morgan, K. and Rossetti, L. (2002) Identification of a biochemical link between energy intake and energy expenditure. *J Clin Invest*, **109**, 1599-1605.

Oliver, W.R., Jr., Shenk, J.L., Snaith, M.R., Russell, C.S., Plunket, K.D., Bodkin, N.L., Lewis, M.C., Winegar, D.A., Sznaidman, M.L., Lambert, M.H., Xu, H.E., Sternbach, D.D., Kliewer, S.A., Hansen, B.C. and Willson, T.M. (2001) A selective peroxisome proliferator-activated receptor delta agonist promotes reverse cholesterol transport. *Proc Natl Acad Sci U S A*, **98**, 5306-5311.

Osuga, J., Ishibashi, S., Oka, T., Yagyu, H., Tozawa, R., Fujimoto, A., Shionoiri, F., Yahagi, N., Kraemer, F.B., Tsutsumi, O. and Yamada, N. (2000) Targeted disruption of hormone-

sensitive lipase results in male sterility and adipocyte hypertrophy, but not in obesity. *Proc Natl Acad Sci U S A*, **97**, 787-792.
Ozes, O.N., Akca, H., Mayo, L.D., Gustin, J.A., Maehama, T., Dixon, J.E. and Donner, D.B. (2001) A phosphatidylinositol 3-kinase/Akt/mTOR pathway mediates and PTEN antagonizes tumor necrosis factor inhibition of insulin signaling through insulin receptor substrate-1. *Proc Natl Acad Sci U S A*, **98**, 4640-4645.
Parimi, P.S., Cripe-Mamie, C. and Kalhan, S.C. (2004) Metabolic Responses to Protein Restriction During Pregnancy in Rat and Translation Initiation Factors in the Mother and Fetus. *Pediatr Res*.
Patti, M.E. (1999) Nutrient modulation of cellular insulin action. *Ann N Y Acad Sci*, **892**, 187-203.
Patti, M.E., Brambilla, E., Luzi, L., Landaker, E.J. and Kahn, C.R. (1998) Bidirectional modulation of insulin action by amino acids. *J Clin Invest*, **101**, 1519-1529.
Pearson, R.B., Dennis, P.B., Han, J.W., Williamson, N.A., Kozma, S.C., Wettenhall, R.E.H. and Thomas, G. (1995) The principal target of rapamycin-induced $p70^{s6k}$ inactivation is a novel phosphorylation site within a conserved hydrophobic domain. *EMBO Journal*, **21**, 5279-5287.
Pende, M., Kozma, S.C., Jaquet, M., Oorschot, V., Burcelin, R., Le Marchand-Brustel, Y., Klumperman, J., Thorens, B. and Thomas, G. (2000) Hypoinsulinaemia, glucose intolerance and diminished beta-cell size in S6K1-deficient mice. *Nature*, **408**, 994-997.
Picard, F., Gehin, M., Annicotte, J., Rocchi, S., Champy, M.F., O'Malley, B.W., Chambon, P. and Auwerx, J. (2002) SRC-1 and TIF2 control energy balance between white and brown adipose tissues. *Cell*, **111**, 931-941.
Pijl, H., Potter van Loon, B.J., Toornvliet, A.C., Radder, J.K., Onkenhout, W., Frolich, M. and Meinders, A.E. (1994) Insulin-induced decline of plasma amino acid concentrations in obese subjects with and without non-insulin-dependent diabetes. *Metabolism*, **43**, 640-646.
Potter, C.J., Huang, H. and Xu, T. (2001) Drosophila tsc1 functions with tsc2 to antagonize insulin signaling in regulating cell growth, cell proliferation, and organ size. *Cell*, **105**, 357-368.
Proud, C.G. (2004a) mTOR-mediated regulation of translation factors by amino acids. *Biochem Biophys Res Commun*, **313**, 429-436.
Proud, C.G. (2004b) Role of mTOR signalling in the control of translation initiation and elongation by nutrients. *Curr Top Microbiol Immunol*, **279**, 215-244.
Puigserver, P., Wu, Z., Park, C.W., Graves, R., Wright, M. and Spiegelman, B.M. (1998) A cold-inducible coactivator of nuclear receptors linked to adaptive thermogenesis. *Cell*, **92**, 829-839.
Pullen, N., Dennis, P.B., Andjelkovic, M., Dufner, A., Kozma, S.C., Hemmings, B.A. and Thomas, G. (1998) Phosphorylation and activation of p70s6k by PDK1. *Science*, **279**, 707-710.
Radimerski, T., Montagne, J., Rintelen, F., Stocker, H., van Der Kaay, J., Downes, C.P., Hafen, E. and Thomas, G. (2002) dS6K-regulated cell growth is dPKB/dPI(3)K-independent, but requires dPDK1. *Nat Cell Biol*, **4**, 251-255.
Rahier, J., Wallon, J. and Henquin, J.C. (1981) Cell populations in the endocrine pancreas of human neonates and infants. *Diabetologia*, **20**, 540-546.
Randle, P.J. (1998) Regulatory interactions between lipids and carbohydrates: the glucose fatty acid cycle after 35 years. *Diabetes Metab Rev*, **14**, 263-283.
Ravussin, E. and Smith, S.R. (2002) Increased fat intake, impaired fat oxidation, and failure of fat cell proliferation result in ectopic fat storage, insulin resistance, and type 2 diabetes mellitus. *Ann N Y Acad Sci*, **967**, 363-378.

Ren, D., Collingwood, T.N., Rebar, E.J., Wolffe, A.P. and Camp, H.S. (2002) PPARgamma knockdown by engineered transcription factors: exogenous PPARgamma2 but not PPARgamma1 reactivates adipogenesis. *Genes Dev*, **16**, 27-32.

Richardson, C.J., Broenstrup, M., Fingar, D.C., Julich, K., Ballif, B.A., Gygi, S. and Blenis, J. (2004) SKAR Is a Specific Target of S6 Kinase 1 in Cell Growth Control. *Curr Biol*, **14**, 1540-1549.

Rigalleau, V., Aparicio, M. and Gin, H. (1998) Effects of low-protein diet on carbohydrate metabolism and energy expenditure. *J Ren Nutr*, **8**, 175-178.

Rohde, J., Heitman, J. and Cardenas, M.E. (2001) The TOR kinases link nutrient sensing to cell growth. *J Biol Chem*, **276**, 9583-9586.

Rosen, E.D., Hsu, C.H., Wang, X., Sakai, S., Freeman, M.W., Gonzalez, F.J. and Spiegelman, B.M. (2002) C/EBPalpha induces adipogenesis through PPARgamma: a unified pathway. *Genes Dev*, **16**, 22-26.

Rossant, J. and Cross, J.C. (2001) Placental development: lessons from mouse mutants. *Nat Rev Genet*, **2**, 538-548.

Rossant, J. and Spence, A. (1998) Chimeras and mosaics in mouse mutant analysis. *Trends Genet*, **14**, 358-363.

Rossetti, L., Rothman, D.L., DeFronzo, R.A. and Shulman, G.I. (1989) Effect of dietary protein on in vivo insulin action and liver glycogen repletion. *Am J Physiol*, **257**, E212-219.

Rui, L., Aguirre, V., Kim, J.K., Shulman, G.I., Lee, A., Corbould, A., Dunaif, A. and White, M.F. (2001) Insulin/IGF-1 and TNF-alpha stimulate phosphorylation of IRS-1 at inhibitory Ser307 via distinct pathways. *J Clin Invest*, **107**, 181-189.

Rupnick, M.A., Panigrahy, D., Zhang, C.Y., Dallabrida, S.M., Lowell, B.B., Langer, R. and Folkman, M.J. (2002) Adipose tissue mass can be regulated through the vasculature. *Proc Natl Acad Sci U S A*, **99**, 10730-10735.

Saltiel, A.R. and Kahn, C.R. (2001) Insulin signalling and the regulation of glucose and lipid metabolism. *Nature*, **414**, 799-806.

Saucedo, L.J., Gao, X., Chiarelli, D.A., Li, L., Pan, D. and Edgar, B.A. (2003) Rheb promotes cell growth as a component of the insulin/TOR signalling network. *Nat Cell Biol*, **5**, 566-571.

Savinska, L.O., Lyzogubov, V.V., Usenko, V.S., Ovcharenko, G.V., Gorbenko, O.N., Rodnin, M.V., Vudmaska, M.I., Pogribniy, P.V., Kyyamova, R.G., Panasyuk, G.G., Nemazanyy, I.O., Malets, M.S., Palchevskyy, S.S., Gout, I.T. and Filonenko, V.V. (2004) Immunohistochemical analysis of S6K1 and S6K2 expression in human breast tumors. *Eksp Onkol*, **26**, 24-30.

Schaffer, J.E. and Lodish, H.F. (1994) Expression cloning and characterization of a novel adipocyte long chain fatty acid transport protein. *Cell*, **79**, 427-436.

Schalm, S.S. and Blenis, J. (2002) Identification of a conserved motif required for mTOR signaling. *Curr Biol*, **12**, 632-639.

Schalm, S.S., Fingar, D.C., Sabatini, D.M. and Blenis, J. (2003) TOS motif-mediated raptor binding regulates 4E-BP1 multisite phosphorylation and function. *Curr Biol*, **13**, 797-806.

Schuppin, G.T., Bonner-Weir, S., Montana, E., Kaiser, N. and Weir, G.C. (1993) Replication of adult pancreatic-beta cells cultured on bovine corneal endothelial cell extracellular matrix. *In Vitro Cell Dev Biol Anim*, **29A**, 339-344.

Segal, K.R., Dunaif, A., Gutin, B., Albu, J., Nyman, A. and Pi-Sunyer, F.X. (1987) Body composition, not body weight, is related to cardiovascular disease risk factors and sex hormone levels in men. *J Clin Invest*, **80**, 1050-1055.

Serkova, N., Litt, L., Leibfritz, D., Hausen, B., Morris, R.E., James, T.L., Benet, L.Z. and Christians, U. (2000) The novel immunosuppressant SDZ-RAD protects rat brain slices from cyclosporine-induced reduction of high-energy phosphates. *Br J Pharmacol*, **129**, 485-492.

Shakur, Y., Holst, L.S., Landstrom, T.R., Movsesian, M., Degerman, E. and Manganiello, V. (2001) Regulation and function of the cyclic nucleotide phosphodiesterase (PDE3) gene family. *Prog Nucleic Acid Res Mol Biol*, **66**, 241-277.

Shi, Y. and Burn, P. (2004) Lipid metabolic enzymes: emerging drug targets for the treatment of obesity. *Nat Rev Drug Discov*, **3**, 695-710.

Shima, H., Pende, M., Chen, Y., Fumagalli, S., Thomas, G. and Kozma, S.C. (1998) Disruption of the $p70^{s6k}/p85^{s6k}$ gene reveals a small mouse phenotype and a new functional S6 kinase. *EMBO J*, **17**, 6649-6659.

Shimomura, I., Bashmakov, Y., Ikemoto, S., Horton, J.D., Brown, M.S. and Goldstein, J.L. (1999) Insulin selectively increases SREBP-1c mRNA in the livers of rats with streptozotocin-induced diabetes. *Proc Natl Acad Sci U S A*, **96**, 13656-13661.

Shulman, G.I. (2000) Cellular mechanisms of insulin resistance. *J Clin Invest*, **106**, 171-176.

Sierra-Honigmann, M.R., Nath, A.K., Murakami, C., Garcia-Cardena, G., Papapetropoulos, A., Sessa, W.C., Madge, L.A., Schechner, J.S., Schwabb, M.B., Polverini, P.J. and Flores-Riveros, J.R. (1998) Biological action of leptin as an angiogenic factor. *Science*, **281**, 1683-1686.

Smith, S., Witkowski, A. and Joshi, A.K. (2003) Structural and functional organization of the animal fatty acid synthase. *Prog Lipid Res*, **42**, 289-317.

Snyder, E.E., Walts, B., Perusse, L., Chagnon, Y.C., Weisnagel, S.J., Rankinen, T. and Bouchard, C. (2004) The human obesity gene map: the 2003 update. *Obes Res*, **12**, 369-439.

Soeder, K.J., Snedden, S.K., Cao, W., Della Rocca, G.J., Daniel, K.W., Luttrell, L.M. and Collins, S. (1999) The beta3-adrenergic receptor activates mitogen-activated protein kinase in adipocytes through a Gi-dependent mechanism. *J Biol Chem*, **274**, 12017-12022.

Stocker, H., Radimerski, T., Schindelholz, B., Wittwer, F., Belawat, P., Daram, P., Breuer, S., Thomas, G. and Hafen, E. (2003) Rheb is an essential regulator of S6K in controlling cell growth in Drosophila. *Nat Cell Biol*, **5**, 559-565.

Sul, H.S. and Wang, D. (1998) Nutritional and hormonal regulation of enzymes in fat synthesis: studies of fatty acid synthase and mitochondrial glycerol-3-phosphate acyltransferase gene transcription. *Annu Rev Nutr*, **18**, 331-351.

Swenne, I., Borg, L.A., Crace, C.J. and Schnell Landstrom, A. (1992) Persistent reduction of pancreatic beta-cell mass after a limited period of protein-energy malnutrition in the young rat. *Diabetologia*, **35**, 939-945.

Swenne, I., Crace, C.J. and Milner, R.D. (1987) Persistent impairment of insulin secretory response to glucose in adult rats after limited period of protein-calorie malnutrition early in life. *Diabetes*, **36**, 454-458.

Tam, P.P. and Rossant, J. (2003) Mouse embryonic chimeras: tools for studying mammalian development. *Development*, **130**, 6155-6163.

Tamemoto, H., Kadowaki, T., Tobe, K., Yagi, T., Sakura, H., Hayakawa, T., Terauchi, Y., Ueki, K., Kaburagi, Y., Satoh, S. and et al. (1994) Insulin resistance and growth retardation in mice lacking insulin receptor substrate-1 [see comments]. *Nature*, **372**, 182-186.

Tanaka, M., Hadjantonakis, A.K. and Nagy, A. (2001) Aggregation chimeras. Combining ES cells, diploid and tetraploid embryos. *Methods Mol Biol*, **158**, 135-154.

Tanaka, T., Yamamoto, J., Iwasaki, S., Asaba, H., Hamura, H., Ikeda, Y., Watanabe, M., Magoori, K., Ioka, R.X., Tachibana, K., Watanabe, Y., Uchiyama, Y., Sumi, K., Iguchi, H., Ito, S., Doi, T., Hamakubo, T., Naito, M., Auwerx, J., Yanagisawa, M., Kodama, T. and Sakai, J. (2003) Activation of peroxisome proliferator-activated receptor delta induces fatty acid beta-oxidation in skeletal muscle and attenuates metabolic syndrome. *Proc Natl Acad Sci U S A*, **100**, 15924-15929.

Tanaka, T., Yoshida, N., Kishimoto, T. and Akira, S. (1997) Defective adipocyte differentiation in mice lacking the C/EBPbeta and/or C/EBPdelta gene. *Embo J*, **16**, 7432-7443.

Tansey, J.T., Huml, A.M., Vogt, R., Davis, K.E., Jones, J.M., Fraser, K.A., Brasaemle, D.L., Kimmel, A.R. and Londos, C. (2003) Functional studies on native and mutated forms of perilipins. A role in protein kinase A-mediated lipolysis of triacylglycerols. *J Biol Chem*, **278**, 8401-8406.

Taylor, S.I. and Arioglu, E. (1998) Syndromes associated with insulin resistance and acanthosis nigricans. *J Basic Clin Physiol Pharmacol*, **9**, 419-439.

Tiraby, C. and Langin, D. (2003) Conversion from white to brown adipocytes: a strategy for the control of fat mass? *Trends Endocrinol Metab*, **14**, 439-441.

Tontonoz, P., Hu, E., Graves, R.A., Budavari, A.I. and Spiegelman, B.M. (1994) mPPAR gamma 2: tissue-specific regulator of an adipocyte enhancer. *Genes Dev*, **8**, 1224-1234.

Toyoshima, Y., Ohne, Y., Takahashi, S.I., Noguchi, T. and Kato, H. (2004) Dietary protein deprivation decreases the serine phosphorylation of insulin receptor substrate-1 in rat skeletal muscle. *J Mol Endocrinol*, **32**, 519-531.

Tremblay, F. and Marette, A. (2001) Amino acid and insulin signaling via the mTOR/p70 S6 kinase pathway. A negative feedback mechanism leading to insulin resistance in skeletal muscle cells. *J Biol Chem*, **276**, 38052-38060.

Tuttle, R.L., Gill, N.S., Pugh, W., Lee, J.P., Koeberlein, B., Furth, E.E., Polonsky, K.S., Naji, A. and Birnbaum, M.J. (2001) Regulation of pancreatic beta-cell growth and survival by the serine/threonine protein kinase Akt1/PKBalpha. *Nat Med*, **7**, 1133-1137.

Ueki, K., Yamamoto-Honda, R., Kaburagi, Y., Yamauchi, T., Tobe, K., Burgering, B.M., Coffer, P.J., Komuro, I., Akanuma, Y., Yazaki, Y. and Kadowaki, T. (1998) Potential role of protein kinase B in insulin-induced glucose transport, glycogen synthesis, and protein synthesis. *J Biol Chem*, **273**, 5315-5322.

Um, S.H., Frigerio, F., Watanabe, M., Picard, F., Joaquin, M., Sticker, M., Fumagalli, S., Allegrini, P.R., Kozma, S.C., Auwerx , J. and Thomas, G. (in press) Absence of S6K1 Protects Against Age and Diet-Induced Obesity While Enhancing Insulin Sensitivity. *Nature*.

Unger, R.H. (2003) Lipid overload and overflow: metabolic trauma and the metabolic syndrome. *Trends Endocrinol Metab*, **14**, 398-403.

Vaisse, C., Clement, K., Durand, E., Hercberg, S., Guy-Grand, B. and Froguel, P. (2000) Melanocortin-4 receptor mutations are a frequent and heterogeneous cause of morbid obesity. *J Clin Invest*, **106**, 253-262.

van der Leij, F.R., Huijkman, N.C., Boomsma, C., Kuipers, J.R. and Bartelds, B. (2000) Genomics of the human carnitine acyltransferase genes. *Mol Genet Metab*, **71**, 139-153.

Vassileva, G., Huwyler, L., Poirier, K., Agellon, L.B. and Toth, M.J. (2000) The intestinal fatty acid binding protein is not essential for dietary fat absorption in mice. *Faseb J*, **14**, 2040-2046.

Vega, G.L. (2004) Obesity and the metabolic syndrome. *Minerva Endocrinol*, **29**, 47-54.

Von Manteuffel, S.R., Gingras, A.-C., Ming, X.-F., Sonenberg, N. and Thomas, G. (1996) 4E-BP1 phosphorylation is mediated by the FRAP-p70^{s6k} pathway and is independent of mitogen-activated protein kinase. *Proceedings of the National Academia of Science USA*, **93**, 4076-4080.

Wang, Q., Somwar, R., Bilan, P.J., Liu, Z., Jin, J., Woodgett, J.R. and Klip, A. (1999) Protein kinase B/Akt participates in GLUT4 translocation by insulin in L6 myoblasts. *Mol Cell Biol*, **19**, 4008-4018.

Wang, Y.X., Lee, C.H., Tiep, S., Yu, R.T., Ham, J., Kang, H. and Evans, R.M. (2003) Peroxisome-proliferator-activated receptor delta activates fat metabolism to prevent obesity. *Cell*, **113**, 159-170.

Werner, E.D., Lee, J., Hansen, L., Yuan, M. and Shoelson, S.E. (2004) Insulin resistance due to phosphorylation of insulin receptor substrate-1 at serine 302. *J Biol Chem*, **279**, 35298-35305.

Whitehead, J.P., Clark, S.F., Urso, B. and James, D.E. (2000) Signalling through the insulin receptor. *Curr Opin Cell Biol*, **12**, 222-228.

Wilkinson, D.G. and Nieto, M.A. (1993) Detection of messenger RNA by in situ hybridization to tissue sections and whole mounts. *Methods Enzymol*, **225**, 361-373.

Winder, W.W. and Hardie, D.G. (1996) Inactivation of acetyl-CoA carboxylase and activation of AMP-activated protein kinase in muscle during exercise. *Am J Physiol*, **270**, E299-304.

Withers, D.J., Burks, D.J., Towery, H.H., Altamuro, S.L., Flint, C.L. and White, M.F. (1999) Irs-2 coordinates Igf-1 receptor-mediated beta-cell development and peripheral insulin signalling. *Nat Genet*, **23**, 32-40.

Withers, D.J., Gutierrez, J.S., Towery, H., Burks, D.J., Ren, J.M., Previs, S., Zhang, Y., Bernal, D., Pons, S., Shulman, G.I., Bonner-Weir, S. and White, M.F. (1998) Disruption of IRS-2 causes type 2 diabetes in mice. *Nature*, **391**, 900-904.

Wu, Z., Puigserver, P., Andersson, U., Zhang, C., Adelmant, G., Mootha, V., Troy, A., Cinti, S., Lowell, B., Scarpulla, R.C. and Spiegelman, B.M. (1999a) Mechanisms controlling mitochondrial biogenesis and respiration through the thermogenic coactivator PGC-1. *Cell*, **98**, 115-124.

Wu, Z., Rosen, E.D., Brun, R., Hauser, S., Adelmant, G., Troy, A.E., McKeon, C., Darlington, G.J. and Spiegelman, B.M. (1999b) Cross-regulation of C/EBP alpha and PPAR gamma controls the transcriptional pathway of adipogenesis and insulin sensitivity. *Mol Cell*, **3**, 151-158.

Yamagata, K., Sanders, L.K., Kaufmann, W.E., Yee, W., Barnes, C.A., Nathans, D. and Worley, P.F. (1994) rheb, a growth factor- and synaptic activity-regulated gene, encodes a novel Ras-related protein. *J Biol Chem*, **269**, 16333-16339.

Yang, Z.Z., Tschopp, O., Baudry, A., Dummler, B., Hynx, D. and Hemmings, B.A. (2004) Physiological functions of protein kinase B/Akt. *Biochem Soc Trans*, **32**, 350-354.

Yeh, W.C., Bierer, B.E. and McKnight, S.L. (1995a) Rapamycin inhibits clonal expansion and adipogenic differentiation of 3T3-L1 cells. *Proc Natl Acad Sci U S A*, **92**, 11086-11090.

Yeh, W.C., Cao, Z., Classon, M. and McKnight, S.L. (1995b) Cascade regulation of terminal adipocyte differentiation by three members of the C/EBP family of leucine zipper proteins. *Genes Dev*, **9**, 168-181.

Yu, C., Chen, Y., Cline, G.W., Zhang, D., Zong, H., Wang, Y., Bergeron, R., Kim, J.K., Cushman, S.W., Cooney, G.J., Atcheson, B., White, M.F., Kraegen, E.W. and Shulman, G.I. (2002) Mechanism by which fatty acids inhibit insulin activation of insulin receptor substrate-1 (IRS-1)-associated phosphatidylinositol 3-kinase activity in muscle. *J Biol Chem*, **277**, 50230-50236.

Zhang, Y., Gao, X., Saucedo, L.J., Ru, B., Edgar, B.A. and Pan, D. (2003) Rheb is a direct target of the tuberous sclerosis tumour suppressor proteins. *Nat Cell Biol*, **5**, 578-581.

Zhu, S. and Gerhard, D.S. (1998) A transcript map of an 800-kb region on human chromosome 11q13, part of the candidate region for SCA5 and BBS1. *Hum Genet*, **103**, 674-680.